



Durham E-Theses

The determination and interpretation of ground movements caused by shield tunnelling in Silty Alluvium at Willington Quay, north-east England

Sizer, K. E.

How to cite:

Sizer, K. E. (1976) *The determination and interpretation of ground movements caused by shield tunnelling in Silty Alluvium at Willington Quay, north-east England*, Durham theses, Durham University. Available at Durham E-Theses Online: <http://etheses.dur.ac.uk/9220/>

Use policy

The full-text may be used and/or reproduced, and given to third parties in any format or medium, without prior permission or charge, for personal research or study, educational, or not-for-profit purposes provided that:

- a full bibliographic reference is made to the original source
- a [link](#) is made to the metadata record in Durham E-Theses
- the full-text is not changed in any way

The full-text must not be sold in any format or medium without the formal permission of the copyright holders.

Please consult the [full Durham E-Theses policy](#) for further details.

THE DETERMINATION AND INTERPRETATION
OF GROUND MOVEMENTS CAUSED BY SHIELD
TUNNELLING IN SILTY ALLUVIUM AT
WILLINGTON QUAY, NORTH-EAST ENGLAND

-by-

K. E. Sizer

The copyright of this thesis rests with the author.
No quotation from it should be published without
his prior written consent and information derived
from it should be acknowledged.



ACKNOWLEDGEMENTS

The author is grateful to the following:

Northumbrian Water Authority (Resident Engineer : Mr. P.G.Gough)
for information, facilities and assistance at various times
during the progress of the measurement work.

Messrs. Charles Brand (Agent Mr. A.Benson) for the provision of
in-tunnel facilities at various times.

Messrs. Bridon Fibres and Plastics for tolerating the measurement
work outside the factory and for arranging periodical inspections
inside the factory.

N.H. Glossop, B. McEleavey and P. Kay for their assistance in field
measurement and laboratory experimentation.

R. Hardy for the provision of X-ray facilities and advice on techniques
and T.J. Smith for assistance in interpreting the results.

Dr. I.W. Farmer for supervision, advice and encouragement.

CONTENTS

	Page
Title.....	i
Acknowledgements.....	ii
Contents.....	iii
Illustrations.....	v
Tables and Plates.....	ix
Synopsis.....	1
1. Introduction and Previous Research.....	3
2. Superficial Deposits and Tunnelling Details.....	9
2.1 Superficial Deposits	
2.2 Details of the Tunnel	
3. Instrumentation.....	22
3.1 Location	
3.2 Surface Movements	
3.3 Sub-surface Movements	
3.4 Piezometer Measurements	
4. Results and Interpretation.....	32
4.1 Introduction	
4.2 Surface Settlement	
4.3 Surface Horizontal Movements	
4.4 Sub-surface Settlement	
4.5 Sub-surface Horizontal Movements	
4.6 Vectors of Ground Movement	
5. Laboratory Programme.....	83
5.1 Sampling Procedure	

5.2	Methods of Analysis	
5.3	Results and Interpretation	
5.4	Grainsize Distributions	
5.5	Liquid and Plastic Limits	
6.	Groundwater and Consolidation Studies.....	118
6.1	Moisture Contents in Tunnel Face	
6.2	Piezometer Results	
6.3	Flow-tank Analogue	
6.4	Consolidation Experiment	
6.5	Methane Determination	
7.	Summary and Discussion.....	143
	References.....	155
	Appendix 1 : Calculations.....	162
	Appendix 2 : Field and Experimental Data.....	164

ILLUSTRATIONS

Page

1.1 Site Locality in Lower Tyneside.....4

1.2 Detail of Site Locality.....5

2.1 Geological cross-section along Tunnel Centre Line..11

2.2 Detail of Tunnel Face Geology.....12

2.3 Tunnelling Shield.....20

3.1 Borehole Records.....23

3.2 Instrumentation Array.....26

3.3 Field Instrumentation.....27

3.4 Piezometer Apparatus.....31

4.1 Rate of Tunnel Advance.....33

4.2 Development of Surface Settlement.....36

4.3 Detail of Pre-Array Surface Settlement.....37

4.4 Initial Contours of Surface Settlement.....38

4.5 Surface Settlement vs. Log-Time Plot for station H
above Tunnel Centre Line.....41

4.6 Lateral variation of Maximum Surface Settlement....46

4.7 Development of Transverse Surface Settlement
Profiles.....47

4.8 Theoretical and Measured Surface Settlement,
Lateral Displacement and Strain.....48

4.9 Development of Sub-surface and Surface Settlement..55

	Page
4.10	Development of Settlement with Depth.....58
4.11	Limit of Settlement.....61
4.12	Inclinometer Profiles for Borehole 1.1.....64
4.13	Inclinometer Profiles Normal to the Tunnel Centre Line.....65
4.14	Inclinometer Profile Parallel to the Tunnel Centre Line.....68
4.15	Correlation diagram for Phases of Ground Movement.74
4.16	Vectors of Ground Movement Normal to the Tunnel Centre Line.....75
4.17	Vectors of Ground Movement Parallel to the Tunnel Centre Line.....80
5.1	Localities of samples from Tunnel Face.....84
5.2	Variation in the Absorption of Atmospheric Moisture with Time.....88
5.3	Interpretation of X-ray Diffraction Chart.....92
5.4	Organic content vs. initial Absorbed atmospheric moisture.....95
5.5	Organic content vs. Moisture content.....96
5.6	Moisture content vs. initial Absorbed atmospheric moisture.....97
5.7	Organic content vs. final Absorbed atmospheric moisture.....98
5.8	Organic content vs. clay to quartz ratio.....102

	Page
5.9 X.R.D. chart of Organic-rich sample.....	103
5.10 X.R.D. chart of Organic-poor sample.....	103
5.11 X.R.D. chart of Quartz-rich sample.....	104
5.12 X.R.D. chart of sample containing gravel.....	104
5.13 X.R.D. chart of unweathered Boulder Clay sample...	105
5.14 X.R.D. chart of weathered Boulder Clay sample.....	106
5.15 X.R.D. chart of zone of Carbonate accumulation....	106
5.16 Organic content vs. aluminium to total silica ratio.....	109
5.17 Lateral variation in Geochemistry within the channel.....	110
5.18 Geochemical Profile of weathered surface of Boulder Clay.....	112
5.19 Grainsize distribution for Organic-rich sample....	114
5.20 Grainsize distribution for Organic-poor sample....	114
5.21 Grainsize distribution for sample containing gravel.....	115
5.22 Liquid Limit vs. Plasticity Index.....	115
6.1 Variation in Moisture Content within the Tunnel Face - samples D.....	120
6.2 Variation in Moisture Content within the Tunnel Face - sample E.....	121
6.3 Variation in Moisture Content within the Tunnel Face - sample F.....	122

6.4	Locations of samples taken from cores.....	123
6.5	Change in Pore Pressure with passage of Tunnel Face.....	126
6.6	Diagrammatic representation of the effect of Compressed Air.....	126
6.7	Change in Water-table during consolidation.....	130
6.8	Water-table in Flow-tank Analogue.....	130
6.9	Flow lines for excess pressure inside the tunnel.....	133
6.10	Consolidation curve.....	135
6.11	Gas extraction apparatus.....	140
6.12	Mass Spectrometer Results.....	140
7.1	Relationships between Depth z , Diameter D and the distance between the points of Inflexion of the trough z_i for Tunnels in various types of ground.....	150
7.2	Relationships between Depth z , Diameter D and Maximum Surface Settlement $S_{g \max}$ for Tunnels in Stiff Clays..	152

TABLES

Page

1. Atterberg Limits and Cohesion Values for borehole samples.....	18
2. Initial depths of Magnetic Rings below ground surface.....	24
3. Minerals identified in Alluvium and Boulder Clay samples.....	91
4. Comparative Geochemistry of Alluvium and Boulder Clay samples.....	111
5. Liquid and Plastic Limits.....	116
6. Piezometer Results.....	127
7. Gas Analysis Results.....	141
8. Measured and Calculated Settlement Volumes.....	148
9. Depth-settlement case histories for Stiff Clays.....	153

PLATES

1. Regions of reclaimed alluvial flats in Lower Tyneside.....	14
2. Structural Damage caused by Settlement.....	42
3. Flow-tank Analogue with Flow Lines.....	129

SYNOPSIS

Settlement and ground deformation were measured around a horizontal, 4.25m external diameter, shield-driven tunnel at an axis depth of 13.375m at Willington Quay on the north bank of the River Tyne, using an instrumented borehole and surface survey array normal to the tunnel centre line.

The particular length of tunnel under investigation was constructed to accommodate an inverted sewage siphon passing beneath a brick panel infilled frame factory structure at ground surface.

The tunnel passed through a recently deposited channel of soft alluvial silt having an average undrained cohesion of 25 kN/m² giving a stability ratio of 9.58 at axis level. This was reduced to 5.97 by the use of compressed air at a pressure of 90 kN/m². The silt had an average bulk density of 1.82 Mg/m³, a moisture content of 42 to 46% and an organic content of 2.5 to 4.0%. Analyses showed an interrelationship between the moisture content, organic content and clay content of various samples. The original water table level was 2.25m below ground level and therefore 9.0m above the tunnel crown.

Surface and sub-surface settlement profiles (Figures 4.2 and 4.9) show that there was a continuation of settlement after completion of the tunnel and removal of the supporting air pressure. At 224 days a maximum settlement of 66mm at the surface and 88mm above soffit level at the side of the tunnel were observed. Settlement



was continuing at a logarithmically-decaying rate (Figure 4.5).

Ground movement vectors in the vertical plane of the instrument array (Figure 4.16) serve to isolate several major settlement phases. Up to 51 days after the tunnel had passed the array deformation was predominantly towards the tunnel annulus. Between 51 and 91 days, movement was away from the tunnel under the influence of secondary grouting at pressures of 690 kN/m^2 . Thereafter deformation occurred in a vertical direction, although the process was interrupted at about 162 days by significant ground uplift which coincided with the demolition of a settlement-damaged surface wall close to the instrument array. Uplift may be due to unloading from the removal of the wall or to further secondary grouting around the tunnel.

Pore pressure measurements (Figure 6.5 and Table 6) indicated a rise in the water table to a level of 1.2m below ground surface during passage of the tunnelling shield. This level fell to 3.5m below the surface at 119 days after the tunnel face had passed the instrument array, and it subsequently rose almost to the ground surface between 176 and 224 days after shield passage.

The main conclusion from the work is that the substantial ground movement around the tunnel was caused principally by consolidation of the saturated, high moisture content silt, the tunnel acting as a drain for the displaced porewater which was permitted access following removal of the compressed air pressure from the tunnel.

Chapter 1

INTRODUCTION AND PREVIOUS RESEARCH

This thesis is based upon a programme of fieldwork designed to provide data on the aground movement caused by the construction of a shield-driven tunnel in soft alluvium. The tunnel is located at Willington Quay in North Tyneside (Figures 1.1 and 1.2) and is the third in a series of projects undertaken by the Department of Engineering Geology in Durham for the Transport and Road Research Laboratory.

The instrumentation was based on experience gained from the previous two projects with small refinements to suit the differing conditions. The first project was at Green Park, London and concerned a tunnel 4m in diameter, lined with cast iron segmented rings and at 30m depth in the stiff, over-consolidated London Clay. The second was at Hebburn, part of South Tyneside, and concerned a 2m diameter tunnel, lined with concrete segmented rings and at an average depth of 7.5m in soft, normally consolidated and strongly laminated lacustrine clay. It was overlain by a layer of stiffer stony clay.

These projects form the subject of two research reports, provided for T.R.R.L., and several papers by P.B. Attewell and

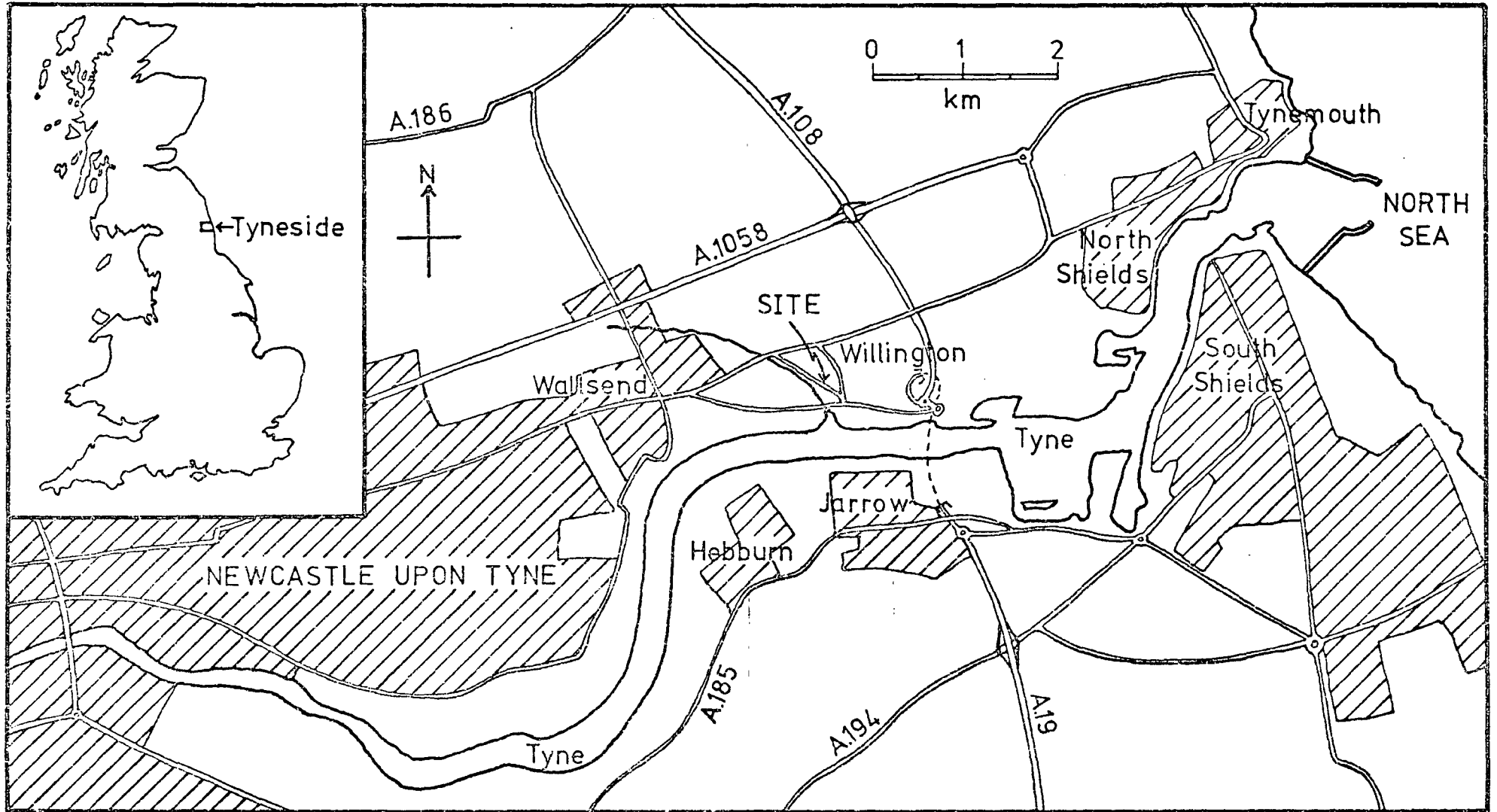


Figure 11: SITE LOCALITY IN LOWER TYNESIDE

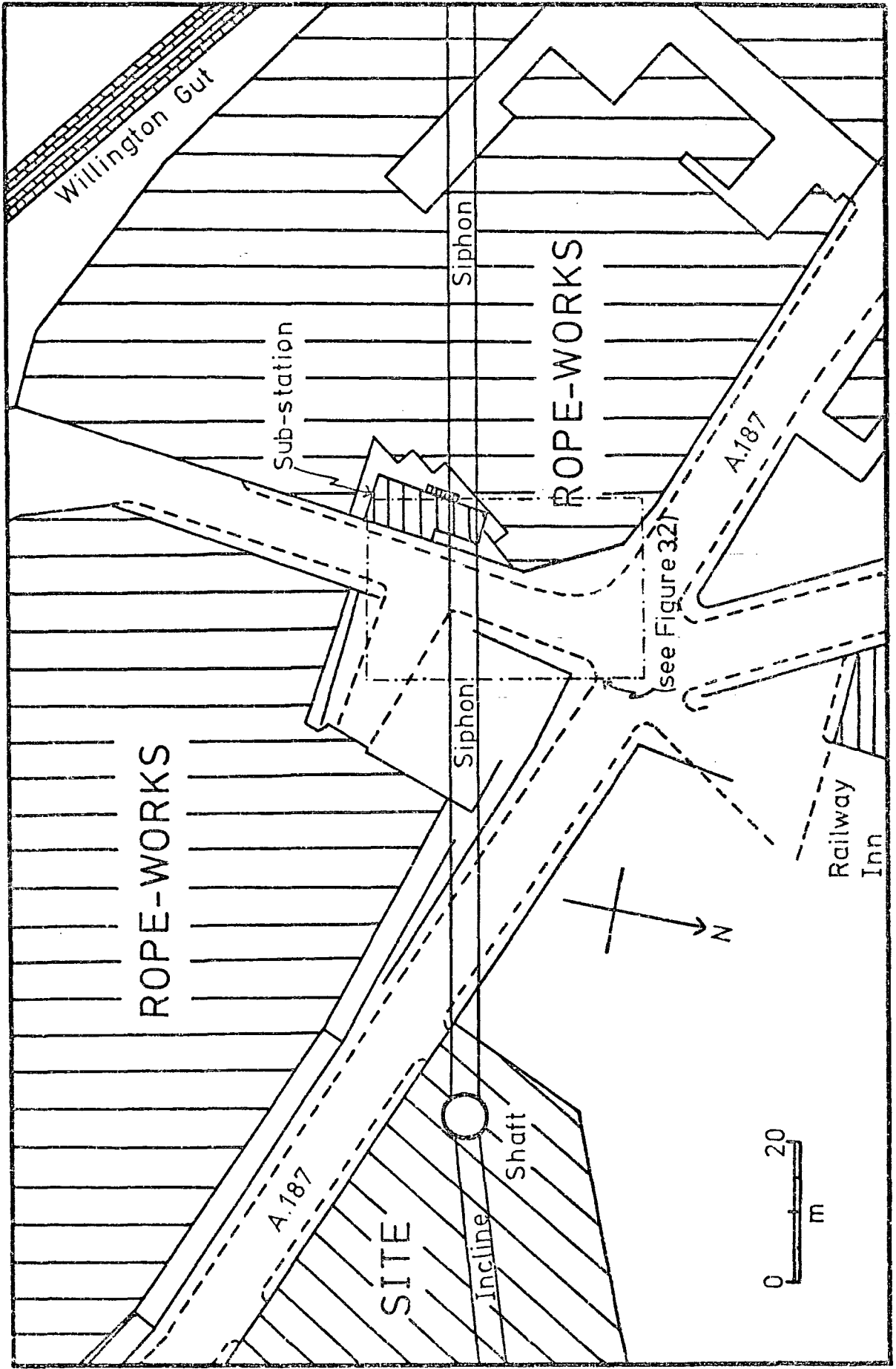


Figure 12: DETAIL OF SITE LOCALITY

I.W. Farmer. This literature formed the core of information upon which the instrumentation and interpretation of data was based. Similar studies of ground movements, caused by tunnelling in soft ground, can be found in J.V. Bartlett and B.L. Bubbers (1970), R.A. Butler (1975), W.H. Hansmire and J.E. Cording (1972), R.B. Peck (1969) and B. Schmidt (1969). However, the conditions and characteristics of the various tunnels were different from the one which is to be subsequently examined. Closer comparisons can be found in H. Hartmark (1964) and K. Henry (1974), both of which are accounts of tunnels driven in very soft, normally consolidated and recently deposited silts and clays. The former was located at Trondheim, Norway and the latter at Grangemouth, Scotland and, although compressed air was used in both the drives, extensive ground movements occurred. The Grangemouth tunnel produced many of the features observed at Willington Quay, in particular the long settlement process, which was caused by the release of compressed air in the drive when the tunnel was completed.

Several comparisons are made between the observed ground movements and those which have been predicted by the "Stochastic Theory". These comparisons were derived from research currently being carried out in this department by N.H. Glossop into the applications of this theory, which is based upon original work done by J. Litwiniszyn (1956). The research will be published in 1976 as part of a Ph.D. thesis.

The remaining references concerning tunnelling form a background of information. The most important of these is the State-of-the-Art

report on "Deep Excavations and Tunnelling in soft ground", by R.B. Peck (1969). This was presented at the 7th International Conference on Soil Mechanics and Foundation Engineering and its content, which summarises the available knowledge on the subject at that time, was considerably augmented by the discussions which followed. The Ph.D. thesis submitted by B. Schmidt (1969) contains several case histories of ground movements associated with tunnelling and some of the theoretical aspects of these. Also the extensive work of K. Szechy (1966) in "The Art of Tunnelling" forms a comprehensive account of the various methods of tunnelling and their effects on the ground.

The laboratory testing programme on samples of the alluvium incorporated standard tests taken mainly from T.N.W. Akroyd (1964) and the British Standards Institution publication (1967). The results obtained showed similarities to those of V. Milligan, L.G. Soderman and A. Rutka (1962) working on Canadian varved clays. Further work on samples, using X-ray techniques for quantitative analysis, was interpreted using extracts from G.W. Brindley (1961) and R.E. Grim (1962). This also required the use of calibration curves developed by the X-ray Laboratory and the Department of Engineering Geology at Durham.

The information available on the geology of the superficial deposits of the North-east is largely of a general nature and frequently deals with areas to the north and south of Tyneside without including Tyneside itself. Various workers, notably D. Woolacott (1905) and (1921) and C.T. Trechmann (1952), have contributed to the

understanding of the glacial deposits of East Durham and various sequences have been erected.

P. Beaumont (1967) provides the most recent analysis of the sequence of deposits together with a map of the buried valleys in the region. However, only G. Armstrong and J. Kell (1951) deal specifically with the lower Tyne valley using information gained during the construction of the pedestrian Tyne Tunnel. This revealed it to be an overdeepened valley with thick deposits of alluvium underlying the present river bed. It will be shown that the channel through which the tunnel passes is a small version of the main Tyne valley and has a similar origin.

Chapter 2

SUPERFICIAL DEPOSITS AND TUNNELLING DETAILS

It is proposed first to outline the nature and possible origins of the ground deposits through which the tunnel was driven, since these factors have some bearing on the choice of tunnelling procedure. The results of detailed investigations into the various properties and characteristics of the deposits will be presented in Chapters 5 and 6.

2.1 Superficial Deposits.

The site of investigation was located at a point where a 4.25 m diameter tunnel was being driven at an axis depth of 13.375 m through a buried channel of alluvium. This alluvium was underlain by beds of sand and gravel with water under artesian pressure, and by boulder clay which extended down to a rock-head of Coal Measures strata. The surface of the channel is now overlain by 3 to 5 m of fill (Figure 2.1).

The drift succession generally accepted as being reasonably representative of the surrounding region consists of three glacial episodes. Separating these are two interglacial periods. The upper

interglacial material shows that this was a period of widespread deposition whilst the lower interglacial is only represented at a single locality. The general succession is as follows:

Upper Till
 Middle Sands - interglacial
 Lower Till
 Hutton Henry Peat -- interglacial
 Scandinavian Till

The channel in question is almost certainly of post-glacial origin and it has been eroded into the underlying till by glacial outwash. The glaciation which formed the Upper Till was not widespread and produced only thin deposits in North-east England. Consequently, the channel may have cut through the Upper Till - if indeed any Upper Till was ever present - making the underlying material the Lower Till. The deposit is found in the floor of a present-day valley occupied by Wallsend Burn which becomes the tidal Willington Gut in its lower reaches where the instrumentation was located.

A plausible origin for the channel is that de-glaciation of the last glacial period produced meltwater which cut a deep valley into the glacial deposits. Flowing water initially laid down sands and gravels carrying the finer sediment further downstream. The post-glacial rise in sea-level flooded the lower part of the valley to produce a brackish, elongate estuary, a tributary to the Tyne estuary. This resulted in silt accumulating in the channel up to the present-day inter-tidal level (Figure 2.1). The estuary, which must have consisted of inter-tidal mudflats, was partly reclaimed by channelling Willington Gut down the west side of the valley and covering the mudflats with 3 to 5 m of fill. A rope factory and access roads were subsequently built on this

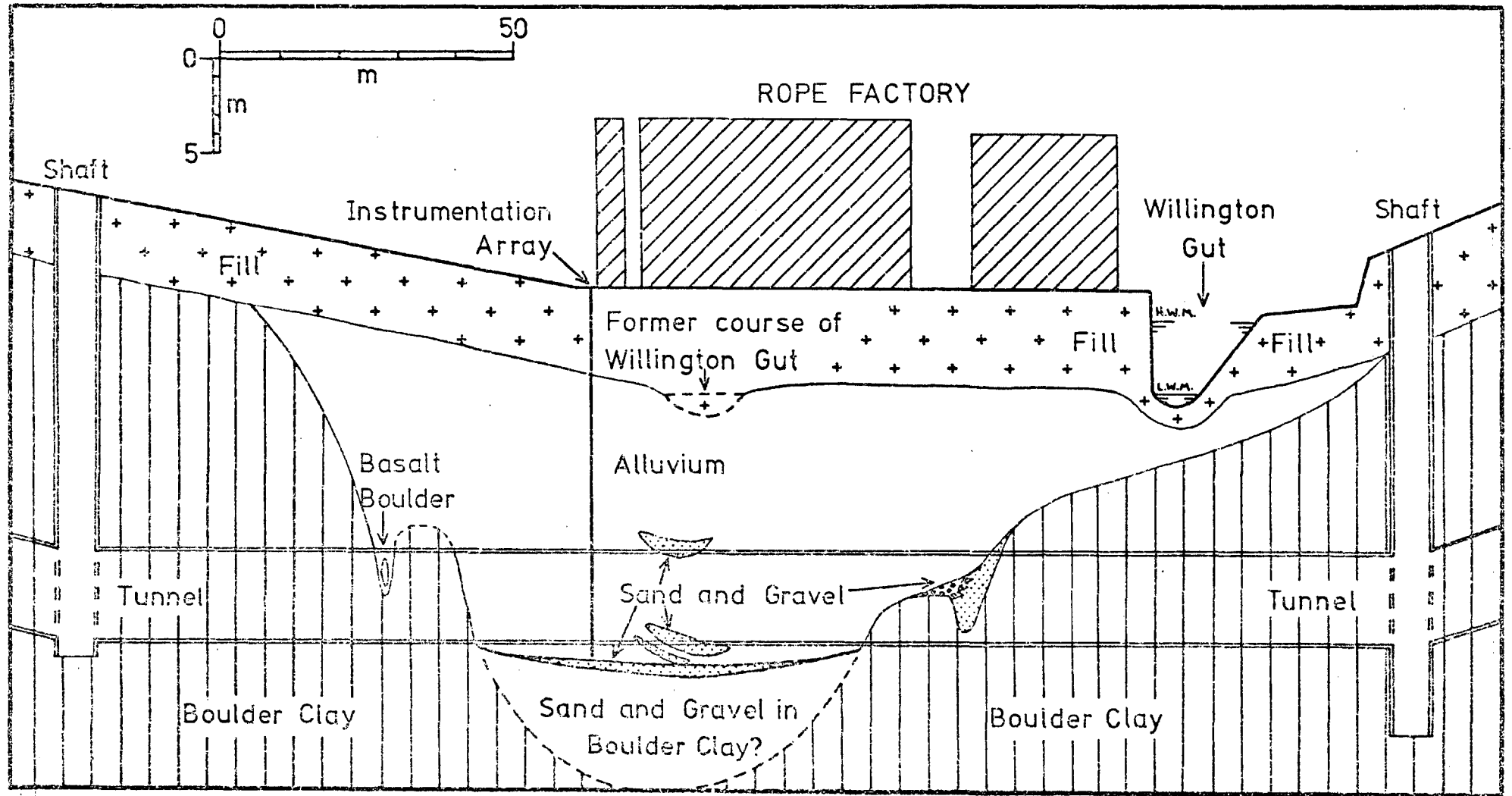


Figure 21: GEOLOGICAL CROSS-SECTION ALONG TUNNEL CENTRE LINE

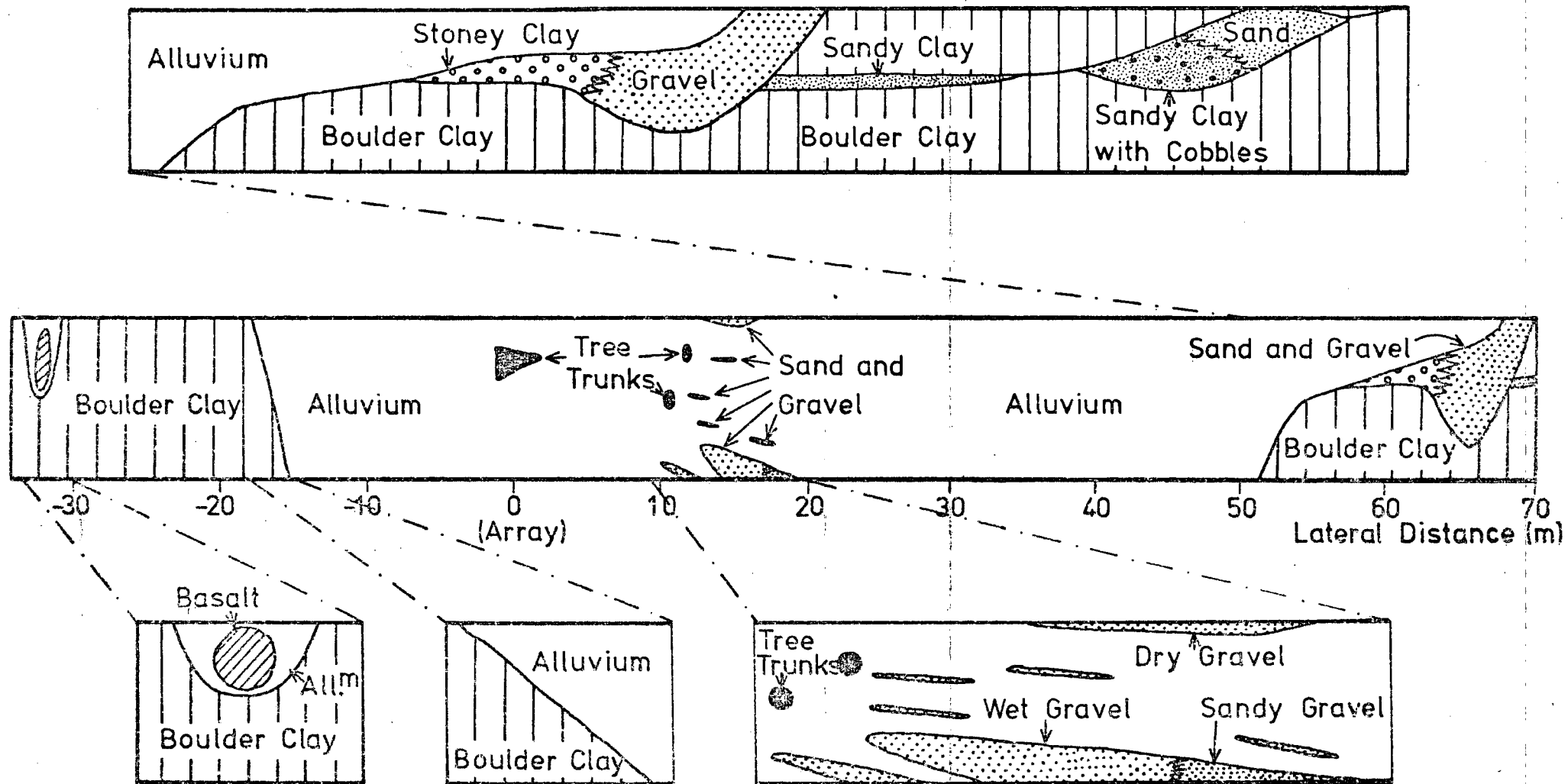


Figure 22: DETAIL OF TUNNEL FACE GEOLOGY

at a level which was 2 m above the High Water Mark in the Gut.

The former course of Willington Gut has been inferred from the pre-1933 ward boundary. Further evidence of its course was found when sand and gravel beds were encountered in the tunnel face when it passed below the inferred position. This indicates that a channel of flowing water must have persisted at Low Water, when the mudflats were exposed, depositing the sand and gravel in its bed as the estuary silted up. The geology of the channel is shown in Figure 2.1 which is a cross-section taken along the centre line of the tunnel using borehole evidence and the geology of the tunnel face.

Organic debris from the established vegetation was washed down into the estuary making the silt very organic. Large tree trunks were also included in the sediment and several were removed from the tunnel face by the contractors. These were saturated with water, but reducing conditions had preserved them in their original state. One large specimen was identified as oak (*Quercus*). The locations of the tree trunks, and the sand and gravel deposits encountered in the tunnel face, are shown in more detail in Figure 2.2. The enlarged sections have a horizontal scale equal to the vertical scale to show the true shape of the deposits.

The alluvium, therefore, mainly consisted of a soft, dark grey organic silt with about 2.5 to 4.0% organic material and 42 to 46% moisture content relative to dry weight. Small variations in the organic content produced dark and light laminations of about 2 to 5 cm thickness which were occasionally discernable at the tunnel face. It is possible that these laminations were caused by seasonal variations in the rate of sedimentation, similar to the variations which form

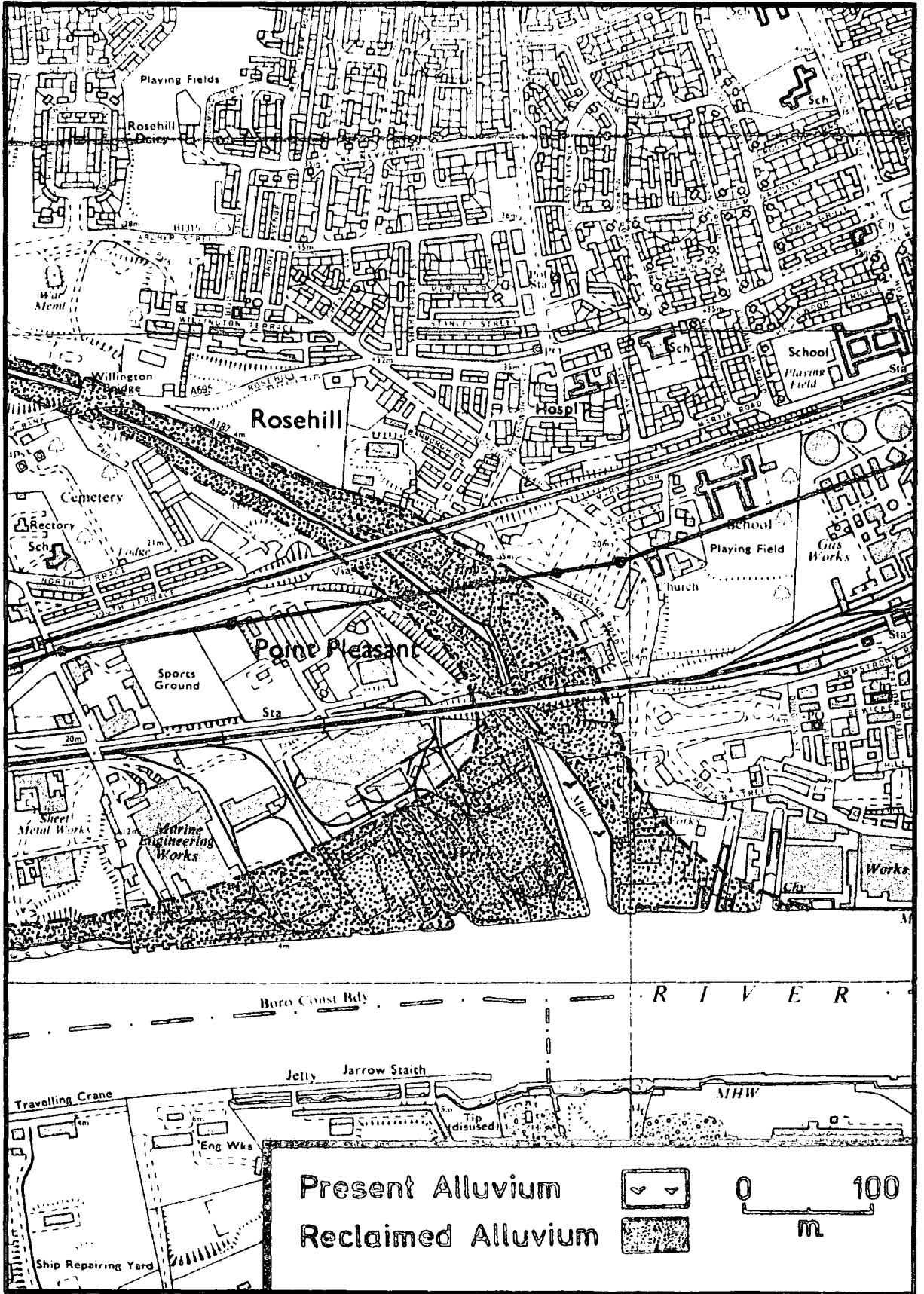


Plate 1a: REGIONS OF RECLAIMED ALLUVIAL FLATS IN LOWER TYNESIDE
-WILLINGTON GUT CHANNEL.

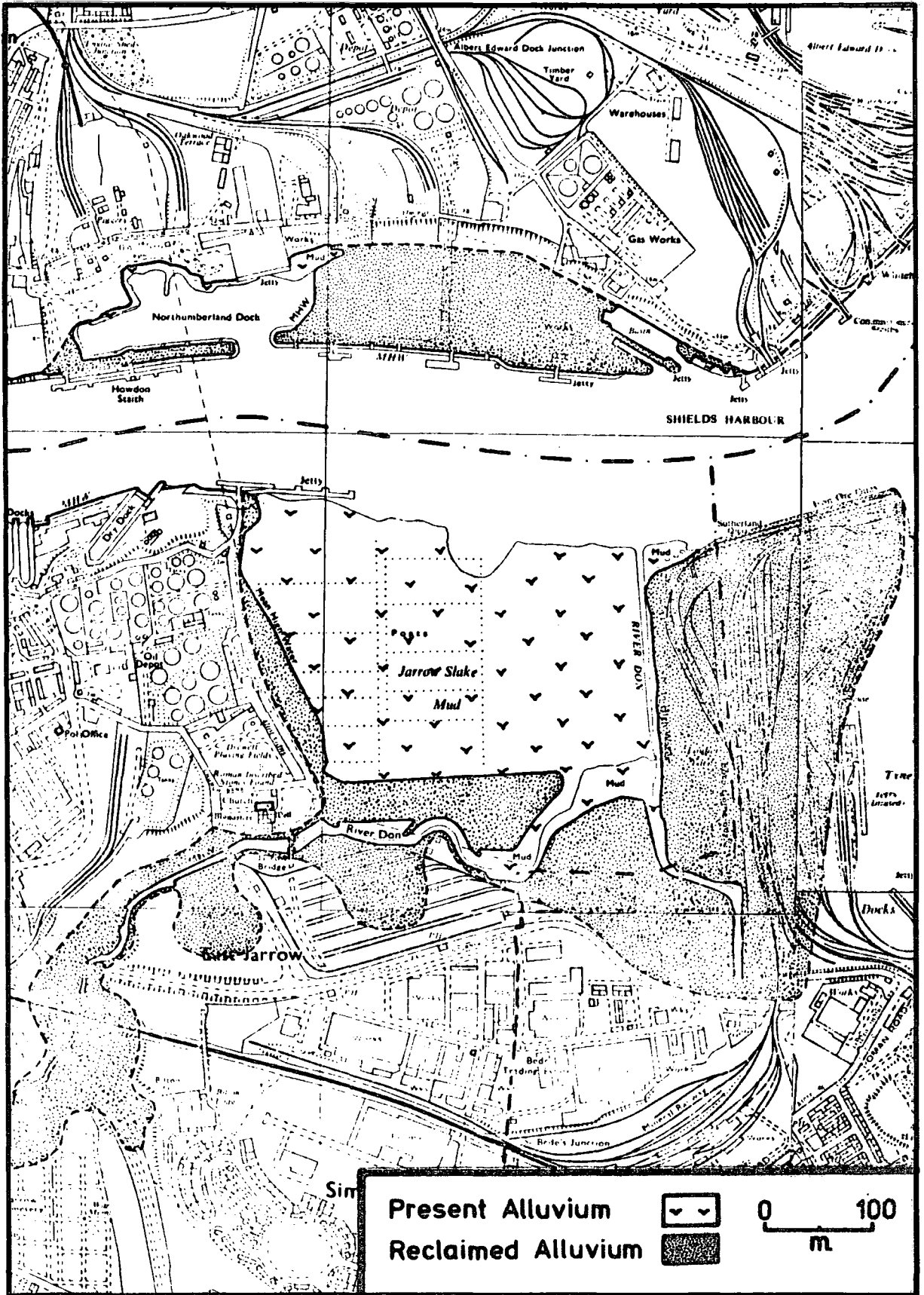


Plate 1b: REGIONS OF RECLAIMED ALLUVIAL FLATS IN LOWER TYNESIDE SHOWING THE WIDESPREAD NATURE OF THESE DEPOSITS.

varved clays. The properties of the silt are discussed further in Chapters 5 and 6.

2.2 Details of the Tunnel.

The tunnel under investigation was the lower section of the Point Pleasant Siphon passing under the valley of Willington Gut at Willington Quay, North Tyneside. This forms part of the North Bank Interceptor Sewer being constructed for the Northumbrian Water Authority as part of the extensive updating of the Tyneside sewerage system.

A large part of the tunnel, between the two inclines of the siphon under the valley sides, passed through the channel of alluvium already described. The instrumentation proved to be located at a point where the tunnel was 18 m into the east side of this channel. Here the axis depth was 13.375 m below the ground surface.

In order to determine the stability of the tunnel face the stability ratio of Simple Overload Factor was calculated. This is dependent upon the relationship of the overburden pressure acting upon the centre of the tunnel face and the undrained shear strength of the alluvium resisting the pressure. The relationship was proposed by B.B. Broms and H. Bennermark (1967) in the form:

$$N = \frac{\gamma \cdot H}{c_u}$$

where γ is the natural wet density of the clay

H is the depth to the centre of the face

c_u is the undrained shear strength of the clay

N is the value of the stability ratio.

Theoretical analysis originally gave a critical value for $N = 6.28$, above which the tunnel face would be unstable resulting in higher intrusion rates of the tunnel face causing large surface settlements and the increasing possibility of failure in the face at higher values of N . The critical value was reinforced using laboratory extrusion tests which produced values in the region of 6 to 8. Evidence of large surface settlements and high tunnel face intrusion rates in tunnels with lower stability ratios resulted in P.B. Attewell and J.B. Boden (1971) suggesting a value of 4.5, based upon the overburden pressure required to produce maximum acceleration of the rate of extrusion in a laboratory extrusion test.

The calculation required the determination of the bulk density and undrained shear strength by triaxial tests which were carried out by N. El-Naga according to B.S. 1377. Table 1 lists the values obtained and also various other properties using samples taken from boreholes 1 and 2 which were drilled for the instrumentation of the tunnel. The shear strengths obtained for the samples from borehole 1 were averaged to give a mean $c_u = 24.9 \text{ kN/m}^2$ or 36.1 lbf/in^2 and a bulk density $\gamma = 1.82 \text{ Mg/m}^3$ or 113.6 lb/ft^3 , which produces a stability ratio of 9.58. Consequently an air pressure of 90 kN/m^2 (13 lbf/in^2) was used in the drive to stabilize the face and reduce the rate of intrusion by lowering the stability ratio to 5.97. As a result of the air pressure the alluvium, although of a plastic consistency, appeared to be firm and stable in the tunnel face.

The compressed air also had the effect of reducing the amount of water made by the tunnel to a minimum despite the water-table being about 10 m above the tunnel soffit.

Sample	1a	1b	1c
Depth m	11.00-11.45	13.00-13.45	14.50-14.95
Liquid Limit	48.50%	48.50%	46.50%
Plastic Limit	28.20%	26.60%	25.54%
Plasticity Index	20.30%	19.80%	20.96%
Moisture Content	38.30%	39.10%	38.75%
c_u kN/m ²	25.99	25.20	23.54

Results for borehole 1.

Sample	2a	2b	2c
Depth m	13.00-13.45	14.00-14.45	15.00-15.45
Liquid Limit	42.60%	44.50%	41.80%
Plastic Limit	28.49%	28.19%	27.23%
Plasticity Index	13.11%	16.31%	14.57%
Moisture Content	40.22%	38.52%	36.53%
c_u kN/m ²	17.65	18.63	20.59

Results for borehole 2.

Table 1: ATTERBERG LIMITS AND COHESION VALUES FOR BOREHOLE SAMPLES.

Excavation of the alluvium was carried out by hand using compressed air clay spades ahead of a 4.31 m diameter shield (Figure 2.3). The bead was removed from the shield before the channel was entered in order to reduce ground loss around the tunnel. This was a deliberate decision based on earlier analyses on the south bank of the Tyne. The shield was 2.4 m long with a 1.2 m tailskin inside which the rings of tunnel lining were built. These rings consisted of 7 concrete segments bolted together to form a 0.6 m (2ft) long ring. When the shield was jacked forward against each newly-erected ring the annulus left between the ring and the ground was filled with a water-cement grout injected under pressure through holes in the lining. The grouting operation was usually carried out every two rings of lining. The cement used was "sulphacrete", a sulphate-resisting cement.

The tunnelling sequence was generally as follows:

- a) The ground was excavated by pneumatic spade to a distance of about 0.6 m (2 ft) ahead of the hood of the shield and to slightly less than the same diameter.
- b) The shield was then shoved forward against the previously erected ring, the cutting edge of the shield peeling off the final layer of ground resulting in a precise fit of the outside of the shield against the alluvium. About 10 cm of the previous ring were left resting on the tailskin of the shield to prevent the tunnel from dipping.
- c) A further ring was erected inside the tailskin and the annulus produced from the shield advance was filled with grout through pre-formed holes in the lining segments.

The grouting operation tended to leave an ungrouted void in the

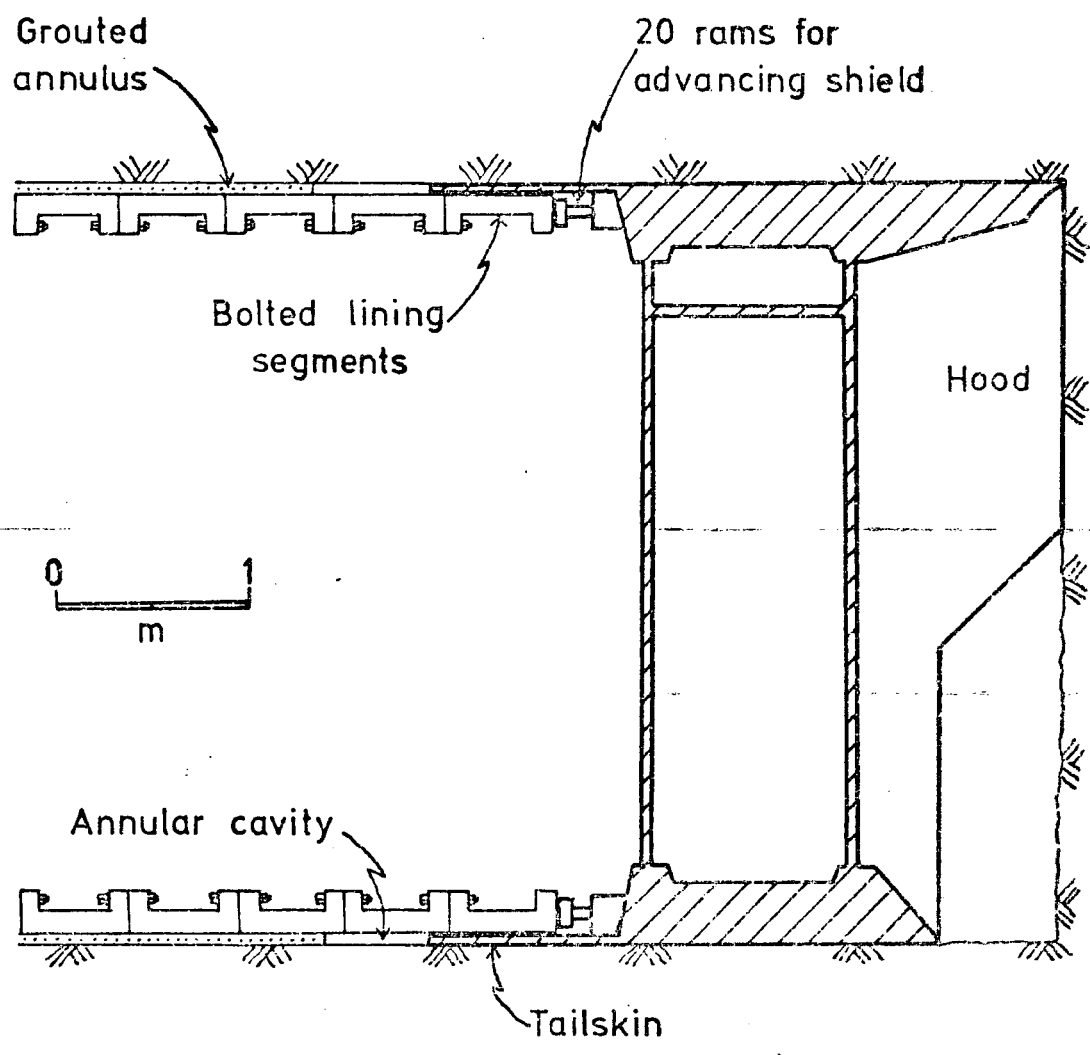


Figure 2.3: TUNNELLING SHIELD

soffit. This was later back-grouted at a higher pressure of 690 kN/m^2 (100 lb/in^2). The back-grouting of the tunnel within the channel was not carried out until the tunnel had reached the far side of the channel and even then the process was not completely successful in eliminating all the voids.

On average, two cycles of excavation and lining erection were completed per 12 hour shift and two shifts per day were worked during the period when the tunnel was in the channel. After the boulder clay had been re-entered three 8 hour shifts a day were worked to maintain rapid progress. At weekends, the face was boarded up with thick breast-boards held in position by four rams projecting forwards from the shield.

Chapter 3

INSTRUMENTATION

3.1 Location.

Four boreholes were drilled vertically through Gut Road to a depth of 16m (just below invert) forming an array in a line normal to the extrapolated centre line of the tunnel. Borehole 1 was located over the centre line and borehole 2 was fixed at about 1m beyond the point through which the tunnel wall would pass. Holes 3 and 4 were located at a distance of 3.96m and 7.65m from the centre line respectively. The records for each of these boreholes are illustrated in Figure 3.1.

Lengths of Soil Instruments inclinometer tube with collapsible telescopic joints were inserted into these boreholes and grouted in with a water-cement-bentonite grout. This grout was designed to have a similar cohesive strength when set to that of the alluvium. Five magnetic settlement rings were taped to each tube before emplacement in order to monitor vertical movement (see Table 2 for initial location). This installation operation was completed 7 months before the drive reached the measurement array and numerous calibration measurements were taken.

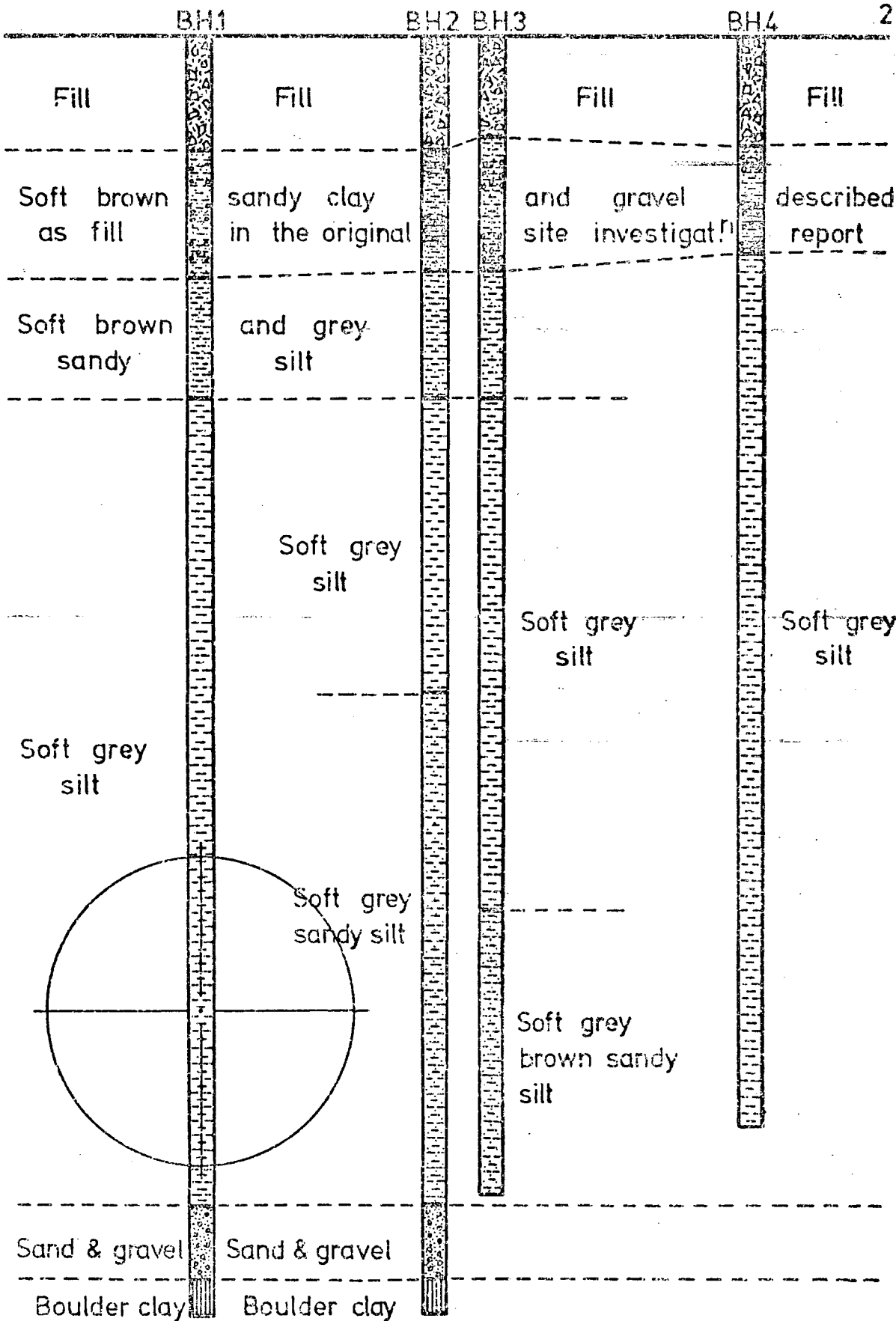


Figure 3.1: BOREHOLE RECORDS (FOR INSTRUMENTATION ARRAY)

Ring	<u>Borehole</u>			
	1	2	3	4
1	1.33	1.54	3.20	2.79
2	4.34	3.09	5.94	6.14
3	7.35	7.65	8.81	8.86
4	10.40	8.60	11.50	12.21
5	15.88	10.99	13.76	
6		15.18		

Table 2: INITIAL DEPTHS OF MAGNETIC RINGS
BELOW GROUND SURFACE.

The keyways in the inclinometer tubes were orientated normal to and parallel to the tunnel centre line. When the tunnel reached the measurement array a section of tube 1 was exposed in the centre of the face. Visual examination of this showed that the tube had not spiralled through the joints and that the borehole had not deviated from the vertical.

Surface levelling stations consisted of a nail inserted through a washer into the road or footpath surface. These were positioned to form an array of 10 stations, 8 of which were on the same side of the centre line as the inclinometer tubes and the remaining two were positioned on the opposite side of the centre line (Figure 3.2). These stations were installed 2 months before the drive reached the array.

Two piezometers were also installed in boreholes 1 and 2. In the former, the piezometer was located about 1m above soffit level and in the latter at axis level. They were positioned by being fastened to the inclinometer tubes at their design depths before the latter were inserted. At these depths, grouting was interrupted and the piezometers were surrounded by a sand filter to provide continuity with the water-table in the alluvium. After this operation, grouting was resumed, so sealing the piezometers in from the surface (Figure 3.3b)

3.2 Surface Movements.

a) Levelling.

Vertical settlement at the surface was measured using a Cooke S.440 precise level and a one-piece metric staff. The staff was

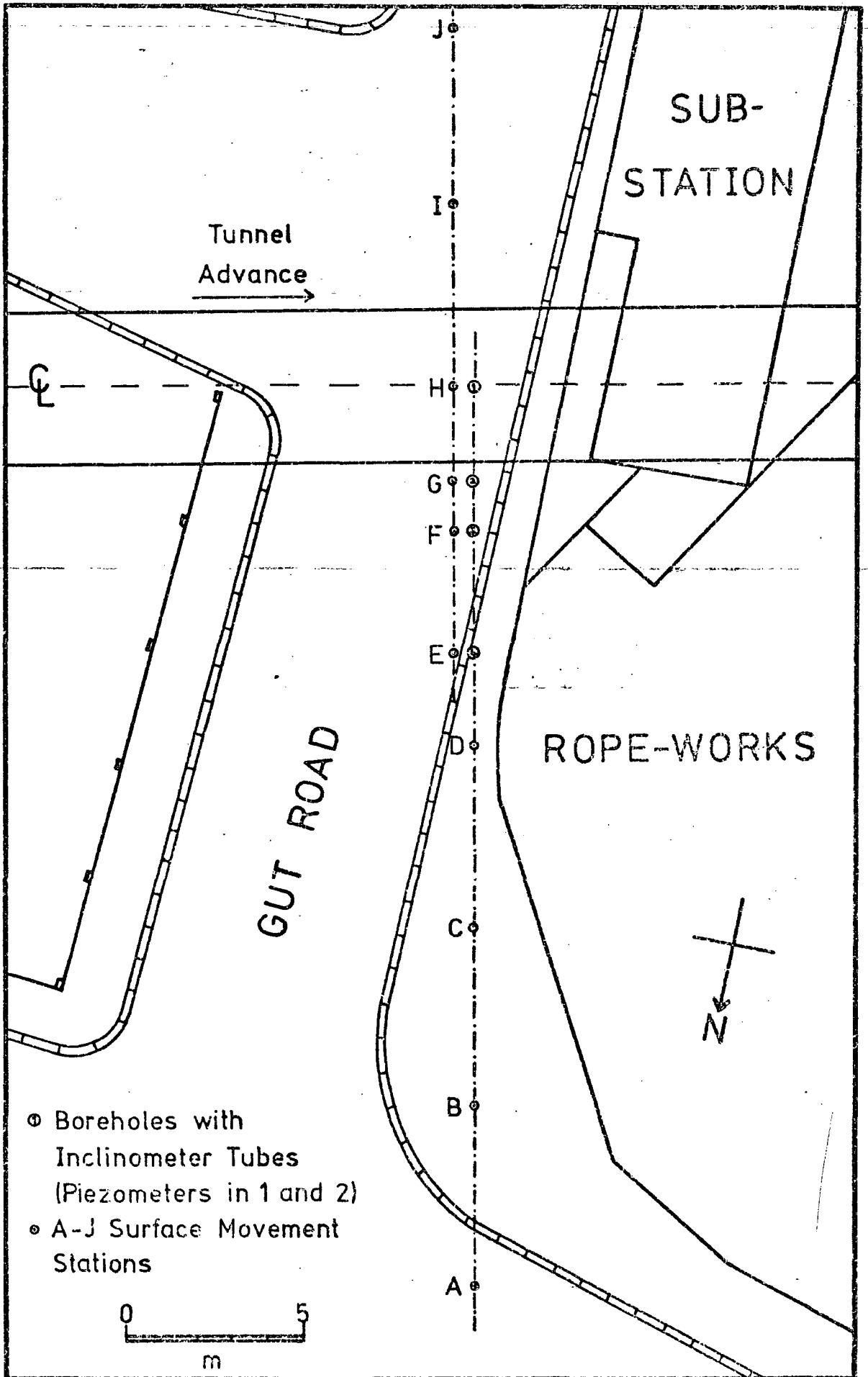
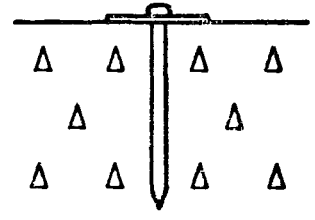
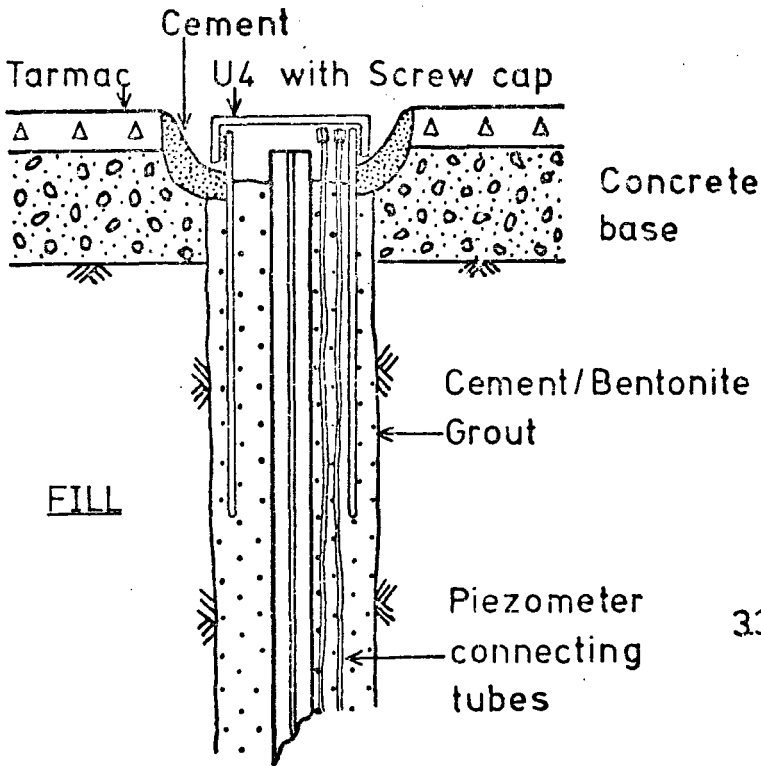
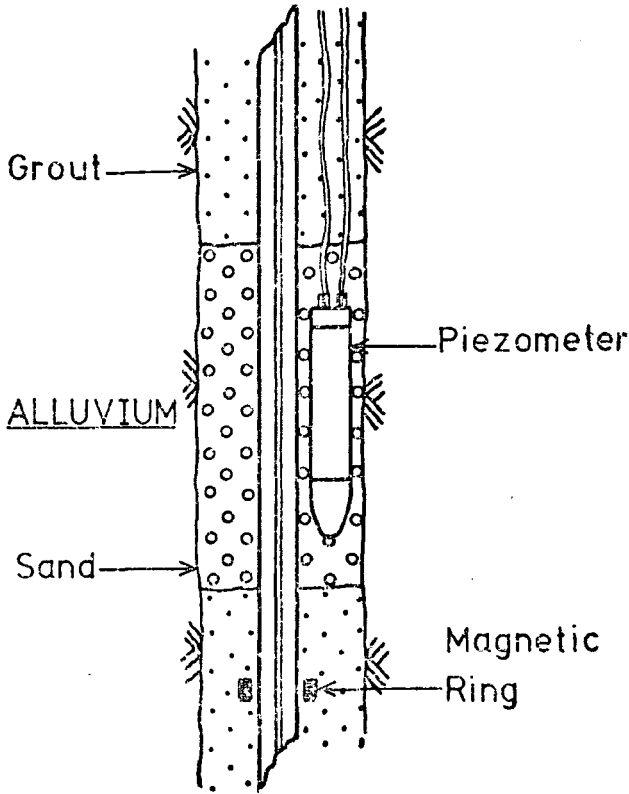


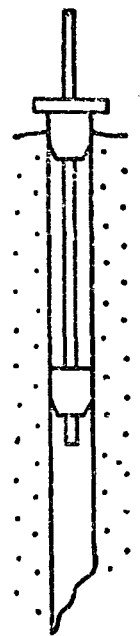
Figure 3.2: ARRAY OF INSTRUMENTATION



33a. Installation of Inclinometer Tubes



33b. Piezometer Cell



33d. Plug for Inclinometer Tubes for Lateral Distance Determination

Figure 33: FIELD INSTRUMENTATION

allowed to rest on the heads of the nails sunk into the road and footpath surface (Figure 3.3c). The array A to J was surveyed using station B as a Temporary Bench Mark (TBM) which was itself compared to a TBM outside the Railway Inn (Figure 1.2) and therefore beyond the influence of the tunnel settlement trough.

A base-level was established prior to the onset of settlement. During settlement development frequent readings were taken and referred back to this datum. Settlement was measured to the nearest 0.1mm with an experimented accuracy of $\pm 0.2\text{mm}$.

b) Horizontal Measurement

A steel band was used to measure the horizontal displacements towards the centre line of the surface levelling stations. The band was kept at a constant tension of 44N (10lb force) in order to reduce any errors that might otherwise have arisen where the band had passed over kerbs. Readings were estimated to 0.3mm (0.001ft) so giving an overall accuracy of $\pm 0.6\text{mm}$ (0.002ft). Undulations in the path and the road may have increased this value slightly.

Inward movements of the tops of the inclinometer tubes towards the centre line were also monitored by inserting specially designed close-fitting plugs into them (Figure 3.3d). Distances between the centre-punch marks in the tops of these plugs were measured and the relative movements were used as the surface datum for the tops of the horizontal ground movement profiles.

Again, datum values for all the measurements were established before settlement began.

3.3 Sub-surface Movements.

a) Magnetic Rings.

Vertical movements were measured using the magnetic rings taped to the outside of the inclinometer tubes. These were located by lowering a reed switch down the tubes on the end of a steel tape. The reed switch closed in the magnetic field of each ring so emitting an audible signal at the surface. Four readings were taken at the top of the tape, two going down as the switch closed and opened, and two coming up as it again closed and opened. Readings were taken to the nearest 0.5mm and averaging these gave an estimated accuracy of $\pm 0.25\text{mm}$. A datum was established before settlement began.

b) Inclinometer Tubes.

Horizontal movements were measured by lowering a Soil Instruments inclinometer torpedo (1 metre long) down each of the four installed tubes in turn. Two sets of readings, one going down and one coming up, were taken with the fixed wheels in each of the four keyways in turn, readings from opposite keyways being averaged to reduce summation errors. Plotting the changes in the profiles of the tubes generated horizontal displacement data for planes normal and parallel to the tunnel centre line at intervals of 1m depth initially and $\frac{1}{2}\text{m}$ intervals when a replacement $\frac{1}{2}\text{m}$ torpedo had to be used.

Datum lines were established by averaging the results taken before surface settlement began, after which frequent readings were taken. However, tube 4 was blocked at a depth of 6m until settlement had begun. This movement caused the object creating the blockage to drop to a depth of 14m. Thus, no datum was established for this particular tube

until just before the tunnel reached the array. The movement up to this time would probably have been very small, so the subsequent profiles can be regarded as a good representation of the total ground movement.

3.4 Piezometer Measurements.

The depth of the water-table below the ground surface was measured every day whilst the tunnel face was passing under the array and until fluctuations had ceased. In order to take these readings, water was pumped down to the piezometer through one connecting tube and back up the other to fill a graduated column attached to it. The base of the graduated tube was filled with mercury supplied through a U-tube from a reservoir open to the atmosphere (Figure 3.4). When all the air was expelled from the system, the water pump was disconnected from the connecting tube and the water levels allowed to stabilize. The level of mercury drawn up into the graduated column was then noted and when the apparatus had been disconnected from the piezometer the level was taken again. The difference between the readings was equivalent to the depth of water-table below the ground surface.

The piezometer in borehole 2 at axis level continued to provide readings throughout the passage of the face. However, the piezometer in borehole 1 at 1m above the tunnel soffit was affected by compressed air leaking through the grout when the tunnel reached the array. This penetrated the instrument and escaped through the connecting tubes making the collection of further data impossible.

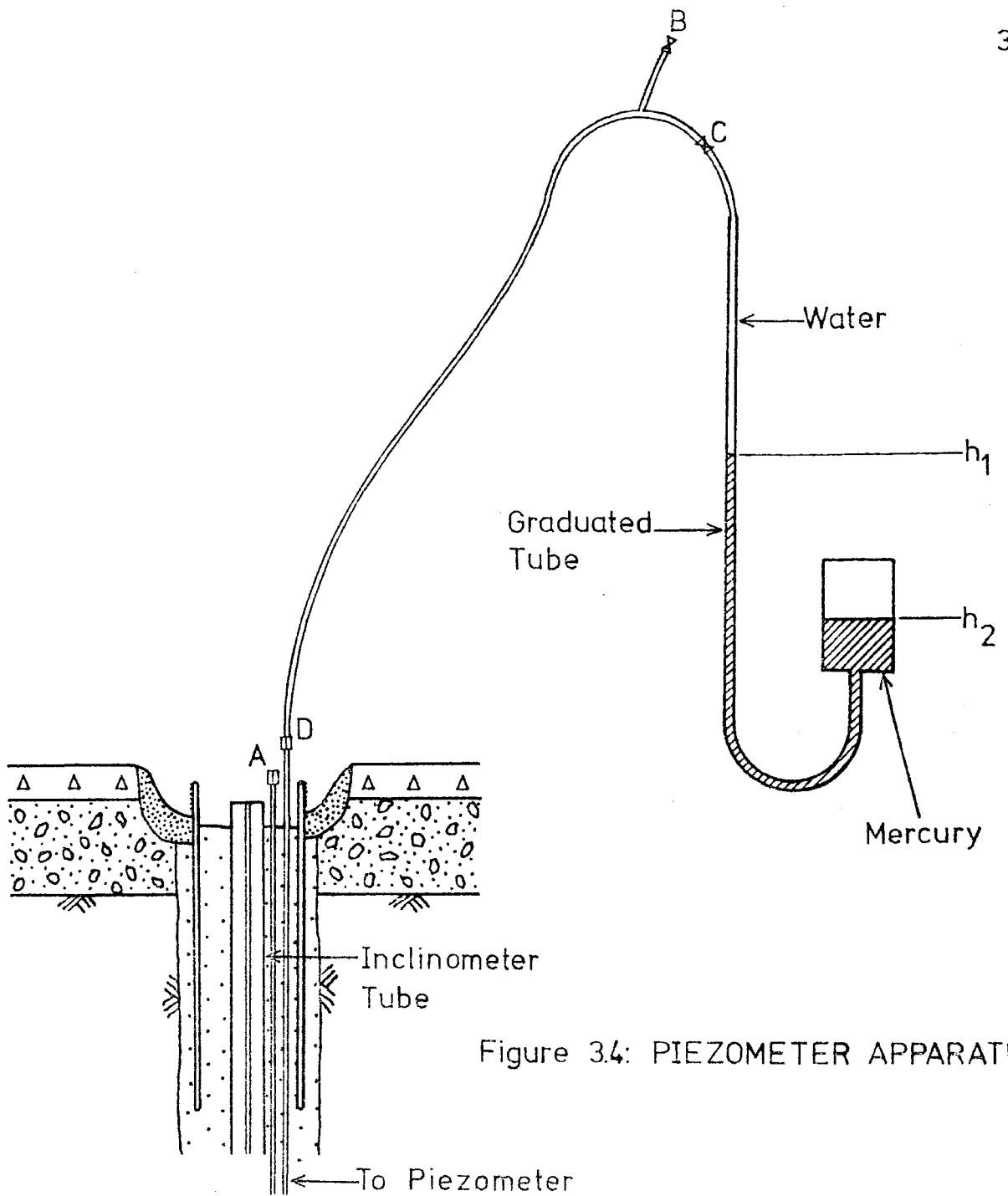


Figure 3.4: PIEZOMETER APPARATUS

Operation Sequence

- 1) Water pumped down through Piezometer at A and out at B thus filling system with water.
- 2) Tube sealed at B with clip.
- 3) Pump disconnected and clip at C removed thereby connecting system to graduated tube.
- 4) Reading h_1 taken after mercury has stopped rising.
- 5) Instrument disconnected at D and reading h_2 taken.
- 6) $h_1 - h_2 =$ depth to water in mm. mercury.

Chapter 4

RESULTS AND INTERPRETATION

4.1 Introduction

The majority of the results are presented graphically to show the development of surface settlement and sub-surface ground movement with respect to time. Time was preferred to tunnel face position as a reference base because of the on-going nature of the settlement. The majority of the settlement took place after the tunnel face was too far away from the instrumentation to have any effect. However, for the period when the tunnel face was within 34m of the array, some reduction in settlement resulted from boarding up the face for the 48 hour weekend breaks. In order to remove this effect the weekends are omitted from the reference base for the period when the face was within 34m of the array. This gives a more realistic representation of the rates of settlement within this critical period.

As a result of a fairly constant rate of progress of the drive, as shown by the site records and illustrated in Figure 4.1, the corrected time plots agree closely with the tunnel face position for this period. However, some of the illustrations use the tunnel face position in metres. These refer specifically to events which occurred when the tunnel face was within 34m of the array. Over this limited period the alternative reference base is a more accurate representation

1975

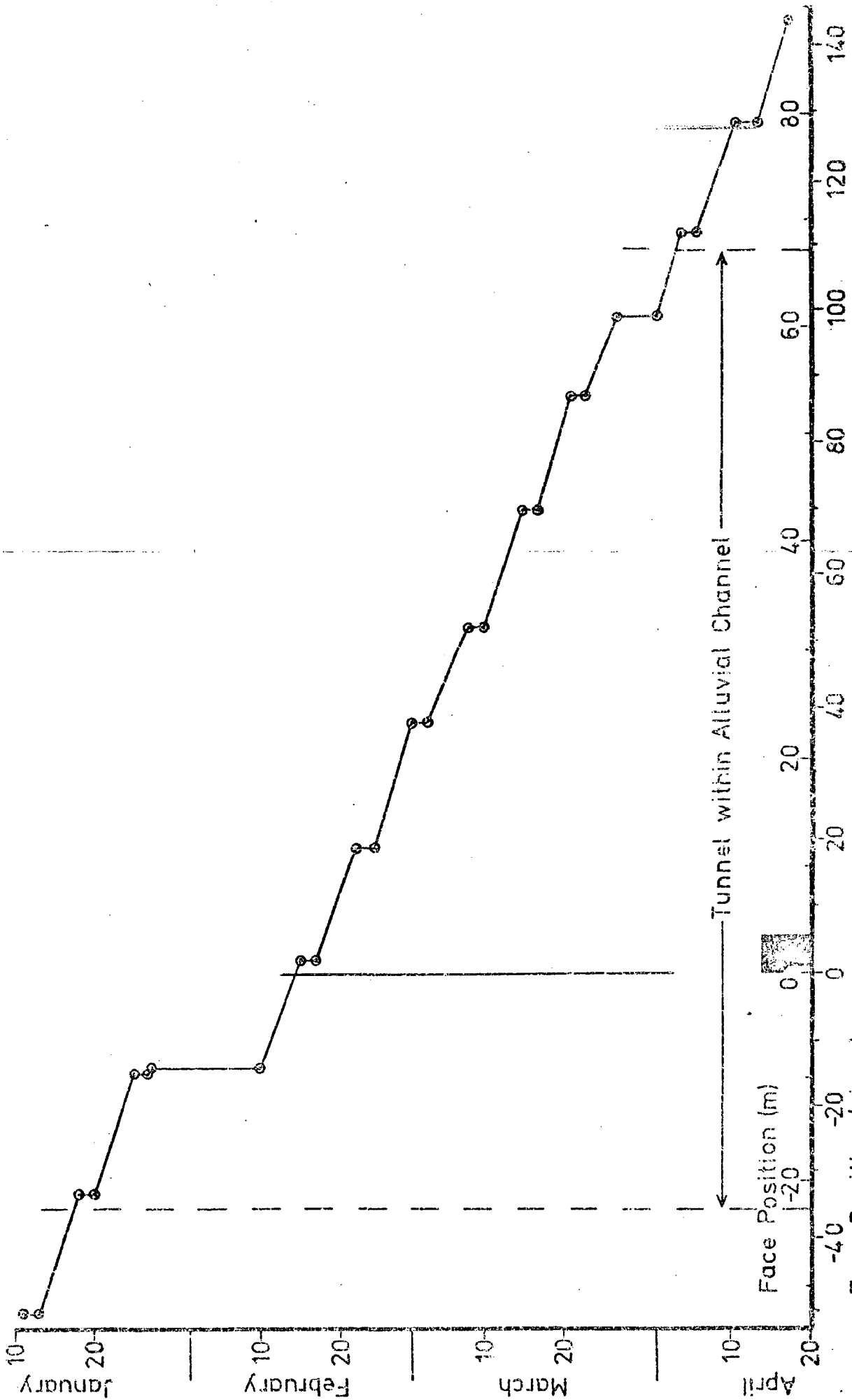


Figure 4.1: RATE OF TUNNEL ADVANCE

of the events, particularly for large scale illustrations.

In all cases the datum was taken as being the time when the tunnel face reached the instrumentation array, that is, when the inclinometer tube in borehole 1 was exposed in the face. The only major interruption to the tunnel progress was for two weeks when the face was -4 days (-8.53m) from the array. This resulted from a report of gas seeping into the tunnel and the hold-up was to allow flameproof lighting and equipment to be installed. The effects of this break will be discussed later.

The various graphs give horizontal and vertical components of movement. By combining these components vectors of ground movement have been produced.

4.2 Surface settlement.

It can be seen in Figure 4.2 that the surface settlement development profiles for stations A to H show a complex settlement history. The various stages of this history are examined separately and some attempt is made to account for their origins.

In the Pre-array stage settlement began, much earlier than expected, at a time when the face was -19 days (-33.75m) from the array and initially formed a trough 28m wide. The width increased during the development, thereby involving more surface stations. The premature onset of movement may have been due to the presence of the organic alluvium just above the tunnel soffit level (Figure 2.1).

At -4 days (-8.53m) from the array the uplift of all the settlement stations coincides with the two week hold-up after gas was stated to have been detected. During this time, the face was timbered up as during a normal weekend and the breasting boards were held in place by

four hydraulic rams projecting forwards from the shield. A combination of possibly excessive pressure on the face from the rams and the proximity to the array probably caused the reversal of the established settlement.

It is debatable whether the uplift was permanently subtracted from the maximum settlement or only temporarily subtracted and the settlement rate subsequently increased until equilibrium was restored. For the purposes of this thesis the latter was assumed to be the case. Some evidence of the instability of the alluvium can be seen at -3 days (-6.71m) in Figure 4.3. It is unlikely that the readings exceed an accuracy of $\pm 0.2\text{mm}$, therefore the ground surface must be oscillating as a result of settlement and heave, the latter being caused by the advance of the tunnel shield. The oscillation appears to take place between two envelopes, the upper envelope has been taken as the main profiles of settlement, the lower envelope is dotted in to show its relationship to the main profiles. The ground surface in the line of the array shows a particular facility for heave when the tunnel face is between -9m and -4m from the array.

The contours of surface settlement (Figure 4.4) further illustrate the uplift due to the two week hold-up and also show the limits of influence of the tunnel upon the surface settlement ahead of the tunnel face. The contours in front of the face show initially a zone of approximately equal width to the tunnel which settled more rapidly than the rest of the trough until such time as the face came within -2 days (-4.27m) of the array. This could be a result of the high face-take of about $0.82\text{mm}/\text{hour}$ which was not fully distributed over the trough (see Appendix 1). The face-take was estimated from the volume of ground lost at the time when the tunnel reached the array (Figure 4.8a).

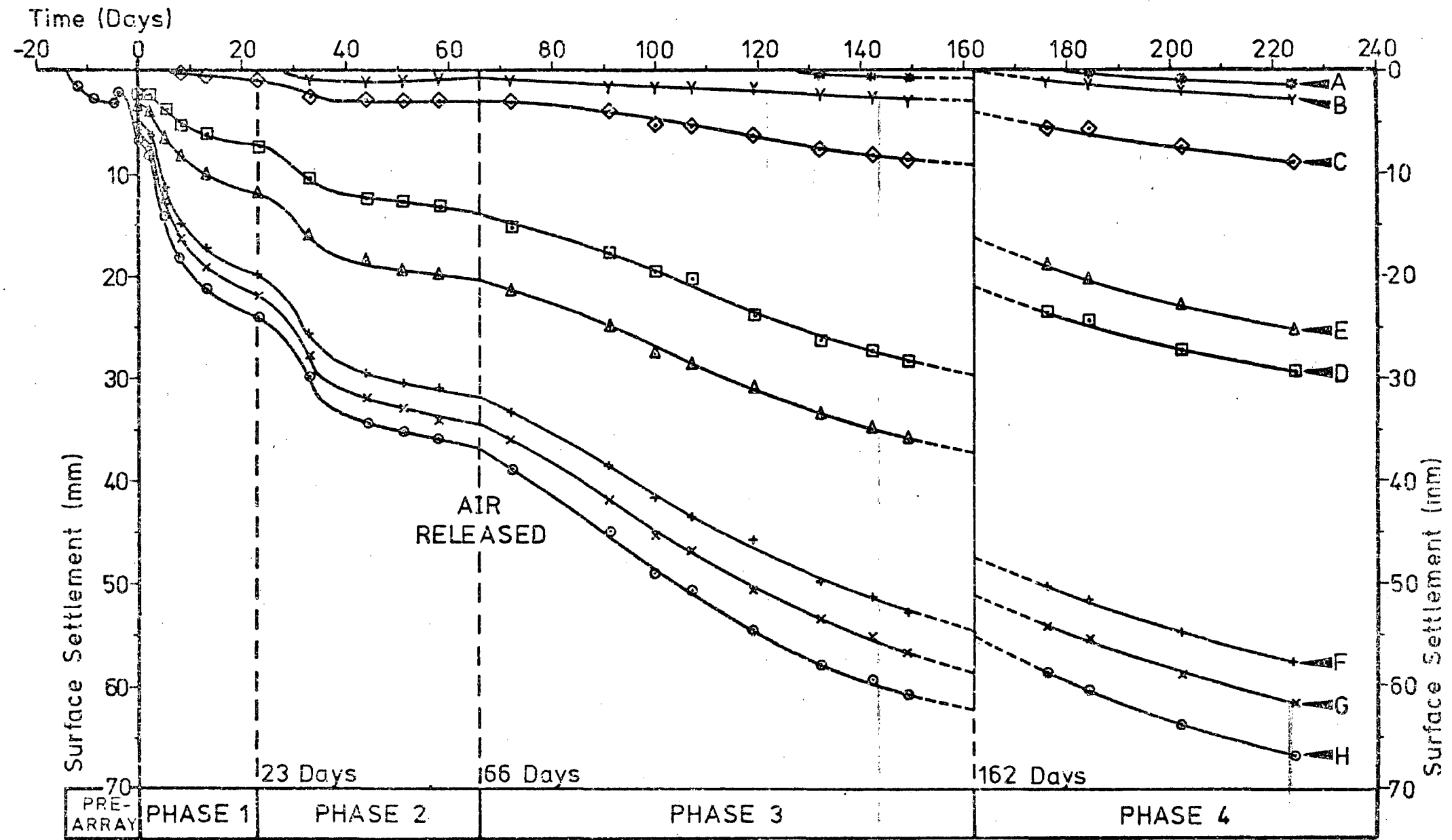


Figure 4.2: DEVELOPMENT OF SURFACE SETTLEMENT

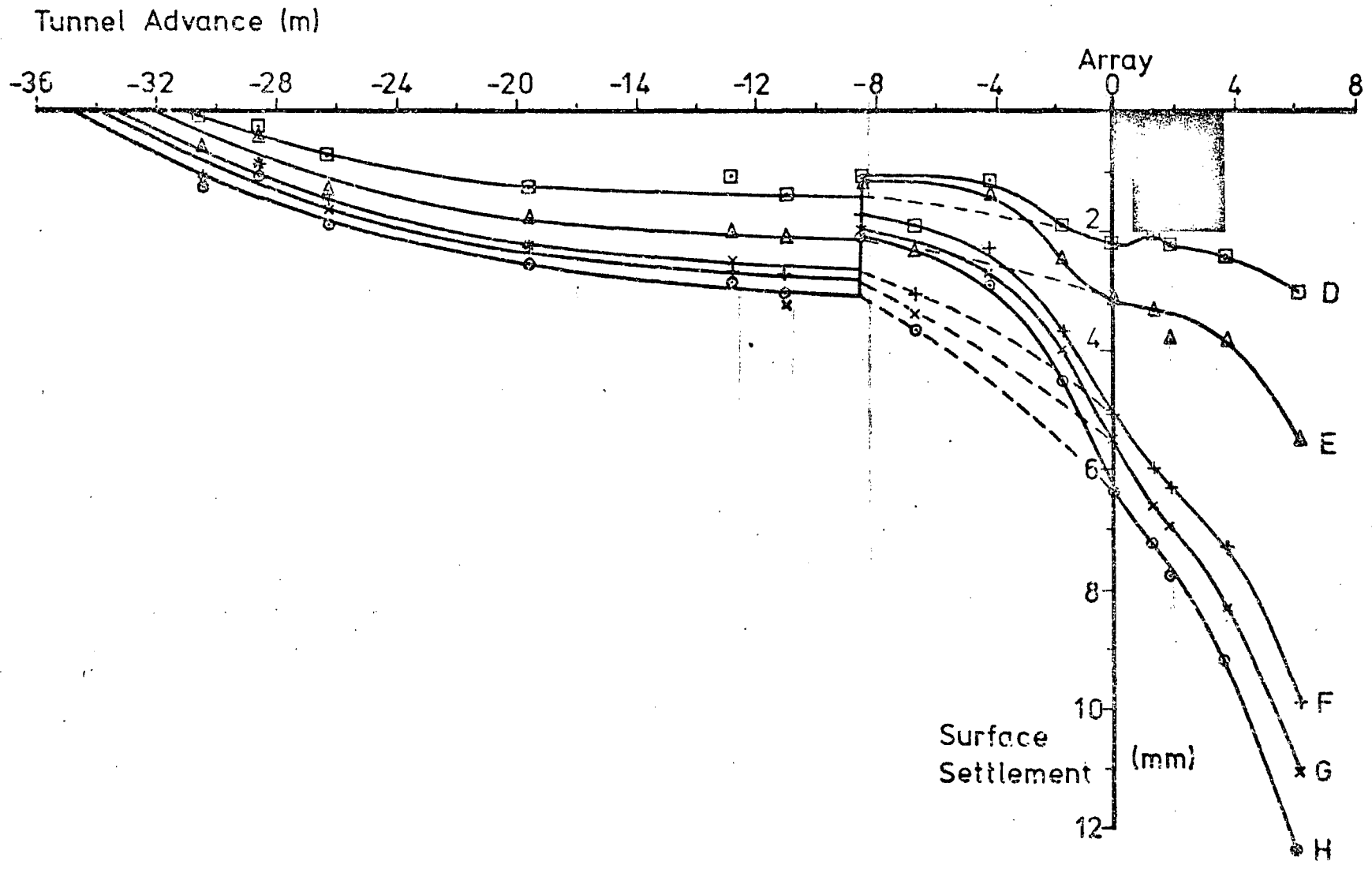


Figure 4.3: DETAIL OF PRE-ARRAY SURFACE SETTLEMENT

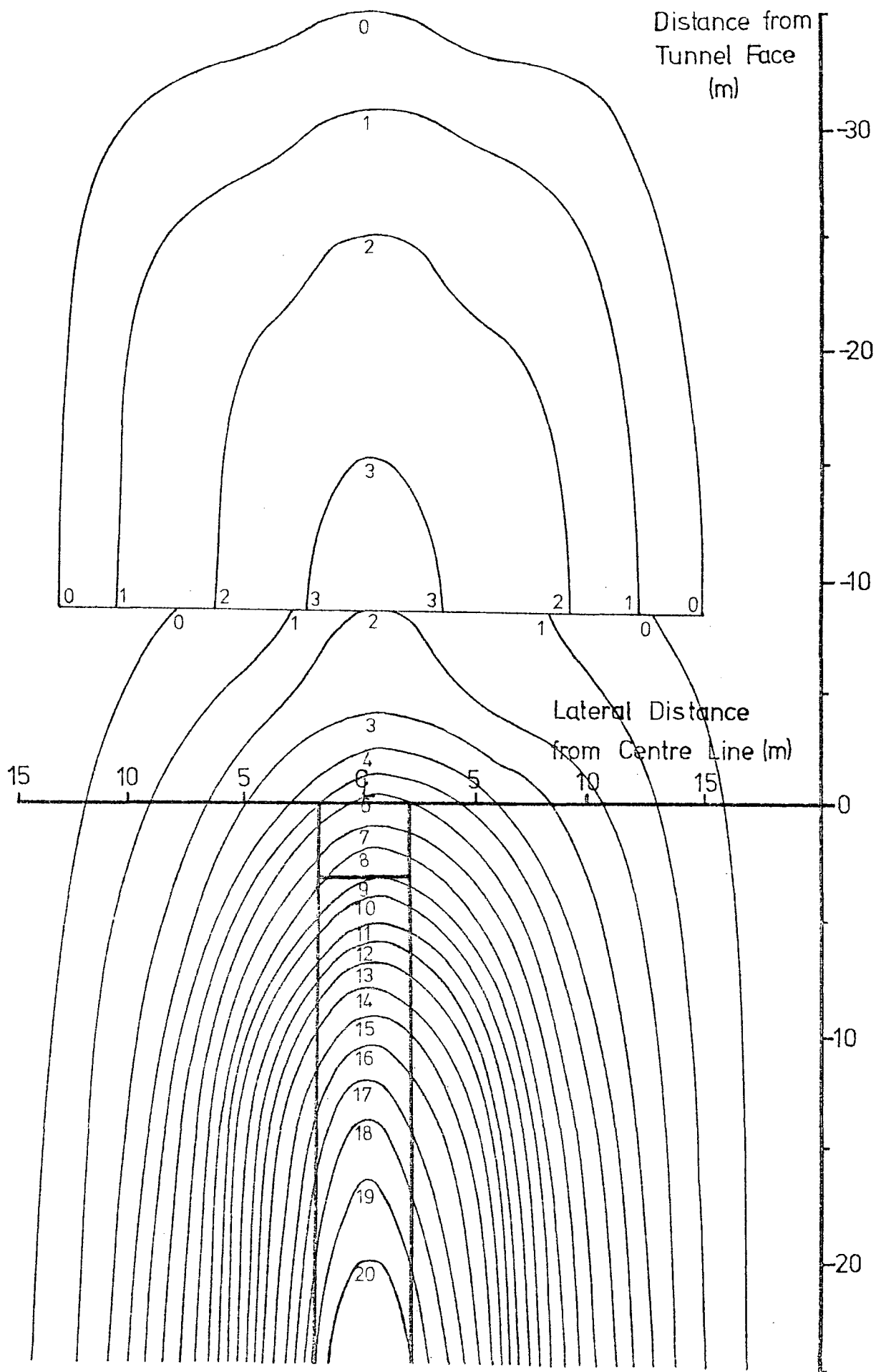


Figure 44: CONTOURS OF SURFACE SETTLEMENT (mm intervals)

This requires the assumption that the volume of lost ground was entirely due to face-take, although it is probable that some post-shield ground losses are included in the value of 0.32mm/hour. The value can therefore only be regarded as approximate. The boarding up of the tunnel face at weekends prevented the in situ measurement of face intrusion.

Extrusion tests were performed by N. El-Naga upon samples from axis depth in borehole 3 to find the change in lateral extrusion rate through a 10mm hole for increasing vertical stress. During these experiments the rates of extrusion of the alluvium were measured under constant stress and the results obtained were extrapolated to include the overburden pressure operative at Willington Quay. This value of 238 kN/m^2 was reduced by the air pressure of 90 kN/m^2 to 148 kN/m^2 and gave an equivalent extrusion rate of 6.1mm/minute or 366mm/hour. The result is obviously much higher than what was actually operating in the tunnel face and points to the limitations of the extrusion test for soft silts and clays. Also the sample may have been disturbed during collection or may have had an abnormally low shear strength. Alternatively, the shear strength may have been reduced in the tunnel face by the compressed air draining the alluvium, although it is unlikely that this would account for the discrepancy.

The post-array stage typically accounted for the bulk of the settlement which occurred. The settlement has been divided into several phases of movement which can be broadly attributed to events which occurred in and around the tunnel. Immediately after the array was reached a significant decrease in the rate of settlement was observed (Figure 4.3), particularly at stations D and E. The feature may be due to heave, or alternatively it may be caused by the presence of the shield below the array providing support to the ground. The

effect persisted until the shield had passed beyond the array suggesting the latter to be the case.

The rapid settlement which followed must have been largely caused by compression of the grout and by the closure of voids left by the grouting process. The ground was beginning to stabilize when the settlement rate suddenly increased again for a short period, after which the slower rate of movement was resumed. No suitable explanation for this second phase has yet been found. The site records show that there was no change in the air pressure in the drive during this period and sub-surface results show that the characteristics of the movement were the same as the first phase of movement. It is possible, therefore, that high pressure backgrouting at 690 kN/m^2 (100 lb/in^2), carried out at this time in the vicinity of the array disturbed the ground sufficiently to produce the movement.

After a period of slow settlement the rate again increased to form a third phase, coinciding with the reduction and final release of air pressure in the drive thereby allowing porewater to drain into the tunnel. This resulted in consolidation of the ground which in turn caused the settlement seen at the surface. When the settlement is plotted against log time (Figure 4.5) a straight line, characteristic of primary consolidation, is produced from this phase of the profile. Figure 4.5 is confined to post-array settlement in order to allow comparisons to be made with the time scale of Figure 4.2.

The prolonged movement caused damage to surface structures near to the array and, as a result of this, a brick wall adjacent to the array had to be demolished before consolidation was completed (Plates 2). The unloading of the ground, a reduction of 50.19 kN/m^2 along the base of the wall, coincided with extensive uplift at the ground surface with a maximum of 7mm on the centre line and would appear to be the cause of the

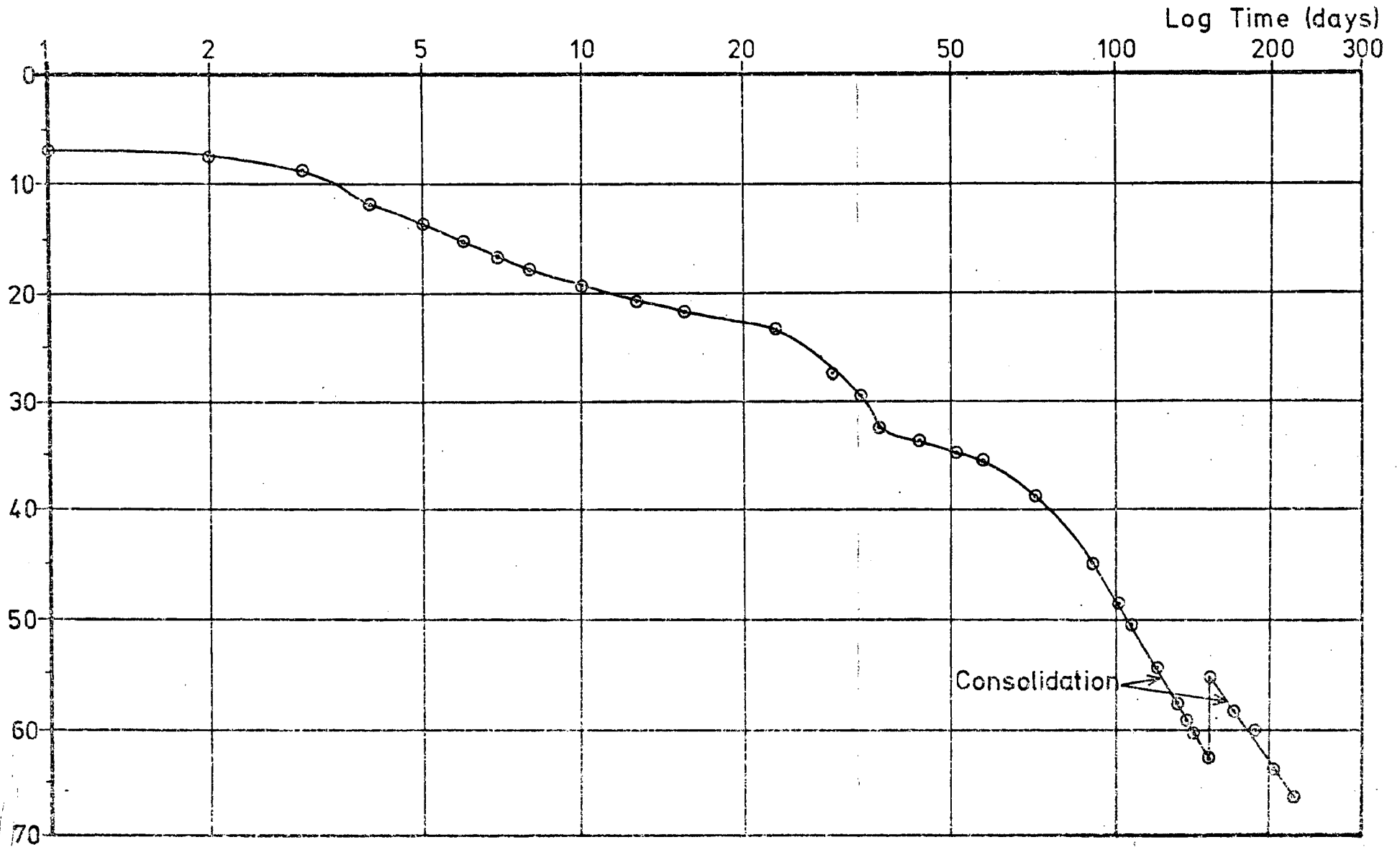
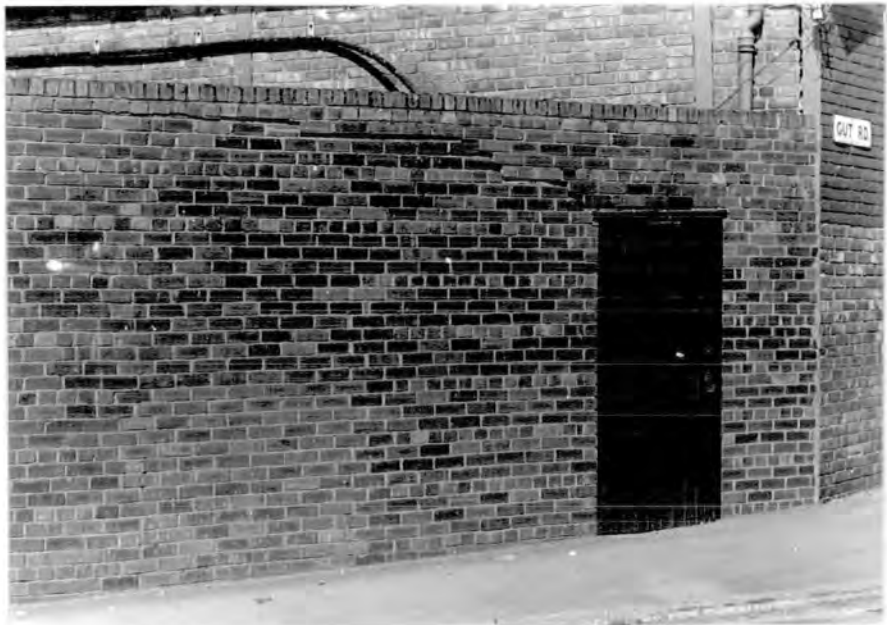
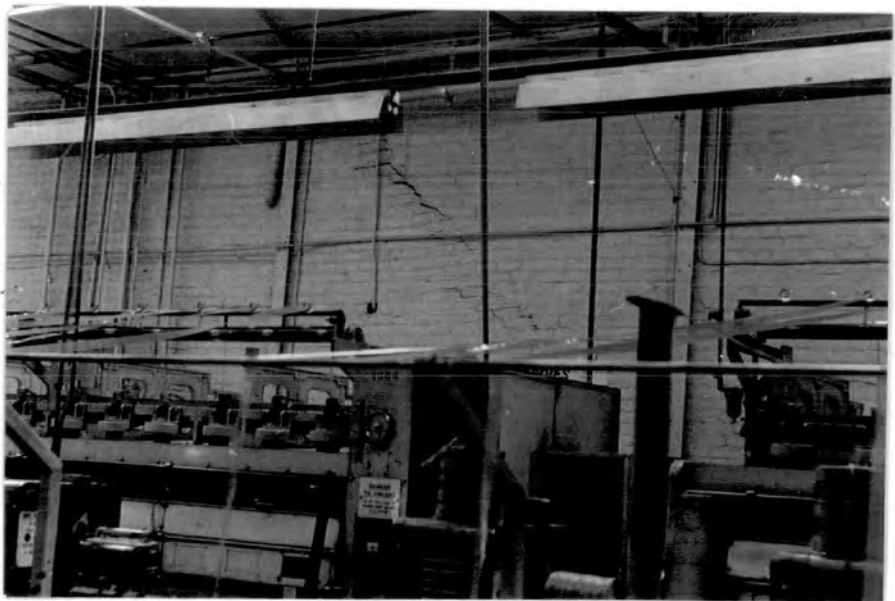


Figure 45: SURFACE SETTLEMENT vs. LOG-TIME PLOT FOR STATION H ABOVE TUNNEL CENTRE LINE



Plates 2a and 2b : STRUCTURAL DAMAGE CAUSED BY SETTLEMENT



Plates 2c and 2d : STRUCTURAL DAMAGE CAUSED BY SETTLEMENT

uplift. The renewal of consolidation after this formed the fourth and final phase recorded. At the time of writing, the process was still taking place and, if the settlement history so far is any indication, movement will continue for some considerable time.

Surface settlements were also recorded by the contractors at several stations located inside the rope factory. Examination of the maximum values for stations above the centre line at 224 days show that much larger settlements developed under the factory (Figure 4.6). The feature may have several causes, most important of which must be the additional weight of the structure upon the ground surface increasing the overburden pressure and additionally the presence of vibrating machinery inside the factory. Both of these factors would greatly facilitate settlement during the consolidation phase. Consolidation in turn was possibly aided by the sand and gravel deposits located in the middle of the channel. These deposits, having a much higher permeability than the alluvium, can be expected to provide much more rapid drainage to the middle of the channel (located under the factory) and hence more rapid consolidation.

The development of the transverse settlement profiles is shown in Figure 4.7 with profiles given at 20 day intervals from zero to 220 days advance beyond the array. The most notable feature of these is the widening of the trough from 30m to 45m during the second phase of rapid settlement. Similarly, during the consolidation phases the trough widened to almost 60m. In addition to Figure 4.7 four transverse profiles are included with Lateral Displacement and Strain profiles in Figures 4.8a to 4.8e. These were selected to illustrate the effects of the phases of movement upon the ground surface and were located at the time when the instrument array was reached, i.e. zero days, and thereafter at 23, 51, 149 and 224 days advance beyond the array

respectively. Overlays to these figures give comparisons with Gaussian Distribution or Error Curves given by:

$$S_s = S_s \max \exp.(-y^2/2i^2)$$

where y is the transverse distance from the tunnel centre line and S_s is the surface settlement at that point, i is the distance from the centre line of the point of inflexion of the settlement profile, (all three being along a line normal to the direction of tunnel advance) and $S_s \max$ is the maximum surface settlement.

The value of i is found from the settlement at the point of inflexion where the settlement $S_s = 0.606 S_s \max$. The area under the Error Curve is found from:

$$A = 2\pi.i S_s \max$$

The shapes of the Error Curves and their areas thus calculated compare closely with the measured areas of the troughs in Figures 4.8a to 4.8e and the results are included on the diagrams. The Error Curve is therefore a good approximation of the settlement profile developed in this case history.

There is a marked difference of up to 3.5mm between the opposite sides of the transverse profile in Figures 4.8a to 4.8c. Stations A to G settled more rapidly than stations I and J (Figure 3.2). This may be due to the closer proximity of vibrating factory machinery to stations A to G than the latter two, thereby causing more rapid settlement on that side of the array. Alternatively, the difference may be due to variation in the resistance of the road and path surface to deformation by settlement. The discrepancy persisted until the phase of consolidation began when it was reduced to less than 1mm (Figures 4.8d and 4.8e).

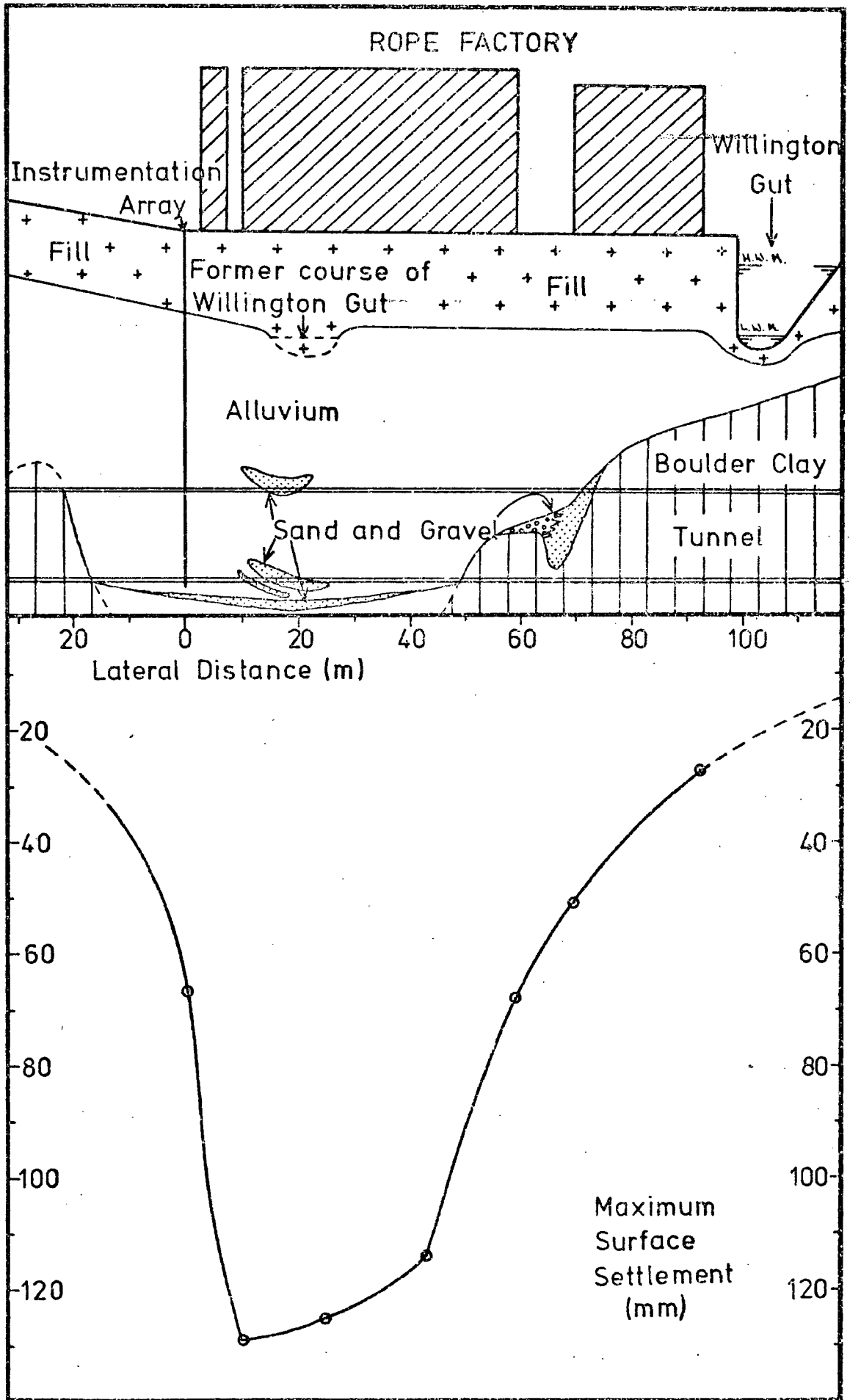


Figure 4.6: LATERAL VARIATION OF MAXIMUM SURFACE SETTLEMENT (224 DAYS)

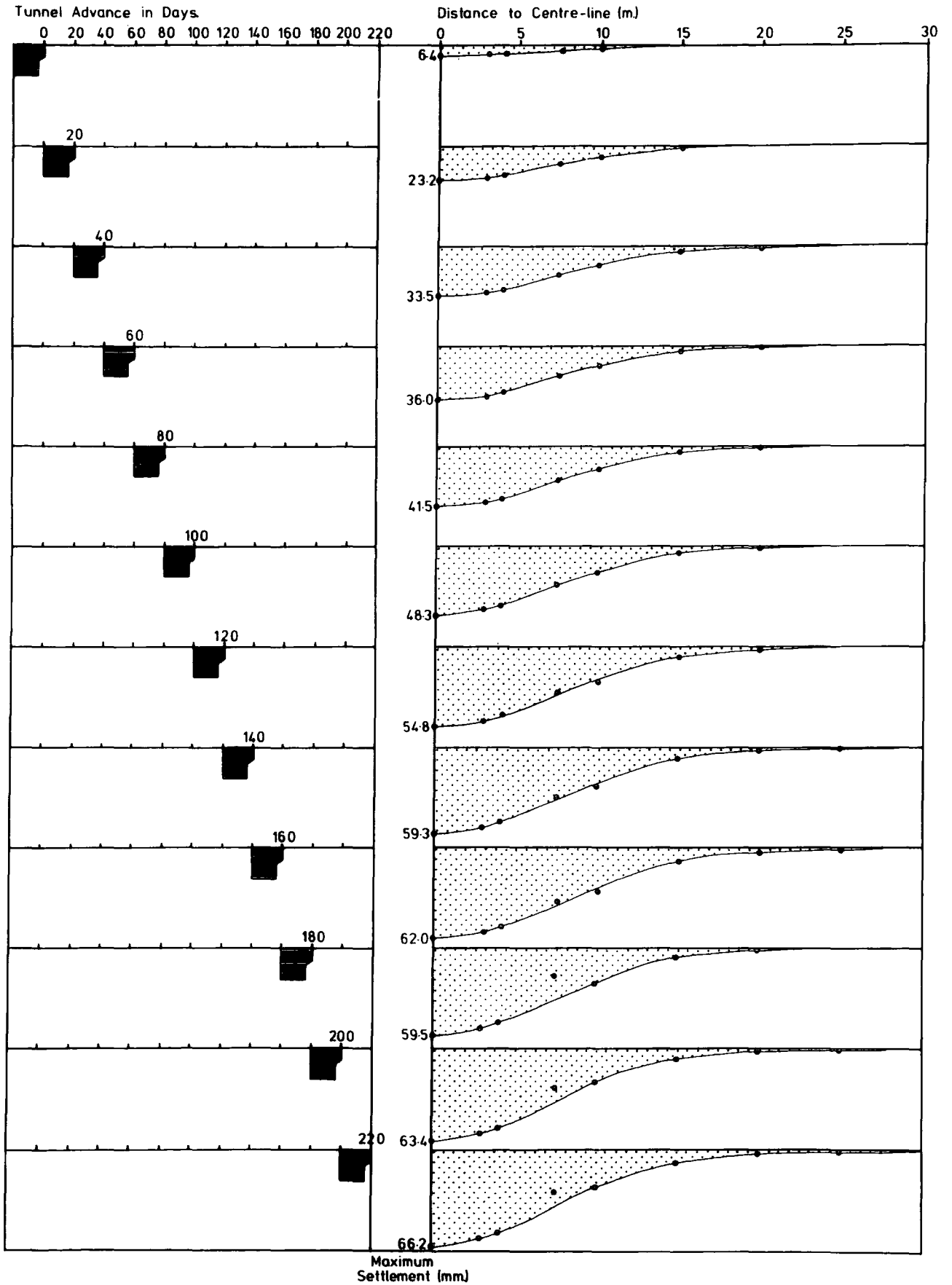


Figure 4.7: TRANSVERSE SURFACE SETTLEMENT PROFILES

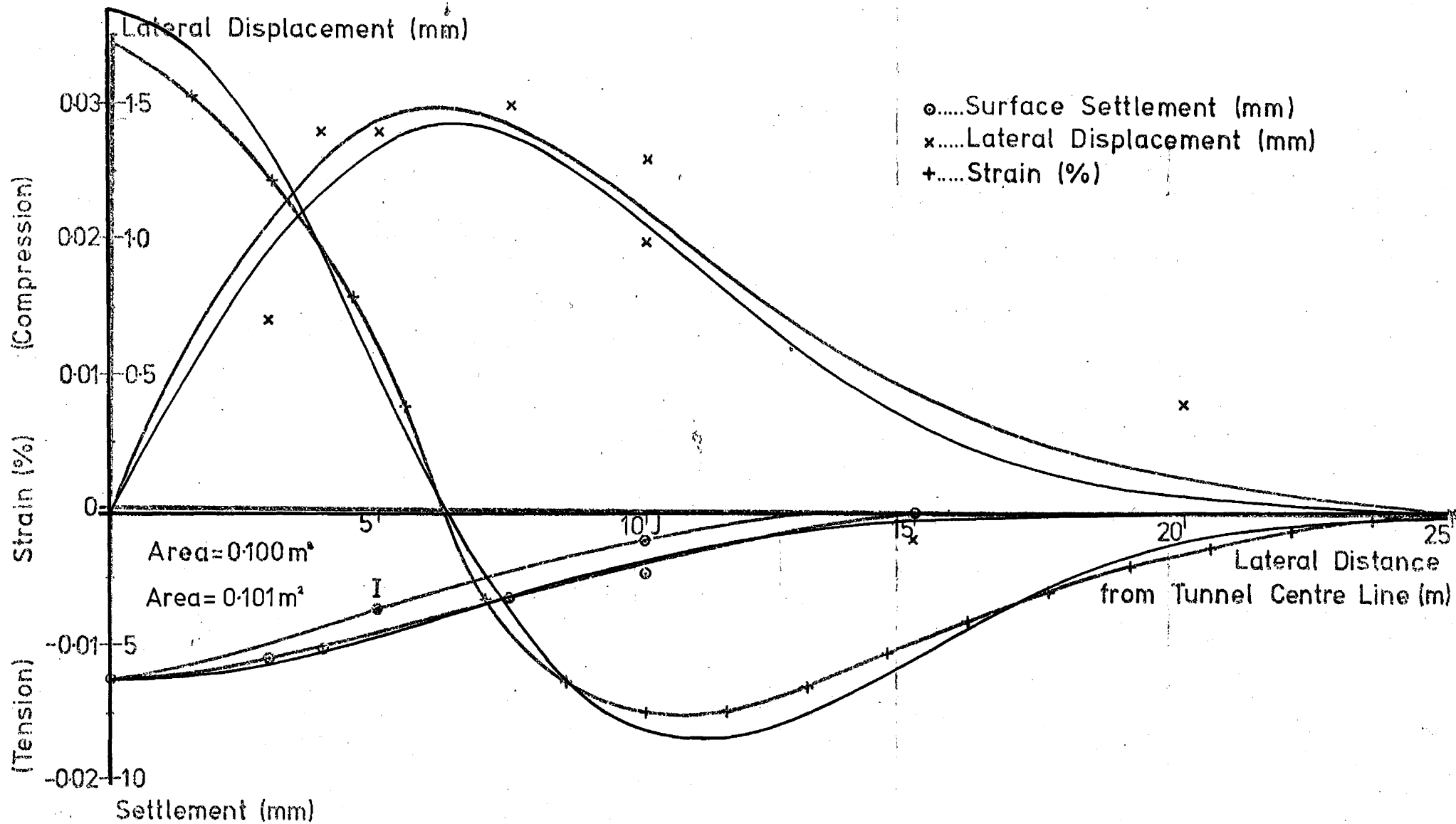


Figure 4.8a: THEORETICAL AND MEASURED SURFACE SETTLEMENT, LATERAL DISPLACEMENT AND STRAIN TUNNEL FACE AT ZERO DAYS FROM ARRAY

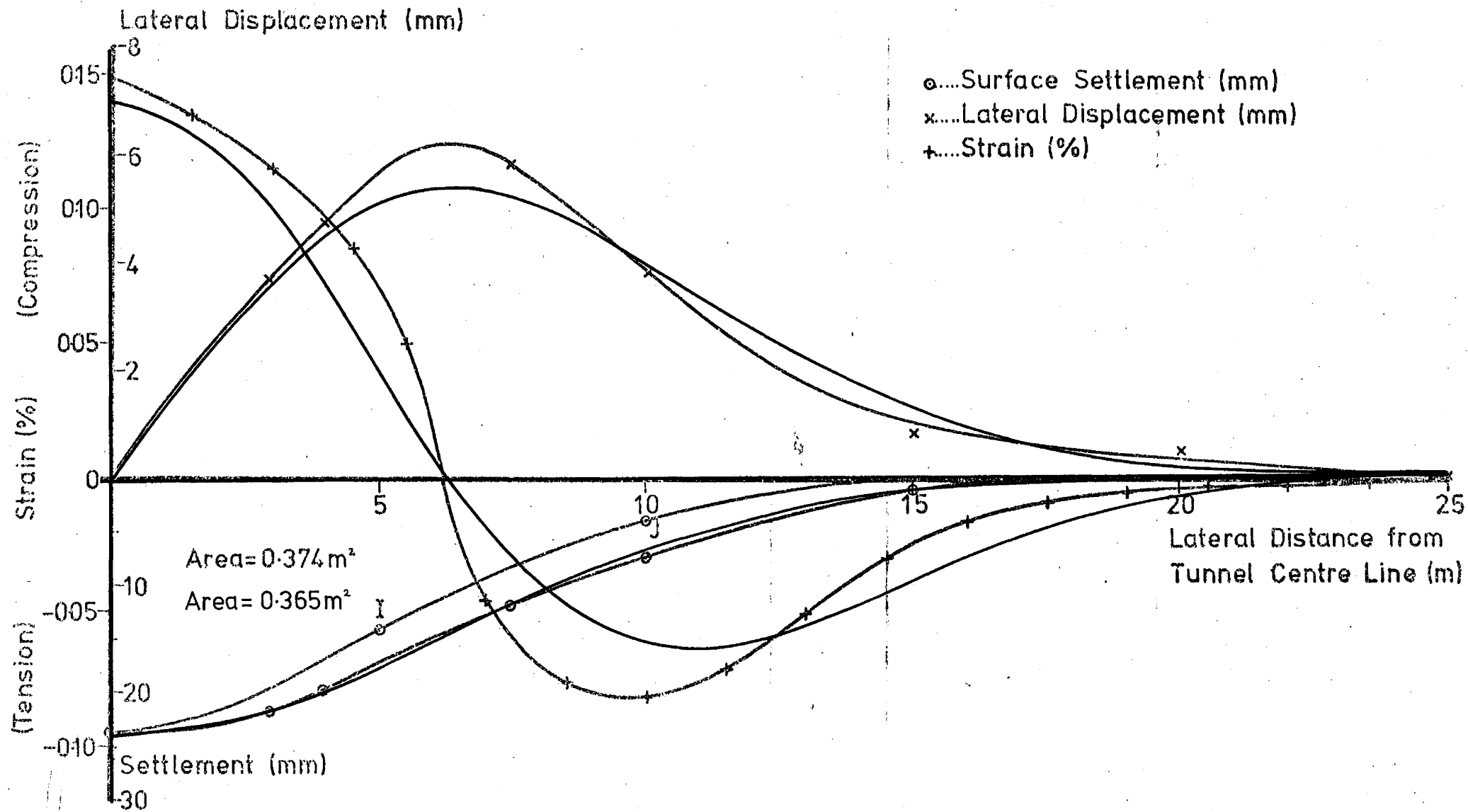
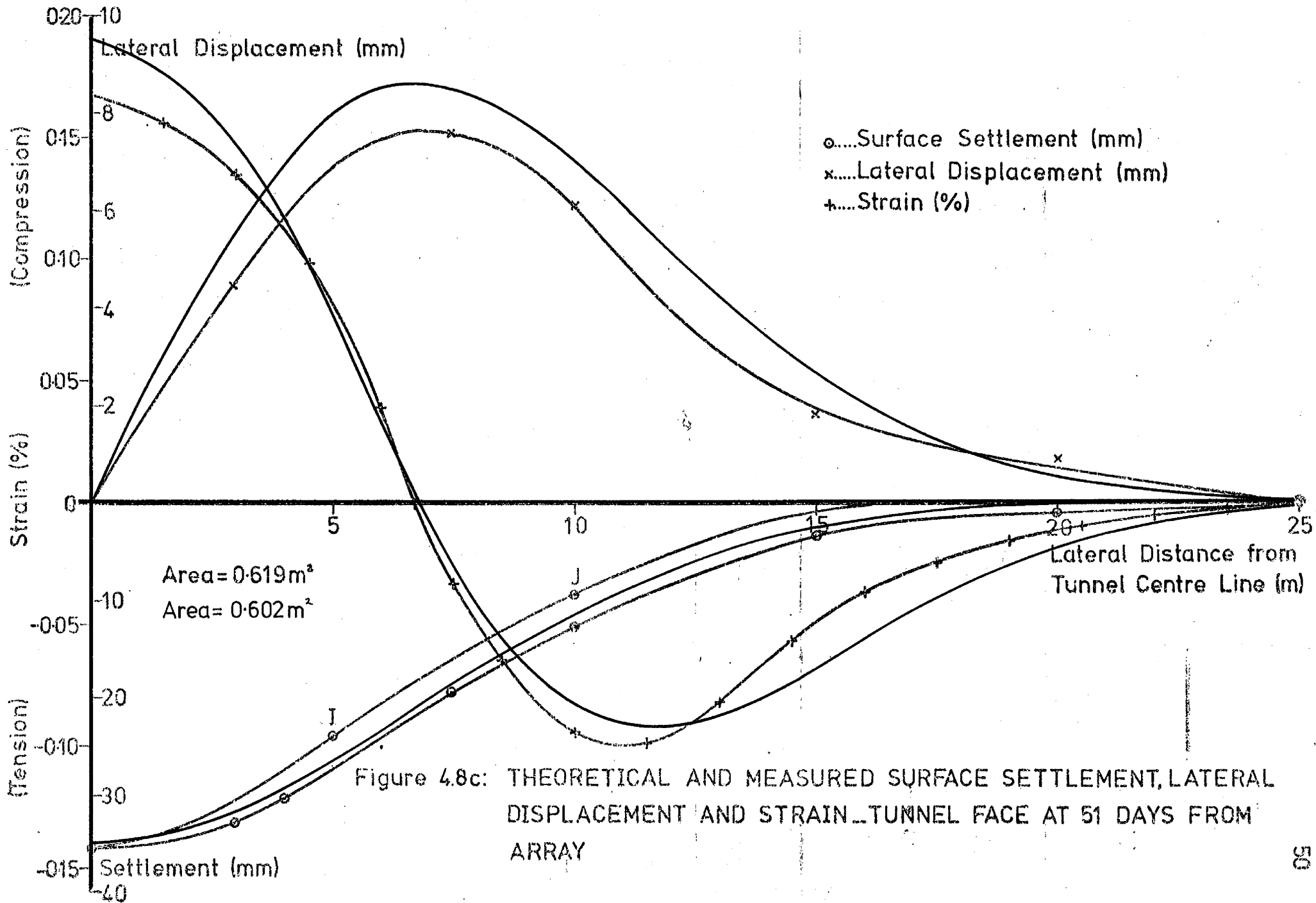


Figure 4.8b: THEORETICAL AND MEASURED SURFACE SETTLEMENT, LATERAL DISPLACEMENT AND STRAIN_TUNNEL FACE AT 23 DAYS FROM ARRAY



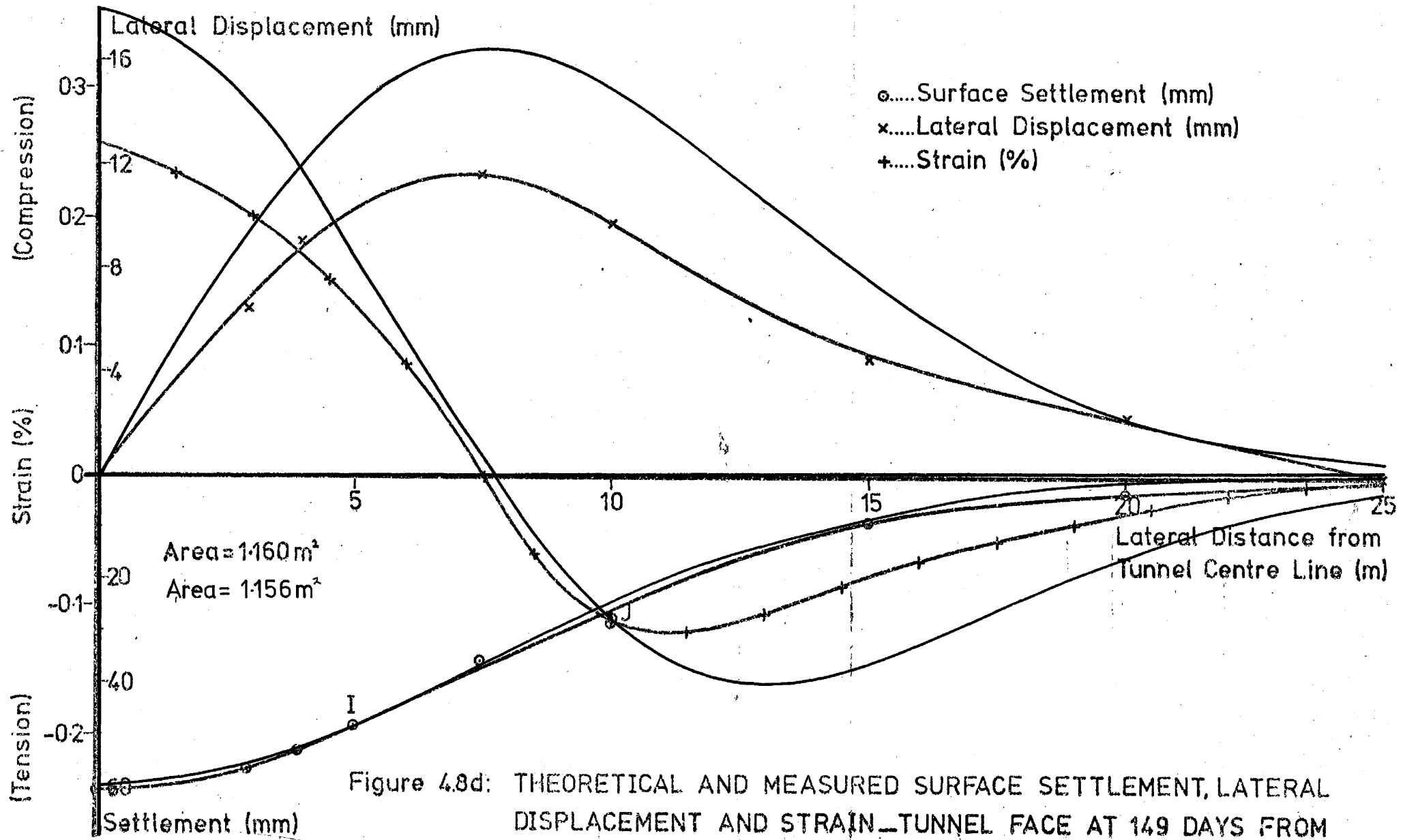


Figure 4.8d: THEORETICAL AND MEASURED SURFACE SETTLEMENT, LATERAL DISPLACEMENT AND STRAIN_TUNNEL FACE AT 149 DAYS FROM ARRAY

4.3 Surface Horizontal Movements.

Five profiles of the horizontal movement of the ground surface towards the centre line have been selected and included with the transverse profiles of the trough in Figures 4.8a to 4.8e. The original data for these profiles were normalised with respect to station A in order to remove variations, caused by expansion and contraction of the steel tape used for the measurements, under the varying atmospheric temperatures encountered in the field. Maximum movement in each case coincides with the point of inflexion of the transverse profiles, making that point the boundary between tension and compression in the ground surface. This is shown by the percentage strain plots included in the same diagrams.

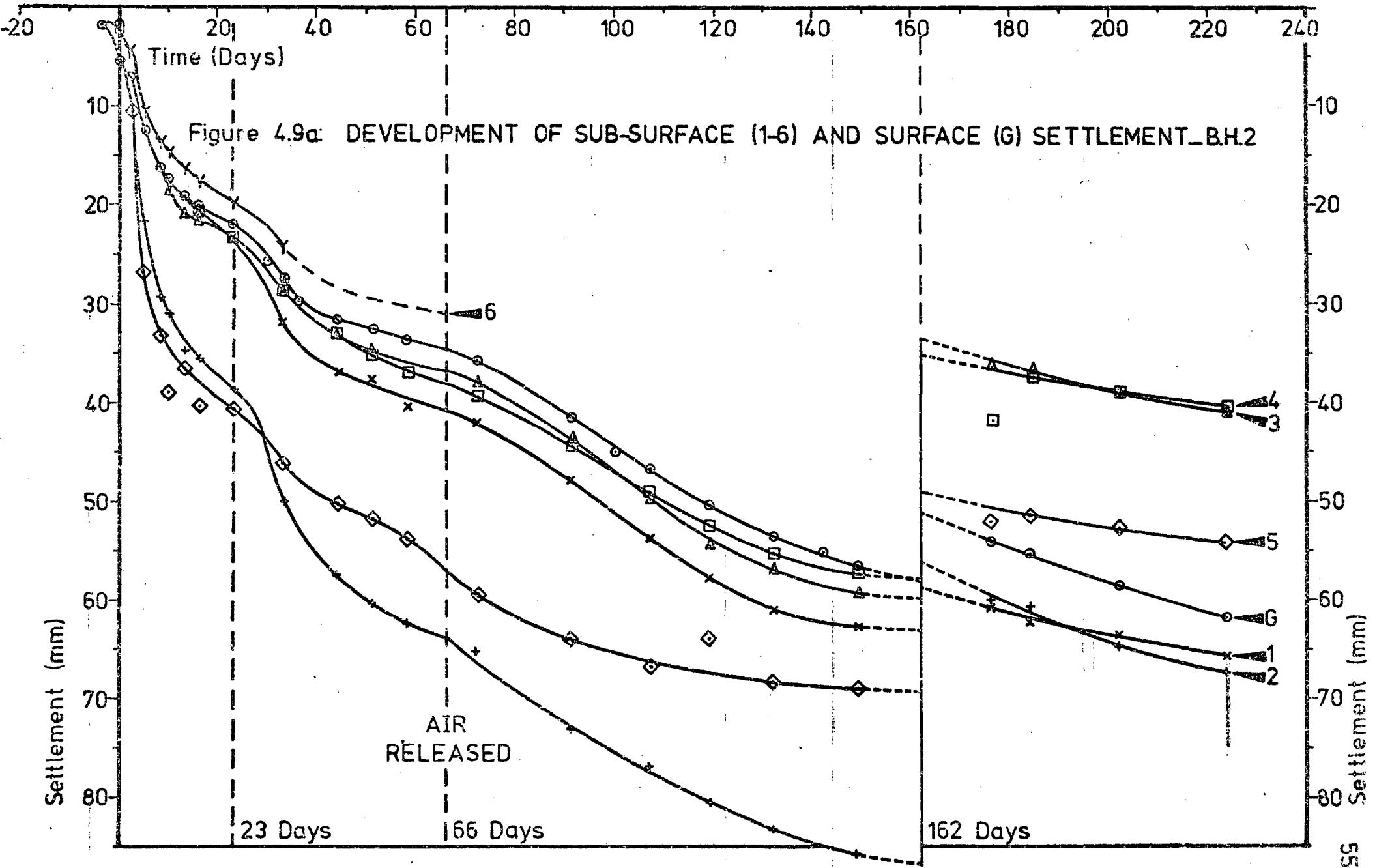
In the overlays the theoretical profiles corresponding to the measured profiles of surface settlement, lateral displacement and strain are shown. These are calculated using a stochastic model for ground settlement and show good correlation with the measured profiles (N.H. Glossop, 1976). The measured profiles and strain curves in Figures 4.8a to 4.8c, that is movement caused by ground losses at the tunnel, correspond closely with the theoretical profiles. However, in Figures 4.8d and 4.8e, where settlement has been attributed to consolidation, the horizontal movements are considerably less than the theoretical values despite the error curves retaining a close agreement with the measured settlement curves. Therefore, the different characteristics of the two processes which caused surface movement have produced different degrees of lateral movement. Initially ground losses at the tunnel caused lateral as well as vertical movement in contrast to

consolidation, which is predominantly a vertical process and caused relatively smaller lateral displacement at the ground surface.

4.4 Sub-surface Settlement

The complex settlement profiles (Figures 4.9a to 4.9c) derived from the magnetic ring results show that movement occurred in the same phases as had been observed at the surface. Not all the profiles are complete for one of two reasons. First, in borehole 1 it was necessary to fill in the lower part of the tube with grout to prevent air leaking out when the tube was cut off just above the soffit level. Unfortunately, the tube was overfilled by the contractor and only the uppermost magnetic ring was accessible. Second, some of the deepest rings in the boreholes became inaccessible before settlement was completed as a result of sediment gradually accumulating in the bottoms of the tubes. This was washed in from the surface during persistent and heavy rainfall in spite of attempts to build temporary "coffer dams" around the heads of the tubes. The sediment reduced the maximum depth to which the reed switch could be lowered. In this way the remaining magnetic ring in borehole 1 became inaccessible before any significant deviation from the surface settlement had been measured.

The results can be clarified somewhat by plotting the maximum settlement against depth (Figures 4.10a to 4.10c). The profiles selected were again at 23, 51 and 149 days of settlement, the movement at zero days was too small to be significant and has not been included. Similarly, no profiles are included after the reversal of settlement at 162 days. This is because the uplift made the profiles irregular and a better representation of the movement can be found in the vector diagrams.



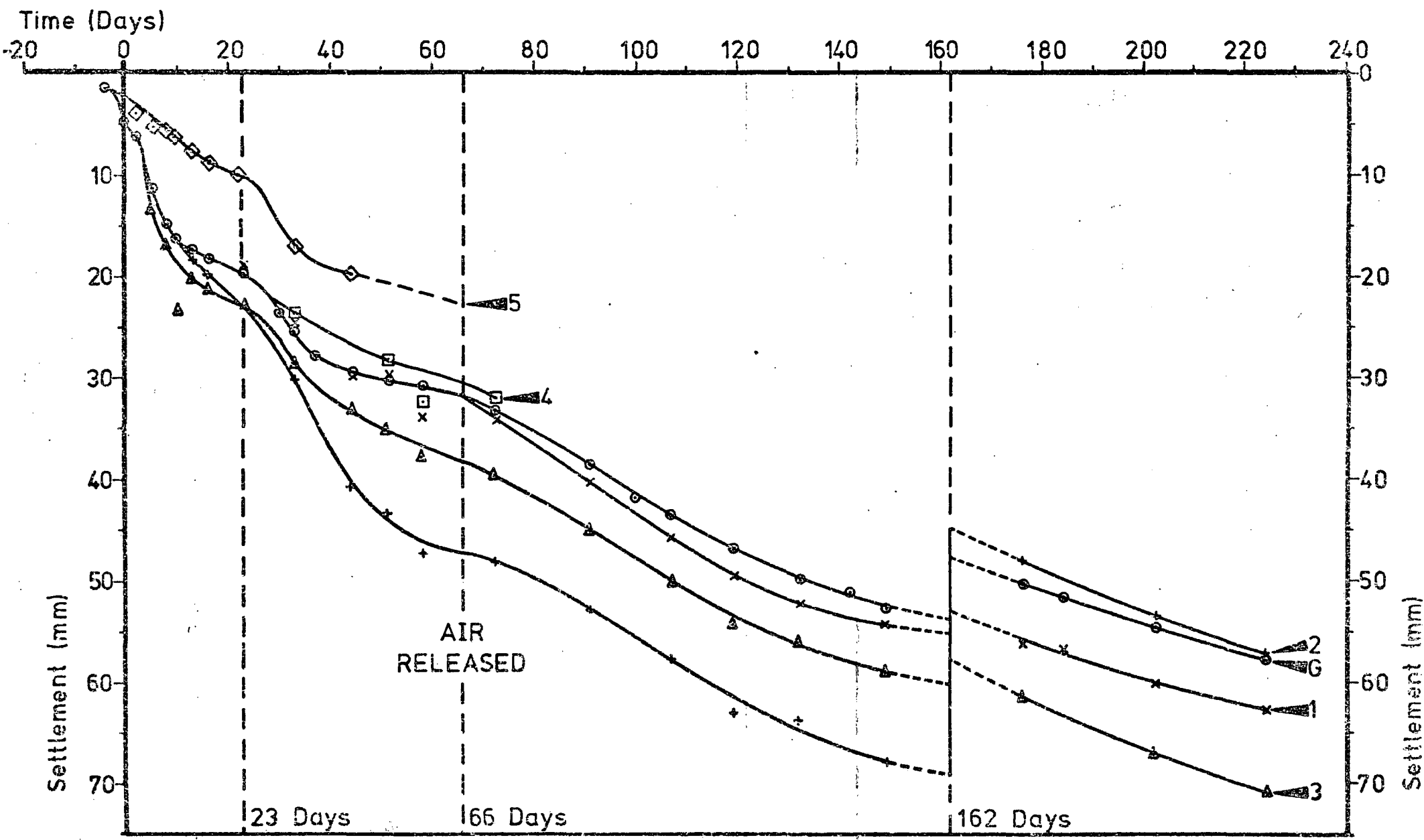


Figure 4.9b: DEVELOPMENT OF SUB-SURFACE (1-5) AND SURFACE (G) SETTLEMENT_BH.3

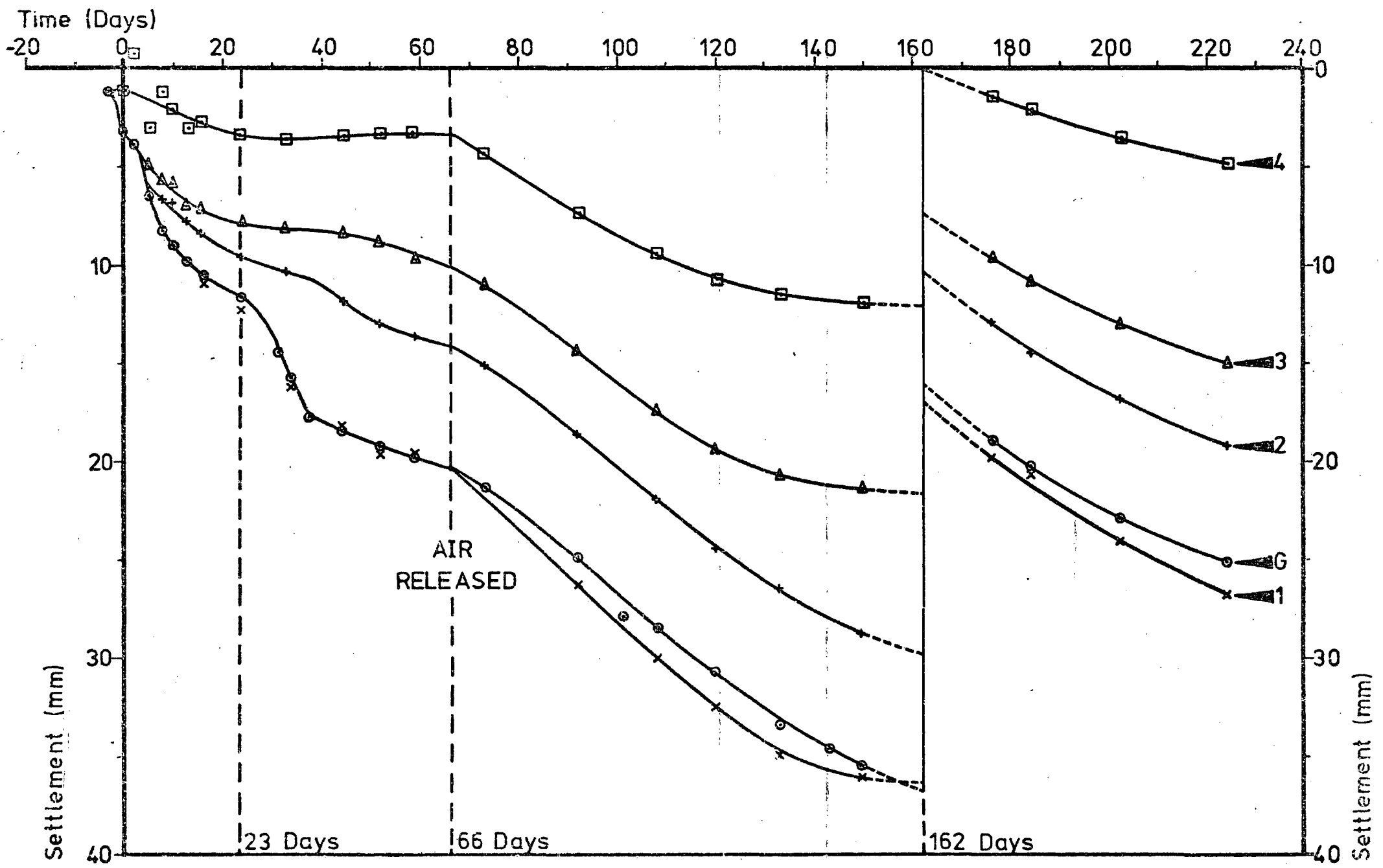


Figure 4.9c: DEVELOPMENT OF SUB-SURFACE (1-4) AND SURFACE (G) SETTLEMENT_BH.4

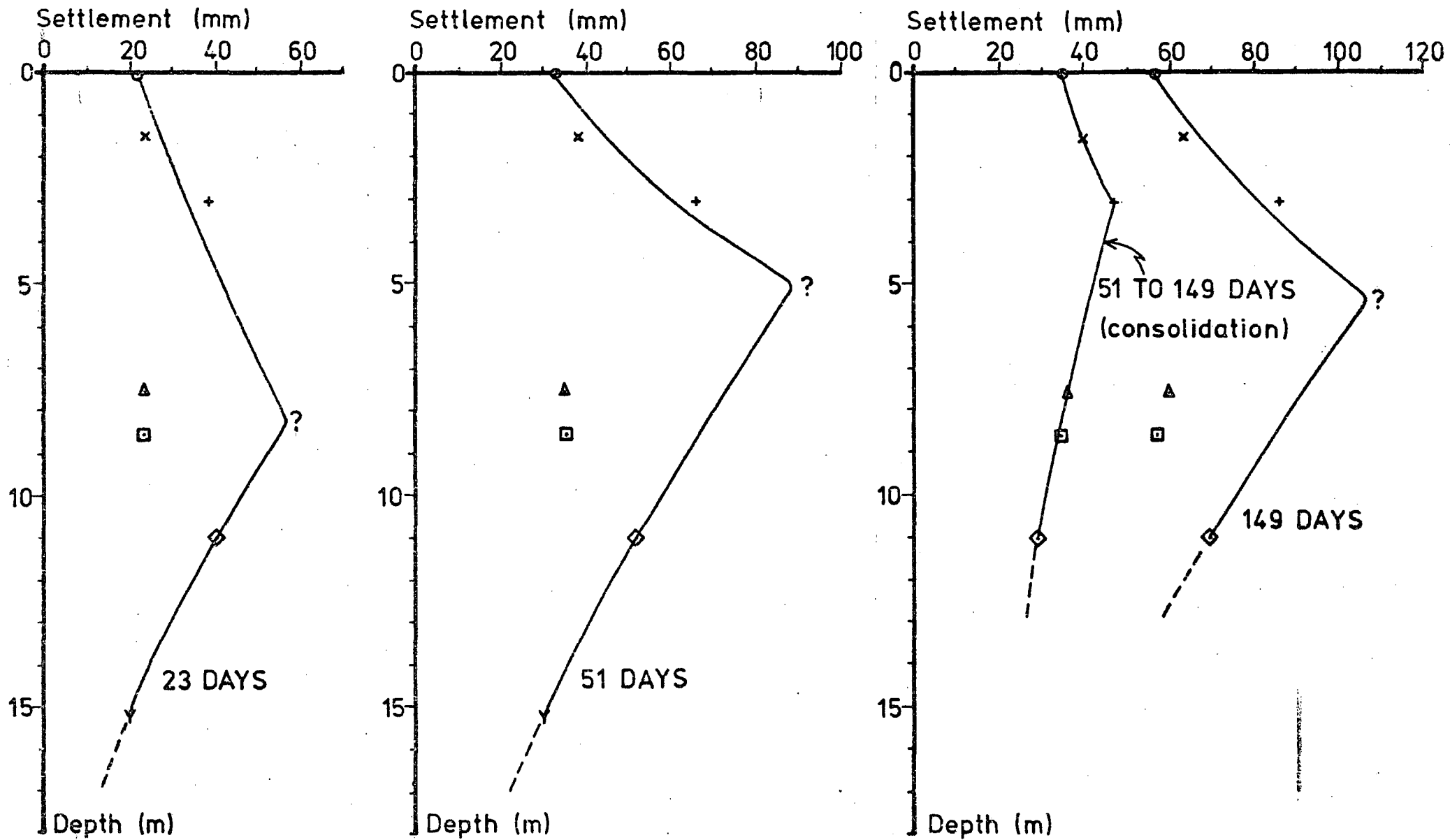


Figure 4.10a: DEVELOPMENT OF SETTLEMENT WITH DEPTH (BOREHOLE 2)

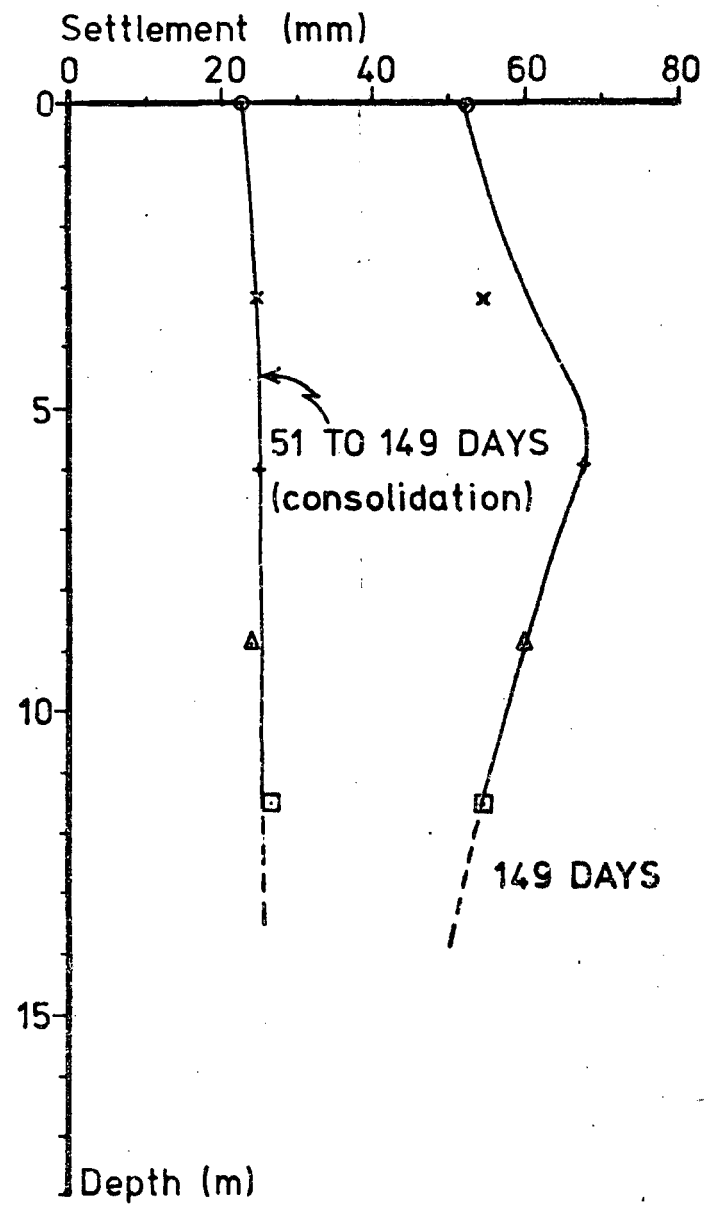
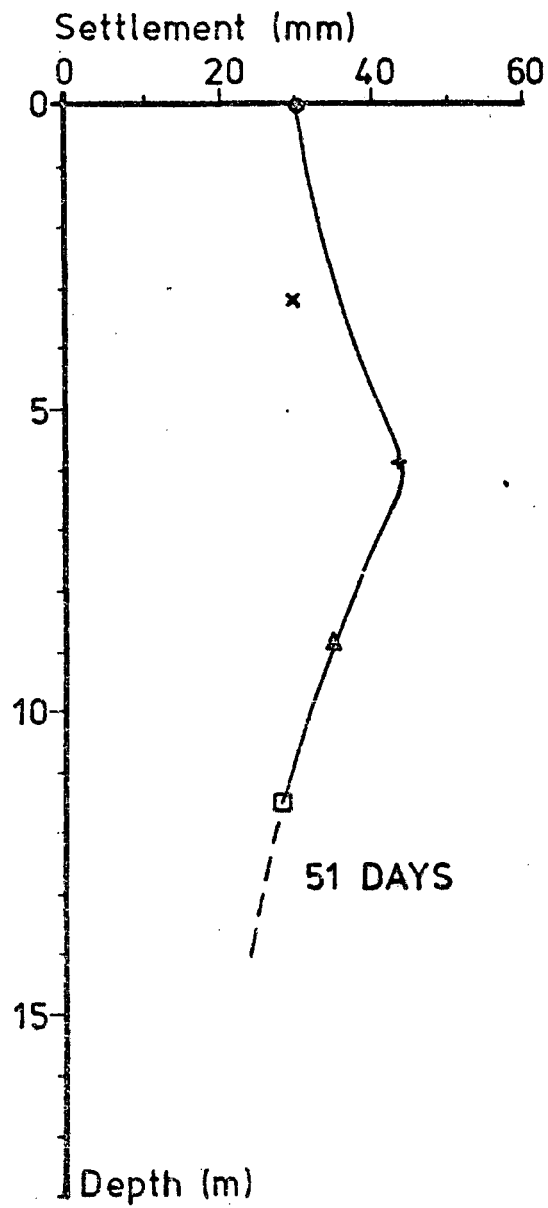
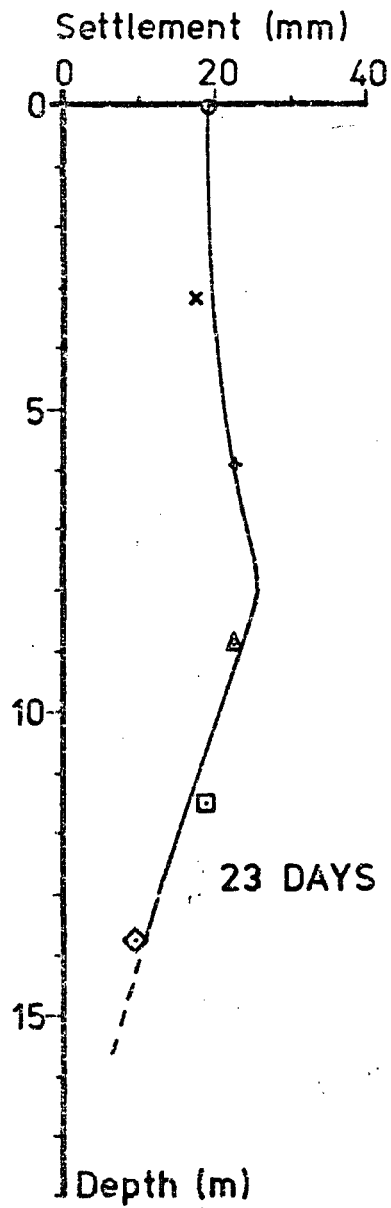


Figure 4.10b: DEVELOPMENT OF SETTLEMENT WITH DEPTH (BOREHOLE 3)

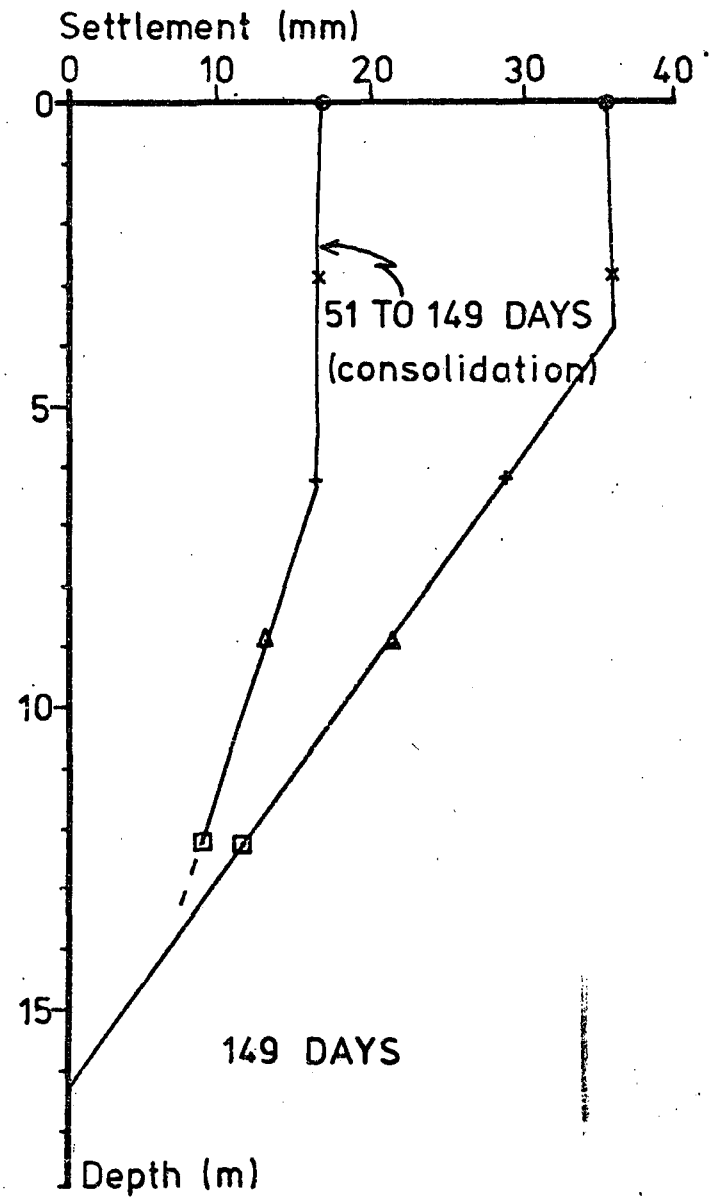
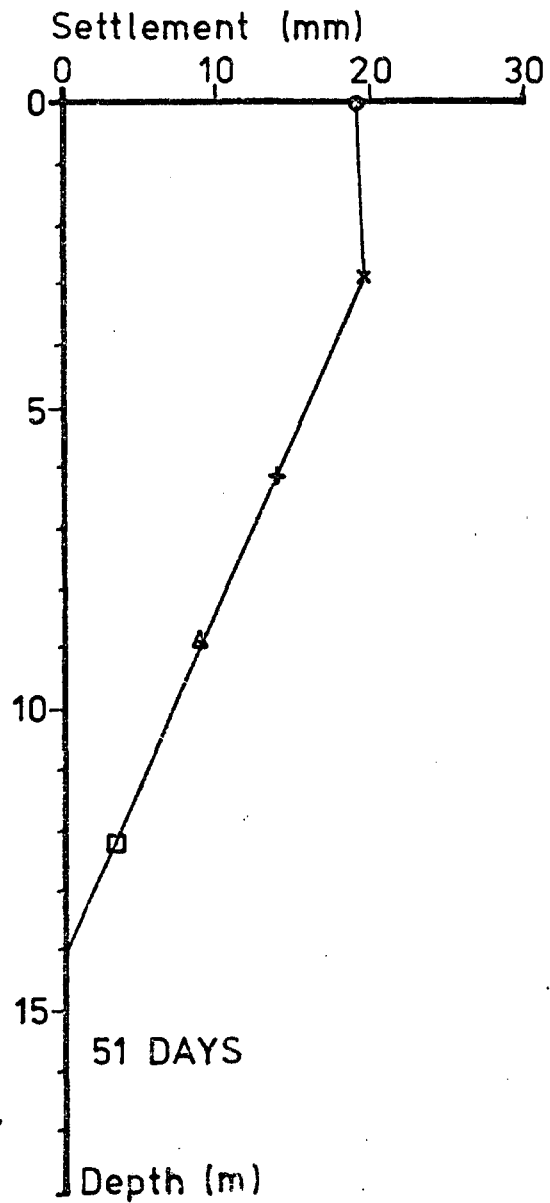
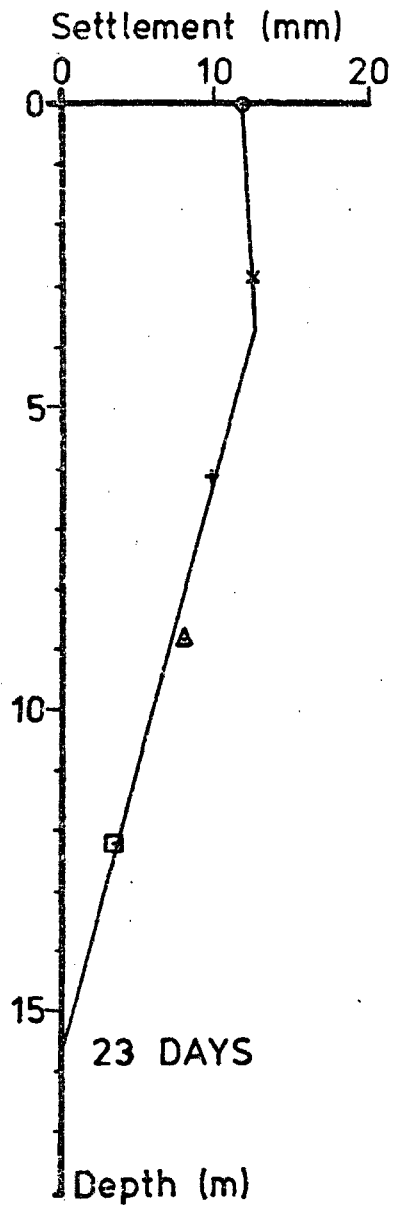


Figure 4.10c: DEVELOPMENT OF SETTLEMENT WITH DEPTH (BOREHOLE 4)

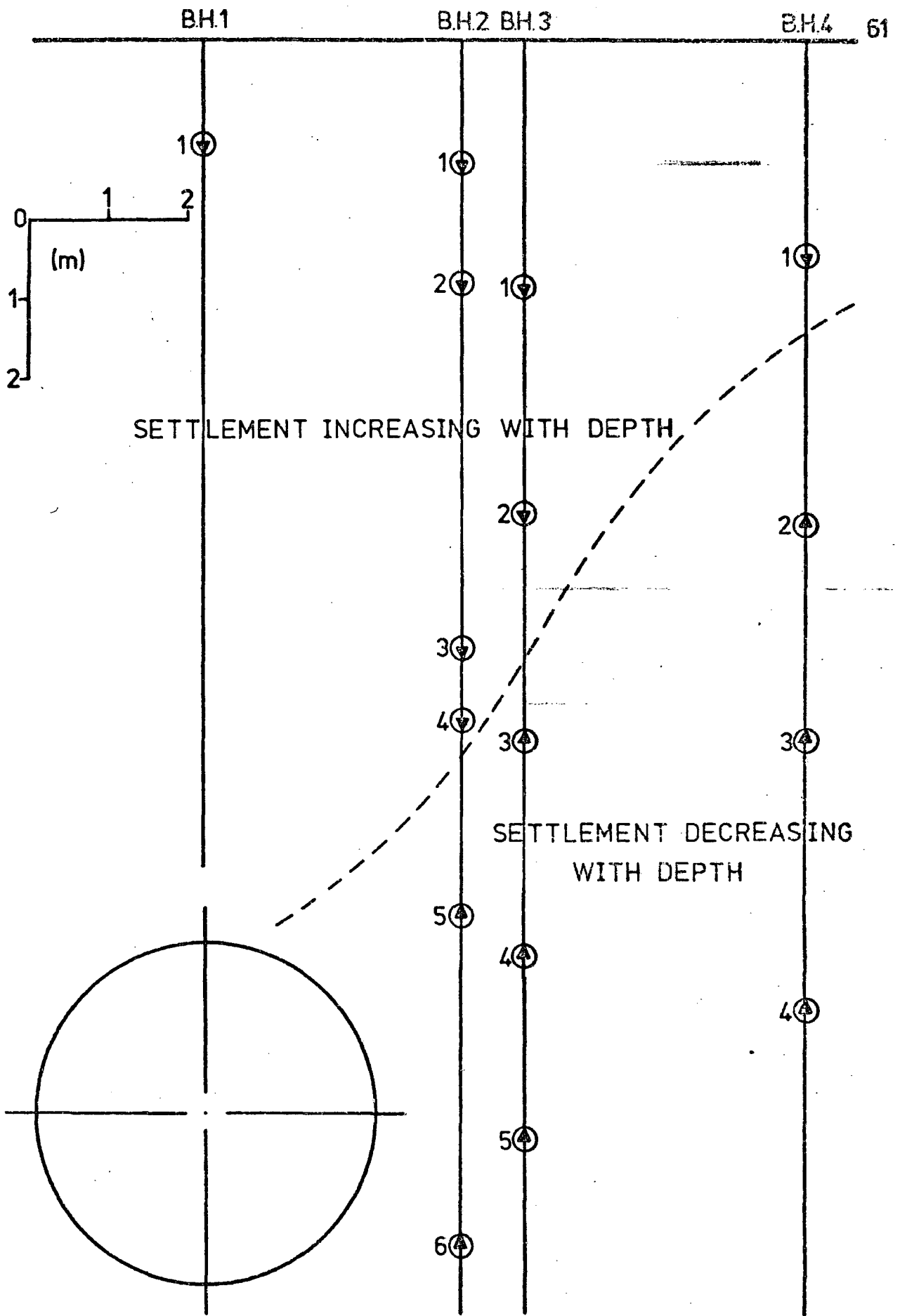


Figure 4.11: LIMIT OF SETTLEMENT (23 DAYS ADVANCE)

In boreholes 3 and 4 all the rings lie close to the profile drawn through them. However, in borehole 2, rings 3 and 4 show a large deviation from the profile and may not have fully taken up the movement of the grout around them. The depths of maximum settlement for each borehole lie on a curve drawn in Figure 4.11. This separates the regions of increasing and decreasing settlement with depth and represents the possible path of a shear failure zone in the clay.

4.5 Sub-surface Horizontal Movements.

The sub-surface horizontal movements are presented as a series of inclinometer profiles taken at regular intervals throughout the case history. The displacements have been calculated in the plane of the array and also in planes parallel to the centre line. These are distinguished by the borehole number with the suffix 1 for profiles parallel to the centre line and 2 for profiles in the plane of the array. Therefore, the profiles for borehole 4 are 4.1 and 4.2 respectively.

The surface displacements for the tops of the boreholes in the plane of the array were measured relative to the centre line. However, the displacements parallel to the centre line were estimated from the relative movements of the upper part of each inclinometer tube. This was necessary in order that vectors of movement could be drawn for planes parallel to the centre line.

In borehole 1 the profiles 1.2 showed no displacement as the tunnel face approached. The profiles for 1.1 however, recorded the displacement of the ground surface as the trough approached and deepened and the face-take around the axis depth for the tunnel (Figure 4.12). Face-take began before -3 days from the array, at which time the face was -6.71m distance. This small movement increased to 3.17mm at 0.7m depth below

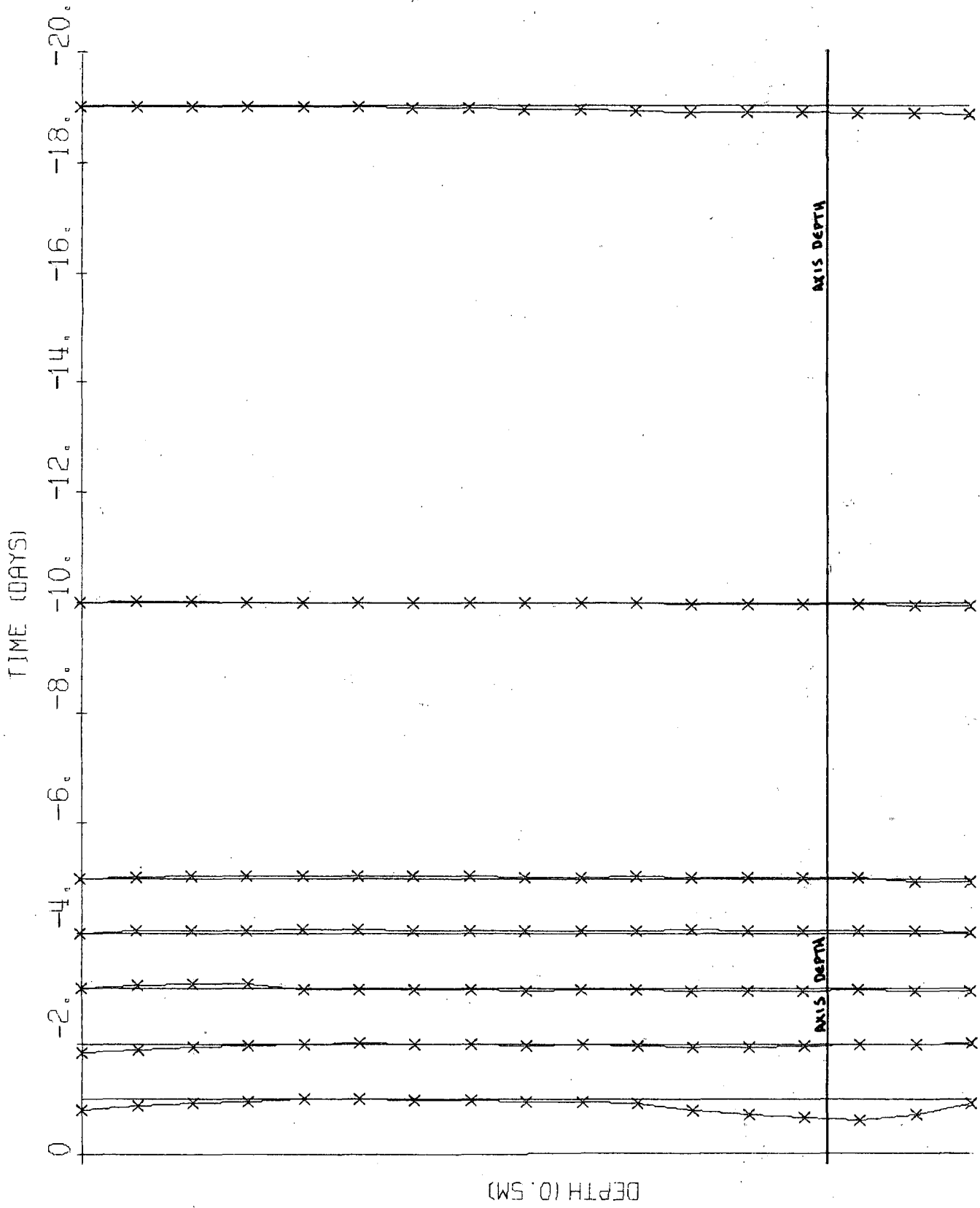
the axis level when the face was -1.83m away at -1 days before the array was intersected. Before intersection the tube was grouted to within 2m of the ground surface preventing further data collection.

The remaining three boreholes (Figures 4.13 and 4.14) gave results which can be divided into phases of movement as with the settlement profiles. The first two post-array phases of the latter correspond to lateral movement of essentially the same character. This period of displacement is progressively towards the centre line in boreholes 2.2, 3.2 and 4.2 whilst 2.1, 3.1 and 4.1 show very much less movement parallel to the centre line. The small displacement which took place was generally towards the alluvium filled channel, a feature which will be discussed later. The movement towards the tunnel reached a maximum at 10m depth in 2.2, at 9m in 3.2 and at 8m in 4.2. The shape of the profiles, and the depths to maximum displacement, are characteristic of gravity settlement caused by the closure of voids and compression of grout around the tunnel.

The movement corresponding to the consolidation phases of settlement development began after the air pressure was released from inside the tunnel. However, the process was interrupted by two events which changed the direction of displacement. Site records show that back-grouting was carried out in the section of the tunnel directly below the array at 71 days advance. The profiles for 2.2 at 72 and 91 days advance show a large reversal of movement around the depth of the tunnel. This must be a result of the high pressure of 690 kN/m^2 (100 lb/in^2) involved in back-grouting forcing the alluvium away from the tunnel.

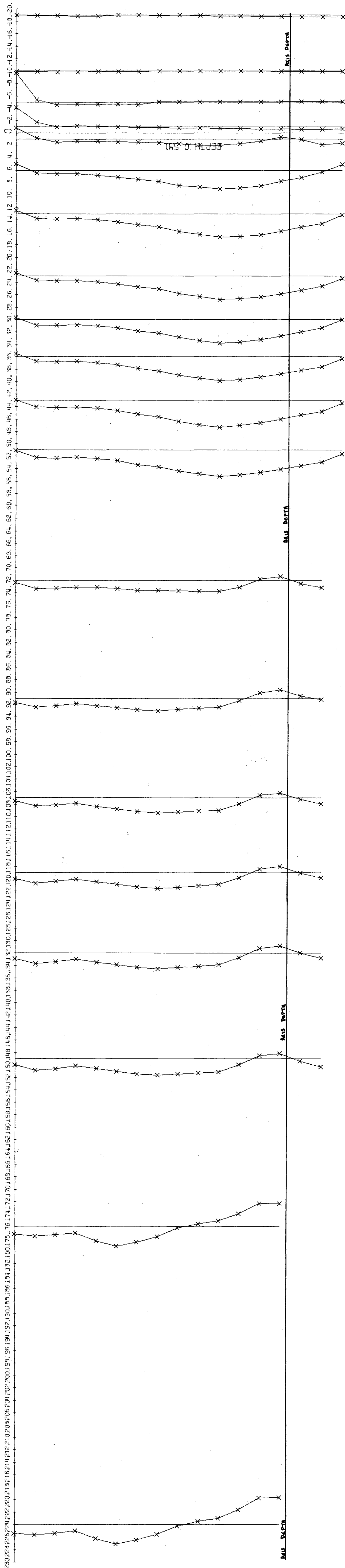
After this event very little lateral movement took place indicating that the settlement was almost vertical, which further points to consolidation as being the operative process. At 162 days advance

INCLINOMETER RESULTS WILLINGTON QUAY



INCLINOMETER RESULTS WILLINGTON QUAY

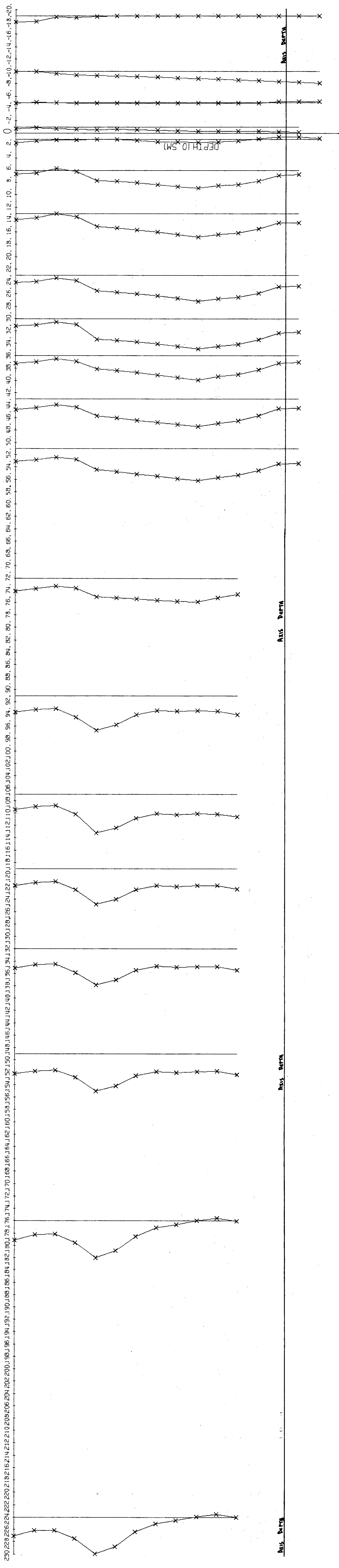
TIME (DAYS)



Figures 4.13: INCLINOMETER PROFILES NORMAL TO THE TUNNEL CENTRE LINE

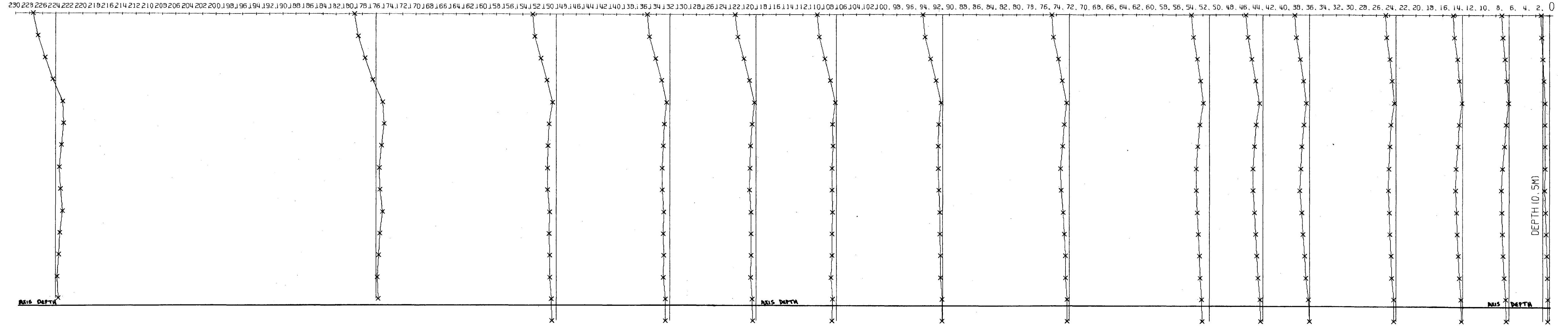
INCLINOMETER RESULTS WILLINGTON QUAY

TIME (DAYS)



INCLINOMETER RESULTS WILLINGTON QUAY

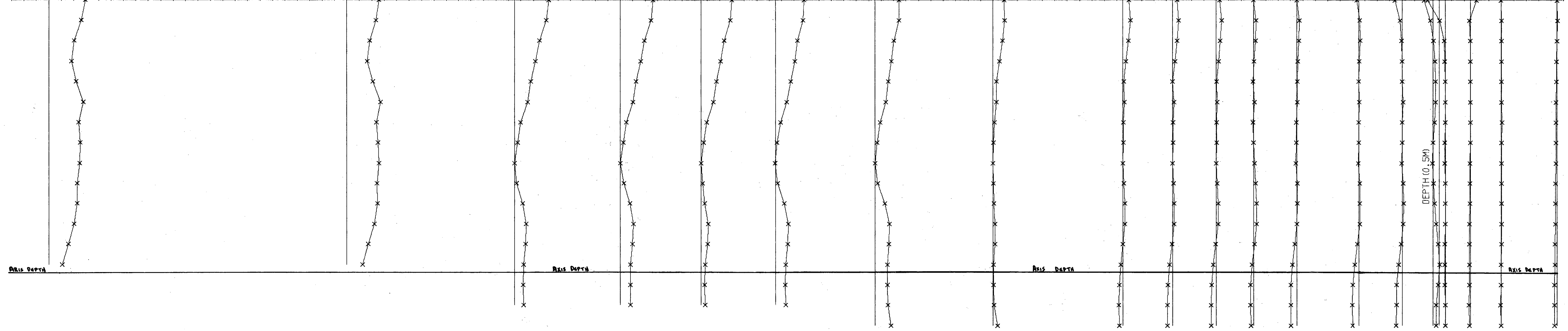
TIME (DAYS)



INCLINOMETER RESULTS WILLINGTON QUAY

TIME (DAYS)

230 228 226 224 222 220 218 216 214 212 210 209 206 204 202 200 199 196 194 192 190 188 186 184 182 180 178 176 174 172 170 168 166 164 162 160 158 156 154 152 150 148 146 144 142 140 138 136 134 132 130 128 126 124 122 120 118 116 114 112 110 108 106 104 102 100 98 96 94 92 90 88 86 84 82 80 78 76 74 72 70 68 66 64 62 60 58 56 54 52 50 48 46 44 42 40 39 36 34 32 30 29 26 24 22 20 18 16 14 12 10 8 6 4 2 0 -2 -4 -6 -8 -10 -12 -14 -16 -18 -20

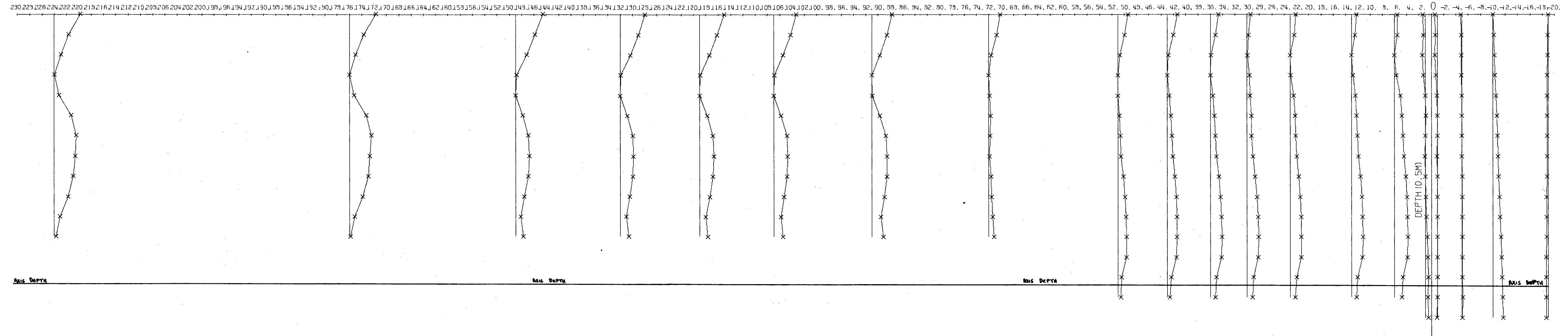


2.1

Figures 4.14: INCLINOMETER PROFILES PARALLEL TO THE TUNNEL CENTRE LINE.

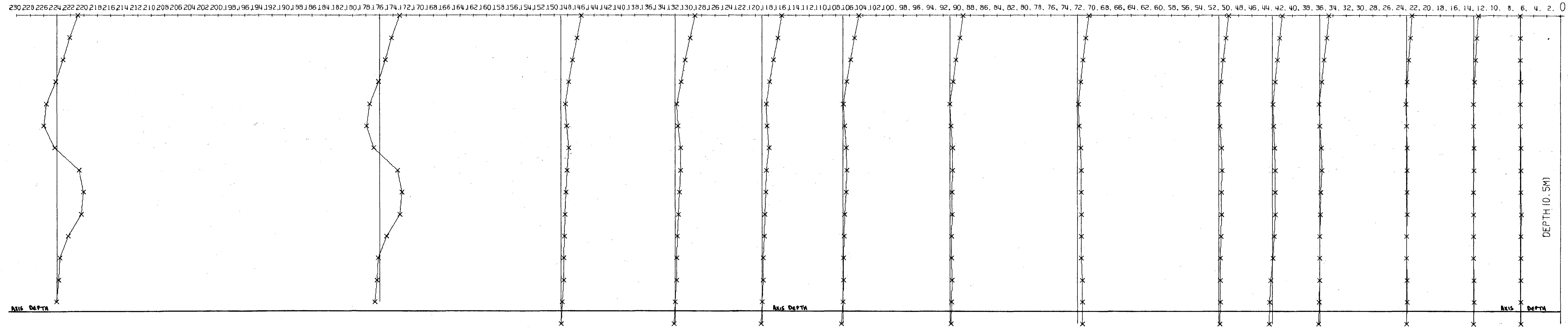
INCLINOMETER RESULTS WILLINGTON QUAY

TIME (DAYS)



INCLINOMETER RESULTS WILLINGTON QUAY

TIME (DAYS)



4.1

beyond the array, the demolition of the wall overlying the tunnel near the array caused widespread uplift. This also caused a renewal of lateral movement seen in all profiles. The nature of the movement suggests a buckling effect, particularly in borehole 4 when the profiles for 162 days and 176 days, that is before and after the uplift, are contrasted. The final profiles normal to the centre line again show little change indicating that consolidation had been resumed.

In the profiles 2.1, 3.1 and 4.1 essentially the same phases of movement took place as described previously. In this case, however, the direction of displacement was towards the middle of the alluvium-filled channel, which became particularly evident after the air in the drive had been released. The displacement was caused by the larger surface settlements above the middle of the channel illustrated in Figure 4.6 with the displacement occurring towards the largest settlement. The profiles are very similar in shape to those normal to the centre line with a large movement at the surface and a second maximum at depth.

4.6 Vectors of Ground Movement.

In order to illustrate and clarify the phases of movement further, the settlements and lateral displacements have been combined to produce vectors of ground movement for the post-array movements which occurred. The pre-array movement was relatively small and has not been shown separately. The profiles for 1.1 (Figure 4.12) indicate that the ground loss for this period was due to a high face-take.

The vectors of the post-array movements have been selected to illustrate the phases which were previously erected in describing individual profiles. However, the combination of data requires that certain intermediate events are also included to provide complete history.

The periods chosen to delineate these movements are also restricted by the availability of data. In order to clarify this Figure 4.15 should be consulted to show the correlation of the vectors, settlement and lateral movement diagrams.

The initial movement covers the period from the beginning of settlement to 51 days advance, the majority of which was post-array (Figure 4.16a). This includes the first two phases of post-array settlement and is therefore made up of two periods of rapid movement, both of which have their origin around the tunnel lining. The first rapid phase has already been attributed to the closure of voids and compression of grout, and the second, tentatively to disturbances caused by back-grouting in a nearby section of the tunnel. The evidence gained from the vectors makes the latter seem a more probable cause for the second phase of rapid movement than an unrecorded reduction in air pressure in the drive, although this is still uncertain.

The vectors from 51 to 91 days advance (Figure 4.16b) include the release of air pressure from the tunnel at 66 days although the movement represented was mainly caused by further back-grouting. This was carried out at 71 days advance and caused movement of the alluvium away from the tunnel. The vectors include a substantial vertical settlement component which is shown to be diverted away from the tunnel. If the data had permitted the movement caused by the back-grouting to be isolated it is very probable that it would be directly away from the tunnel.

The phase attributed to consolidation began at 66 days although, as a result of back-grouting at 71 days it was necessary to use the vectors from 91 days to 149 days advance to represent this movement (Figure 4.16c). The vectors support the consolidation hypothesis in that they are almost vertical and decrease in magnitude with depth.

This shows that the movement originates from a process occurring within the body of the alluvium and not around the tunnel lining.

At 162 days the process was interrupted by the demolition of a nearby wall. The vectors for the period of 149 to 176 days advance delineate the uplift which resulted from this unloading (Figure 4.16d). The uplift was greatest in borehole 4 because this was the nearest to the demolished wall. The vectors for the remaining period of 176 to 224 days are again almost vertical showing that the consolidation process had been resumed (Figure 4.16e).

Ground movement vectors parallel to the tunnel centre line (Figures 4.17a to 4.17c) have been divided into the same periods of movement as vectors normal to the tunnel. The first phase of movement was largely vertical corresponding to the predominance of ground movement normal to the centre line. Thereafter the vectors show a consistent movement towards the middle of the channel, which is somewhat better illustrated by the inclinometer profiles (Figures 4.14a to 4.14c).

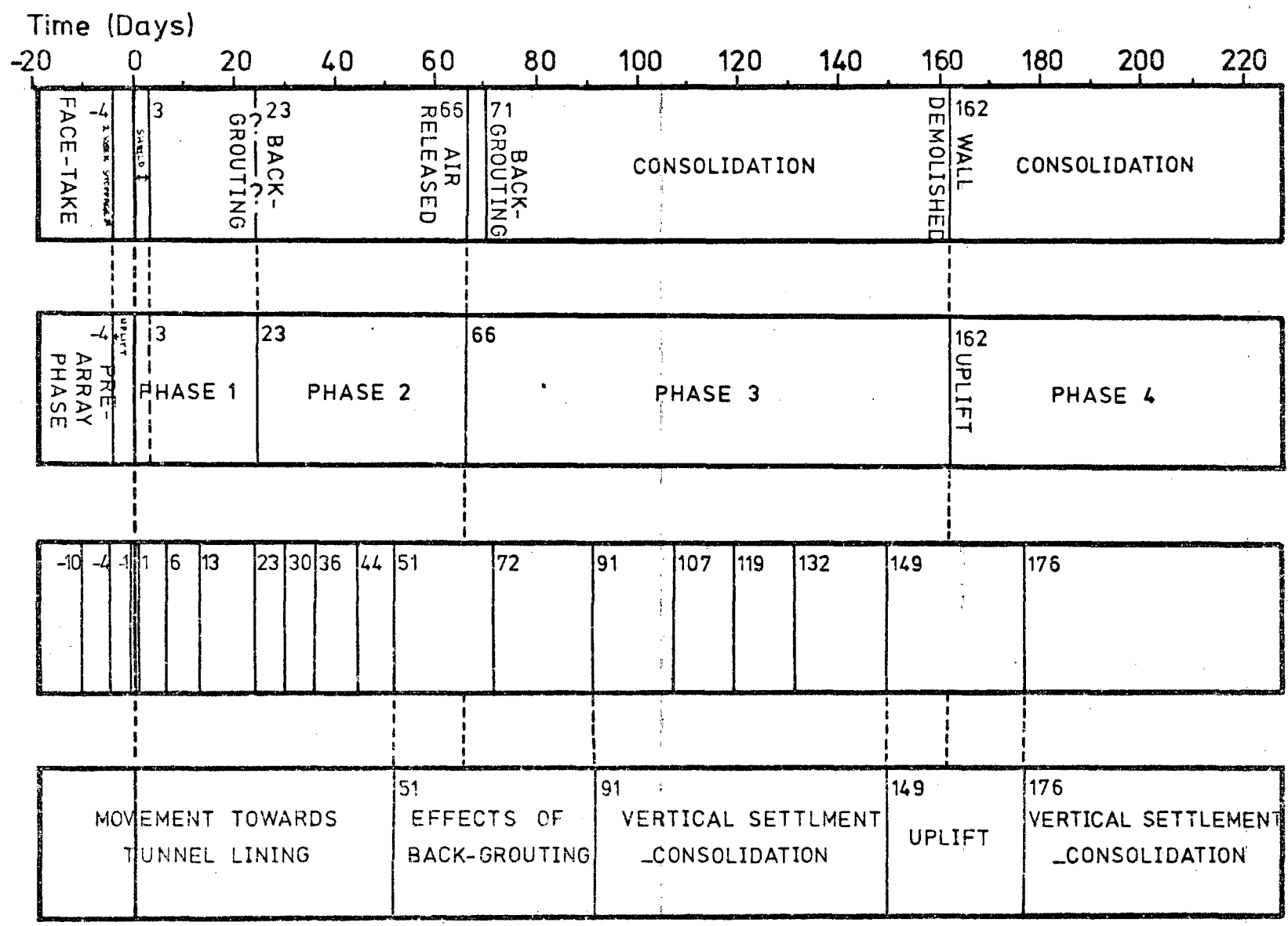


Figure 4.15: CORRELATION DIAGRAM FOR PHASES OF GROUND MOVEMENT

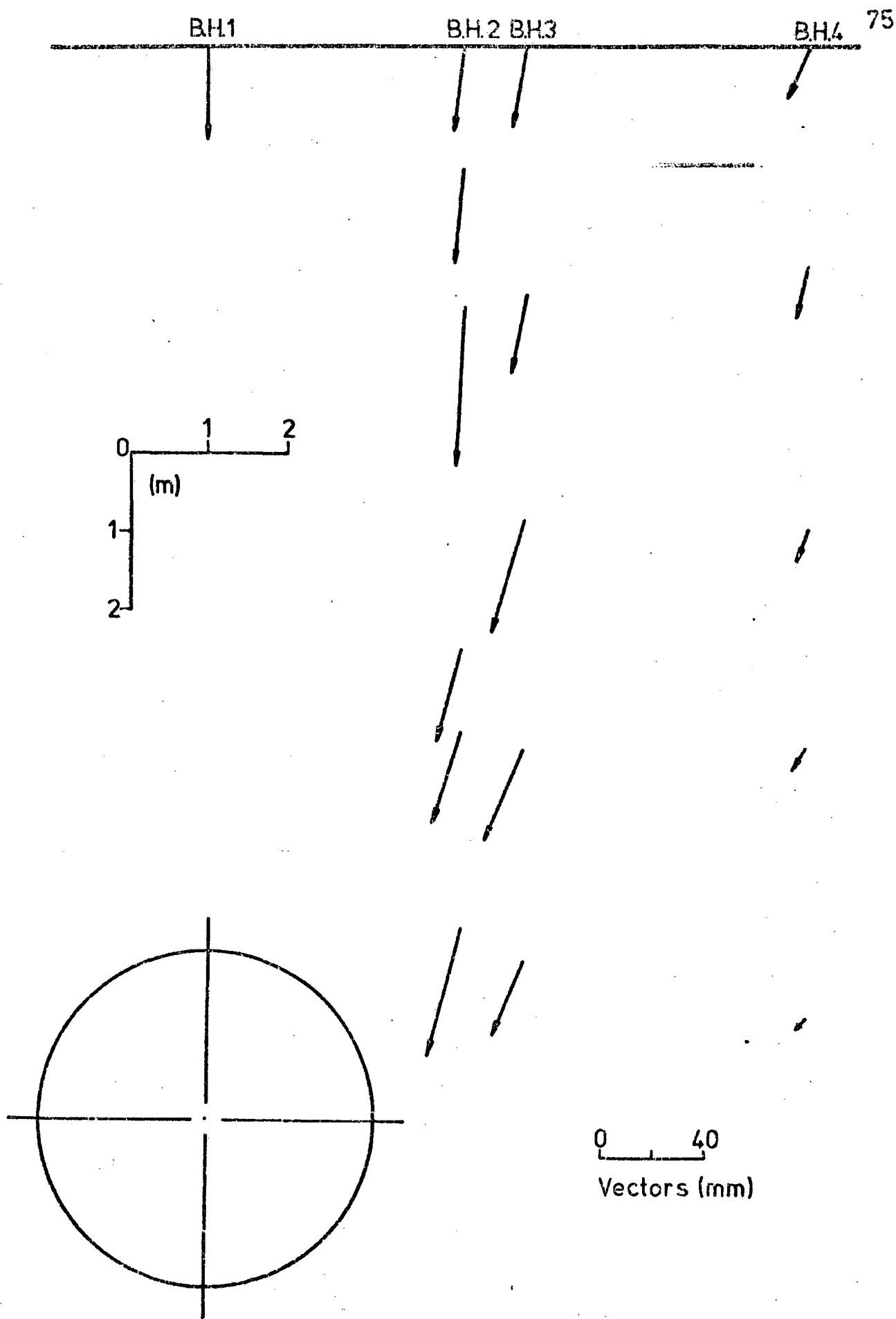


Figure 4.16a: VECTORS OF GROUND MOVEMENT NORMAL TO THE TUNNEL CENTRE LINE AT 51 DAYS

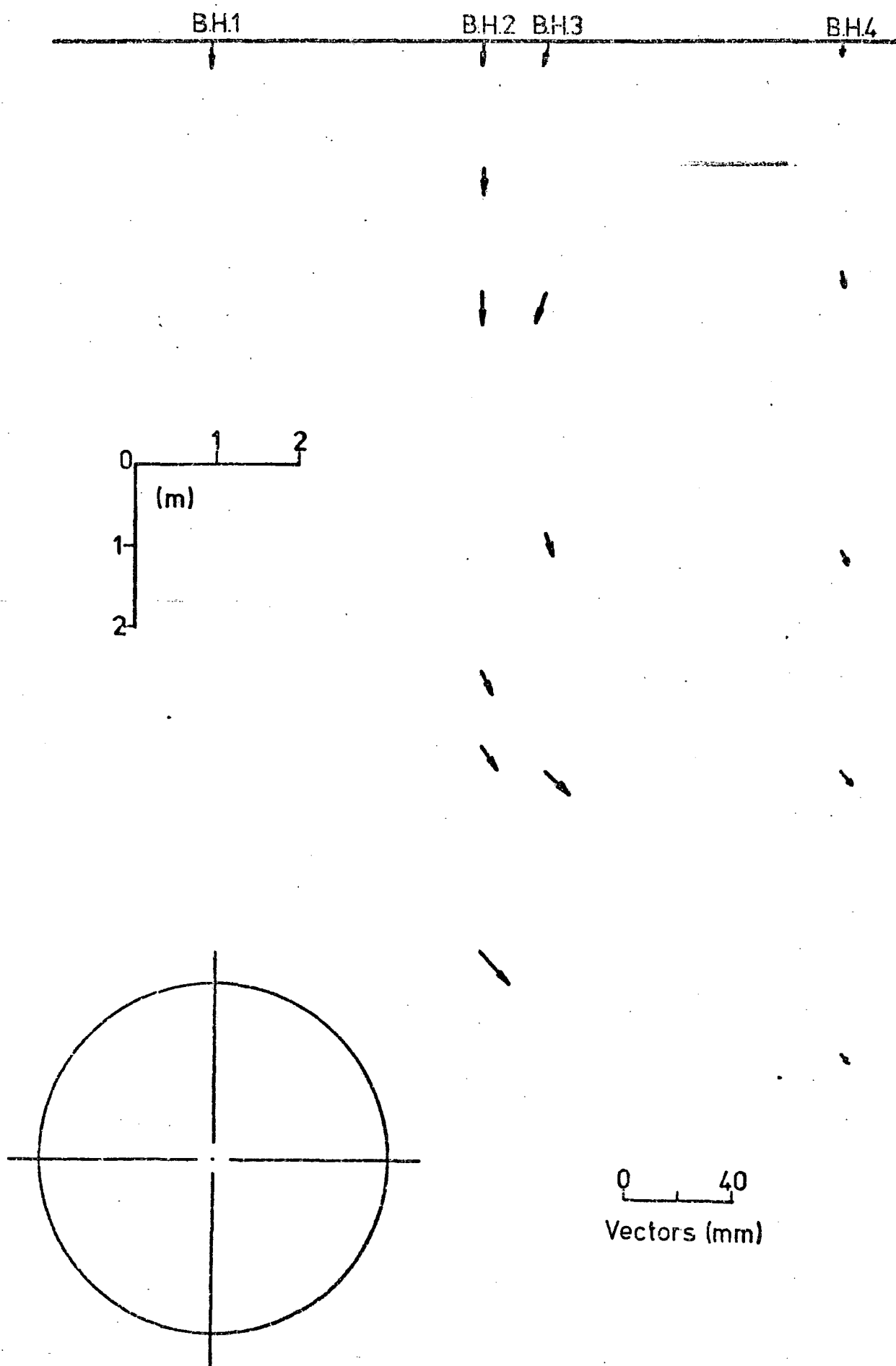


Figure 4.16b: VECTORS OF GROUND MOVEMENT NORMAL TO THE TUNNEL CENTRE LINE BETWEEN 51 AND 91 DAYS

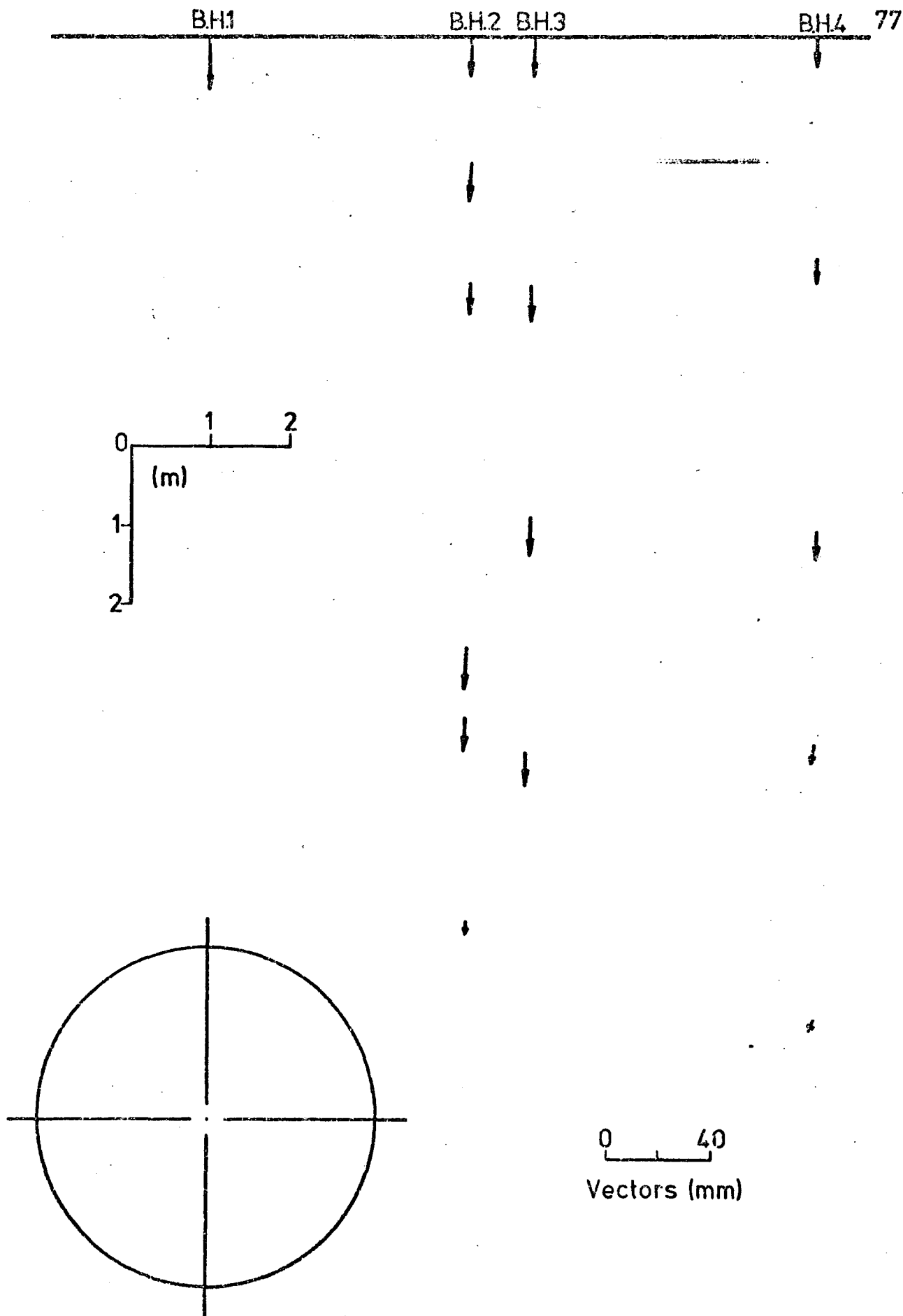


Figure 4.16c: VECTORS OF GROUND MOVEMENT NORMAL TO THE TUNNEL CENTRE LINE BETWEEN 91 AND 149 DAYS

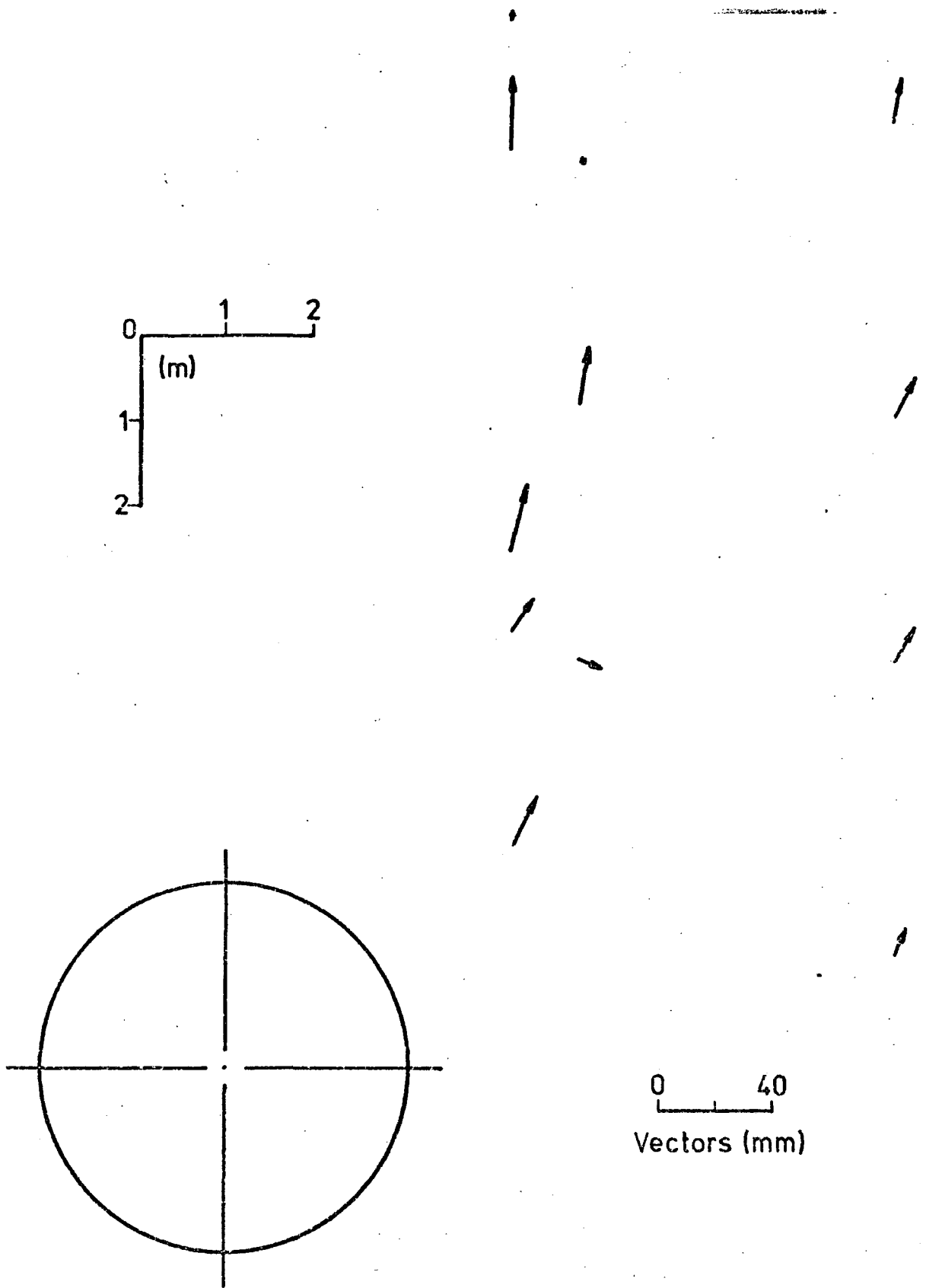


Figure 4.16d: VECTORS OF GROUND MOVEMENT NORMAL TO THE TUNNEL CENTRE LINE BETWEEN 149 AND 176 DAYS

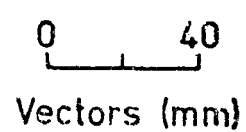
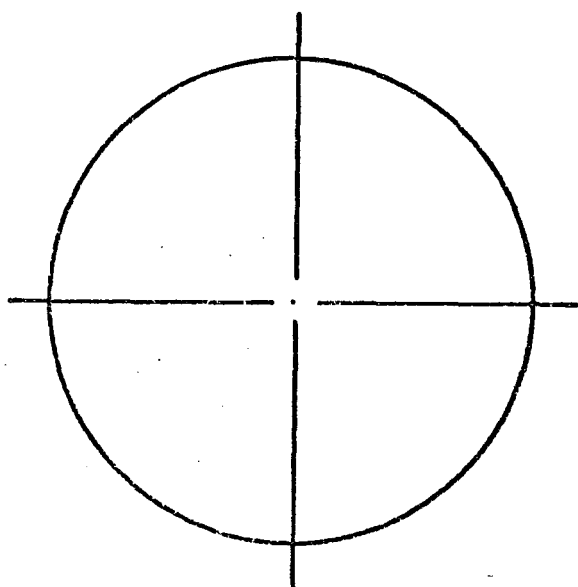
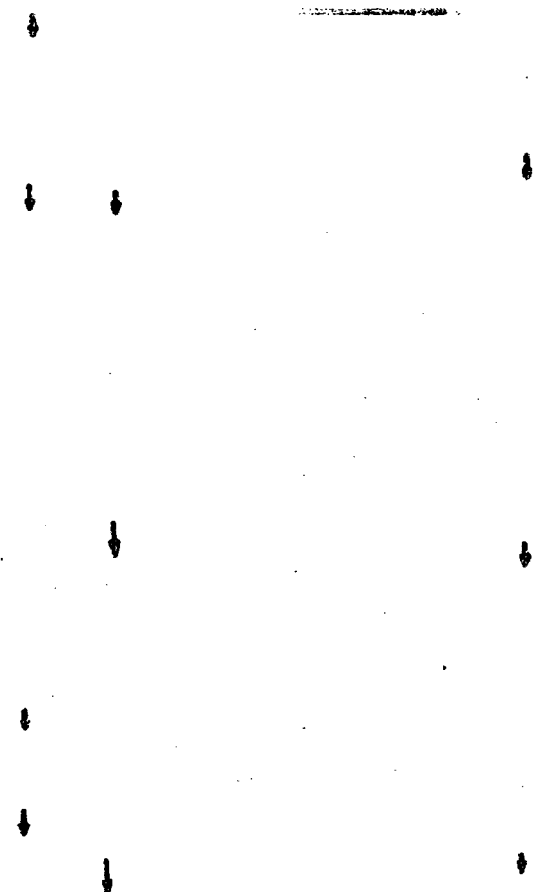
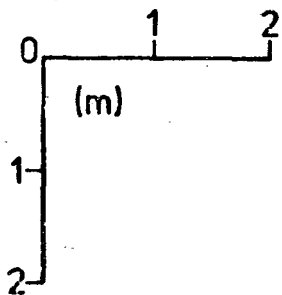


Figure 4.16e: VECTORS OF GROUND MOVEMENT NORMAL TO THE TUNNEL CENTRE LINE BETWEEN 176 AND 224 DAYS

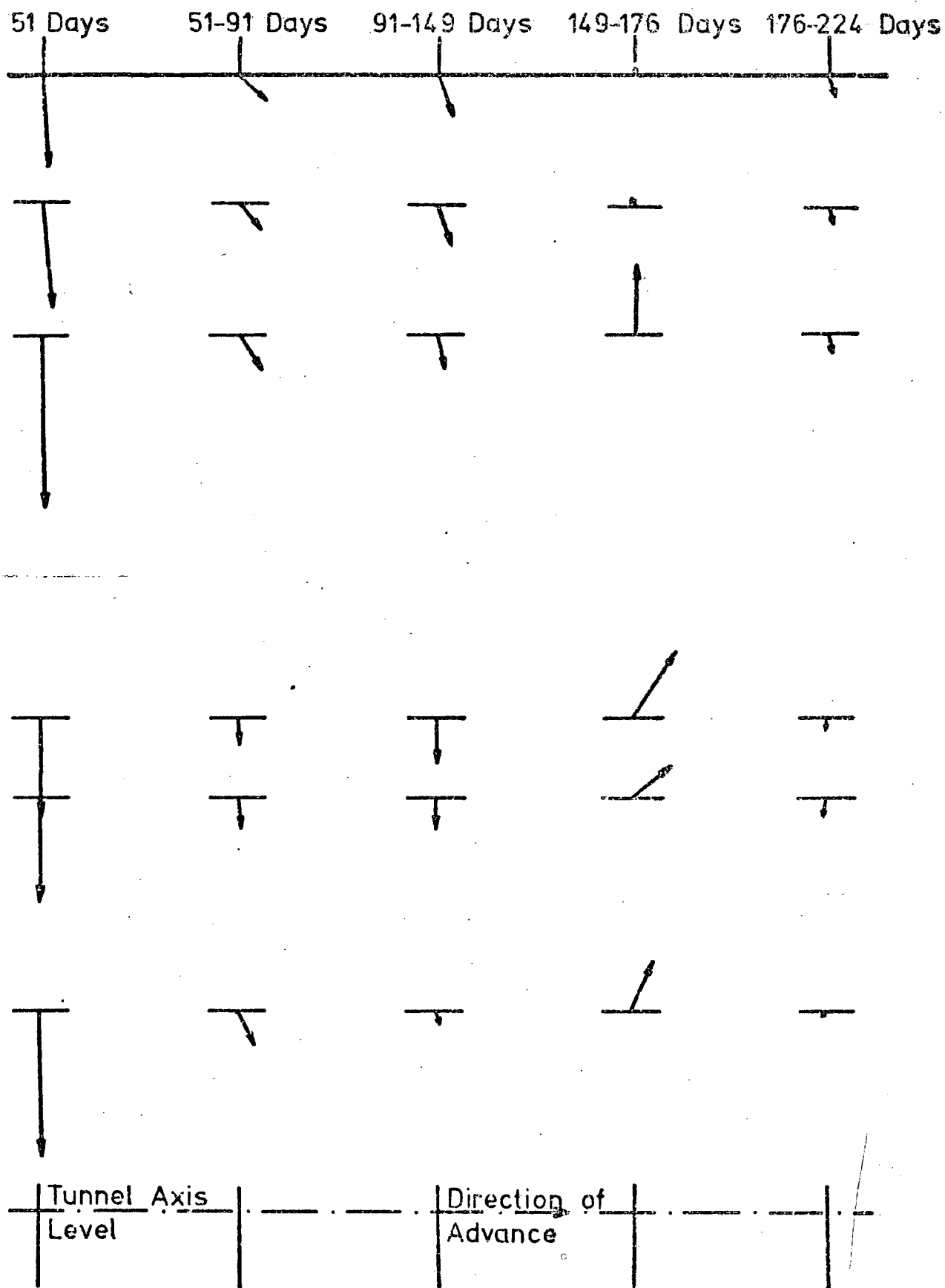


Figure 4.17a: VECTORS OF GROUND MOVEMENT PARALLEL TO THE TUNNEL CENTRE LINE. BOREHOLE 2 OFFSET 293m FROM \mathcal{C} (Scales as in Figure 4.16)

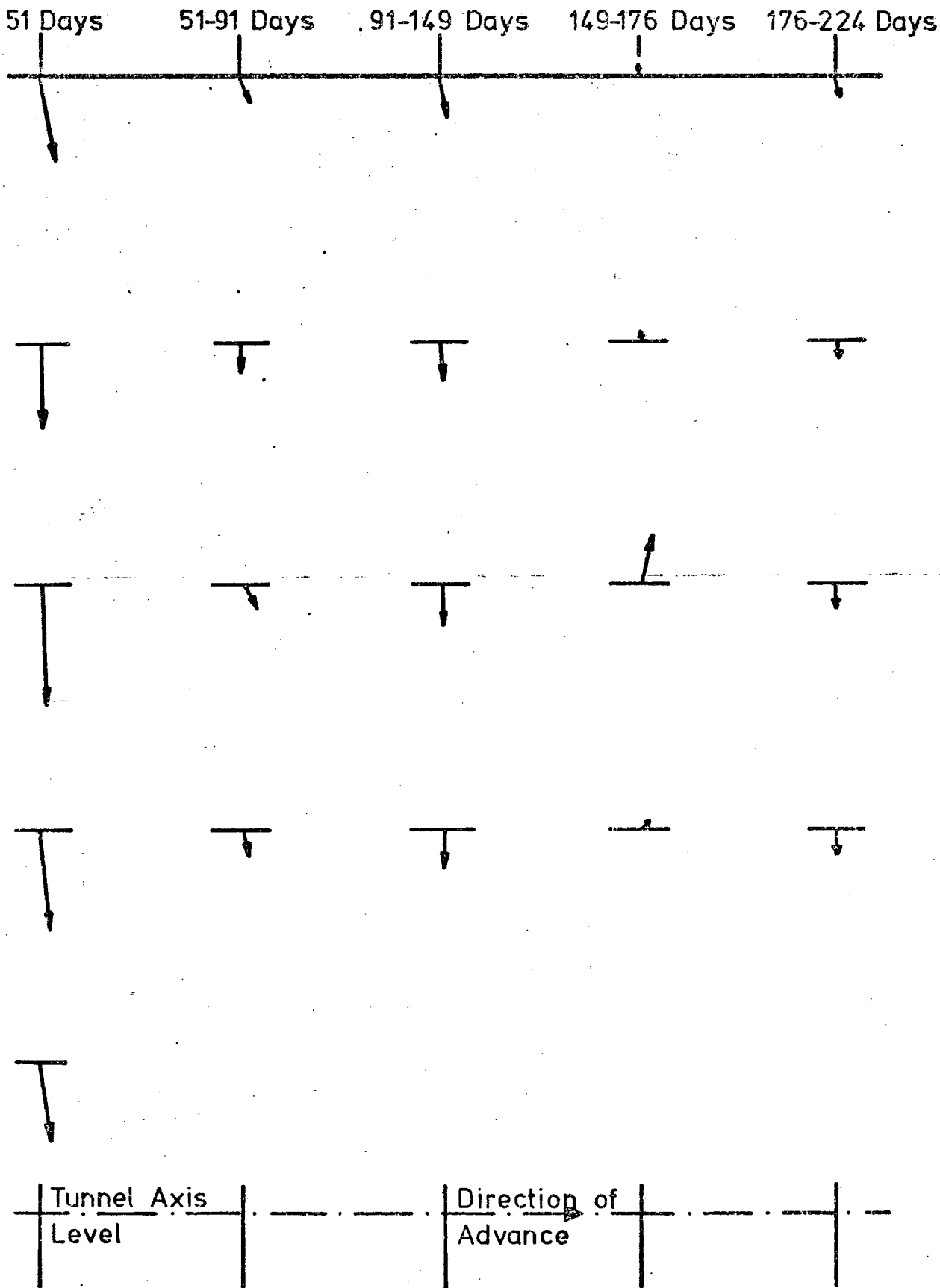


Figure 4.17b: VECTORS OF GROUND MOVEMENT PARALLEL TO THE TUNNEL CENTRE LINE..BOREHOLE 3 OFFSET 396m FROM ζ (Scales as in Figure 4.16)

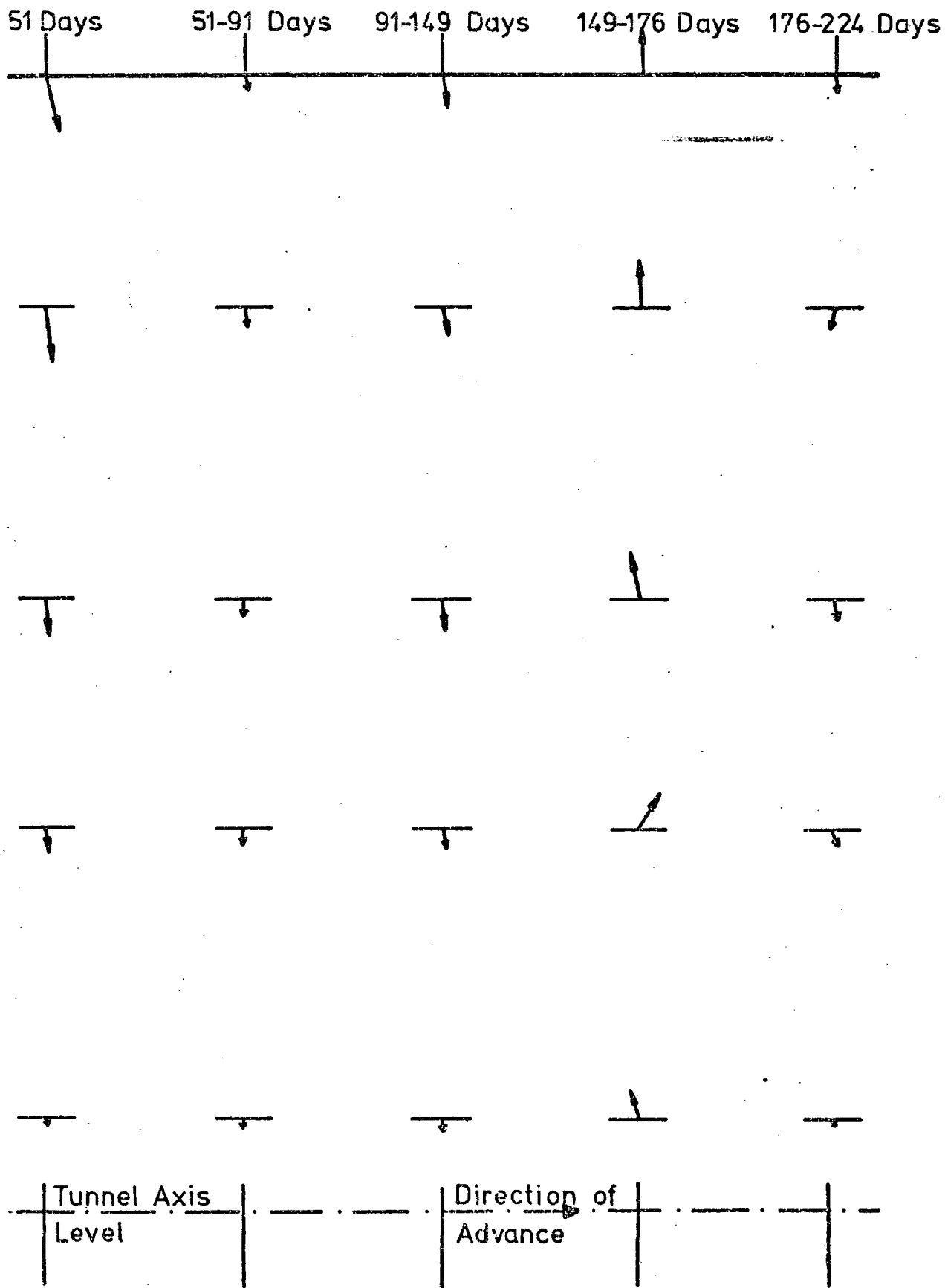


Figure 4.17c: VECTORS OF GROUND MOVEMENT PARALLEL TO THE TUNNEL CENTRE LINE - BOREHOLE 4 OFFSET 7.65m FROM ϕ (Scale as in Figure 4.16)

Chapter 5

LABORATORY PROGRAMME

During the passage of the drive through the channel a number of samples of the alluvium were taken from the tunnel face. These were used for a variety of laboratory tests and analyses to provide data on the physical properties, mineralogy and geochemistry of the sediment.

5.1 Sampling Procedure.

The tunnel face was sampled at six stages during the passage of the drive through the alluvium. The first two, labelled A and B, were relatively close together whilst the rest from C to F were evenly distributed across the width of the channel (Figure 5.1). At each of these stages from 4 to 8 samples were taken, mainly in a line from soffit level to invert of the accessible face. Sampling was carried out as rapidly as possible so as not to hinder the work of the miners, particularly when they were excavating the face without a break throughout a shift. Therefore no regular pattern could be established. Subsequent examination of the results has shown that more regular sampling would not have affected their interpretation (Figure 5.1).

About 1 Kg of alluvium was taken from each of the sample localities A to C and these were stored in sealed polythene bags. This method of

Lateral Distance (m)

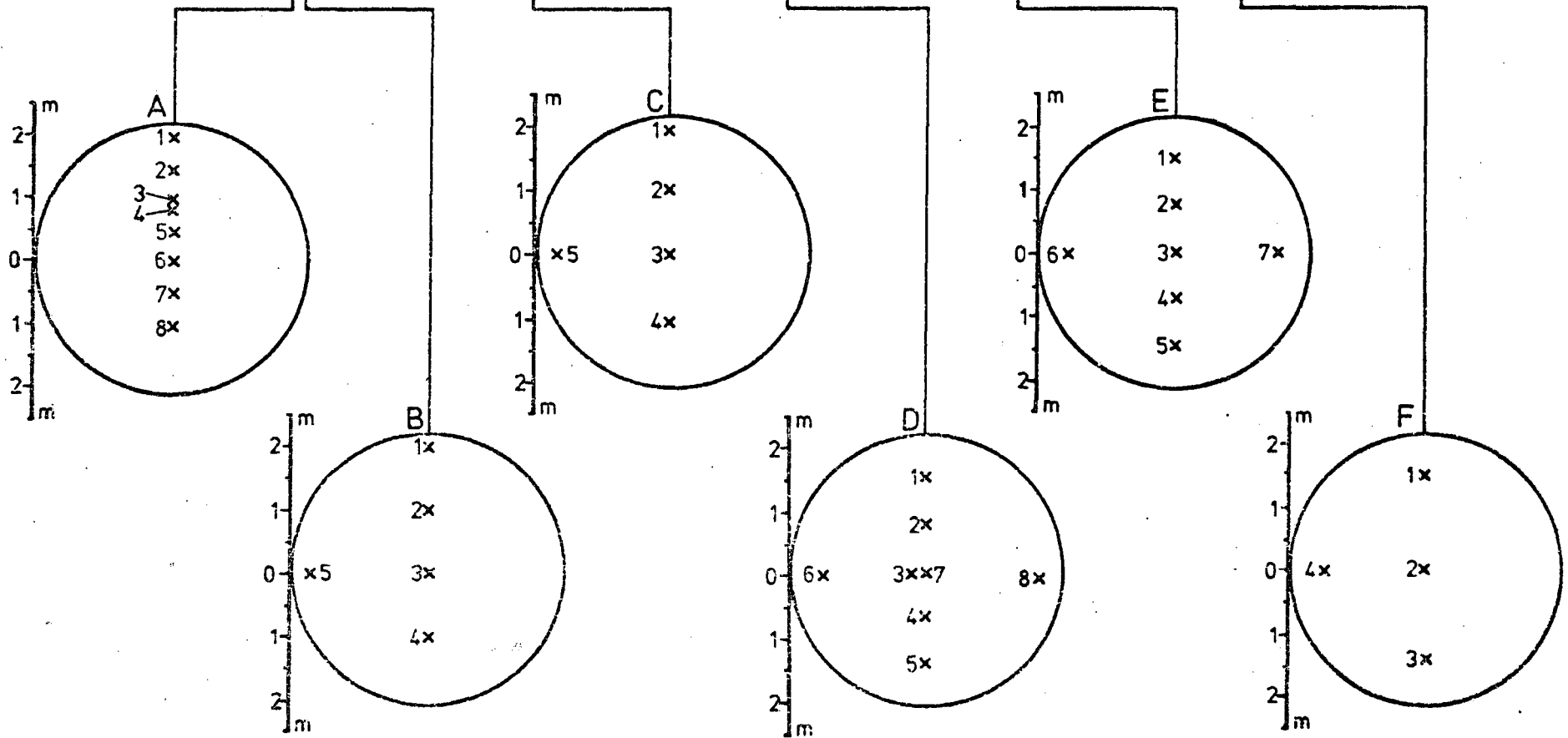
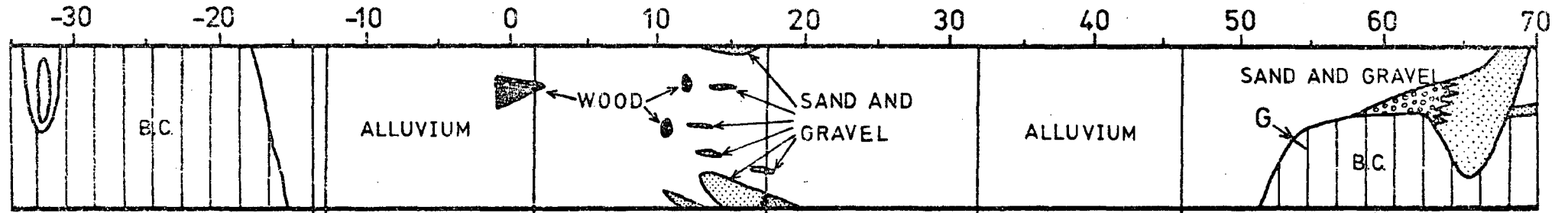


Figure 51: LOCALITIES OF SAMPLES FROM TUNNEL FACE

storage had proved to be the most efficient in preventing the loss of moisture from the samples. A different procedure was used for samples D to F in order to obtain information on the effect of air pressure on the moisture content of the alluvium in the tunnel face. For these samples several $\frac{1}{2}$ m long steel tubes were driven horizontally into the face to produce cores of about 35cm in length and 4cm in diameter. Polythene bags were used as temporary seals for ends of the tubes until the cores were extruded.

As the drive re-entered the boulder clay on the west side of the channel, two samples were taken from the weathered surface of the boulder clay. Again the samples were extracted by driving two of the steel tubes into the face, in this case at an angle which would obtain a core normal to the boulder clay-alluvium interface. These cores were labelled G whilst a final specimen of unweathered boulder clay H was taken from the tunnel face when the drive had passed several metres into the boulder clay.

5.2 Methods of Analysis

a) Moisture content, Organic content and Absorbed moisture.

About 30 to 40gm of sediment were removed from the middle of each of the samples A to C and the various experiments were carried out upon these smaller samples. Similar samples were cut at intervals from the cores taken at localities D to F. Work commenced on the samples as soon as possible after their collection, particularly in the case of D to F where the delay between collection and the determination of moisture content was kept below $1\frac{1}{2}$ hours. The cores of boulder clay G were similarly treated and a smaller sample of unweathered boulder clay H was extracted from the specimen which had been collected.

Almost 150 samples of alluvium and boulder clay were produced and subsequently submitted to the following experimental procedures:

1) Samples from localities A to F were weighed and dried at 105°C to constant weight, which frequently took several days, in order to determine their moisture contents by weight loss. The samples were cooled to room temperature in a desiccator before the dry weight was found.

2) The samples were then allowed to absorb atmospheric moisture at room temperature for 7 days before being weighed again to determine the quantity absorbed.

3) Samples from G and H were similarly dried but no determinations were carried out. All the samples A to H were ground down by pestle and mortar and two portions of the powdered samples, of about 1.5 gm each, were again dried at 105°C to constant weight in small test tubes. Usually the drying stage took 48 hours and was necessary for removing the absorbed mixture.

4) An estimation of the organic content was subsequently obtained by placing the test tubes in an oven at 350°C for 48 hours, cooling then in a desiccator to room temperature and weighing to find the weight loss. Some loss of carbon dioxide from the carbonates may have caused the values to be slightly too high.

5) Finally, the samples were again allowed to absorb atmospheric moisture for 7 days and the weight absorbed was determined.

All the weights were found to the nearest milligram whilst the quantities of moisture, absorbed moisture and organic material are expressed as percentages relative to the dry weight of the sample to the nearest 0.001%, (see Appendices).

Stages 1 and 2 were carried out upon batches consisting of all the samples from each locality in turn, whilst for stages 3,4 and 5 batches of

20 samples were used. In addition to these a control experiment was performed to monitor any differences in the experimental conditions for each batch. A group of samples was assembled using one from each of the above batches and these were subjected to the process outlined above. Each sample, therefore, underwent the process under exactly the same conditions.

Any variations between the control results and those obtained previously pointed to an inconsistency in the experimental conditions for the batch from which the sample came. The moisture contents could not be checked in this fashion because of the difficulty in retaining the original amount of moisture until all the samples had been collected. The results for the organic content proved to be in agreement for all the batches, however, considerable variation was found in some of the absorbed moisture contents determined both before and after the removal of the organic material. This resulted from the day to day variations in atmospheric humidity, to which the quantity of absorbed moisture was related. These variations can be seen in Figure 5.2 which shows the absorbed moisture contents of five samples measured over a period of 10 days after drying. The samples were from locality B and the absorbed moisture values were those of stage 2 in the experimental procedure. Inconsistencies in the results for both stage 2 and stage 5 have, therefore, been corrected using the control values as follows:

$$\frac{\text{Control Percentage}}{\text{Corresponding Experimental Percentage}} \times \text{Experimental Percentage for rest of the batch} = \text{Corrected Experimental Percentage}$$

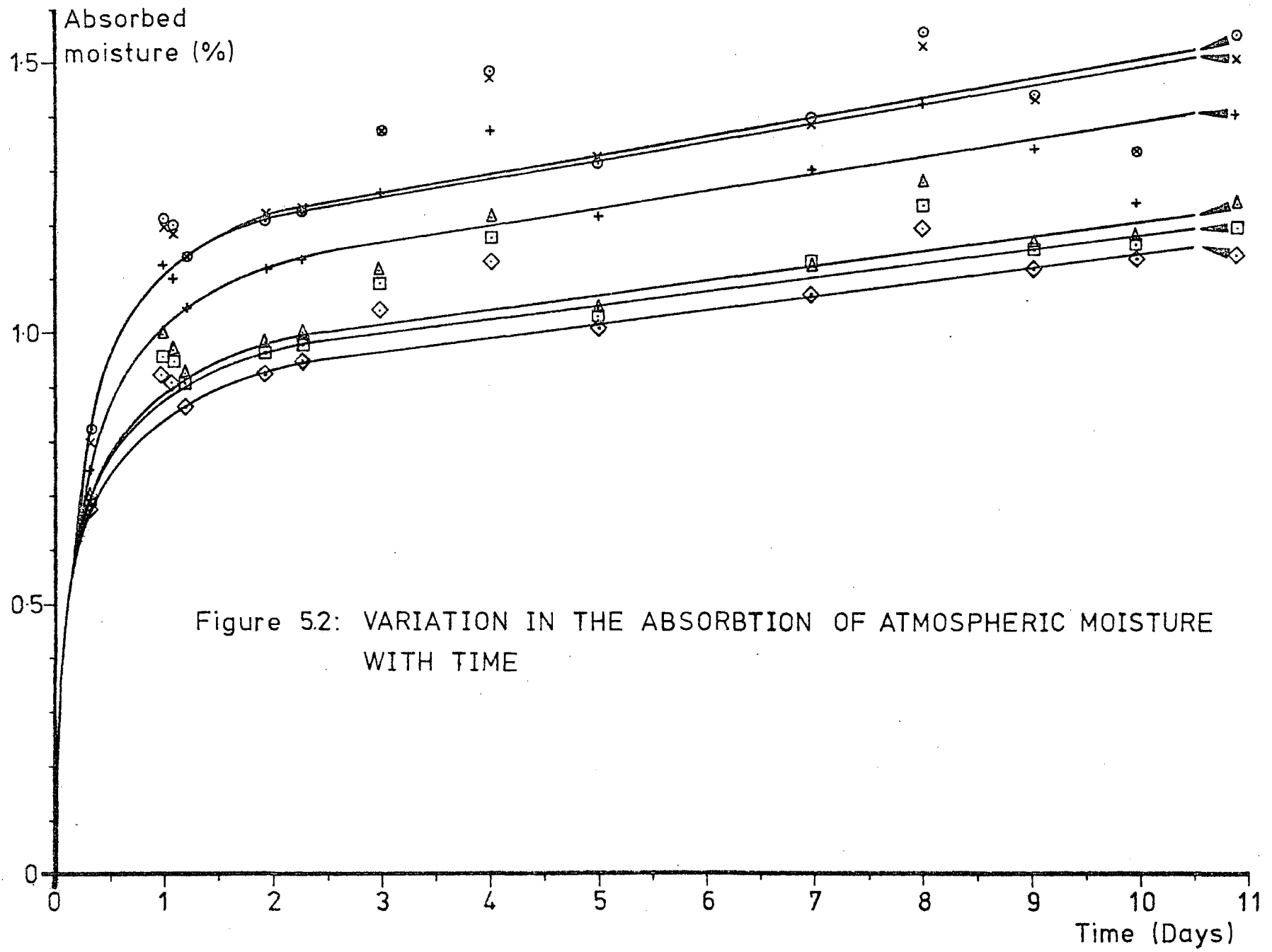


Figure 52: VARIATION IN THE ABSORPTION OF ATMOSPHERIC MOISTURE WITH TIME

b) X-Ray Diffraction.

In order to investigate variations in the mineralogy of the samples, some of them were analysed by X-ray Diffraction. The samples used were further portions of the dried and powdered samples which were produced for stage 3 described above. Analysis was carried out on all samples from A to C and one sample from each of the cores D to F of the alluvial material. The cores of weathered boulder clay each provided eight samples, all of which were analysed to provide some information upon the possible development of a weathered profile in the surface of the boulder clay. Finally, the sample from H was analysed for a comparison between unweathered and weathered boulder clay as it was probable that the cores had not penetrated beyond the weathered layer.

This resulted in 37 samples of alluvium distributed across the channel and 16 samples of weathered boulder clay with one unweathered sample from the west side of the channel. Each of these underwent the following procedure:

- 1) 0.45 gm of powdered sample was weighed out and 0.05 gm of an internal standard Boehmite added to it forming a 90% sample to 10% Boehmite mixture. Both were weighed to the nearest 0.00005 gm.
- 2) The two substances were mixed with an agate pestle and mortar for 5 minutes and the mixture was put in a labelled tube.
- 3) About 0.2 gm of the sample was placed on a clean glass slide and a lake of acetone run around it.
- 4) The powder was then spread out with a spatula and the slide shaken to form an even film of the sample before allowing the acetone to evaporate.
- 5) A slide prepared in this way was placed in an X-ray Diffractometer and bombarded with X-rays at 45 kU and 25 mA. Measurement of the

diffracted radiation took place with the detector moving from 3° to $43^{\circ} 2\theta$ at 1° per minute, the radiation peaks being traced on a chart recorder running at 10 mm/minute making $1^{\circ} 2\theta = 10\text{mm}$ of chart.

For each sample the peak to background ratio was adjusted to a maximum whilst still retaining the relevant quartz peak within the chart span. This was achieved by using electronic filters during the amplification of the detector signal. The ranges used for the samples analysed were 77 to 81 for the Lower Level adjustment and 10 to 34 for the Window adjustment.

Various minerals were found to be present from the 2θ values of the chart peaks. These are listed in Table 3 along with their respective 2θ and D-spacing values. Background radiation resulting from the glass slide was removed as shown in Figure 5.3 and the areas of the various peaks were measured using a planimeter. Peak areas produced by this method vary with the different detector signal amplification conditions and with different sample thicknesses on the glass slide. Therefore, the areas of each mineral peak were expressed as a ratio to the Boehmite peak to remove the effects of this variability.

Boehmite ratios obtained were compared with calibration curves to find the percentage of each mineral. These curves were prepared using various proportions of pure or nearly pure minerals, and Boehmite to give a Boehmite Peak Area Ratio to Percentage of Mineral curve. A curve was required for each of the main minerals present in the alluvium. However, for Kaolinite and Illite several curves were necessary because different degrees of structural disorder in these minerals affected the peak area ratios. The shapes of the peaks were also changed and the relationship between the half peak width and the Boehmite half peak width gave a Shape Factor which was used as a guide to the level of disorder. The Shape

<u>MINERAL</u>	<u>2θ</u>	<u>D-SPACING</u>
Chlorite	7.35	13.96
Muscovite-Illite	10.30	9.92
Kaolinite	14.40	7.14
BOEHMITE	16.90	6.09
Quartz	24.35	4.24
Plagioclase	25.73	4.02
Orthoclase	32.07	3.24
Calcite	34.35	3.03
Dolomite	36.15	2.88
Siderite	37.42	2.79
Pyrite	38.58	2.71

Table 3: MINERALS IDENTIFIED IN ALLUVIUM AND BOULDER CLAY SAMPLES.

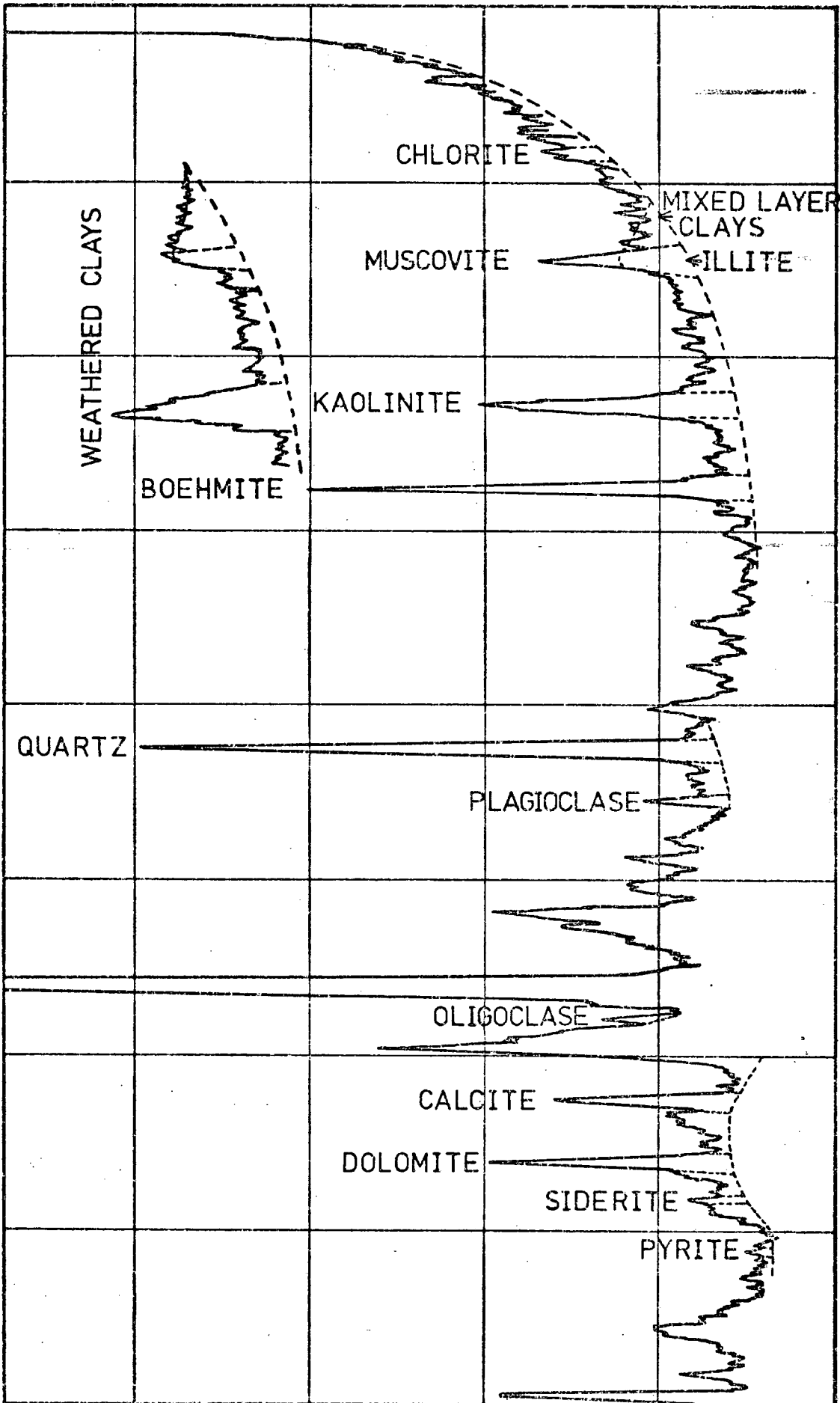


Figure 5.3: INTERPRETATION OF X-RAY DIFFRACTION CHART

Factor was also used to choose which calibration curve should be used for converting the peak area ratios into a percentage of the mineral.

The curves used were developed by T.J. Smith of the Department of Engineering Geology and R. Hardy of the X-ray laboratory for use on Mesozoic and Tertiary clays and Carboniferous shales respectively. This places some limitations upon the interpretation of the results.

Although the absolute values of the percentages may not be completely accurate, which applies particularly to the clays, their relative proportions for the same mineral between different samples should be a good representation of the relative proportions of the minerals.

c) X-ray Fluorescence.

All the specimens analysed by the X-ray Diffraction method also underwent X-ray Fluorescence analysis. The various stages of the method again described forthwith:

1) Further portions of the dried and powdered material were used in the analysis. About 10 gm were mixed with a binding resin Mowiol and placed in a mould.

2) A compressive force of 7 tons pressure was applied for 2 minutes to produce a $1\frac{1}{4}$ inch diameter round pellet of about $\frac{1}{4}$ inch in thickness. Where insufficient sample was available the pellets were given a borax backing for reinforcement and to maintain opacity to the x-rays.

3) The pellets were run on a Phillips P.W. 12-12 Automatic Sequential Analyser using a TE 108 Torrens Industry Automatic Sample Loader. Machine drift was monitored by using a standard analysed for each run. Conditions used for this group of samples are listed in the

appendices.

Samples were run with 12 International Standards for sedimentary material and the results analysed by computer. Those appearing in the appendices are uncorrected for mass absorption and were calculated on a CO_2 , C and H_2O free basis. These constituents make up the remaining 10-12% of the difference between the total of oxides and 100%.

5.3 Results and Interpretation.

a) Moisture Content, Organic Content and Absorbed Moisture.

Various combinations of these results are illustrated in Figures 5.4 to 5.7 to show the relationships between the various properties of the alluvium. In order to reduce the amount of data the values for the samples from cores D to F were averaged to find a mean for each core. The closest correlation was obtained from the combination of the initial absorbed moisture, that is, that of the dried samples, and the organic content (Figure 5.4). These show an increase in the quantity of absorbed moisture with an increase in the organic content. Also the points fall into two distinct groups, one with 2.3 to 3.3% organic material and a smaller group of 3.6 to 4.0% organic content, each group with correspondingly lower and higher absorbed moisture values respectively. The exceptions to this relationship have been shown to have abnormally high clay contents (E.6) or quartz contents (A.4, D.5, E.2), or in the case of C.3 a large piece of organic material such as a twig may have caused the relationship to break down.

By comparing the organic and absorbed moisture contents to the original moisture contents of the samples a similar distribution and grouping of points results (Figure 5.5 and 5.6). However, there is considerably more scatter with respect to the original moisture content values in both cases. The scatter was most probably caused by the

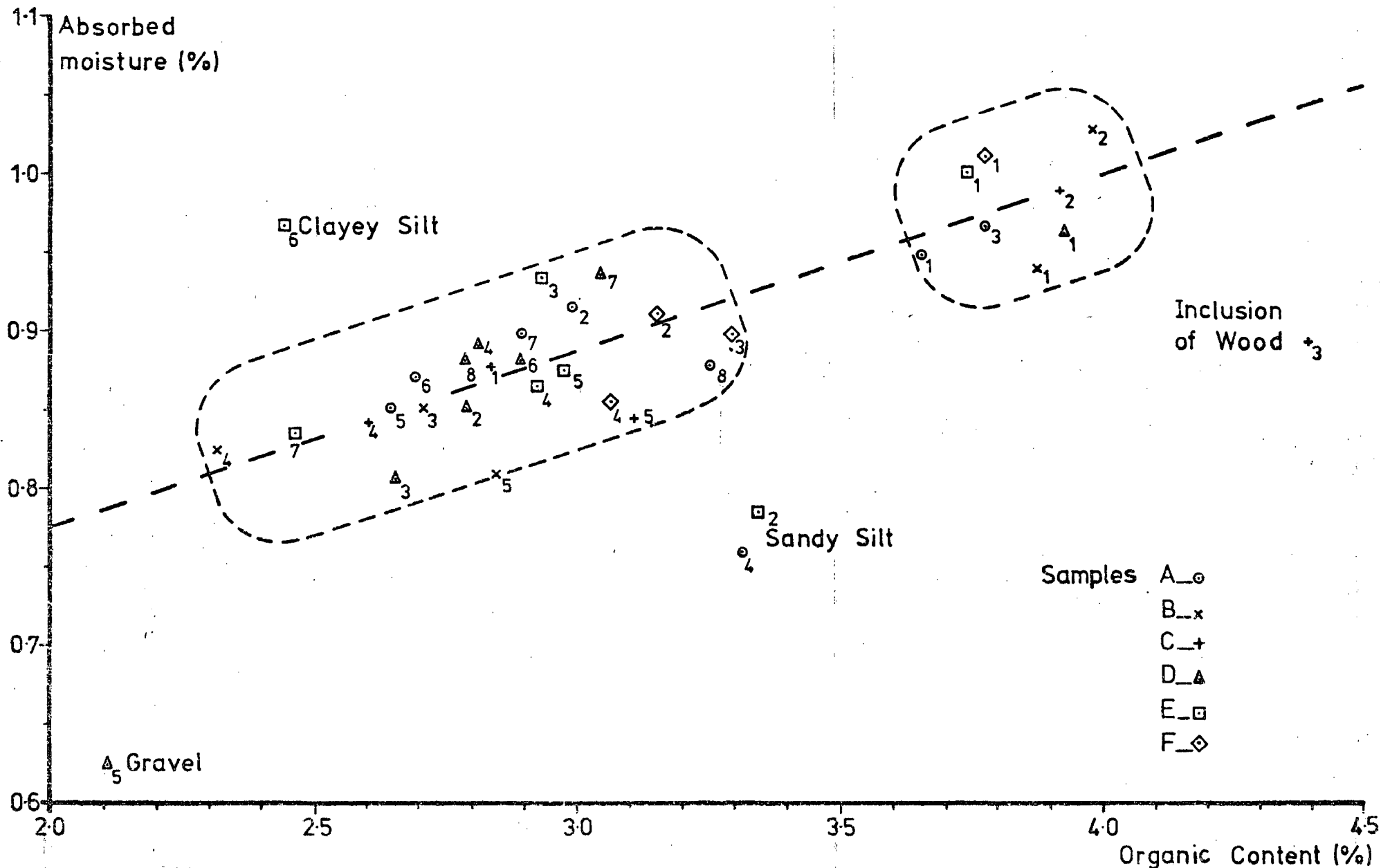


Figure 5.4: ORGANIC CONTENT vs. INITIAL ABSORBED ATMOSPHERIC MOISTURE

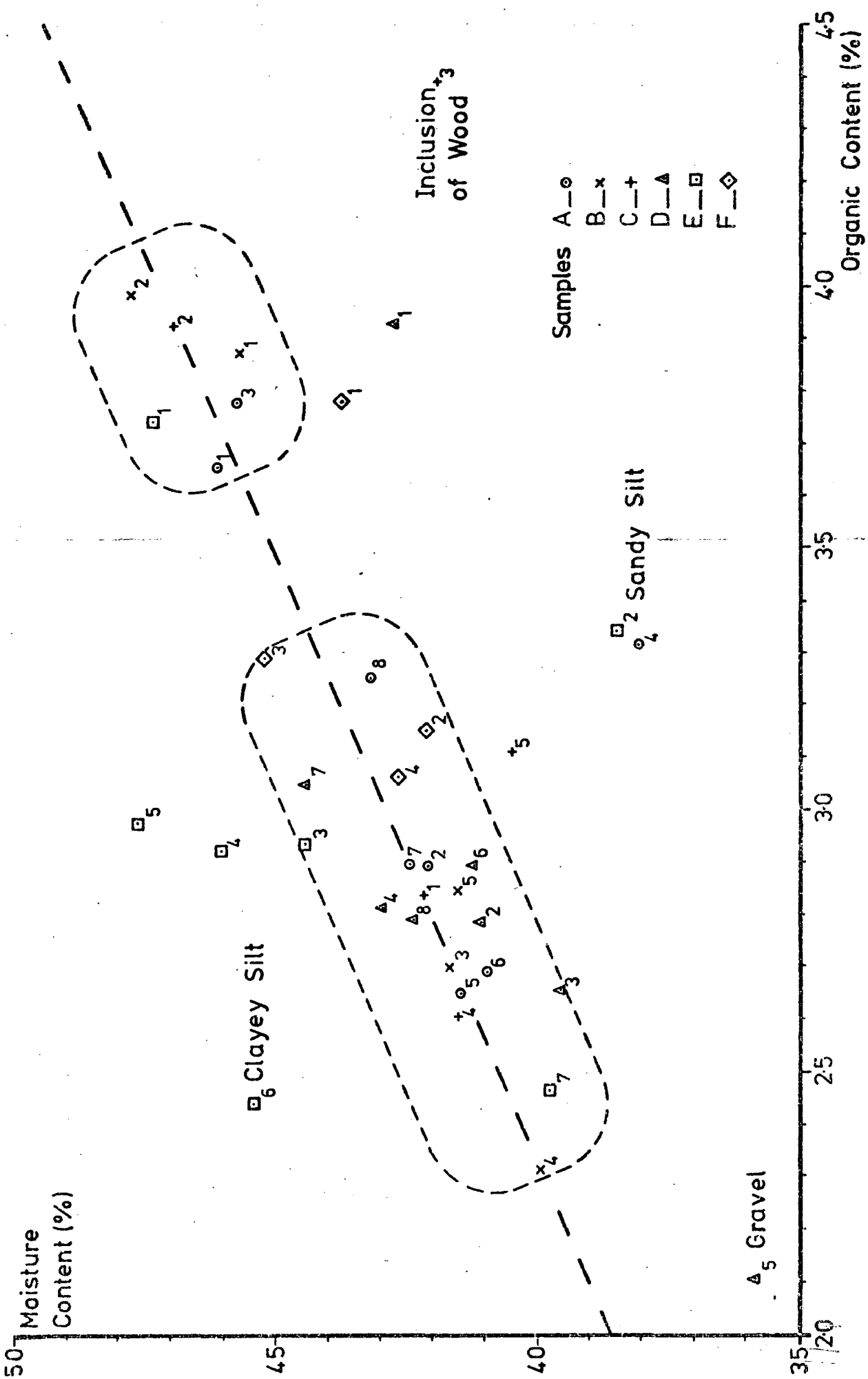


Figure 5.5: ORGANIC CONTENT vs. MOISTURE CONTENT

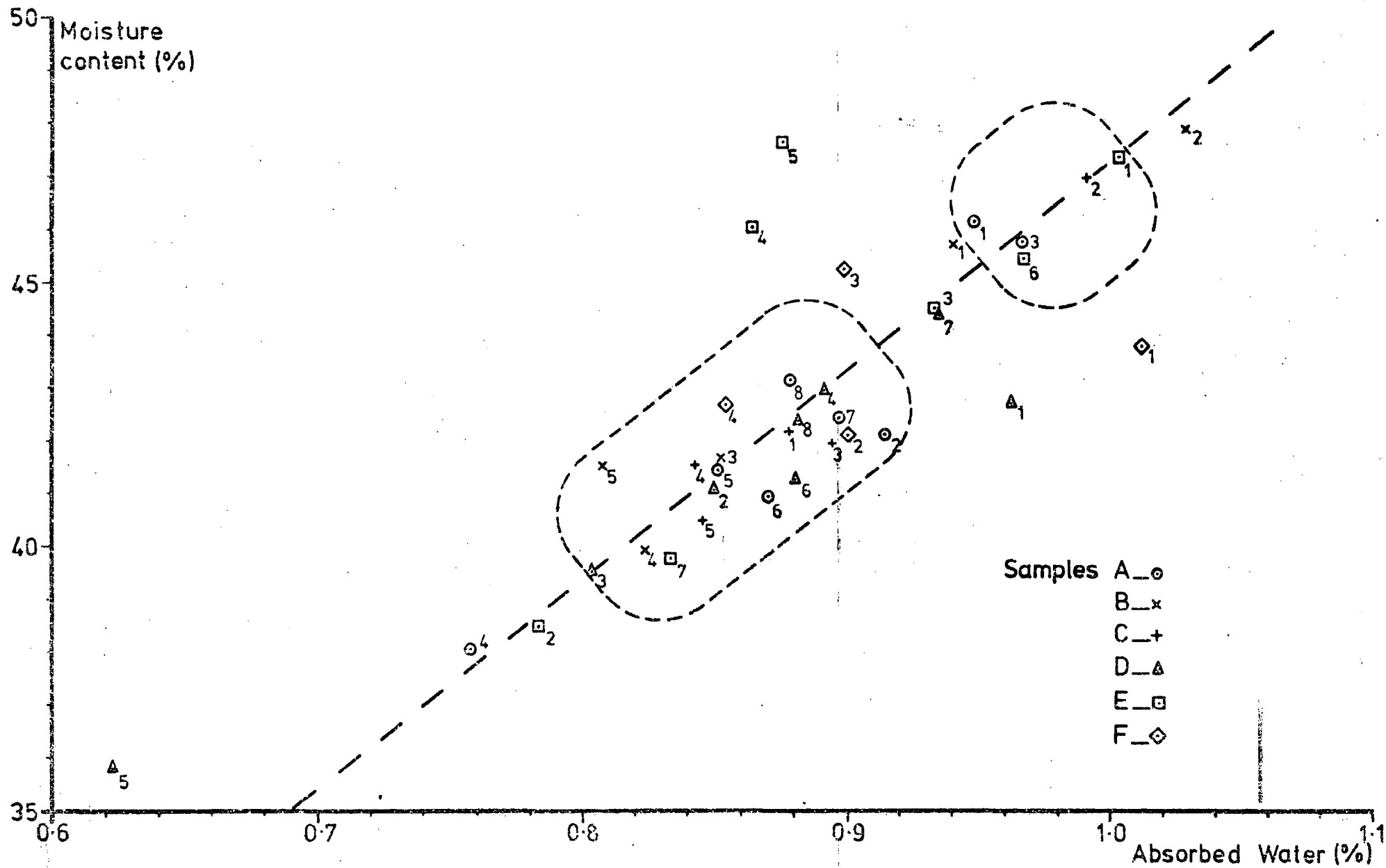


Figure 5.6: MOISTURE vs. INITIAL ABSORBED ATMOSPHERIC MOISTURE

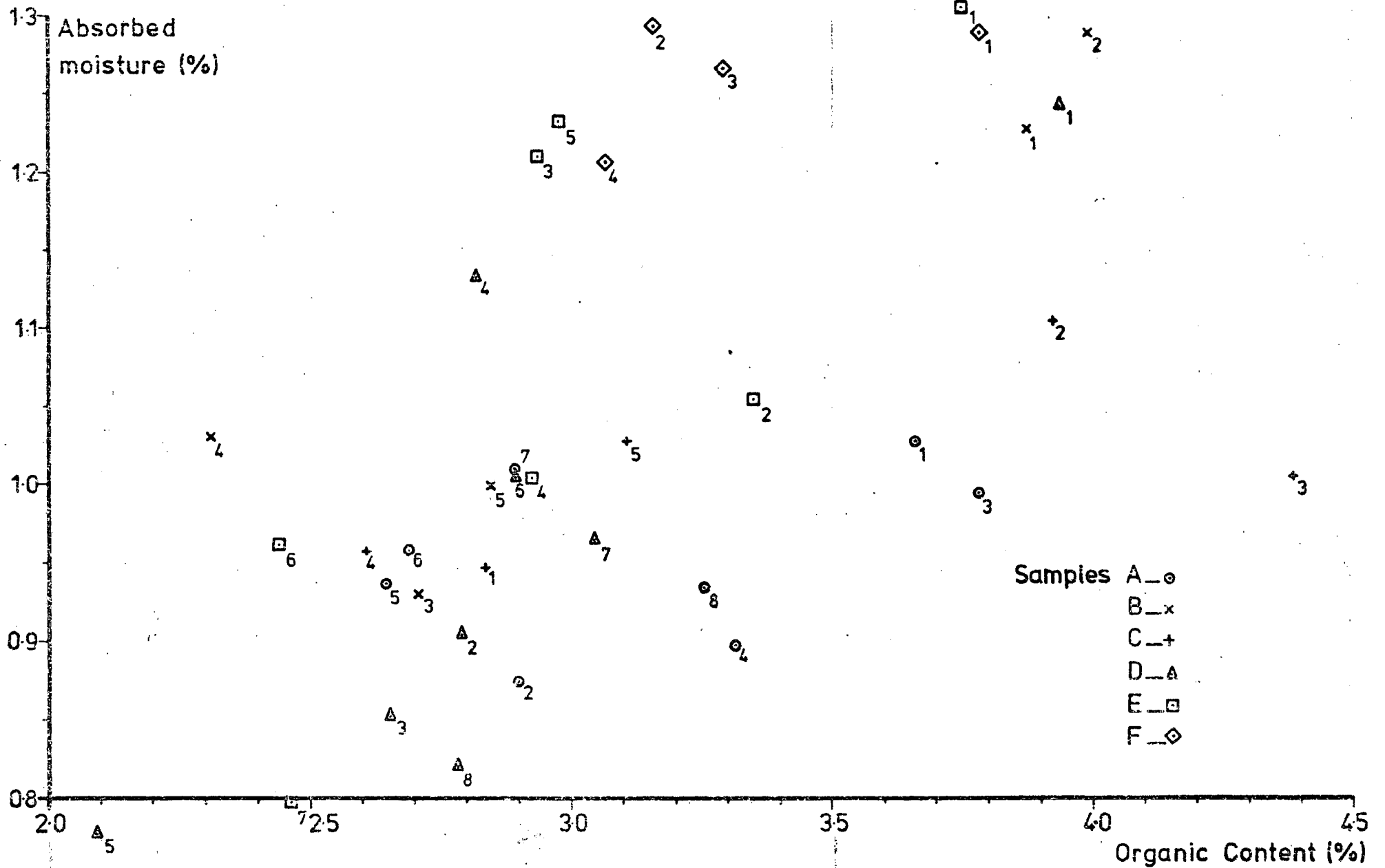


Figure 5.7: ORGANIC CONTENT vs. FINAL ABSORBED ATMOSPHERIC MOISTURE

action of the compressed air in the drive upon the face. This will be examined in more detail in Chapter 6.

Finally, in the comparison of the organic content with the final absorbed moisture, that is, that absorbed after the removal of organic material, the relationship has almost completely broken down (Figure 5.7).

In this latter case two things could explain the breakdown of the relationship, the removal of the organic material and the destruction of the sedimentary structure. Both of these factors must be important in creating the relationships observed between organic content, original moisture content and the absorbed moisture. The presence of finely disseminated organic material within the sediment must have a profound influence upon the openness of the structure of the sediment particles, and hence it is felt that the quantity of organic material is the underlying factor causing the relationships observed above and their breakdown in Figure 5.7.

The distribution of the organic contents into two distinct groups indicates the sediment may be made up of two components. This was observed occasionally in the tunnel face when freshly broken surfaces of the alluvium revealed alternating light and dark grey layers. It would appear from the results so far obtained that these layers are caused by variations in the organic content, the darker layers corresponding to the group with higher organic contents. In the tunnel face the light bands were thicker than the dark bands by approximately 3 to 5 cm for the light bands and 1 to 2 cm for the dark bands, which agrees with the ratio of high to low organic contents of 1 : 3. The layered structure was much more clearly seen in the upper part of the tunnel face, and if the organic contents are averaged for the lower and upper half of each

sample locality the lower half contains 2.974% whilst the upper half contains 3.429%. Similarly the mean organic content for each locality reveals a lateral variation across the width of the channel (Figure 5.17). These variations show a correspondence to the variations of the mineralogy within the channel and will be discussed further in the following sections.

b) X-Ray Diffraction.

The results obtained show most of the samples of alluvium possess a very similar assemblage of minerals. Those which are present are mainly Quartz, Kaolinite, Illite and the Mixed Layer Clays. Quartz and Kaolinite form distinct peaks whilst the Illite and Mixed Layer Clay appear as a series of low peaks forming a diffuse hump. A smaller, sharper peak of Muscovite was usually superimposed upon this hump for the samples of alluvium analysed. The relationship of these latter minerals is such that the Illite is formed from the hydration of Muscovite, a process which progressively lowers the Muscovite peak until only the diffuse hump remains (Figure 5.3). The Illite forms the part of the hump with the lower D-spacing, the part below the Muscovite peak, whilst the Mixed Layer Clays form the part with the higher D-spacing. By further alteration the Illite can become degraded into Mixed Layer Clays which in turn can be altered to minerals of higher D-spacing.

Alteration also causes Kaolinite to become disordered in the 001 plane and the diffraction peak is lowered and widened (Figure 5.3). Hence the presence of a tall narrow Kaolinite peak and a substantial Muscovite peak in the majority of the diffraction charts shows that the clays are relatively fresh, as might be expected, from a recently deposited sediment.

Small amounts of chlorite, calcite, dolomite, orthoclase, plagioclase, siderite and pyrite made up the remainder of the sediment. However, the accuracy of the method was not sufficient for the reliable determination of any trends shown by these minerals. Mineralogical trends were determined for the major constituents in the form of a ratio of Quartz to Total Clays compared with the equivalent organic contents (Figure 5.8). A very general relationship is shown in which samples having a high organic content were more clay rich than those with a low organic content. However, the relationship is far from conclusive due to the considerable scatter of the Quartz to Clays ratio which may be a result of the inaccuracy of the original percentages (listed in full in the Appendices). The possibility will be examined further using X-ray Fluorescence data.

Figures 5.9 to 5.12 show typical charts of samples with high and low clay contents B.2 and A.6 and of two quartz-rich samples D.2 and D.5, the latter also contained gravel material. Sample D.5 was prepared by sieving with a B.S. 212 sieve, followed by 15 minutes of grinding in a pestle and mortar of both D.2 and D.5 to reduce the size of the quartz particles. This was carried out because large quartz grains produce anomalously low peak area ratios (G.W. Brindley, 1961). Muscovite and carbonate peaks for these latter two are much reduced or absent showing hydration and solution has occurred. Increased ground water percolation in these more permeable beds is probably the cause of this feature.

The unweathered sample of boulder clay H had a very similar mineralogy to the alluvium samples (Figure 5.13). Two cores of weathered material G.1 and G.2 showed, however, several distinct differences in mineralogy, the most obvious of which was an absence of calcite, dolomite and siderite removed by leaching from percolating rainfall.



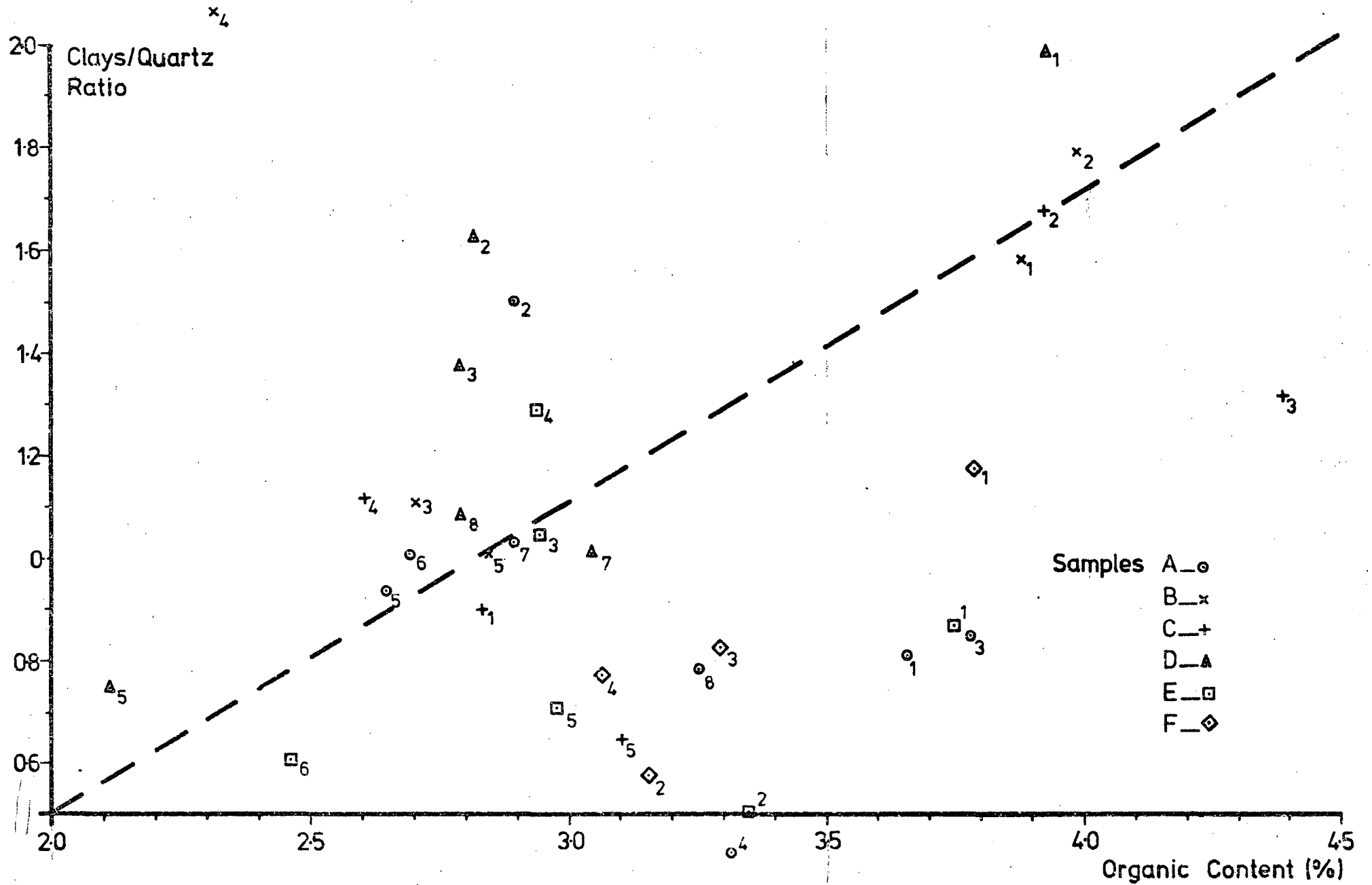


Figure 5.8: ORGANIC CONTENT vs. CLAYS TO QUARTZ RATIO

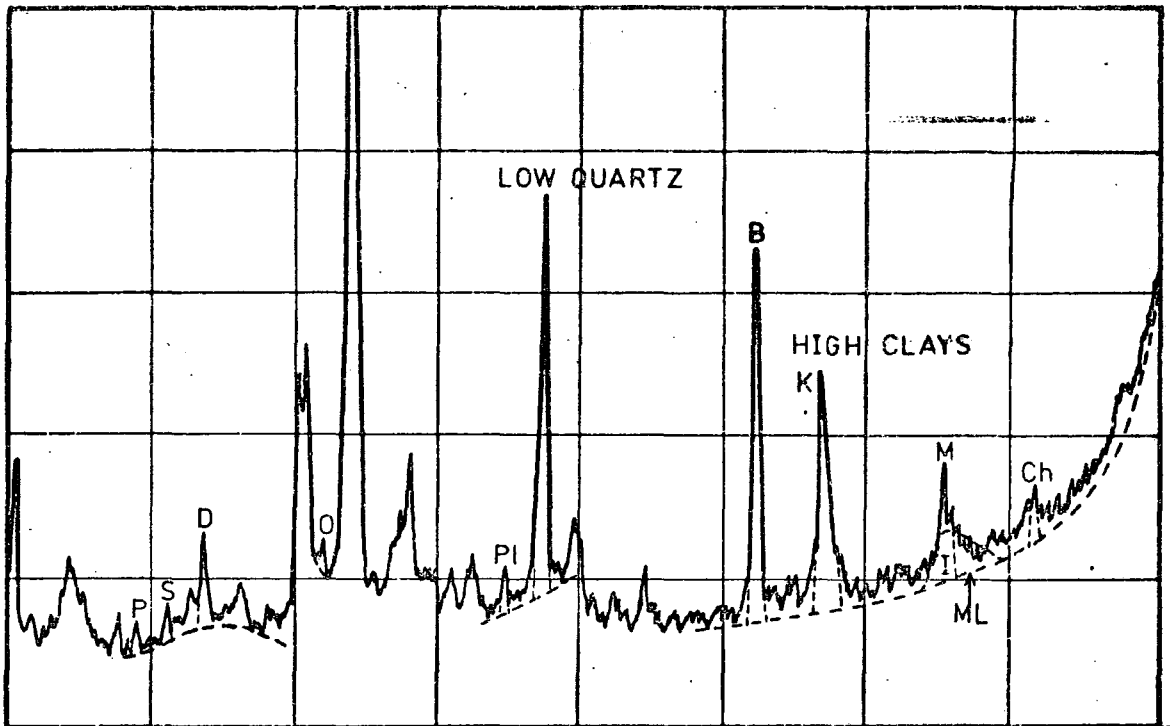


Figure 5.9: XRD. CHART OF ORGANIC-RICH SAMPLE (B.2)

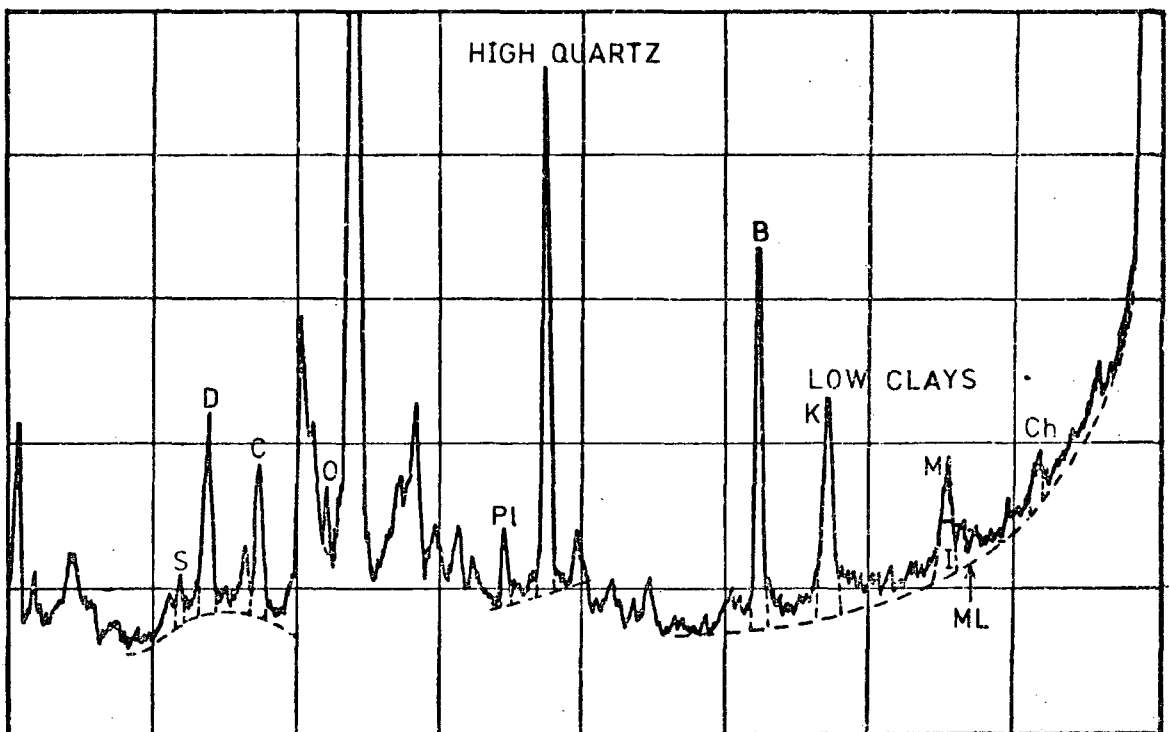


Figure 5.10: XRD. CHART OF ORGANIC-POOR SAMPLE (A.6)

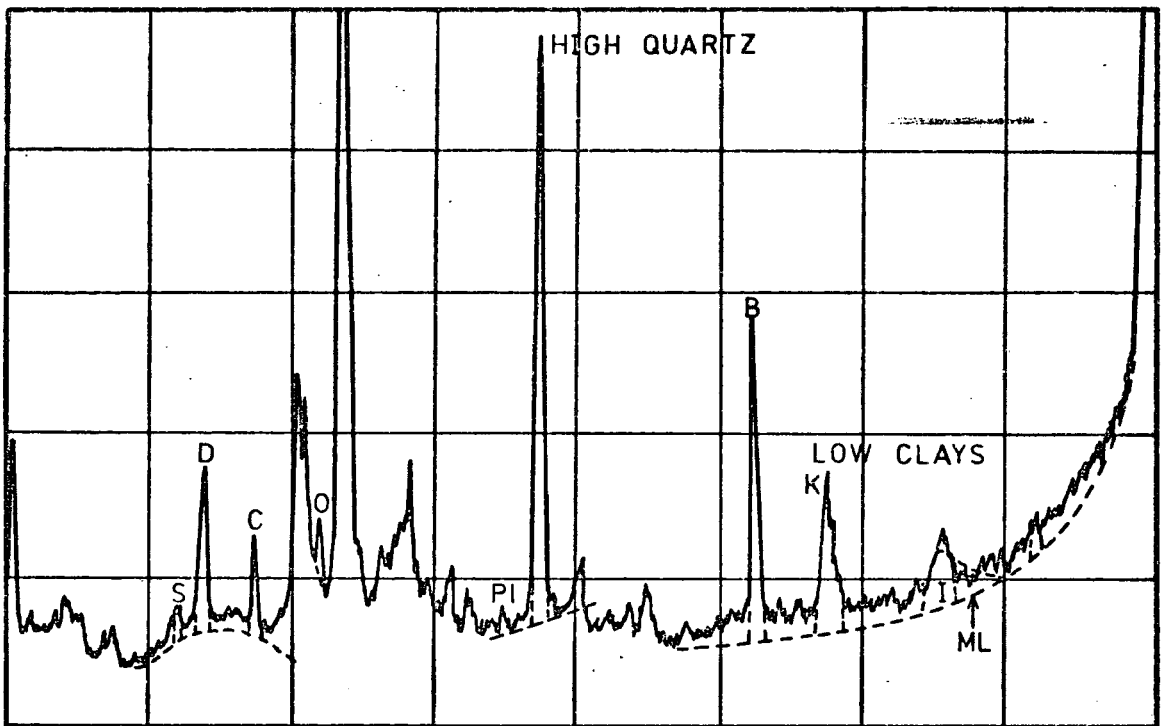


Figure 5.11: XRD. CHART OF QUARTZ-RICH SAMPLE (E2C)

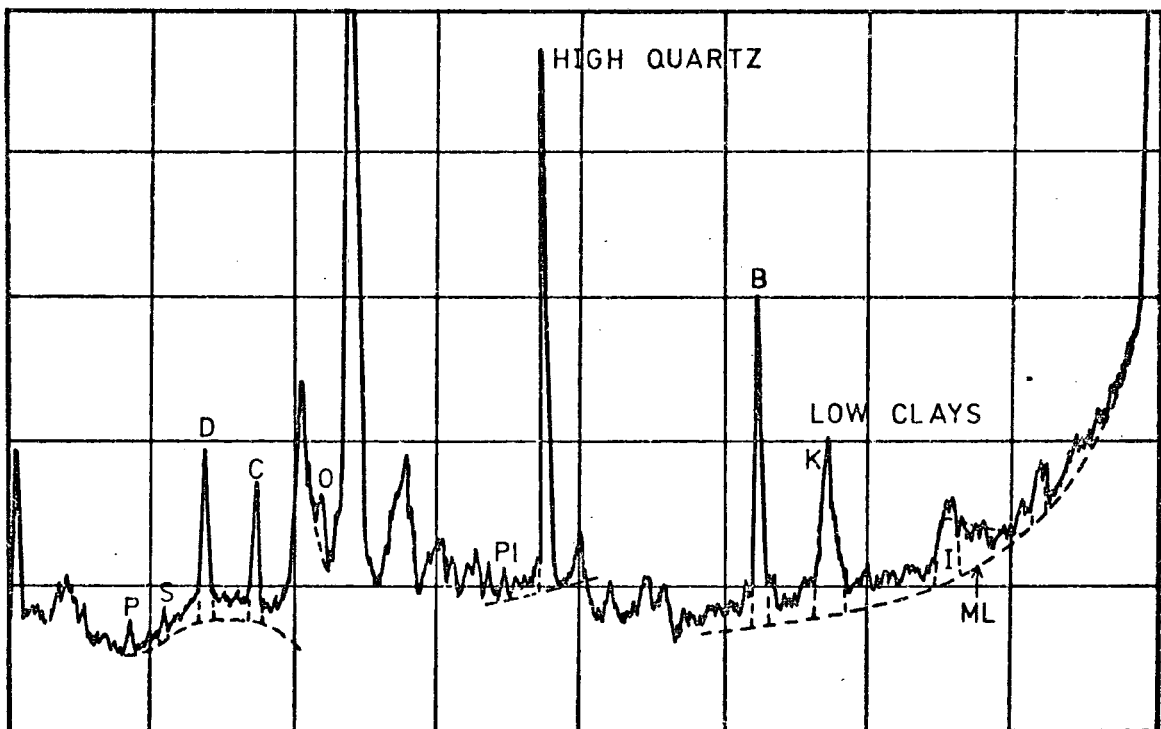


Figure 5.12: XRD. OF SAMPLE CONTAINING GRAVEL (D5C)

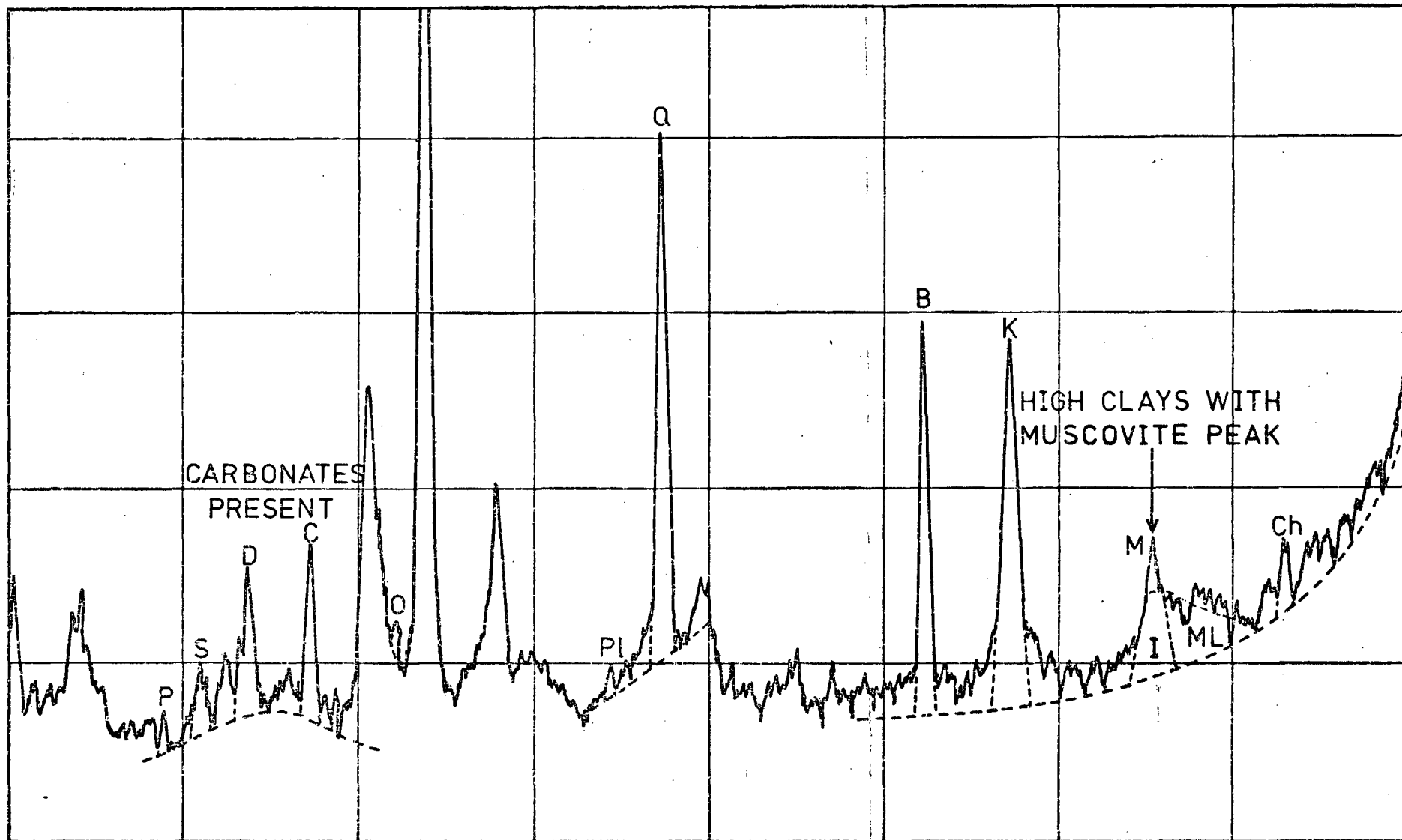


Figure 5.13: XRD. CHART OF UNWEATHERED BOULDER CLAY SAMPLE (H)

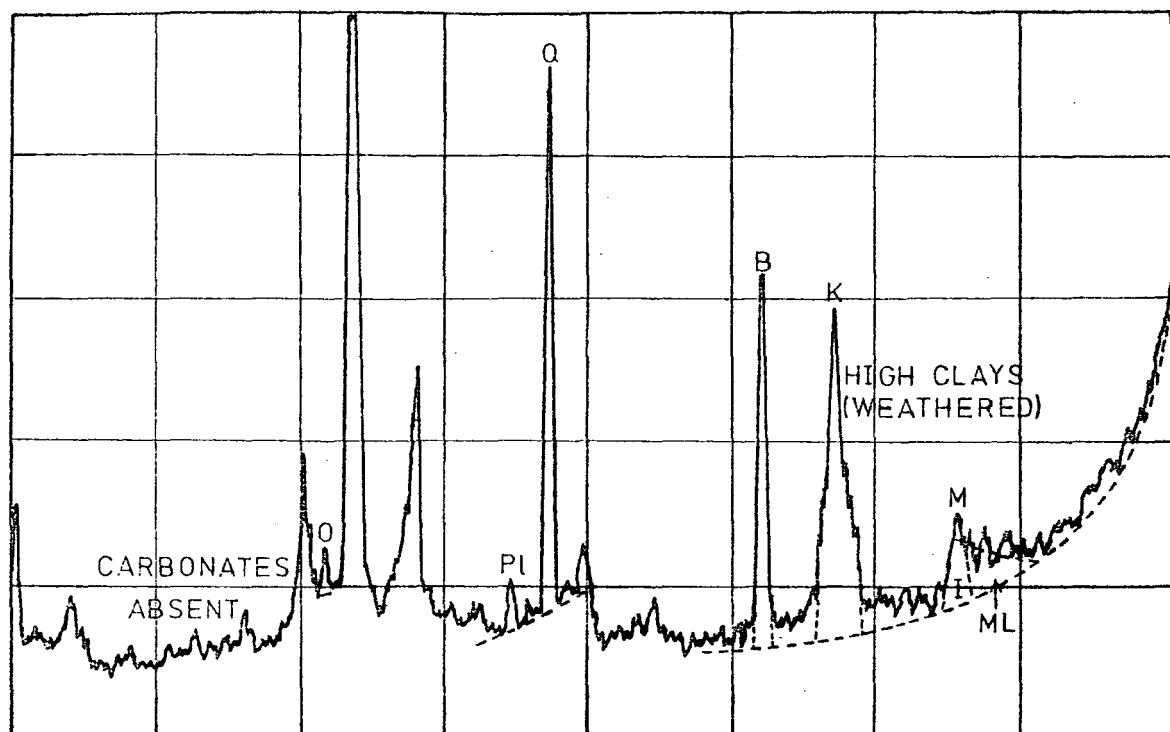


Figure 5.14: XRD. CHART OF WEATHERED BOULDER CLAY SAMPLE (G.1A)

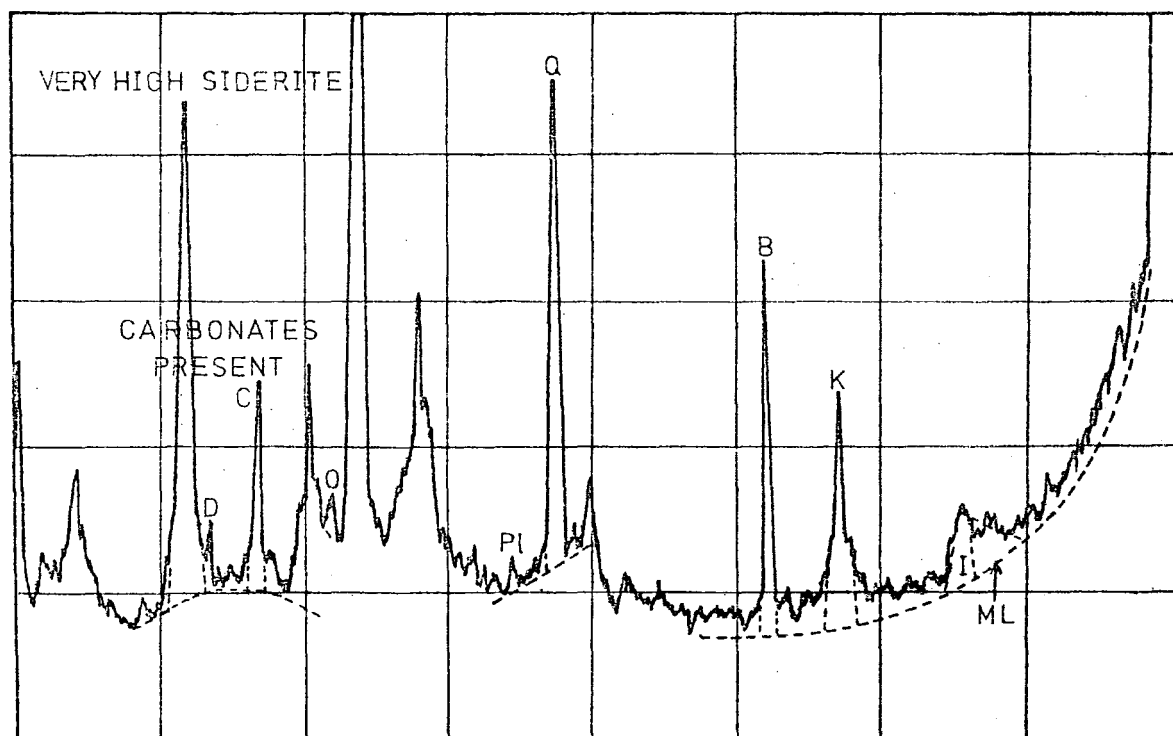


Figure 5.15: XRD. CHART OF ZONE OF CARBONATE ACCUMULATION (G.1H)

In addition to this the Muscovite peak was much reduced or absent due to hydration to Illite by the same process (Figure 5.14). Samples taken from the deepest point in both these cores had a mineralogy in which the carbonate minerals reappeared, in the case of siderite the quantity was higher than that seen in any other sample (Figure 5.15). This feature will be discussed further using X-ray Fluorescence evidence.

Stones found in the samples were mainly of fine grained, laminated sandstones with coarser sandstones, shales and occasional coal fragments indicating probable derivation from the Coal Measures. Examination of the gravel material revealed a similar suite of fragments showing that at least the lenses of gravel were derived directly from the boulder clay by stream action.

c) X-Ray Fluorescence.

The X-ray Fluorescence results express the geochemistry of the alluvium and boulder clay as the proportions of the major elements in the form of percentages of their oxides. Some of these can be taken as being representative of the relative proportions of some of the minerals. Sulphur, when present is mainly that which is contained in iron pyrites and changes in the quantities of calcium and magnesium are a good indication of changes in the quantities of calcite and dolomite. In addition variations in the ratio of Total Silica to Aluminium correspond to variations in the proportions of quartz to clays. Although this is only applicable to a group of samples with very similar clay minerals and is not the normal use of the ratio.

When the ratio is compared with the distribution of organic contents of the samples, a better relationship of increasing clay content corresponding to increasing organic content (Figure 5.16). There is

much less scatter from these results which further points to the inaccuracy of the X-ray Diffraction data. By averaging the silica to aluminium ratios for each locality a lateral variation was again found. This shows an increase in the amount of silica in the middle of the channel where the lenses of sand and gravel were encountered (Figure 5.17). Similarly, the mean of the iron oxide percentages for each locality show a minimum content in the middle of the channel which may be related to lateral variations of the clays.

By finding the mean of the oxides for the two main groups in Figure 5.4 the contrast between the geochemistry of samples with low and high organic contents can be demonstrated, Table 4. Samples with a high organic content show an increased mean Silica to Aluminium ratio of 0.2829 compared to 0.2367, which indicates they are more clay rich. These samples also have a higher mean iron oxide content of 5.87% compared to 4.86% and a higher sulphur content of 1.30% to 0.78%. The latter shows a connection between the occurrence of iron pyrites and the quantity of organic material. Pyrites is known to form within a sediment under strong reducing conditions, such as those produced by the anaerobic decay of organic material. Therefore the layers with a higher organic content are the most favourable for pyrites formation.

As with mineralogy, the geochemistry of the boulder clay H was very similar to that of the alluvium. Notable exceptions are the higher Silica to Aluminium ratio of 0.3624 compared to 0.2383, which indicates a higher proportion of clays in the boulder clay, and the sulphur content of 0.31% which is much lower than the mean of 0.91% for the alluvium. Since the latter indicates there is much less pyrites in the boulder clay it is unlikely that the pyrites of the alluvium was derived from the drift.

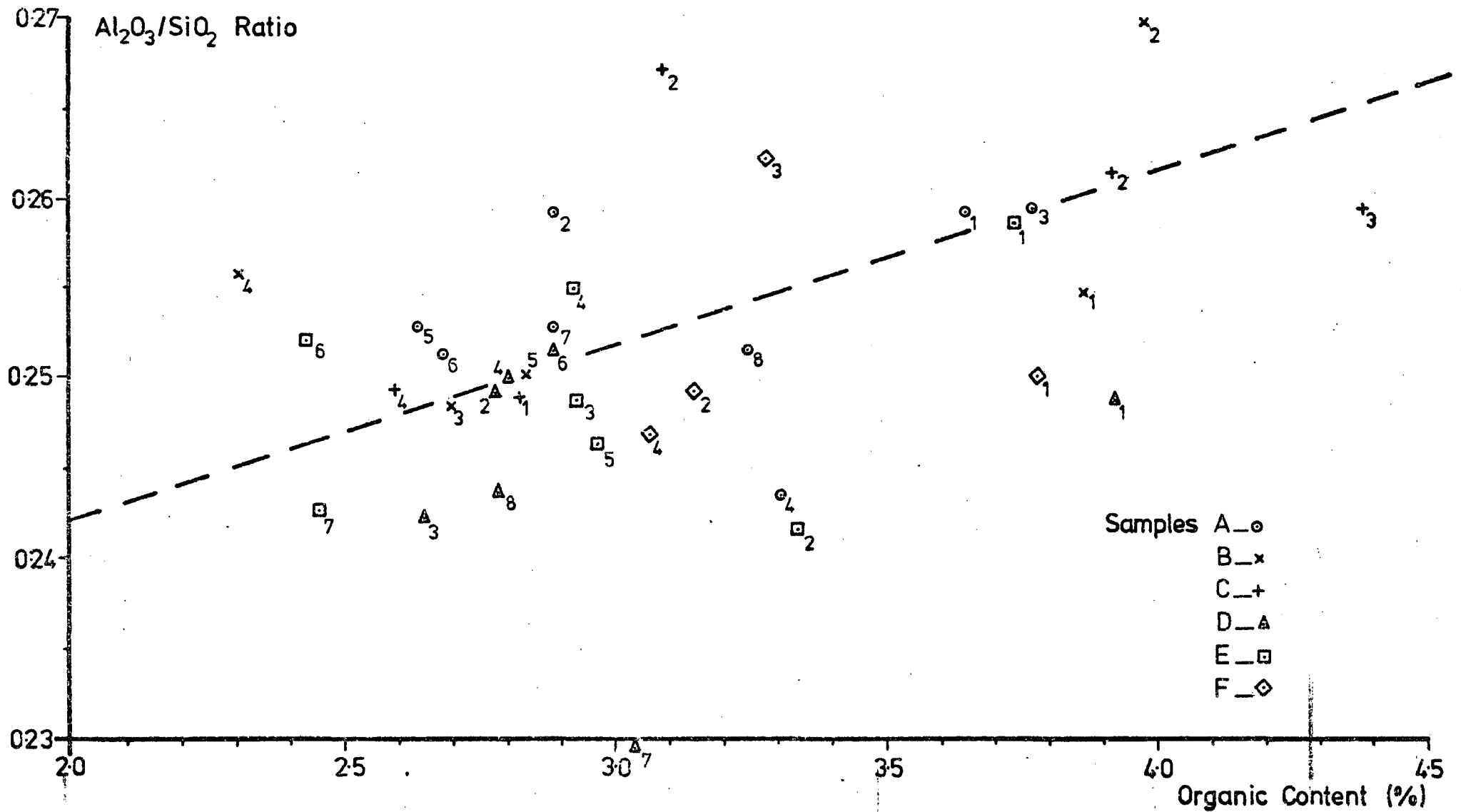


Figure 5.16: ORGANIC CONTENT vs. ALUMINIUM TO SILICA RATIO

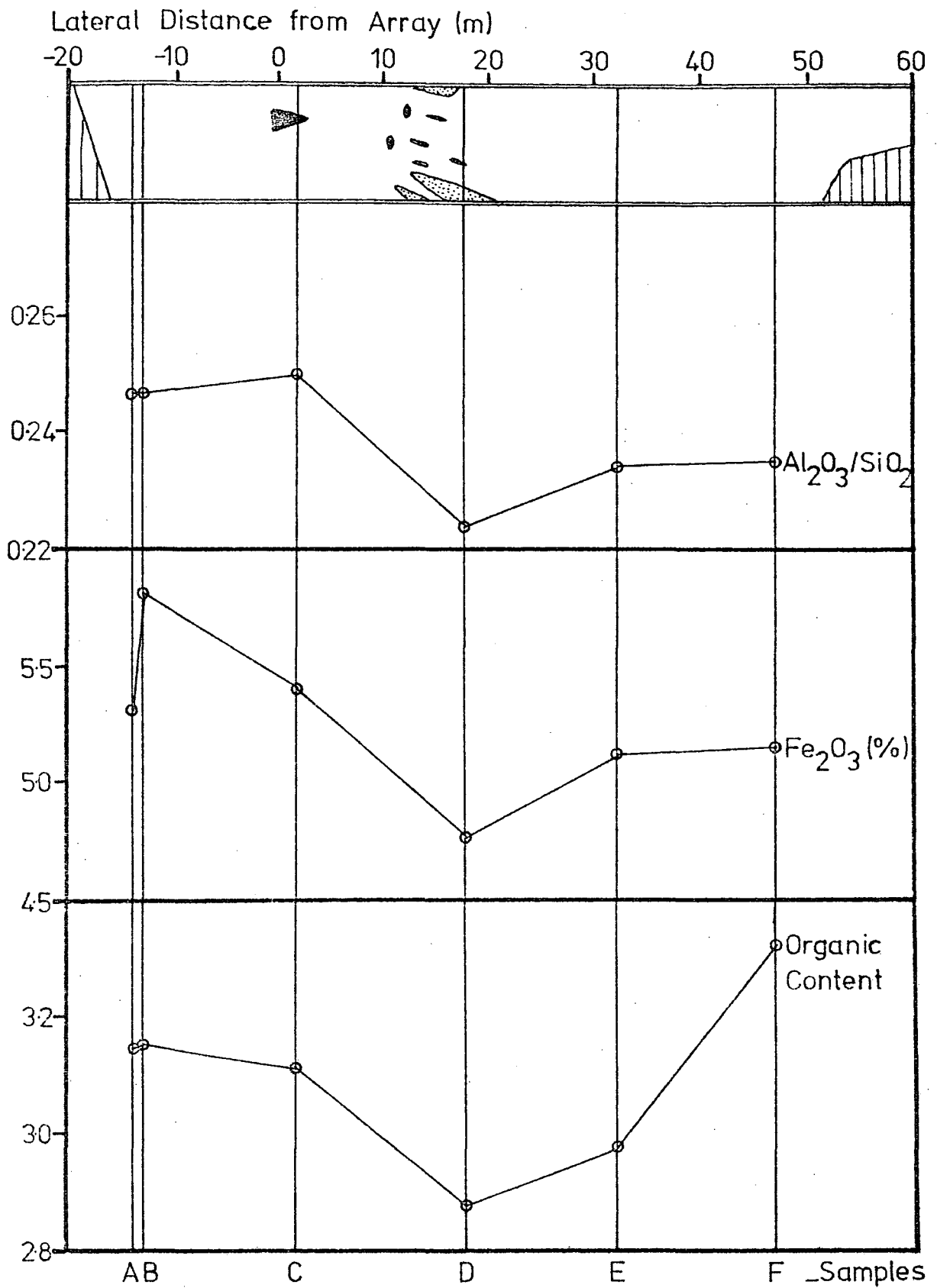


Figure 5.17: LATERAL VARIATION IN GEOCHEMISTRY WITHIN THE CHANNEL

Oxide	Low Organic Alluvium	High Organic Alluvium	Unweathered Boulder Clay	Weathered Boulder Clay
SiO ₂	55.10	56.51	53.67	55.29
Al ₂ O ₃	13.04	15.99	19.45	20.57
Fe ₂ O ₃	4.86	5.87	6.15	5.07
MgO	2.61	2.60	2.40	5.73
CaO	4.41	3.52	4.15	0.41
Na ₂ O	0.75	0.72	0.60	0.46
K ₂ O	3.47	3.40	3.19	2.67
TiO ₂	0.77	0.83	0.86	0.98
S	0.78	1.30	0.31	0.20
P ₂ O ₅	0.13	0.13	0.10	0.10
Al ₂ O ₃ /SiO ₂	0.2367	0.2828	0.3624	0.3720

Table 4: COMPARATIVE GEOCHEMISTRY OF ALLUVIUM AND BOULDER CLAY SAMPLES.

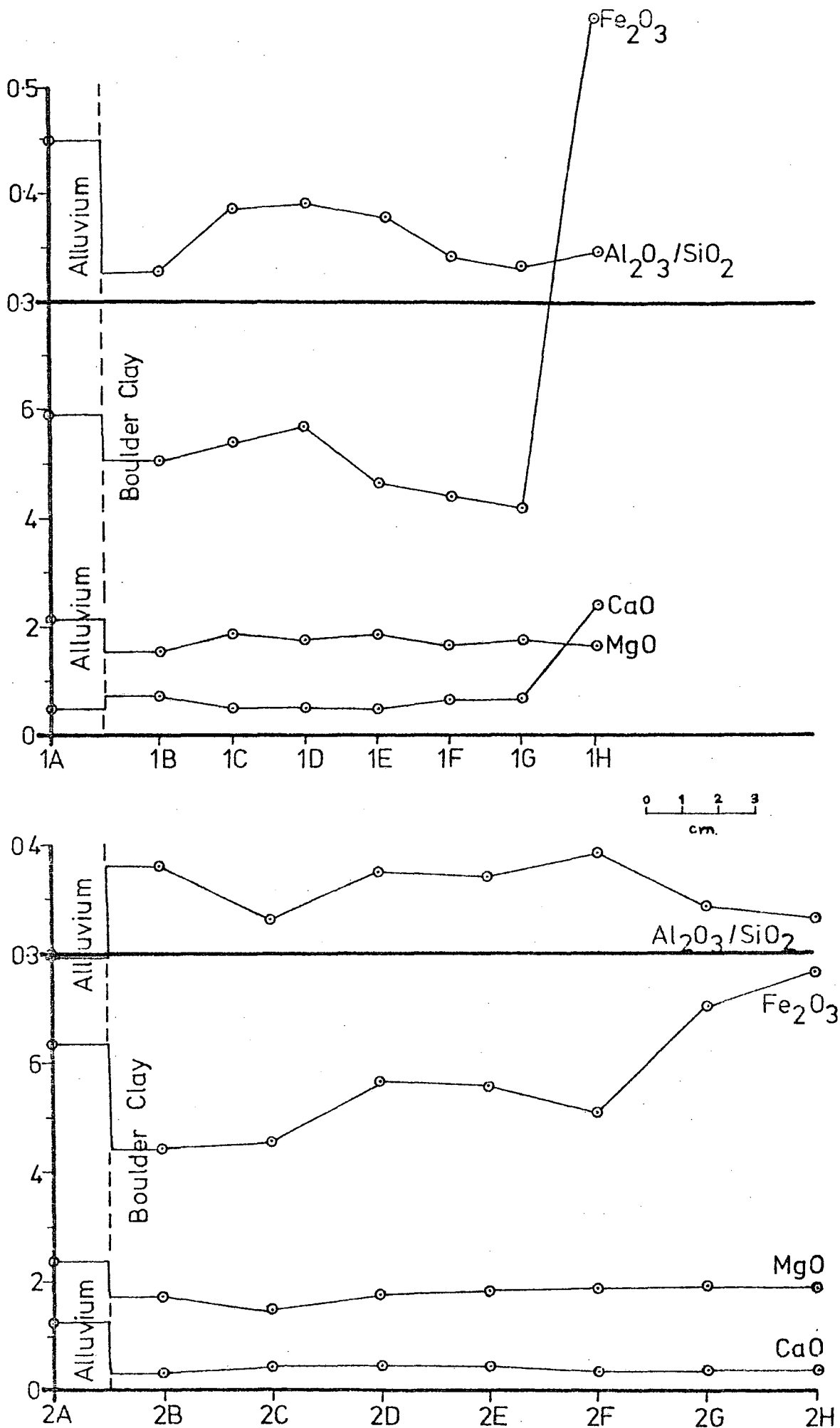


Figure 5.18: GEOCHEMICAL PROFILE OF WEATHERED SURFACE OF BOULDER CLAY

The geochemistry of samples G.1 and G.2 clearly illustrate the effects of leaching upon the boulder clay (Figure 5.18). Leaching has removed much of the calcium, magnesium and iron from the upper samples and redeposited them in the deepest samples, which corresponds to the distribution of calcite, dolomite and siderite in the mineralogy. Iron was particularly concentrated to between 7.5% and 13%, which is shown to be mainly siderite by the mineralogy. An accumulation of iron and carbonates in a weathered profile suggests the presence of a hard iron pan at 10 to 20cm depth below the surface. A feature which is commonly found in present day soils and weathered horizons. The evidence shows, therefore, that it is very probable that in the past the surface of the boulder clay was exposed to sub-aereal weathering processes for a period of time.

5.4 Grainsize Distribution.

Grainsize distribution determinations of three samples were carried out by wet sieving and pipette analysis according to B.S. 1377.

The results illustrated in Figures 5.19 and 5.20 show examples of each of the two main groups of samples, A.6 with a low organic content of 2.693 and B.2 with a high organic content of 3.984. These clearly demonstrate the higher clay content of B.2 compared to A.6. Figure 5.21 also illustrates the grainsize distribution of sample D.5 taken from a thin bed of gravelly alluvium. Some of the larger lenses of sand and gravel probably contained much greater proportions of sand and gravel. The skew of these distribution curves is typical of alluvial silts (T.W. Lambe and R.V. Whitman, 1961).

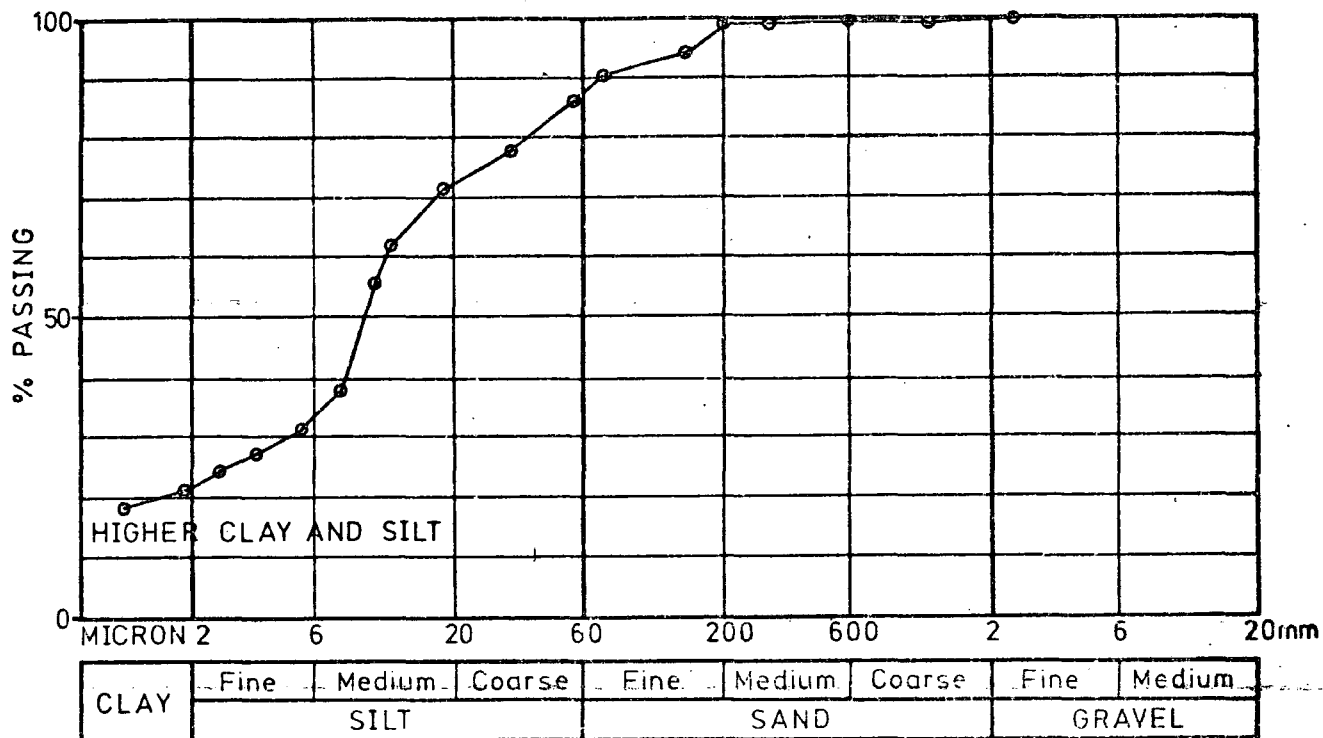


Figure 5.19: GRAINSIZE DISTRIBUTION FOR ORGANIC-RICH SAMPLE (B.2)

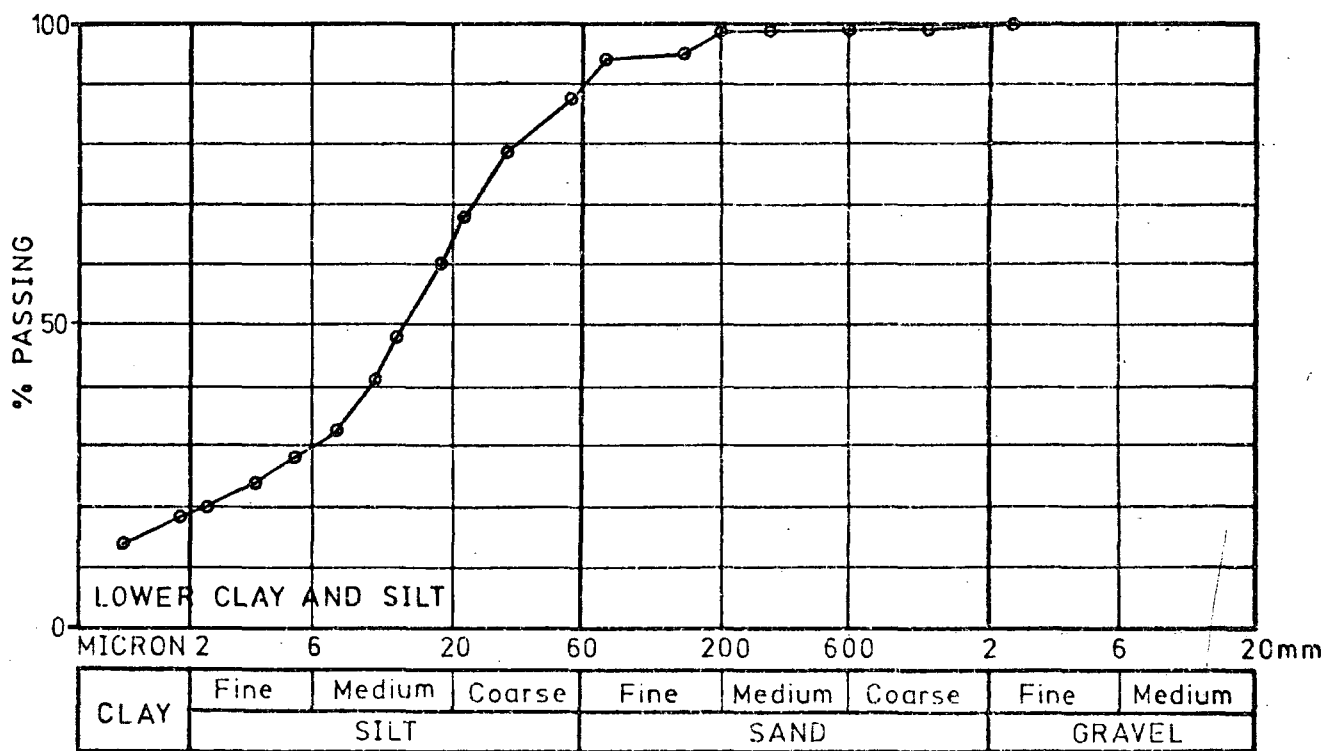


Figure 5.20: GRAINSIZE DISTRIBUTION FOR ORGANIC-POOR SAMPLE (A.6)

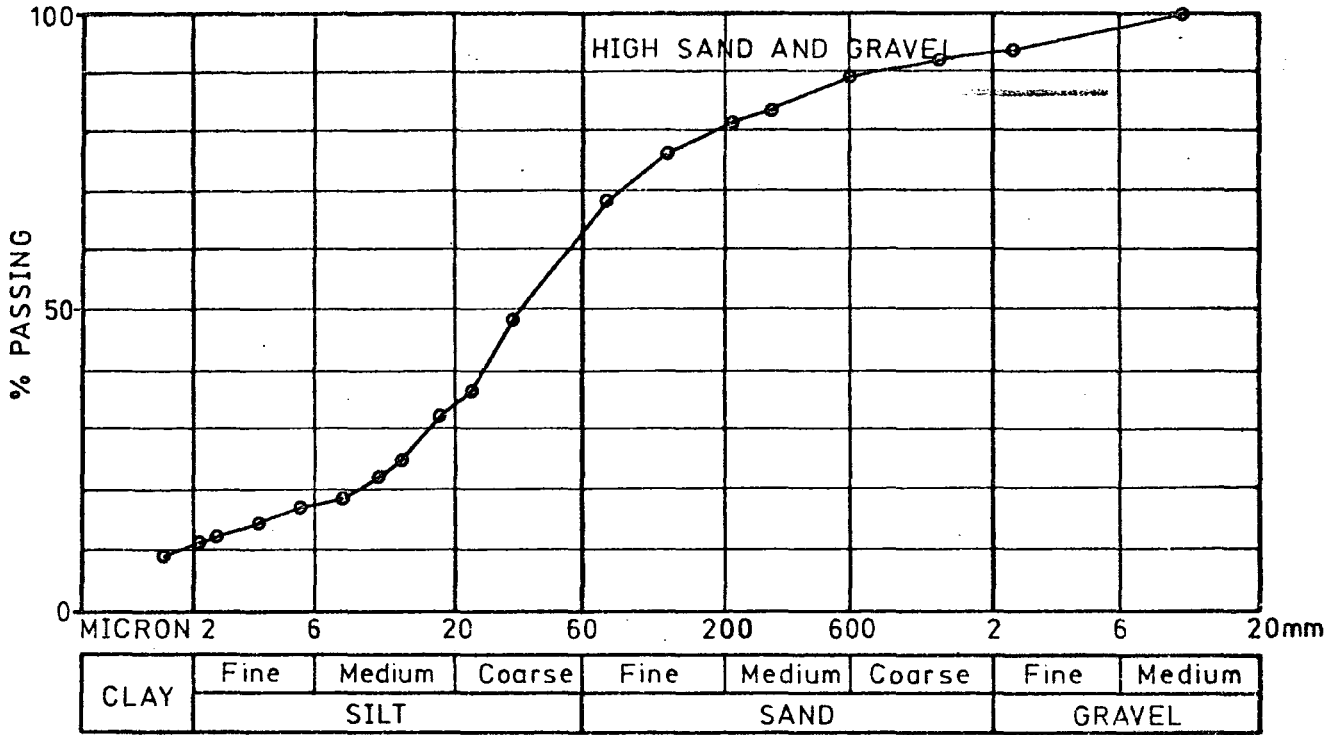


Figure 5.21: GRAINSIZE DISTRIBUTION FOR SAMPLE CONTAINING GRAVEL

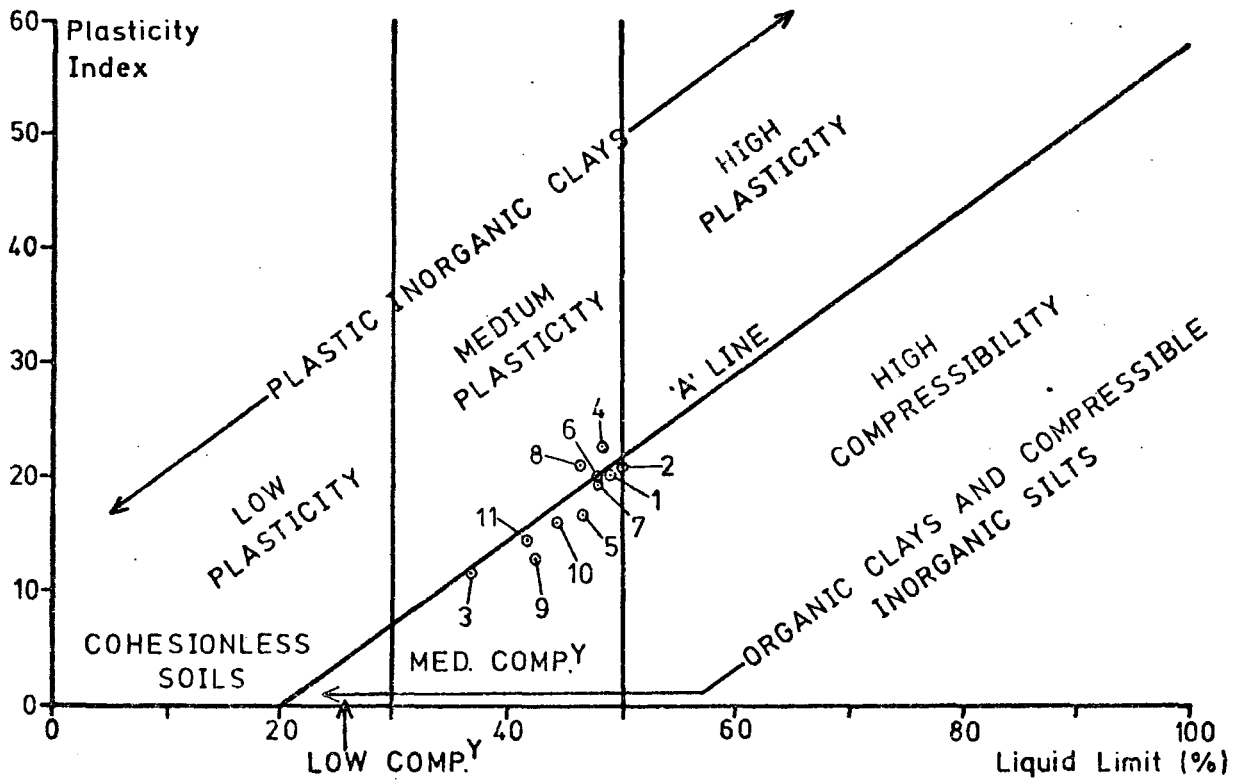


Figure 5.22: LIQUID LIMIT vs. PLASTICITY INDEX

Number	Sample	Plastic Limit(%)	Liquid Limit(%)	Plasticity Index(%)
1	A.6	29.03	49.40	20.37
2	B.2	29.27	50.00	20.73
3	D.S (Gravelly)	24.95	37.05	12.10
4	E.3	26.12	48.63	22.51
5	F.1	29.89	46.71	16.82
6	1.a*	28.20	48.50	20.30
7	1.b*	28.60	48.50	19.80
8	1.c*	25.54	46.50	20.96
9	2.a*	28.49	42.60	13.11
10	2.b*	28.19	44.50	16.31
11	2.c*	27.23	41.80	14.57

* after N. El-Naga

Table 5: LIQUID AND PLASTIC LIMITS.

5.5 Liquid and Plastic Limits.

Liquid and plastic limits were determined for the three samples which were used for the grainsize analysis and for several other samples according to B.S. 1377. The results obtained are listed in Table 5 and have been plotted on Figure 5.22 of Liquid Limit vs. Plasticity Index. The majority of the results fall close to the 'A' line with the region of organic silts, which complies with the analyses of the samples, although some points cross into the region of inorganic clays of medium plasticity.

Chapter 6

GROUNDWATER AND CONSOLIDATION STUDIES

6.1 Moisture Contents in the Tunnel Face.

The stabilization of the tunnel face by compressed air results from the occurrence of two processes. Mainly the face is supported by the force exerted by the air pressure upon the face. Simultaneously the material in the face is strengthened by a reduction in the moisture content, which occurs when the air pressure exceeds the pore water pressure.

In order to investigate the latter phenomenon, the cores from localities D, E and F were analysed in detail for variations in moisture content and organic content with respect to depth into the tunnel face. The results that were obtained are presented in the Appendices. The strong influence of the organic content has already been noted in Chapter 5. Considerable variations in the amount of organic material were encountered from core to core and small variations between different samples from the same core. As a result of this it was necessary that the influence of variations in the organic content, upon the moisture contents of each sample, should be removed.

The gradient of the line through the two main groups of points in Figure 5.4 was used to achieve the correction. For a given organic

content, the intersection of the value with the line gave a moisture content which the sample would have possessed in the absence of any other influence. Therefore, by using the various organic contents, it was possible to find the difference between the moisture content for each sample, and that which it should have possessed under normal conditions:

$$\begin{array}{rcl} \text{Moisture Content} & - & \text{Gradient} \times \text{Organic Content} \\ \text{(Determined)} & & \text{(4.32)} \quad \text{for Sample} \\ & & \text{(Determined)} \end{array} = \text{Deviation from normal m/c.}$$

Although the method relies too heavily upon the controlling effects of the organic content over the moisture content, the corrected results show a much more consistent pattern than before the correction was applied. The results are illustrated in Figures 6.1 to 6.3 for each locality as a percentage deviation from the normal moisture content, varying with depth into the face.

In general these show a reduction of moisture content from the normal in cores taken from the top of the tunnel, and an increase for cores from the bottom of the face. Also the profiles into the tunnel face show a rapid increase in moisture content, followed by a reduction, producing a peak value at between 5 and 10cm into the face. This is particularly evident from cores taken from the lower part of the tunnel face. It is possible that the profiles may be a result of variable compressive forces exerted on the alluvium during the insertion of the sampling tubes and the extrusion of the cores. Alternatively, they may represent the interaction of air pressure and pore pressure at depth within the tunnel face.

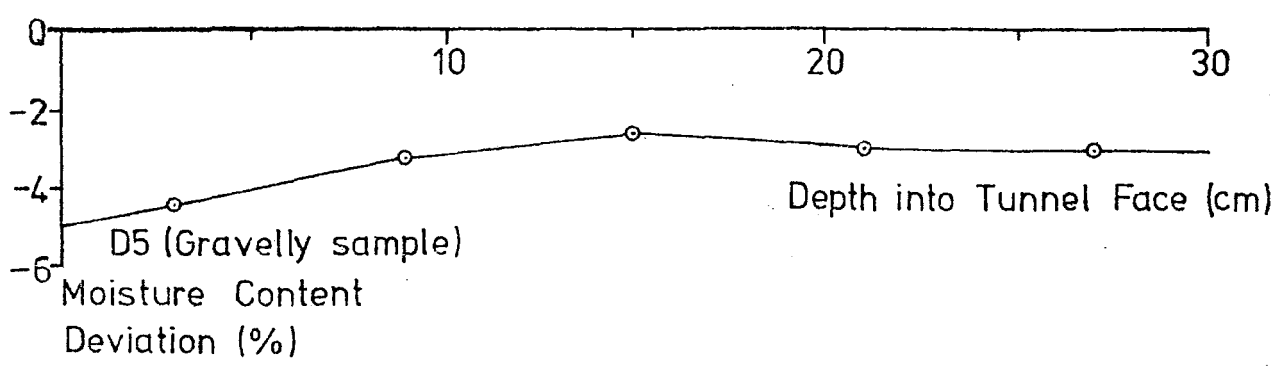
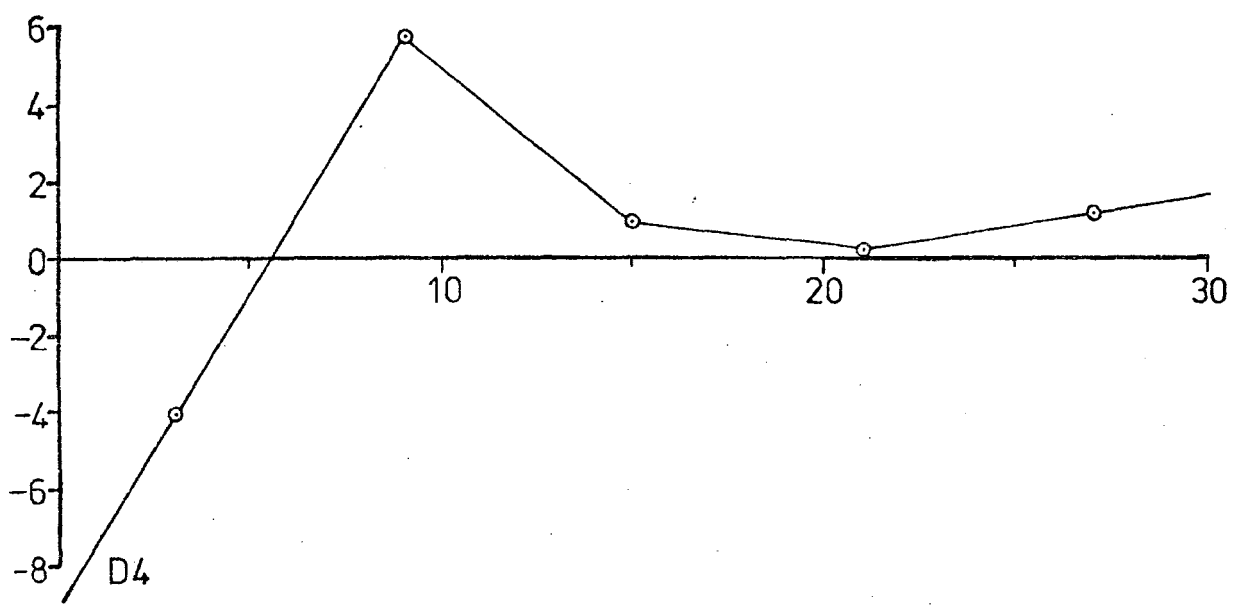
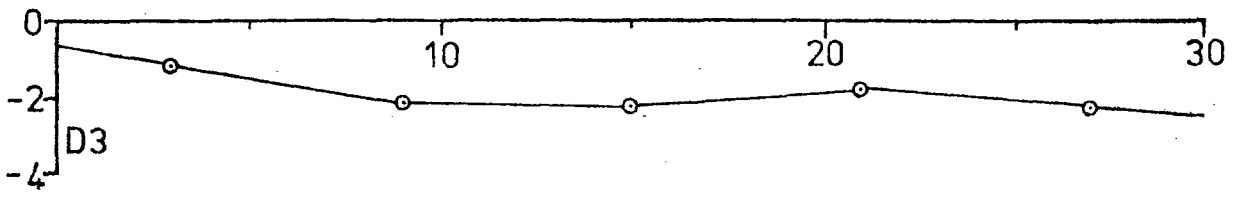
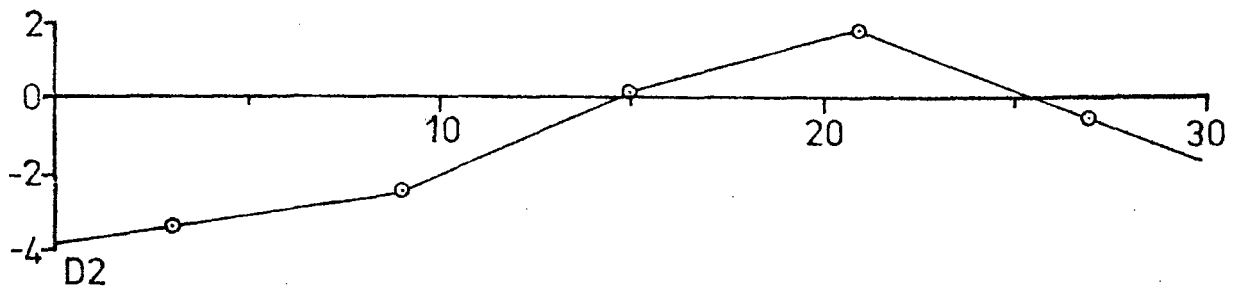
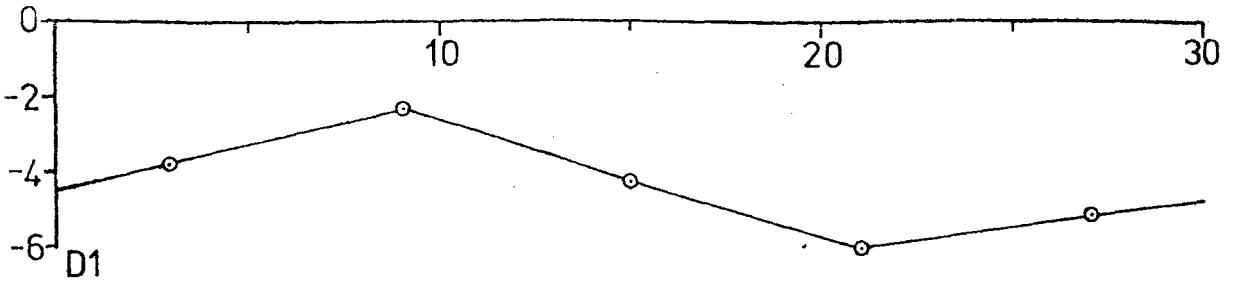
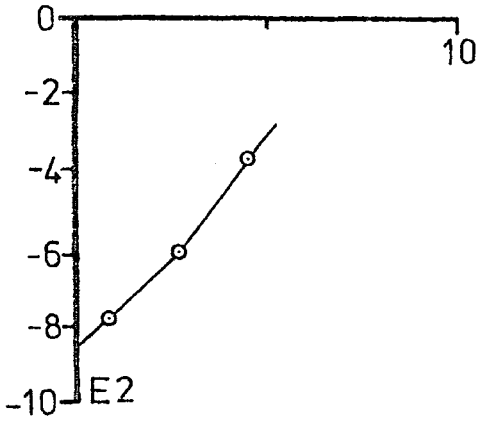
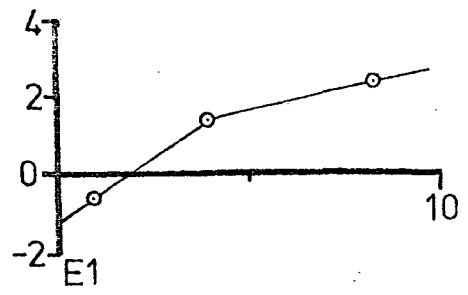


Figure 6.1: VARIATION IN MOISTURE CONTENT WITHIN THE TUNNEL FACE_SAMPLES D (see Figure 5.1)



Moisture Content Deviation (%)

Depth into Tunnel Face (cm)

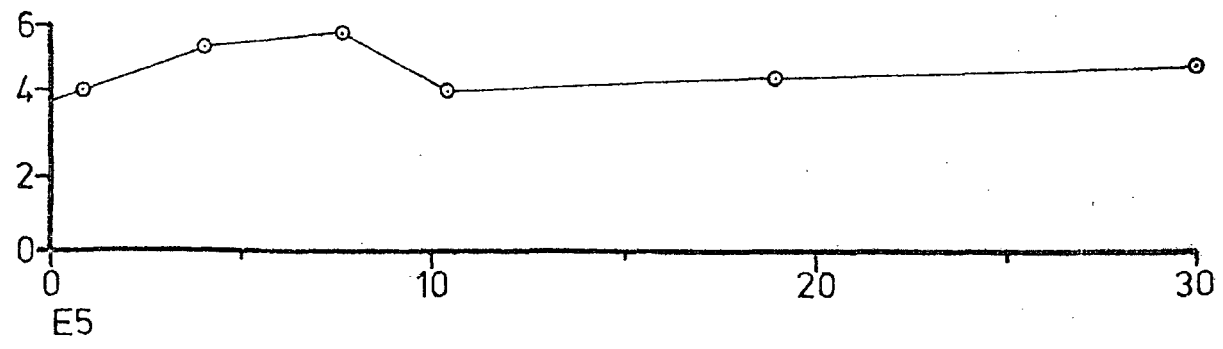
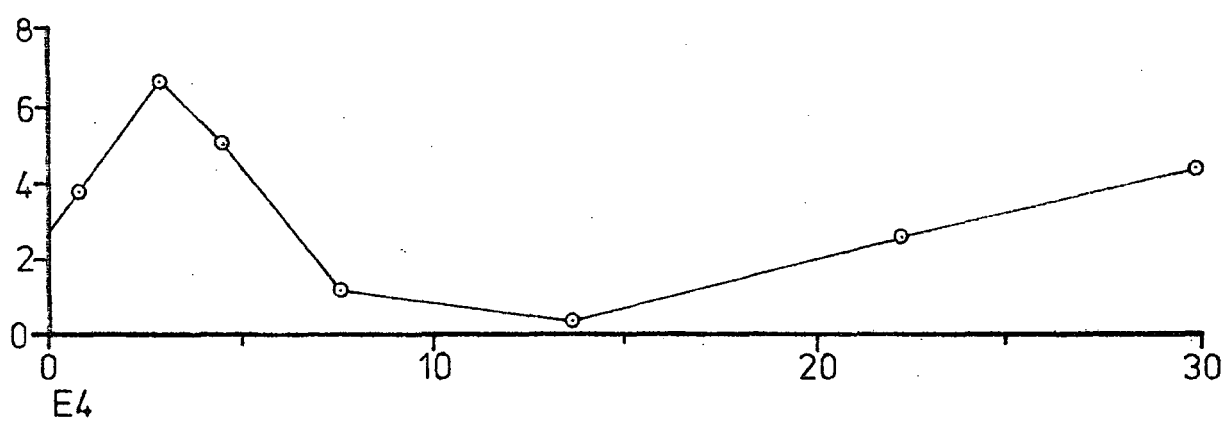
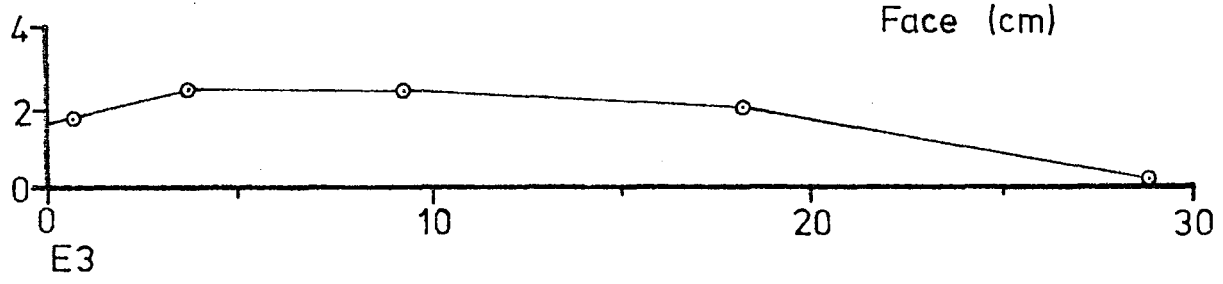


Figure 6.2: VARIATION IN MOISTURE CONTENT WITHIN THE TUNNEL FACE_SAMPLES E (see Figure 5.1)

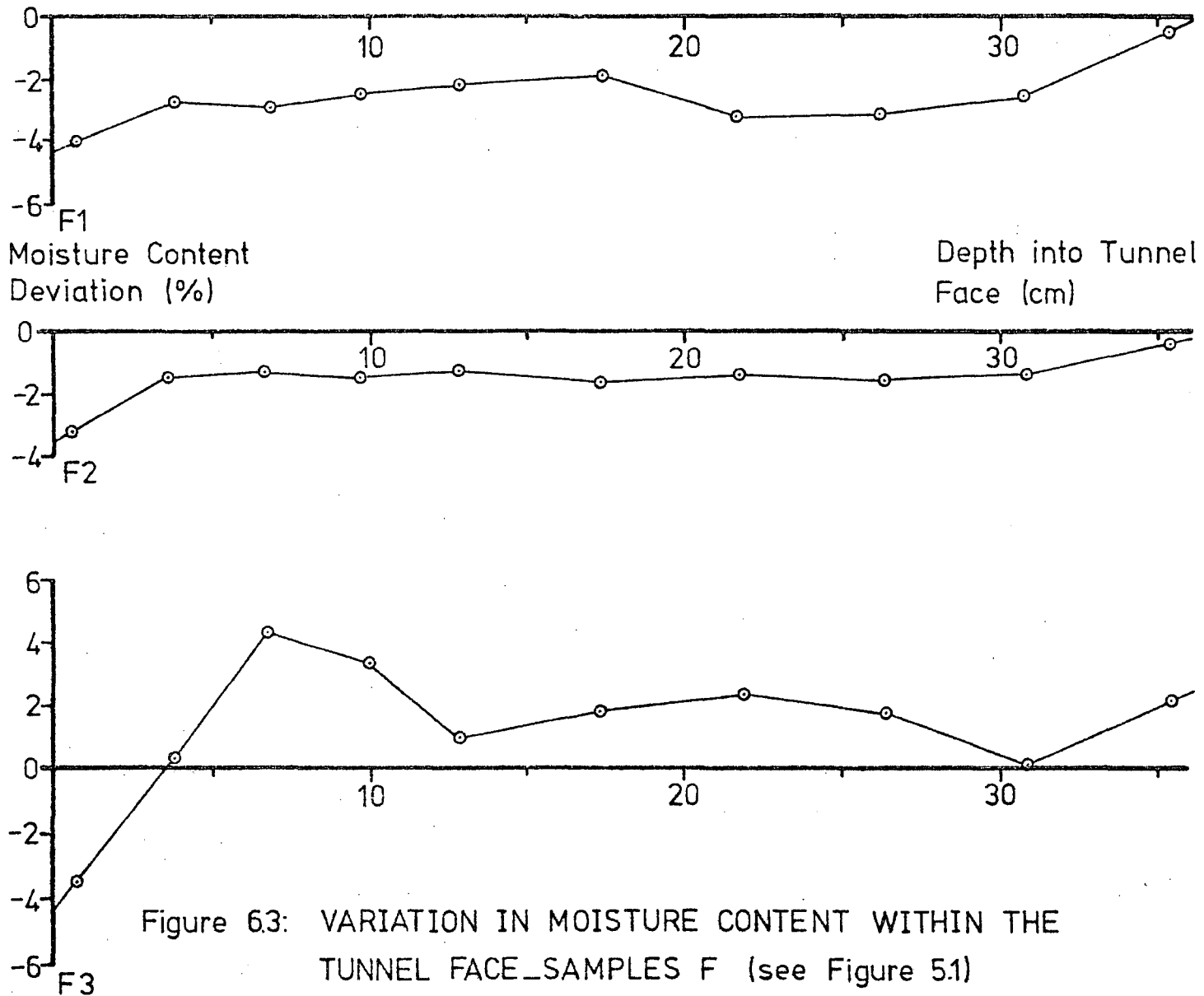
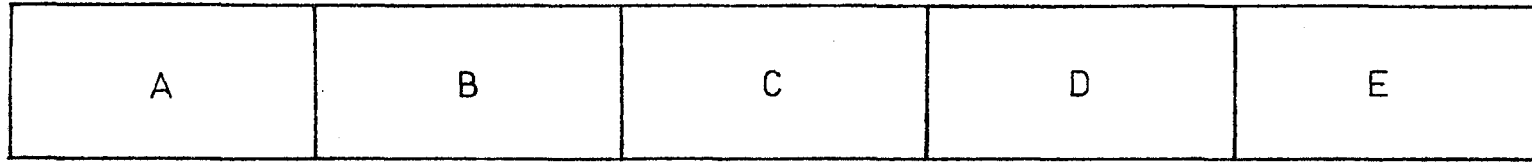


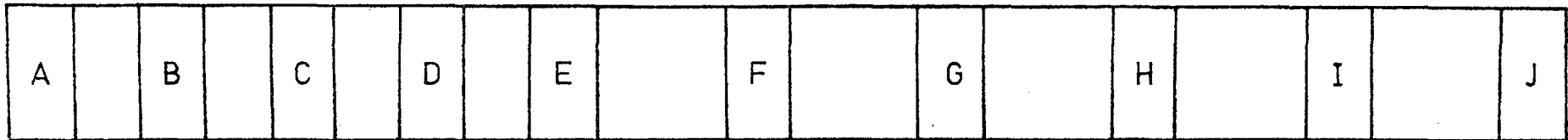
Figure 63: VARIATION IN MOISTURE CONTENT WITHIN THE TUNNEL FACE_SAMPLES F (see Figure 5.1)



Samples D



Samples E



Samples F

Figure 64: LOCATIONS OF SAMPLES TAKEN FROM CORES (see Figure 5.1)

The de-watering of the upper half of the face, with respect to the lower half, is consistent with the increase in pore pressure which occurs with depth relative to the constant air pressure acting over the whole of the face. The de-watering indicates that the pore pressure, in at least the upper part of the face, was overcome by the air pressure in the drive of 90 kN/m^2 , whilst the pore pressure in the lower part was in excess of the air pressure. Observations of sand and gravel beds in the tunnel face show that the upper beds always appeared dry, and those in the lower part of the face always seeped water into the tunnel. This supports the results gained from the samples. Although the level of compensation in the face appeared to vary, probably due to changes in the water-table level across the channel, it was usually located around the middle of the face.

Cores from locality D were divided into five sections which proved an unsatisfactory method, as can be seen from the results, for detecting changes in moisture content over relatively short distances. Also core D.5 gave very low values, due to the samples containing sand and gravel material, despite the fact that the bed was at the base of the accessible face, and was observed to be seeping water into the tunnel. The profiles from localities E and F are more consistent due to an improved sampling process which involved taking smaller samples at intervals along the core. Figure 6.4 illustrates the various methods of sampling of the cores.

6.2 Piezometer Results.

The pore pressures in the alluvium were measured before the tunnel reached the array using the piezometer installed at 1m above soffit and axis depth in boreholes 1 and 2 respectively. When borehole 1 was exposed

in the tunnel face air penetrated the grout above the soffit and leaked into the piezometer and through the connecting tubes to the ground surface making it impossible to take further readings. This leak persisted for several weeks afterwards, however the piezometer in borehole 2 remained operation and recorded a rise in pore pressure as the shield passed the array.

The results are shown in Figure 6.5 with respect to tunnel advance in metres rather than time which is less relevant in this case. Pore pressures before the array was reached were 109.1 kN/m^2 in borehole 2 and 78.4 kN/m^2 in borehole 1 at the piezometer design depths making the water-table 2.25 m below the ground surface, assuming that there is no 'aquiclude' of significantly lower permeability between the piezometer and the ground surface. As the tunnel face passed the array the pore pressure in borehole 2 rose to 119.2 kN/m^2 , which would support a water-table at 1.22 m below ground surface, although the low permeability of the alluvium may have prevented the air pressure from affecting the level of the water-table until some time afterwards. The pore pressure is equivalent to that of 97.9 kN/m^2 at the depth of the excavated surface of alluvium above the soffit of the lining, which is very close to the air pressure of 90 kN/m^2 used in the drive. The increased pore pressure may therefore be a transmittance of the air pressure inside the tunnel, with the compression of the alluvium caused by the forward movement of the tunnelling shield increasing the value from 90 to 97.9 kN/m^2 . Figure 6.6 illustrates the balance between these opposing pressures.

When the compressed air was released the amount of water made by the tunnel increased as a result of the tunnel acting as a drain to the alluvium surrounding it. This drainage facility progressively lowered

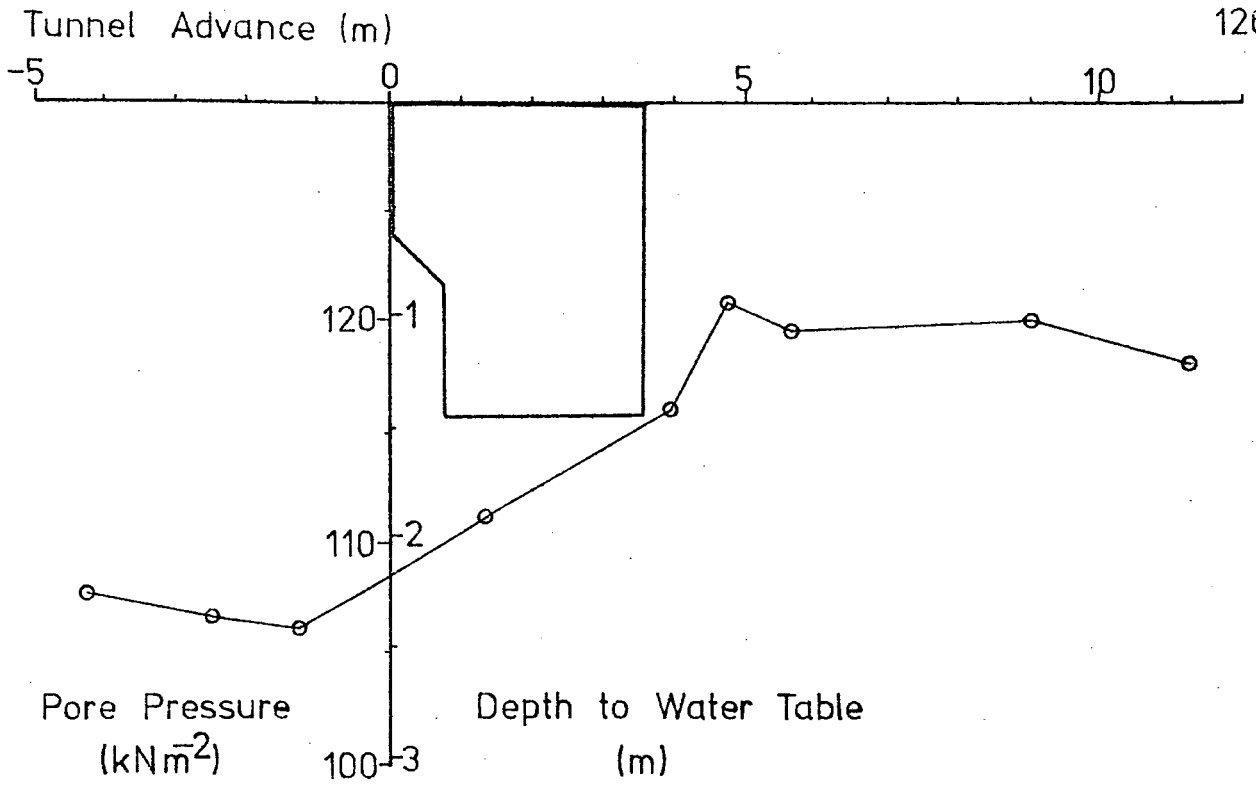


Figure 65: CHANGE IN PORE PRESSURE WITH PASSAGE OF TUNNEL FACE

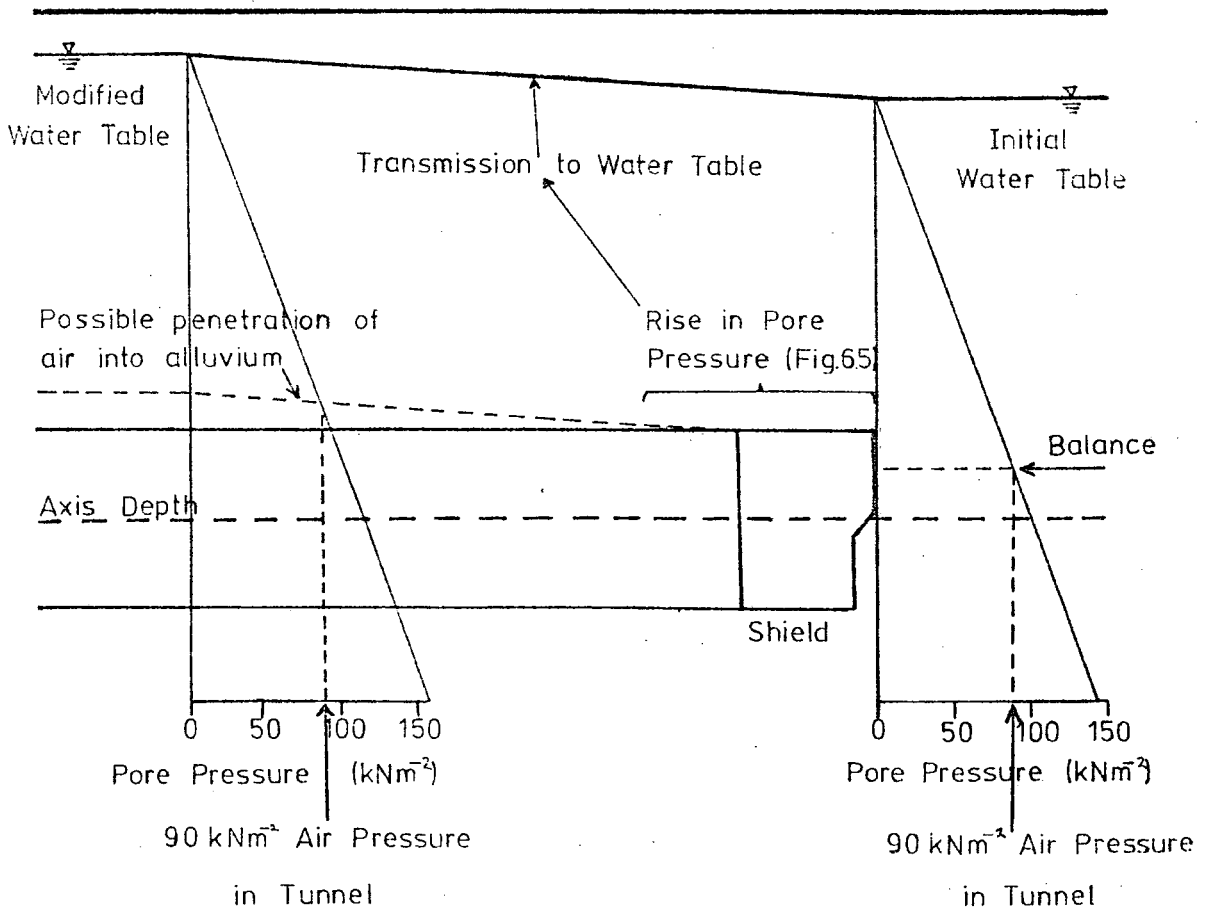


Figure 66: DIAGRAMMATIC REPRESENTATION OF THE EFFECT OF COMPRESSED AIR

Tunnel Face Position (m)	Pore Pressure at Axis depth (kN/m ²)	Depth of water table below surface (m)
- 4.27	109.1	2.25
- 2.50	108.3	2.34
- 1.25	107.6	2.40
- 0.40	107.0	2.25
1.22	112.5	1.90
3.66	117.1	1.43
4.75	121.9	0.94
5.60	120.7	1.07
8.53	121.3	1.01
11.40	119.2	1.22

Data for Figure 6.5

Day	Depth of water table below surface (m)	
	B.H.1.	B.H.2
119	3.52	3.37
176	1.05	0.29
184	1.16	-
202	-	0.69
224	0.38	0.38

Data for latter part of consolidation.

Table 6: PIEZOMETER RESULTS.

the pore pressure in both boreholes until the water-table, which must have been in equilibrium with the pore pressures because of the long time-period over which this took place, was 3.52 m below ground surface in borehole 1 and 3.37 m in borehole 2. These values are equivalent to 66 kN/m^2 and 67.5 kN/m^2 respectively both values calculated to the depth of the piezometer in borehole 1. The measurement results tended to be slightly erratic, however, because of varying weather and tidal conditions.

The lowering of the pore pressure coincided with the consolidation phase of ground settlement. During the latter part of consolidation the joints in the tunnel lining were caulked in order to seal the tunnel prior to carrying out further stages of construction. This process effectively removed the drainage properties of the tunnel and resulted in a gradual increase in pore pressure by the re-establishment of a state of equilibrium.

Readings for piezometer 1 were lower than those for piezometer 2 in each case, until the last results showed the same values for both piezometers with the water-table at 0.38 m below ground surface or 96.8 kN/m^2 in borehole 1 and 127.5 kN/m^2 at axis depth in borehole 2. The lower pore pressure in borehole 1 at a given depth is due to maximum drainage facility occurring along the centre line. An extrapolation of these values is illustrated in Figure 6.7 showing the lowering of the water-table and its subsequent rise.

6.3 Flow-tank Analogue

Investigations were carried out into the drainage process brought about by the tunnel using a flow-tank model in the laboratory (Plate 3). A piezometer was used to simulate a permeable tunnel and the flow-tank was

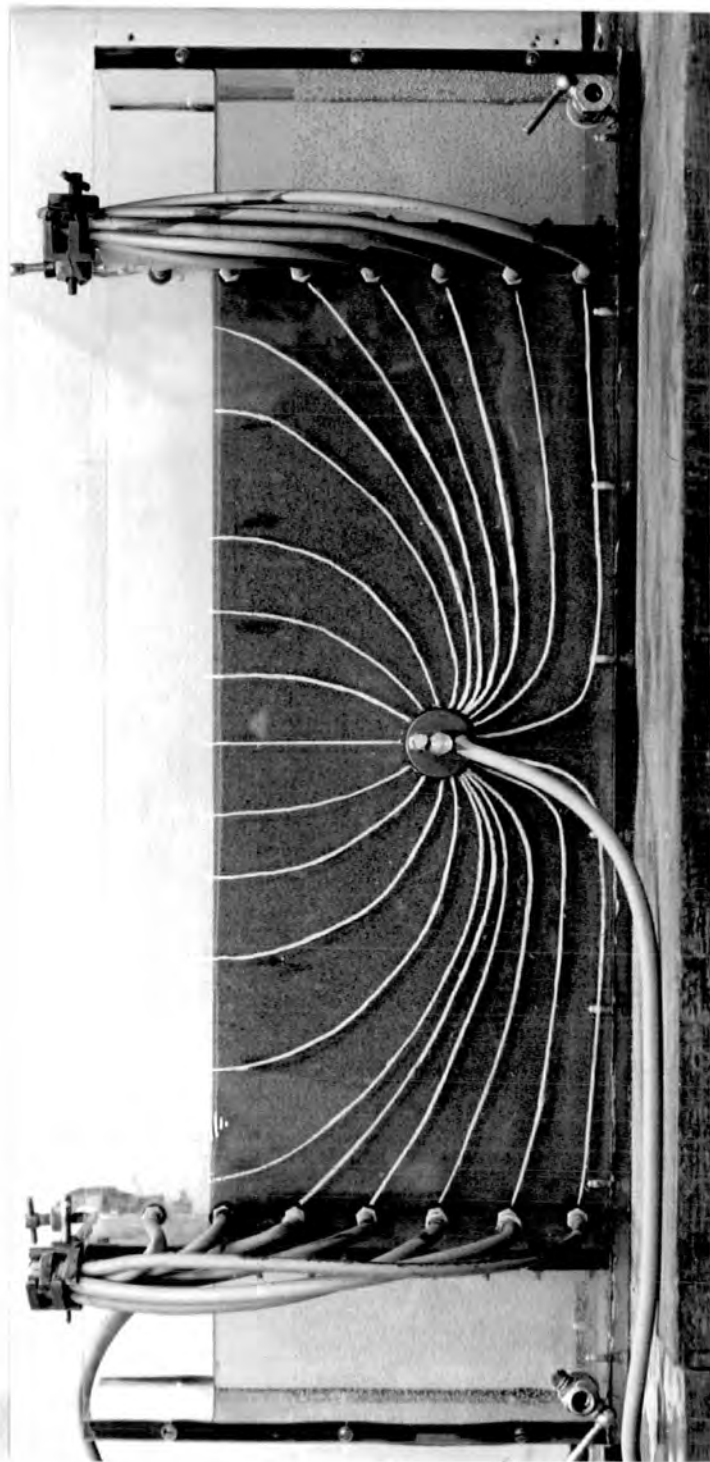


Plate 3 : FLOW -- TANK ANALOGUE WITH FLOW LINES

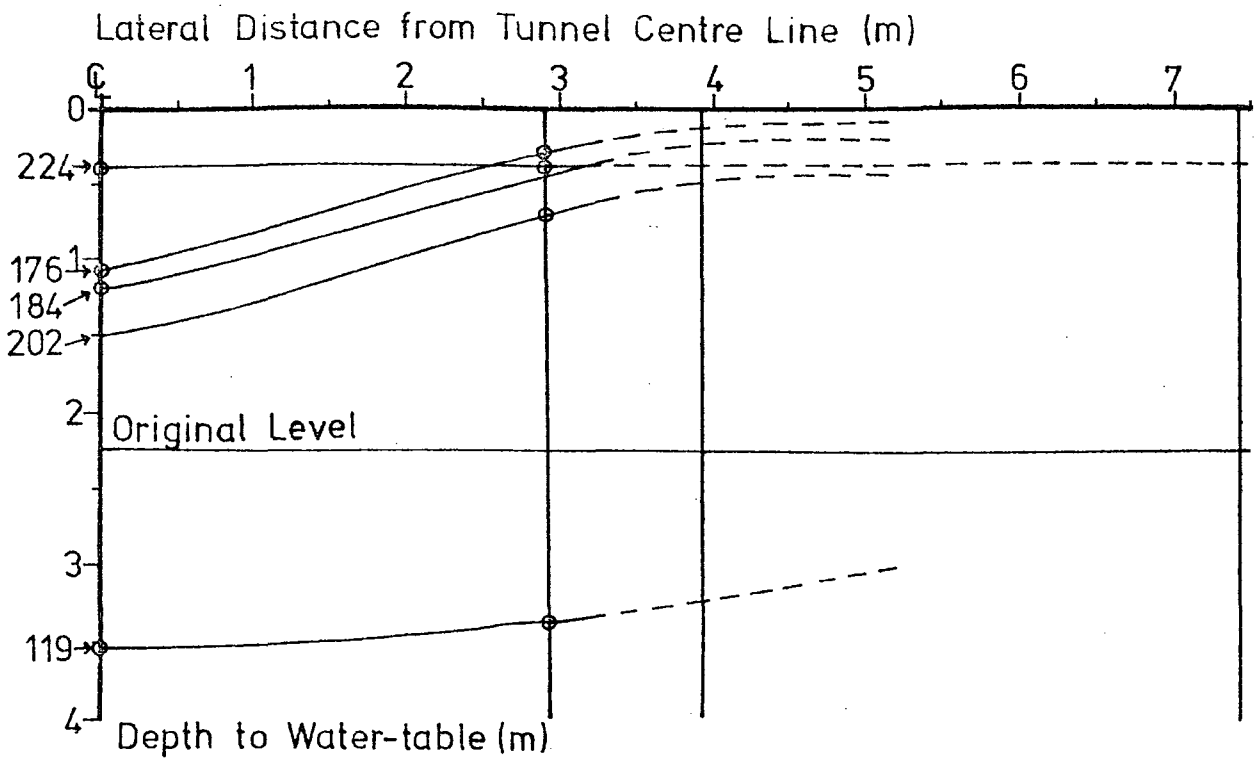


Figure 6.7: CHANGE IN WATER-TABLE DURING CONSOLIDATION

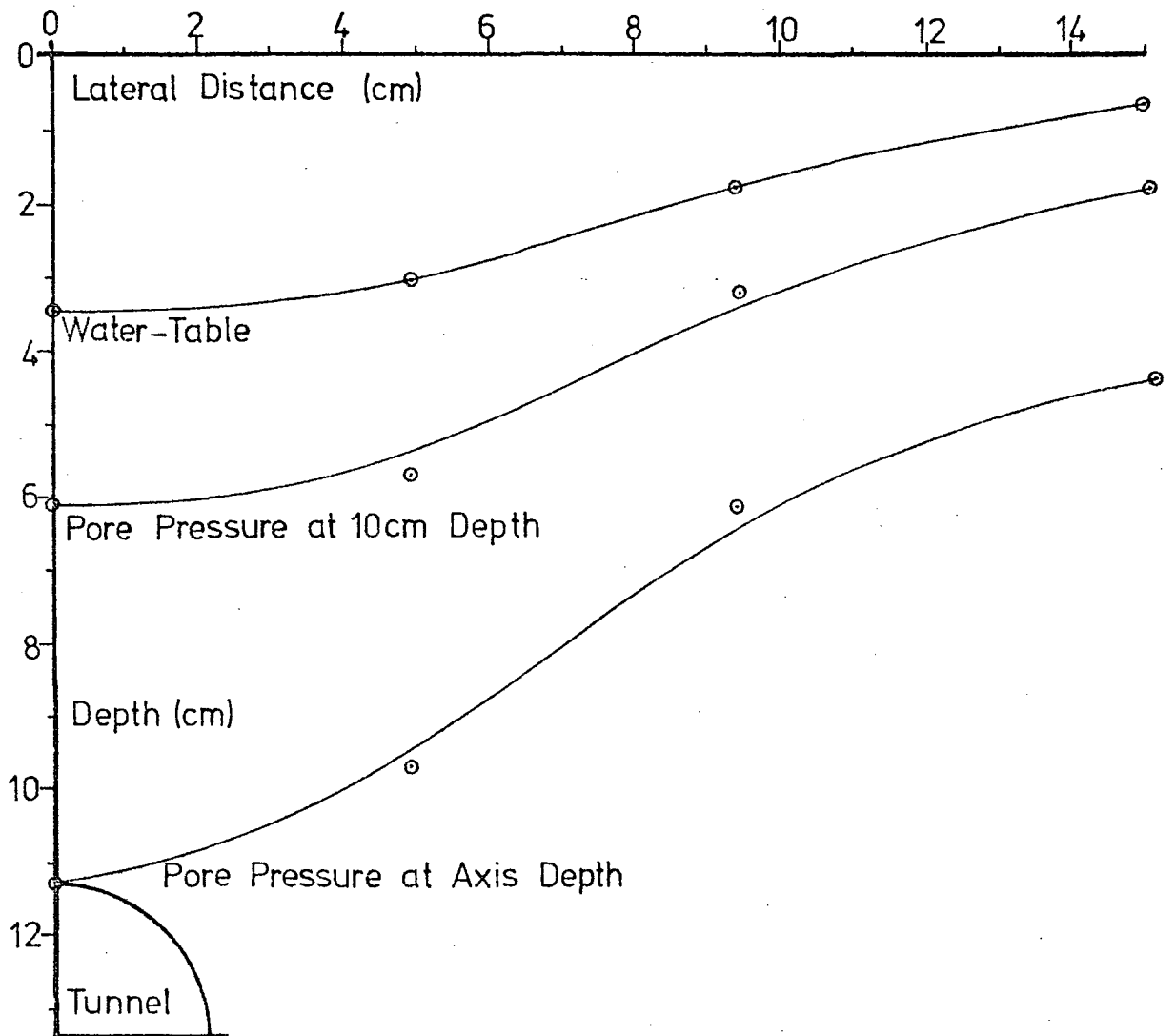


Figure 6.8: WATER-TABLE IN ELOW-TANK ANALOGUE

built around it to accommodate a sufficient depth of sand to give the correct depth to diameter ratio of the Wellington Quay siphon, coincidentally the scale was very close to 100 : 1. The sand was compacted under water by vibration until all the visible voids were eliminated.

Potassium permanganate dye was used to trace the flow lines produced when water was allowed to drain from the piezometer under a head of water kept constant at just above the surface of the sand (Plate 3). The latter was necessary to maintain continuity between the depth of water in the reservoirs at either side of the tank. During the determination of the flow lines, the pore pressures were measured using glass tubes inserted to various depths in the sand, the water levels being read through the side of the tank. Figure 6.8 includes the results obtained for the pore pressures whilst water was draining into the 'tunnel'. These compare well with the distribution of pore pressures measured in the field during the consolidation phase of settlement.

Finally, after the completion of these experiments, a low air pressure was applied to the 'tunnel' to simulate the effects of the air pressure used in the drive to stabilize the face. It has already been noted in the previous section that the air pressure was in excess of the pore pressure at the top of the face. Therefore, some permeation of the alluvium above the tunnel soffit would be expected. However, the air found a channel to the surface and leaked away before it could have any effect, presumably this was due to variations in packing of the sand which proved difficult to eliminate. In order to prevent this the air pressure was replaced by water pressure, which, although not having the buoyancy of air in water, nevertheless produced results consistent with those for air illustrated by K. Szechy (1966). The flow of water was

traced by small quantities of dye distributed around the tunnel, the flow direction of the dye and rates of flow being traced on the side of the tank (Figure 6.9). For this experiment the pressure of water inside the 'tunnel' was maintained at a level which balanced the pore pressure about half way up the 'tunnel'.

The limitations of these experiments are mainly that the permeability of the sand is higher than that measured for the silt. Using a constant head permeability apparatus the coefficient of permeability K , was found in cm/sec from:

$$K = \frac{q \cdot l}{A \cdot H} \text{ cm/sec} \quad (\text{from T.N.W. Akroyd (1964)}).$$

where q = the volume of water passed in cm³/sec.

l = the length of sample in cm.

A = the cross-sectional area of the sample in cm²

H = the head of water in cm.

Using samples of alluvium of 6.7 cm in length and 28.3 cm² area, the volume of water passed per second was measured for various heads of water, after some time had been allowed for the sample to consolidate under the pressure. The vertical permeability was found to be 1.03×10^{-7} cm/sec whilst laterally it was slightly higher at 1.25×10^{-7} cm/sec because of the layers of more silty sediment. The samples were taken from locality C. Permeabilities quoted for medium sand are around 2.95×10^{-7} cm/sec (T.W. Lambe and R.V. Whitman, 1969). The anisotropy of the alluvium is therefore not too great to affect the flow-lines drastically, although the lower permeability makes the processes observed much slower and may prevent the significant permeation of air above the tunnel.

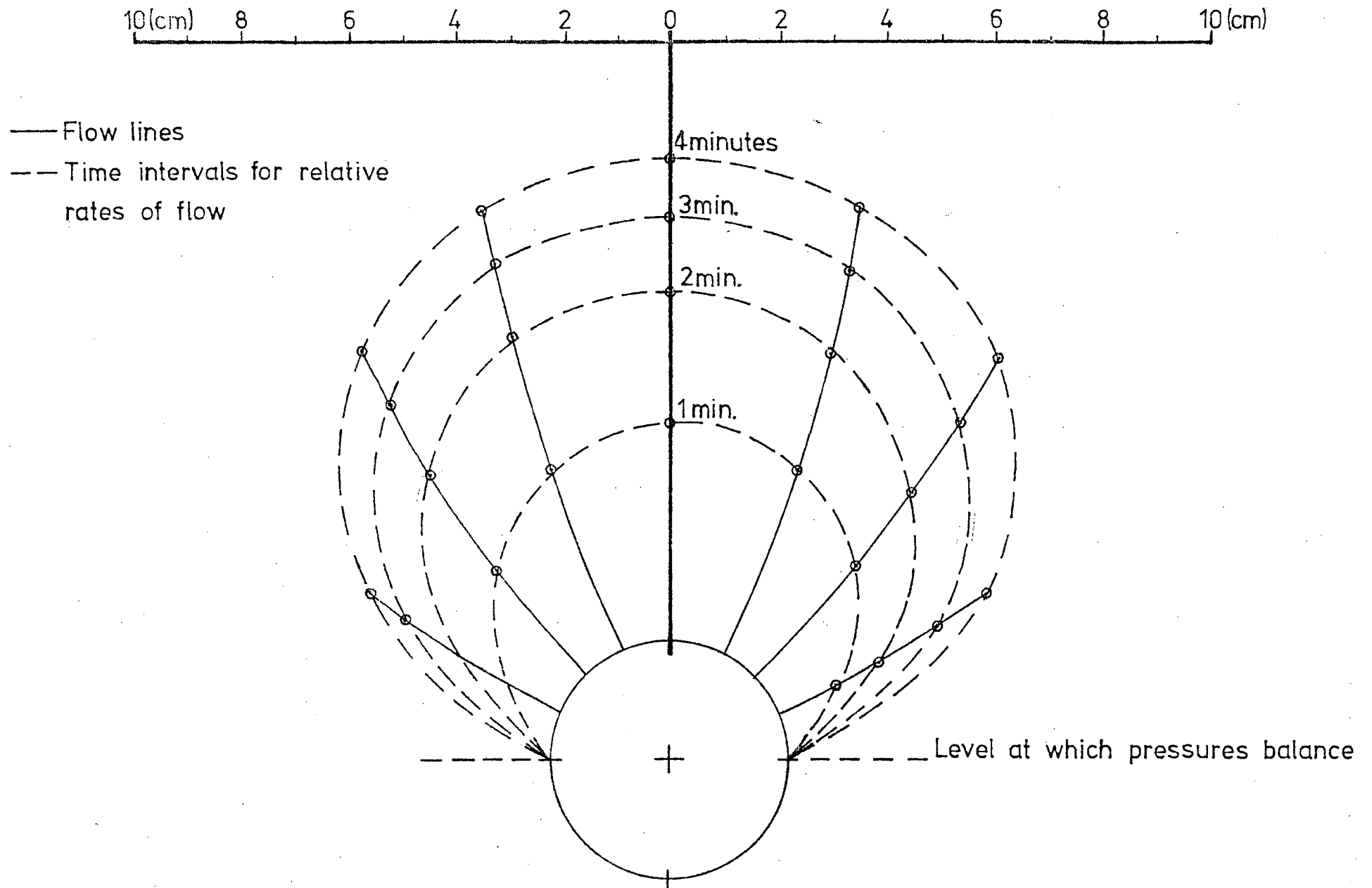


Figure 6.9: FLOW LINES FOR EXCESS PRESSURE INSIDE THE TUNNEL

6.4 Consolidation Experiment.

A large undisturbed block of alluvium was collected from axis depth at locality C and stored in aluminium foil. A sample was later taken from this block and used in a consolidation test carried out according to B.S. 1377. The results of the test are listed in the appendices.

Figure 6.10 shows the decrease of the voids ratio with increasing pressure, the latter being plotted on a log scale. Using the construction shown the original overburden pressure for the sample was found to be 93.2 kN/m^2 . The value corresponds to the calculated effective stress of 108.8 kN/m^2 and shows that the alluvium is normally consolidated supporting the view that it is a post-glacial deposit.

An additional sample was loaded to 93.2 kN/m^2 and unloaded in small increments to give the rate of increase in voids ratio which could be expected to occur if the ground surface above the alluvium was unloaded. The values obtained are included in Figure 6.10. The estimated unloading of the ground surface caused by the demolition of the settlement damaged wall was 50.19 kN/m^2 . Given that the base of the channel was 17 m below ground surface and that the upper 3 m was composed of fill, the unloading at the centre of the alluvium was 1.08 kN/m^2 . This was estimated by spreading the load on a 2(vertical): 1(horizontal) basis. Using the value in the unloading curve in Figure 6.10 an estimate of the increase in voids ratio was determined which was inserted in the following equation:

$$\Delta H = \frac{e_0 - e_1}{1 + e_0} \cdot H$$

where e_0 is the original voids ratio at 93.2 kN/m^2

e_1 is the voids ratio after unloading

H is the thickness of the layer of alluvium in metres

ΔH is the uplift at the ground surface in metres

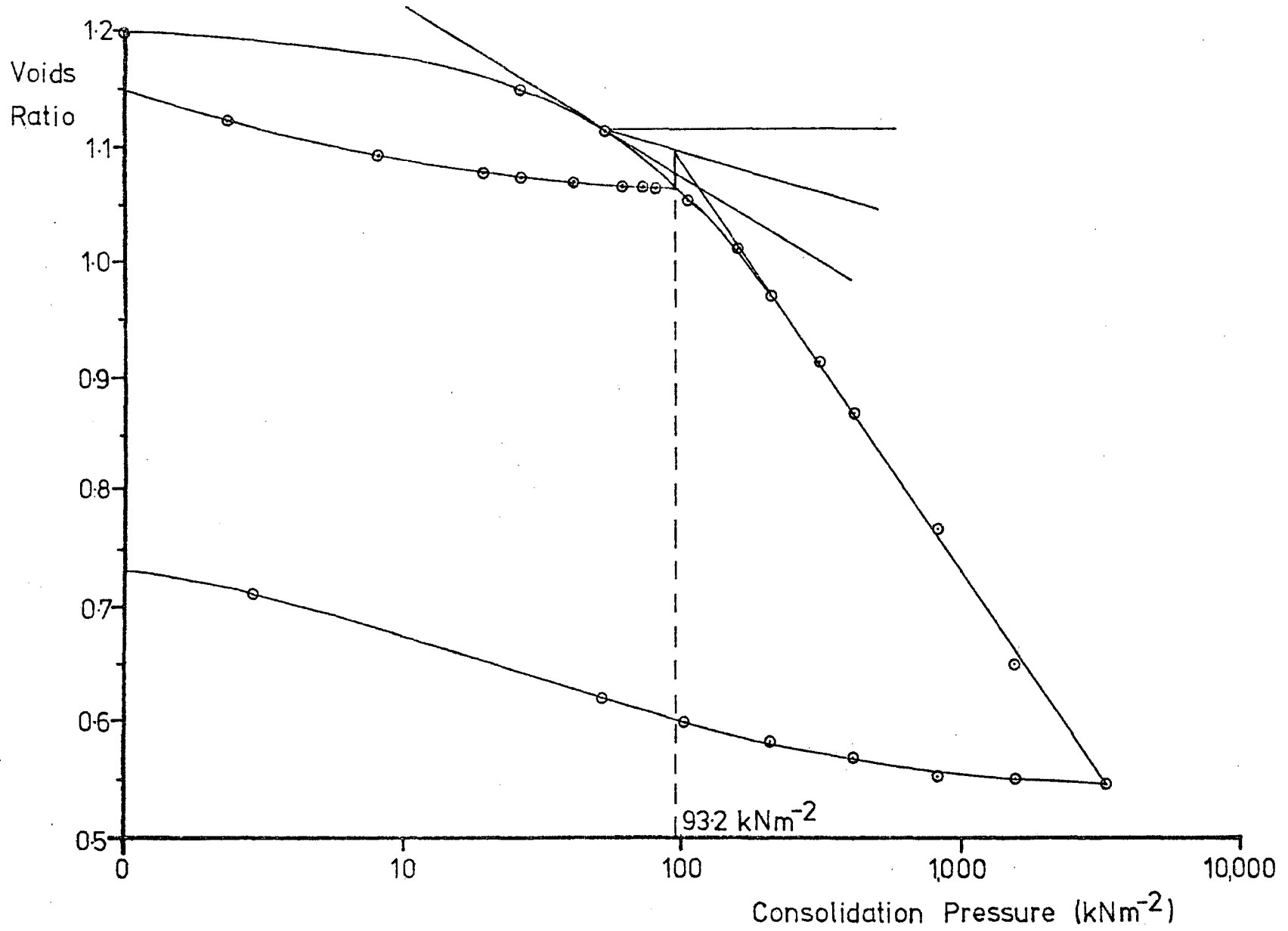


Figure 6.10: CONSOLIDATION CURVE

The uplift predicted was approximately 0.082 mm from a voids ratio increase of 0.000012. This indicates that the unloading was much too small to cause the observed uplift, although a number of features of the uplift make it difficult to explain by any other process:

1. All surface stations were uplifted by different amounts which rules out the possibility of disturbance of the T.B.M. Also the maximum uplift occurred, both at the surface and underground, in borehole 4 and surface station E which was the closest to the demolished wall.
2. A more likely alternative is that back-grouting around the tunnel caused the uplift, although the sub-surface movement particularly in borehole 2 is not directly away from the tunnel lining. The lateral movement which did take place appeared to be more the result of a buckling of the inclinometer tubes rather than a movement controlled by the tunnel.
3. There were no exceptionally high tides or high rainfall around the period of the uplift although an increase in pore pressure was measured after this period. The latter feature may have been brought about by the caulking of the tunnel lining which took place over that period. However, although this could explain the uplift by decreasing the effective stress, the process of consolidation was resumed after the uplift.

Therefore, the unloading of the ground remains the most probable explanation of the observed uplift.

By projecting the present rate of settlement on a log time basis two years of movement will produce a maximum settlement of 100 mm and after three years 112 mm of settlement will have taken place. This

assumes that consolidation is an infinite process which, in practise, is not the case. The consolidation of the alluvium in the field, brought about by the lowering of the pore pressure by drainage of pore-water into the tunnel, can be regarded as an increase in the effective stress acting upon the layer of alluvium. The increase caused by lowering the water-table by 2.3 m is of the order of 9.02 kN/m^2 . Again using this value in the consolidation curve a decrease in voids ratio of 0.008 was determined which gave an approximate predicted maximum surface settlement of 55 mm. When combined with the settlement which had occurred before consolidation began a total settlement of about 101 mm is predicted.

6.5 Methane Determination

During the early stages of tunnel construction gas was stated to have been detected when the tunnel face was within the boulder clay and about 21 m from the edge of the channel, -40.8 m from the instrumentation array. At this point five holes were augered into the tunnel face and soft clay was encountered at between 1.5 and 2 m depth. A safety officer examined these auger holes with a lighted candle and ignited gas at the mouth of one of the holes. The lense of soft clay may have been a distributary of the main channel of alluvium and was rapidly passed through by the tunnel face. However, the detection of gas, probably methane, although unconfirmed by Gas Manometer tests, nevertheless caused concern about the possibility of further gas being encountered when the main channel was intersected. Eventually, when the tunnel was about 9 m into the main channel and at -9 m from the instrumentation array the drive was closed down for two

weeks for the installation of flameproof lighting and equipment. Also the rate of ventilation of the compressed air was increased to prevent the build up of gas.

At locality D a sample of the alluvium from the tunnel face was sealed in a U4 for an analysis of the gas. In the laboratory about 350 gm of wet sample was rapidly transferred to a flask and connected to the apparatus illustrated in Figure 6.11. Initially the apparatus was evacuated of air by means of a vacuum line and this assisted in drawing off the gases from the sample. Then the sample was heated over a water-bath and the gases released were passed through two traps. The first was cooled by acetone-drycol at -78°C to remove the water vapour and the second by liquid air at -190°C to condense the remaining gases.

After about 2 hours of distillation, when most of the water had been driven out of the sample causing a 28% loss in weight, the trap containing the condensed gases was connected to an empty and evacuated flask via a soda-lime container. By warming the condensed gases and cooling the empty flask with liquid air the gases were transferred and at the same time passed over soda-lime which removed most of the carbon dioxide present. Removal of the carbon dioxide was important for the analysis of the gases by Mass Spectrometer due to the dependence of the results upon the molecular weight of the gas. Carbon dioxide dissociates to form oxygen ions (O^{2-}) which have an ionic weight very close to that of methane (CH_4). Therefore the oxygen ions must be kept as low as possible so as not to obscure the methane peak.

The results illustrated in Figure 6.12 indicate the presence of methane in excess of the background which results from machine oils.

Although not quantitative, the peak shows that methane was evidently present in very small quantities. It is unlikely that much interstitial gas was retained during the sampling process, despite careful sealing of the U₄, and compressed air had probably progressively driven the gas away ahead of the advancing tunnel face. Therefore, the gas determined was that which was absorbed onto the clay particles and this may have only been partly driven off by heating to 100°C.

The latter possibility is supported by a test carried out by a consultant on behalf of the construction company in which a small sample was heated by a bunsen in a vacuum. After cooling air was allowed into the container and a sample of the gases and air was analysed by Gas Chromatography using a poropac column. After calibration with a mixture of Methane, Ethane, Propane, Butaine and Ethelene the gases listed in Table 7 were obtained.

A comparison was made with garden soil and in all the saturated hydrocarbons the gases are present in greater quantities in the alluvium with methane being the main component. The unsaturated hydrocarbons were found in greater quantities in the garden soil indicating that these gases are products of the breakdown of humus, which is in turn formed by the aerobic decomposition of organic material. Conversely under anaerobic conditions, such as those found within the alluvium, methane with small amounts of ethane and propane are formed.

The test was performed when methane was detected in the tunnel after the compressed air was released. Using an M.S.A. Combustible Gas Detector a level of 2% of the lower explosive limit of methane was detected three days after the compressed air was released. Subsequently extensive ventilation was installed in the tunnel to flush out the

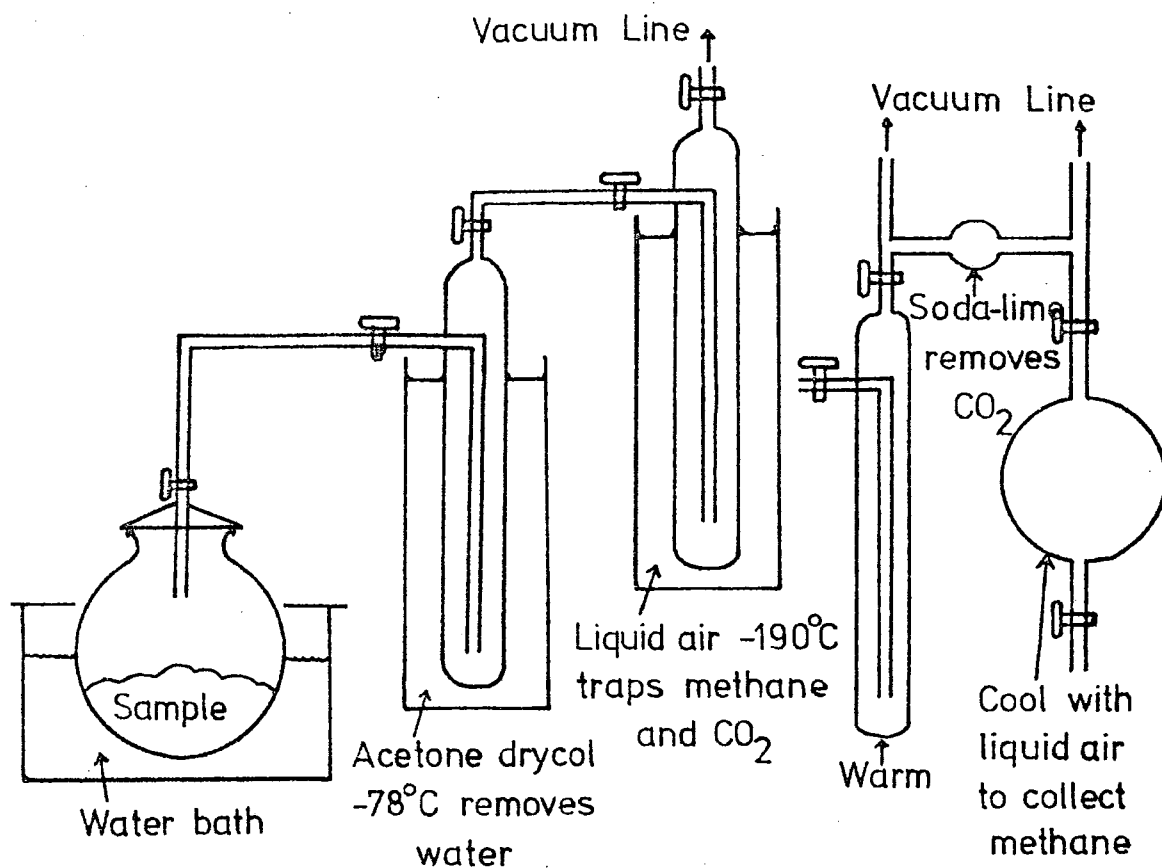


Figure 6.11: GAS EXTRACTION APPARATUS

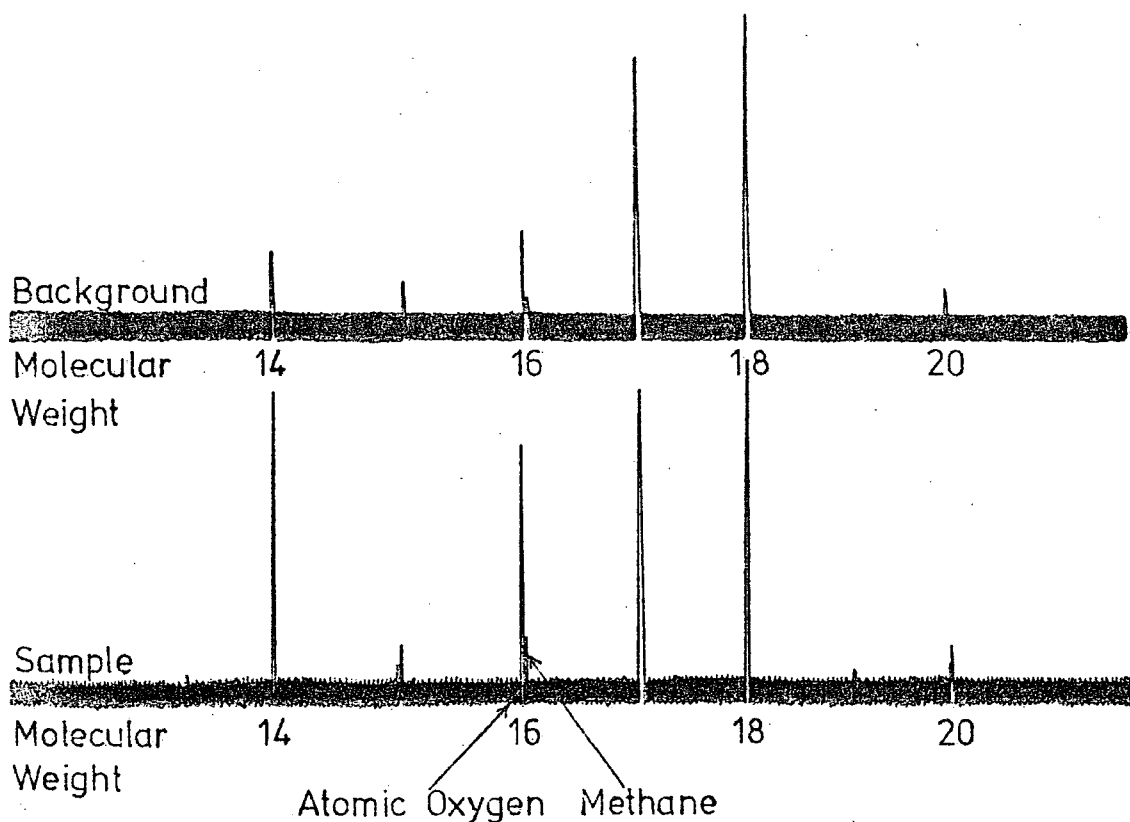


Figure 6.12: MASS SPECTROMETER RESULTS

	GAS	SAMPLE (17g)	GARDEN SOIL (16g)
Saturated Hydrocarbons	Methane	1.32 cc	0.22 cc
	Ethane	0.011 cc	0.007 cc
	Propane	0.033 cc	0.00 cc
Unsaturated Hydrocarbons	Ethylene	0.033 cc	0.06 cc
	Propylene	0.020 cc	0.055 cc

Table 7 : GAS ANALYSIS RESULTS

methane and prevent the build up of pockets of gas in the roof.

It can be concluded that methane was present within the deposit at pressures insufficient to overcome the pressure of the air in the drive of 90 kN/m^2 . However, once the air was released methane was able to seep into the tunnel. Gas was observed bubbling through water in the floor of the tunnel around the locality of the sand and gravel lenses in the middle of the channel. The higher permeability of these beds made them a focus for the seepage of gas into the tunnel.

Methane generation is a common feature of organic silts and in this case the process may still be taking place. There is also an alternative explanation which is plausible, that is, the methane may originate from the old mine workings in the underlying Coal Measures which are very frequent in the surrounding region.

Chapter 7

SUMMARY AND DISCUSSION

The case history describes settlement and ground movement which took place when a 4.25 m diameter tunnel was shield driven at 13.375 m depth through a buried channel of soft organic alluvial silt.

Investigations also revealed a number of features concerning the channel itself which have some bearing upon the nature of the ground movements. The features are listed separately as follows:-

- 1) The channel was formed by post-glacial erosion and subsequently filled with alluvium during the post-glacial rise in sea level (Flandrian Transgression) to form a small tidal estuary, a tributary to the Tyne. The estuary was partly reclaimed about 45 years ago by diverting Willington Gut to one side of the channel and filling with about 5 m of brick, ash, stone and clay fill to about 1.5 m above high tide level (Figure 2.1).
- 2) The alluvium consisted of a soft organic silt with light and dark grey laminae caused by variations in organic content of 2.85% in the light bands and 3.85% in the dark bands (Figure 5.4). The organic contents proved to have a strong influence upon the moisture content and moisture absorbing properties of the silt, with the low organic bands containing 42.25% moisture and absorbing 0.87% and the high organic bands containing 46.60% and absorbing 0.98%, all quantities being means (Figures 5.5 and 5.6). An increase in frequency of the dark bands was found towards the top of the tunnel face and a decrease towards the

middle of the channel. Sand and gravel lenses were found beneath the former course of Willington Gut and some large tree trunks and branches were found within the sediment (Figure 3.2).

3) Organic material, decaying under anaerobic conditions, created significant quantities of methane (Table 7), which readily seeped into the tunnel when the compressed air was released.

4) Laminae with a higher organic content generally contained a higher clay and pyrites content (Figures 5.8 and 5.16) and a larger clay component in the grain size distribution (Figures 5.19 and 5.20). The mineralogy and geochemistry of the boulder clay in the sides of the channel was very similar to that of the alluvium, except for the higher clay content and virtual absence of pyrites in the boulder clay (Table 4). The surface of the boulder clay in contact with the alluvium was leached of carbonates, which were redeposited at 15 to 20 cm depth to form an iron-rich carbonate hard pan typical of sub-aerally weathered soils (Figure 5.18).

5) Moisture contents determined at depth into the tunnel face revealed a dewatering in the upper part of the face to the lower part as a result of compressed air. Samples from the lower part of the tunnel face generally showed a rapid rise in moisture content with a maximum at 5 to 10 cm depth followed by a steady fall (Figures 6.1 to 6.3).

6) The alluvium had an undrained shear strength of 24.9 kN/m^2 and a bulk density of 1.82 Mg/m^3 giving a stability ratio of 9.58 at tunnel axis depth which was reduced to 5.97 by the application of compressed air.

The main features of the settlement and ground movement were as follows:

- 1) Surface settlement began when the tunnel face was 33.75 m from the instrumented array in a plane normal to the tunnel centre line (Figure 4.3). A maximum surface settlement of 35 mm had developed when the compressed air in the drive was released at 66 days after the passage of the tunnel through the array. Consolidation then took place and continued long after the cessation of tunnelling operations increasing the settlement to 66 mm after 224 days (Figure 4.2). Settlement continued to take place as a result of consolidation after 224 days and had reached 74 mm at 296 days. At the time of writing settlement is continuing to increase at a logarithmically decaying rate.
- 2) The surface settlement semi-profiles at all stages of settlement (Figure 4.7) closely followed the form of a normal probability curve (Figures 4.8). Horizontal surface deformation and strain profiles, computed on the basis of the normal probability curve by a stochastic analysis, were similar to the respective measured profiles until consolidation began. During consolidation the measured lateral displacements were significantly smaller than the calculated values.
- 3) Porewater pressure measurements (Figure 6.5 and Table 6) indicated an initial water table 2.25 m below ground surface. This level rose to 1.22 m during passage of the shield, but then fell to 3.52 m below surface level at 119 days, after the release of compressed air. Subsequent rises in the water table to near-surface levels, monitored from 176 to 224 days, followed caulking of the tunnel lining.

- 4) Sub-surface settlement to the side of the tunnel (Figure 4.9) generally increased with depth to a maximum value (Figure 4.10) and then decreased. The depth to the maximum value decreased from borehole 2 to borehole 4. Settlement just above soffit depth to the side of the tunnel was 88 mm at 224 days.
- 5) Ground movement vectors in the plane of the instrument array (Figure 4.16), computed from settlement and inclinometer data, have isolated five main deformation regimes. The time periods which isolate these regimes were subject to the availability of data and therefore do not precisely delineate movement which occurred during each regime. Relative to the time at which the tunnel face passed the instrument array these regimes were:
- (a) Up to 51 days, predominantly deformation into the tunnel annulus.
 - (b) Between 51 and 91 days, deformation away from the tunnel associated with the injection of large quantities of cement grout at 71 days into the ground surrounding the tunnel at pressures of 690 kN/m^2 .
 - (c) Between 91 and 149 days, vertical settlement typical of consolidation of the soil.
 - (d) Between 149 and 176 days, uplift coinciding with the demolition of a wall adjacent to the array. Uplift may have been caused by the unloading of the ground under and alongside the base of the wall.
 - (e) Between 176 and 224 days, continuing vertical settlement of a linear form on a settlement-log time curve (Figure 4.5) and again

typical of primary consolidation.

Ground movement vectors parallel to the tunnel centre line (Figure 4.17) exhibited a tendency for movement towards the middle of the alluvial channel throughout the case history.

6) Local damage to the factory above the tunnel may be related to the measured zones of tensile strain (Figure 4.8) on either side of the tunnel centre line and perhaps, more particularly, be interpreted in terms of ground tilts.

The volumes of settlement which had taken place at selected stages in the case history are listed in Table 8 along with their relative proportions of the total volume of ground loss. The value for settlement which occurred prior to the onset of consolidation will decrease as the proportion of consolidation increases with time.

The volume of ground lost during the first post-array phase can be attributed to deformation into the tunnel annulus. However, this volume of $0.548 \text{ m}^3/\text{m}$ would require the complete closure of an annulus of 80 mm depth around the entire lining circumference. Between a beadless shield 4.31 m in diameter and a lining of 4.25 m diameter, the minimum annulus available was 30 mm deep before any infilling of grout. The method of tunnelling made it unlikely that there was any significant overbreak caused by excavation at the face, therefore several alternatives are suggested to explain the ground loss:

- 1) Face-take continued to contribute to the ground loss after the shield had passed the array.
- 2) Adhesion of silt to the outer surface of the shield created overbreak.
- 3) Grouting compressed the alluvium and created a more deeply grouted

Time (days)	Measured volume of settlement (m ³ /m)	Error curve volume (m ³ /m)	Proportion of total ground loss * (%)
0	0.200	0.202	8
23	0.748	0.731	21
51	1.238	1.205	19
149	2.320	2.313	52
224	2.550	2.417	

* Calculated from measured volume of settlement.

Table 8: MEASURED AND CALCULATED SETTLEMENT VOLUMES

annulus.

The settlement in both the first and second post array phases together would require an annular void 150 mm deep. Clearly the second phase resulted from a disturbance around the lining and the previously suggested hypothesis of back-grouting at 690 kN/m^2 in the vicinity of the array remains the most probable explanation. The second phase of settlement, and evidence of extensive ground movement away from the lining following back-grouting directly under the array, point to the tentative suggestion that high pressure back-grouting should be avoided when tunnelling in compressible ground.

Additionally the bulk of the settlement was due to consolidation with the tunnel acting as a drainage source. It is possible that this process may be reduced or eliminated by caulking the lining prior to the release of compressed air.

The relationships of depth z , diameter D and the distance between the points of inflexion of a trough $2i$, have been included with Peck's original data in Figure 7.1. A line through the points for soft to stiff clays using the original data led Peck to derive the equation:

$$\frac{2i}{D} = \frac{(z)^{0.8}}{(D)}$$

The additional data from this case history and others monitored by the Department suggests the relationship to be closer to:

$$\frac{2i}{D} = \frac{z}{D}$$

The trough width after the first phase of post-array settlement gave a value for z/D of 2.92. It should be noted that the value lies closer to the 'best fit' line than that of 3.41 derived from the trough after consolidation at 224 days.

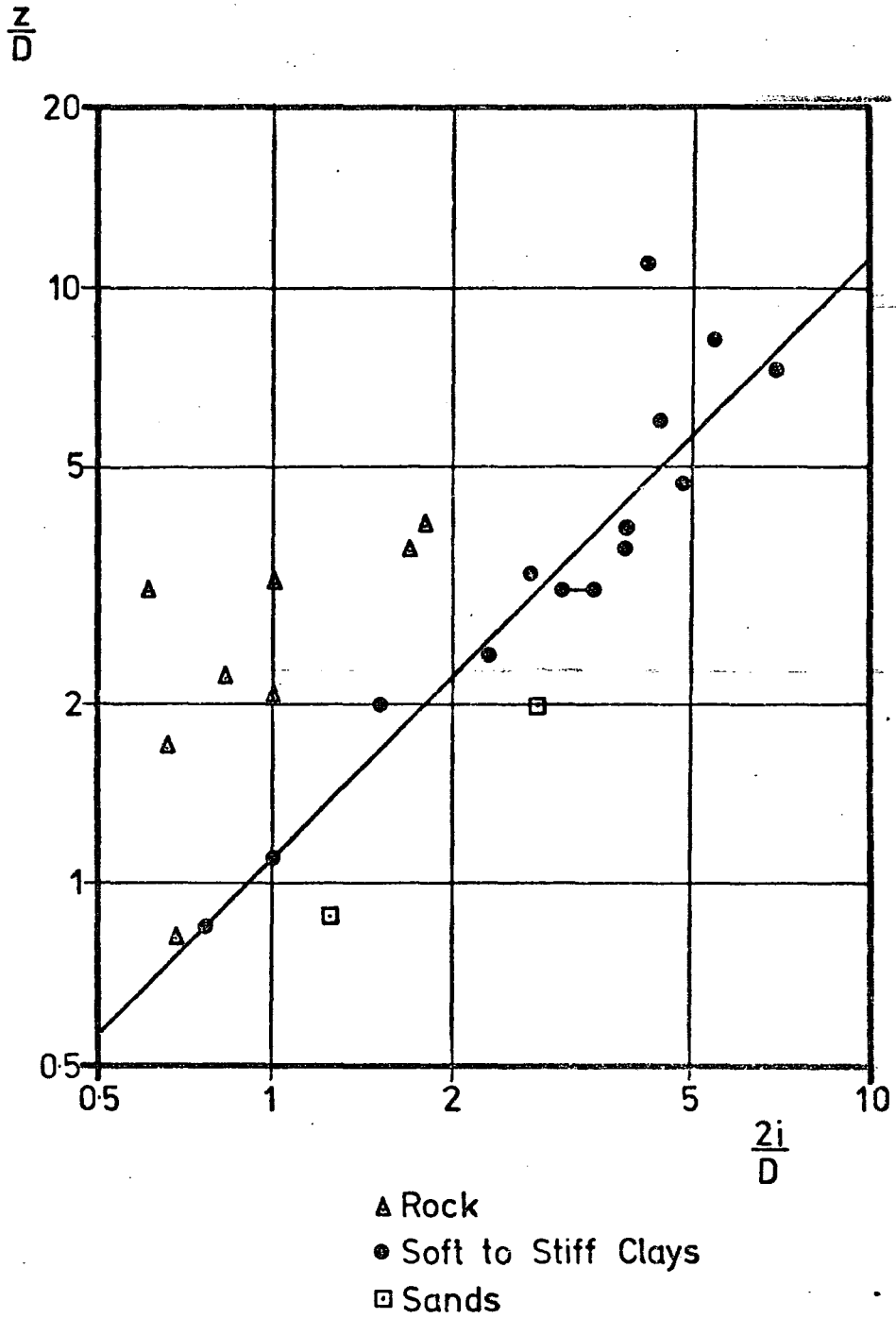


Figure 7.1: RELATIONSHIPS BETWEEN DEPTH z , DIAMETER D AND THE DISTANCE BETWEEN THE POINTS OF INFLEXION OF THE TROUGH $2i$ FOR TUNNELS IN VARIOUS TYPES OF GROUND

The majority of ground loss at the surface is contained within a trough of width $6i$. The relationship can therefore be used as an indication of the trough width which can be expected to develop in soft to stiff clays.

Figure 7.2 similarly relates depth z , diameter D and maximum surface settlement $S_s \text{ max}$ for the case histories listed in Table 9. The data originally compiled by P.B. Attewell and I.W. Farmer (1974) using case histories for stiff clays, has been extended to include more recent examples and three cases of tunnelling in soft ground.

The majority of points show an exponential relationship between z/D and $S_s \text{ max}/D$ down to z/D ratios of about 3.5 (illustrated in a linear fashion by using a log scale for $S_s \text{ max}/D$). Below this ratio there is a tendency for points to depart from the relationship as a result of higher $S_s \text{ max}/D$ values which indicates increasing difficulty in maintaining small ground losses with large and/or shallow tunnels. The deviation of points 16 and 17 from the main group may be due to these two tunnels being horse-shoe shaped as opposed to circular in cross-section. Also they were mined in short timbered drifts without a shield which greatly facilitates ground loss at the tunnel and therefore causes higher surface settlements.

Points 18, 19 and 24 are for tunnels driven in soft ground and have high settlements as a result of the difficulties involved. Consolidation accounted for much of the settlement in 19 and 24 (Willington Quay) and it may be that 18 also underwent a phase of consolidation upon the release of compressed air in the drive.

Point 23 is the value for $S_s \text{ max}/D$ at Willington Quay after the first phase of post-array settlement of about 25 mm and lies close to the data

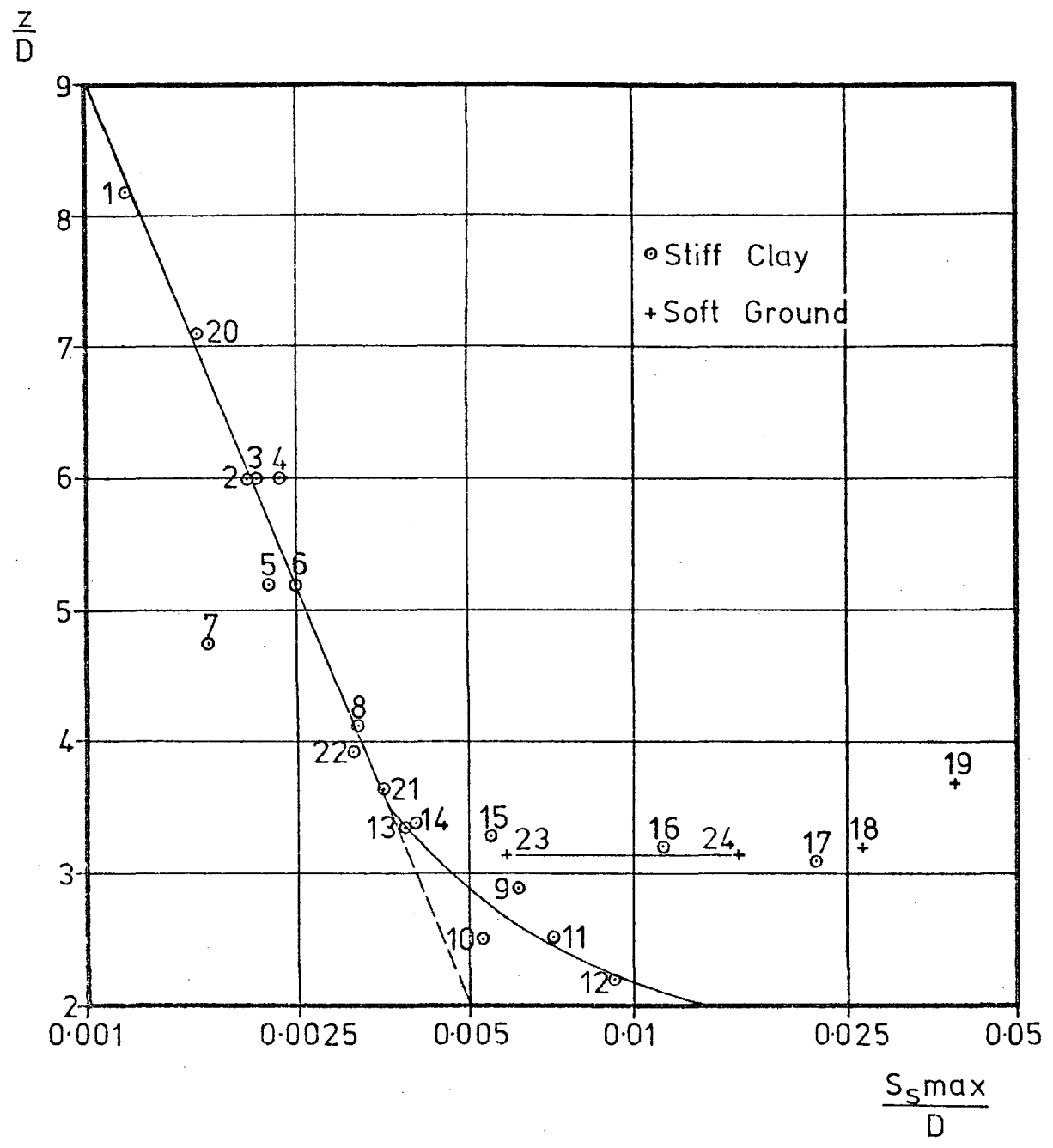


Figure 7.2: RELATIONSHIPS BETWEEN DEPTH z, DIAMETER D AND MAXIMUM SURFACE SETTLEMENT S_{smax} FOR TUNNELS IN STIFF CLAYS

No.	Tunnel	z/D	S_{\max}/D	Reference
1.	Regent's Park (Sthbd)	8.19	1.20×10^{-3}	T.R.R.L.
2.	Ottawa	6.00	2.00×10^{-3}	Peck (1969)
3.	Victoria Line	6.00	2.29×10^{-3}	Peck (1969)
4.	Victoria Line	6.00	2.08×10^{-3}	Schmidt (1969)
5.	Victoria Line	5.29	2.18×10^{-3}	Bartlett & Bubbers (1970)
6.	Victoria Line	5.29	2.43×10^{-3}	Bartlett & Bubbers (1970)
7.	Regent's Park (Nthbd)	4.75	1.69×10^{-3}	T.R.R.L.
8.	Victoria Line	4.13	3.16×10^{-3}	Bartlett & Bubbers (1970)
9.	Victoria Line	2.90	6.14×10^{-3}	Bartlett & Bubbers (1970)
10.	Victoria Line	2.51	5.31×10^{-3}	Bartlett & Bubbers (1970)
11.	Victoria Line	2.51	7.18×10^{-3}	Bartlett & Bubbers (1970)
12.	Victoria Line	2.20	9.24×10^{-3}	Bartlett & Bubbers (1970)
13.	Garrison Dam	3.35	3.87×10^{-3}	Burke (1957)
14.	Oakland	3.38	4.00×10^{-3}	Kuesel (1969)
15.	BART	3.28	5.50×10^{-3}	Peck (1969)
16.	Chicago	3.21	11.25×10^{-3}	Peck (1969)
17.	G.N.R.R.-U.S.	3.10	21.50×10^{-3}	Peck (1969)
18.	Tokyo	3.22	26.10×10^{-3}	Peck (1969)
19.	Grangemouth	3.70	38.90×10^{-3}	Henry (1974)
20.	Fleet Line	7.10	1.61×10^{-3}	Attewell & Farmer (1972)
21.	Hebburn, Tyneside	3.65	3.50×10^{-3}	Attewell & Farmer (1973)
22.	Howdon, Tyneside	3.93	3.10×10^{-3}	(unpublished data)
23.	Willington Quay	3.15	5.88×10^{-3}	present case history
24.	Willington Quay	3.15	15.66×10^{-3}	present case history

Table 9: DEPTH-SETTLEMENT CASE HISTORIES
FOR STIFF CLAYS.

points for stiff clay. This suggests that in the absence of the second rapid phase of movement and consolidation, settlement behaviour would have been comparable to that of stiff clay.

The results indicate therefore, that the exponential relationship may be used to give an indication of the settlement which can be expected to develop when shield tunnelling in stiff clay at $z/D > 3.5$. Where $z/D < 3.5$ it is suggested that the extension plotted in Figure 7.2 may be tentatively used, although additional accurate settlement data is required to confirm this.

The complex case history serves to point out the variety of events and processes which can contribute to surface settlement and ground movement when tunnelling in soft ground. On the basis of the evidence accumulated so far it is reasonable to assume that settlement will persist for some considerable time. Furthermore it is probable that any future disturbance of the present relative equilibrium of slow consolidation will cause a change in the rate of settlement.

The results suggest that tunnelling through recent alluvium is to be avoided wherever possible, particularly where buildings and other sensitive surface structures overlie the path of the tunnel. However, as with this example, the cost of repairing the damage to surface structures compared with the cost of taking an alternative route frequently makes the former a more viable proposition.

REFERENCES

a) TUNNELLING

1. ATTEWELL, P.B. and BODEN, J.B. (1971) Development of stability ratios for tunnels driven in clay. Tunnels and Tunnelling, 3(3), pp.195-198.
2. ATTEWELL, P.B. and FARMER, I.W. (1972) Determination and interpretation of surface and sub-surface ground movements during construction of a tunnel in London Clay, at Green Park, London. Report ref. no. PBA/IWF/TRRL/1972/1 to Transport and Road Research Laboratory.
3. ATTEWELL, P.B. and FARMER, I.W. (1973) Measurement and interpretation of ground movements during construction of a tunnel in laminated clay at Hebburn, County Durham. Report ref. no. PBA/IWF/TRRL/1973/2 to Transport and Road Research Laboratory.
4. ATTEWELL, P.B. and FARMER, I.W. (1974) Ground deformation Resulting from Shield Tunnelling in London Clay. Canadian Geotechnical Journal, vol.11, 3, pp.380-395.
5. ATTEWELL, P.B. and FARMER, I.W. (1974) Ground disturbance caused by Shield Tunnelling in a Stiff, overconsolidated clay. Eng. Geol., 8, pp.361-381.
6. BARTLETT, J.V., BIGGART, A.R. and TRIGG, R.L. (1973) The Bentonite Tunnelling Machine. Proc. Inst. Civ. Eng., Part 1: Design and Construction, Nov. 1973, vol,54, paper 7670, pp. 605-624.
7. BARTLETT, J.V. and BUBBERS, B.L. (1970) Surface movements caused by bored tunnelling. Conf. Subway Constr. Budapest, Hung., paper 3(5), pp. 513-539.

8. BERRY, D.S. (1964) A discussion of the "stochastic" theory of ground movement.
Felsmechanik und Ingenieurgeologie, 2(1), pp.213-227.
9. BODEN, J.B. and McCAUL, C. (1974) Measurement of ground movements during a bentonite tunnelling experiment.
T.R.R.L. Report 653.
10. BUTLER, R.A. (1975) Subsidence over a Soft Ground Tunnel.
Jl. of the Geotech. Eng. Div. (Proc. of the Am. Soc. of Civil Engs.), vol. 100, 1, Jan. 1975.
11. CUEVAS, N.R. (1969) Contribution to panel discussion on Peck, R.B. : Deep Excavations and Tunnelling in Soft Ground.
Proc. 7th Int. Conf. Soil Mech.Found.Eng., Mexico City, 3, pp. 365-367.
12. GLOSSOP, N.H. (1976) Soil Deformation caused by Soft Ground Tunnelling.
Ph.D. Thesis, University of Durham, (in press).
13. HANSMIRE, W.H. and CORDING, J.E. (1972) Performance of a Soft Ground Tunnel on the Washington Metro.
Proc. of Rapid Tunnelling and Exc. Conf., vol. 1, chpt.23, 1972.
14. HARTMARK, H. (1964) Geotechnical observations during construction of a tunnel through soft clay in Trondheim, Norway.
Rock.Mech. Eng. Geol., Vienna, Austria, 2(1), pp.9-21.
15. HENRY, K. (1974) Grangemouth tunnel sewer.
Tunnels and Tunnelling, vol. 6, Jan. 1974, pp.25-26.
16. HEWETT, B.H.M. and JOHANNESSON, S. (1922) Shield and Compressed Air Tunnelling.
McGraw Hill, New York.

17. KUESEL, T. (1969) Contribution to panel discussion of :
Peck, R.B. : Deep Excavations and Tunnelling in
Soft Ground.
Proc. 7th Int. Conf. Soil Mech. Found. Eng.,
Mexico City, 3, pp 312-320.
18. LEE, K.L. and SHEN, C.K. (1969) Horizontal Movements Related
to Subsidence.
Jl. of the Soil Mech. and Found. Div., A.S.C.E.,
vol.95, paper 6336, Jan. 1969, pp 139-166.
19. LITWINISZYN, J. (1955) Displacements in Loess Bodies as
Stochastic Processes.
Bull. de l'Academie Polonaise des Sciences, III,4.
20. LITWINISZYN, J. (1956) Application of the equation of
stochastic processes to mechanics of loose bodies.
Arch. Mech. Stosow., 8(4), pp. 393-411.
21. LUSCHER, U. and HOEG, K. (1965) The action of soil around
buried tubes.
Proc. 6th Int. Conf. Soil Mech. Found. Eng., Toronto,
Ont., 2, pp. 396-400.
22. MORETTO, O. (1969) Contribution to panel discussion on :
Peck, R.B. : Deep Excavations and Tunnelling in
Soft Ground.
Proc. 7th Int. Conf. Soil Mech. Found. Eng.,
Mexico City, 3, pp. 325-328.
23. PECK, R.B. (1969) Deep Excavations and Tunnelling in Soft
Ground. "State of the Art report".
Proc. 7th Int. Conf. Soil Mech. Found. Eng.,
Mexico City, 3, pp. 225-290.
24. PECK, R.B. (1969) Deep Excavations and Tunnelling in Soft
Ground.
Proc. 7th Int. Conf. Soil Mech. Found. Eng.,
Mexico City, 3, pp. 311-373.
25. SCHMIDT, B. (1969) Settlements and ground movements associated
with tunnelling in soil.
Ph.D. Thesis, Univ. of Illinois, Urbana, Ill.

26. SOUTO SILVEIRA, E.B. and GAIOTO, N. (1969) Contribution to panel discussion on : Peck, R.B. : Deep Excavations and Tunnelling in Soft Ground. Proc. 7th Int. Conf. Soil Mech. Found. Eng., Mexico City, 3, pp. 367-369.
27. SZECHY, K. (1966) The Art of Tunnelling Translated from the Hungarian by D. Szechy et al., Akademiai, Kiado, Budapest, Hungary.
28. WARD, W.H. (1969) Contribution to panel discussion on : Peck, R.B. : Deep Excavations and Tunnelling in Soft Ground. Proc. 7th Int. Conf. Soil Mech. Found. Eng., Mexico City, 3, pp. 320-325.
29. WOOD, A.M. MUIR, (1969) Contribution to panel discussion on: Deep Excavations and Tunnelling in Soft Ground. Proc. 7th Int. Conf. Soil Mech. Found. Eng., Mexico City, 3, pp. 363-365.

b) LABORATORY EXPERIMENTATION.

30. AKROYD, T.N.W. (1964) Laboratory testing in Soil Engineering. Geotechnical Monograph 1.
31. BRINDLEY, G.W. (1961) Quantitative Analysis of Clay Mixtures. The X-Ray Identification of Crystal Structures in Clay Minerals, chpt. 14, edited by G. Brown (Mineralogical Society - Clay Minerals Group), London.
32. CLOUGH, K.H. (1936) Study of permeability measurements and their application to the oil industry. Oil Weekly, vol. 83, 4, pp. 27-34.
33. GRIM, R.E. (1953) Clay Mineralogy. McGraw-Hill, New York.
34. GRIM, R.E. (1962) Applied Clay Mineralogy. McGraw-Hill, New York.

35. LAMBE, T.W. and WHITMAN, R.V. (1969) Soil Mechanics.
John Wiley and Sons, Inc., New York.
36. MILLIGAN, V., SODERMAN, L.G. and RUTKA, A. (1962) Experience with
Canadian Varved Clays.
Jl. Soil Mechs. and Found. Division, A.S.C.E.,
paper 3224, Aug. 1962.
37. OHLE, E.L. (1951) The influence of permeability on ore distribution
in limestone and dolomite.
Economic Geology, vol. 46, Nov. 1951, pp. 667-706.
38. TERZAGHI, K. and PECK, R.B. (1967) Soil Mechanics in Engineering
Practise.
John Wiley and Sons Inc., New York.
39. VARIOUS (1951) X-Ray Identification and Structure of Clay Minerals.
Mineralogical Society of Great Britain.
Monograph.
40. VARIOUS (1967) Methods of Testing Soils for Civil Engineering
Purposes.
British Standards Institution, B.S. 1377.

c) GEOLOGY.

41. ANDERSON, W. (1940) Buried Valleys and Late Glacial Drainage Systems
in North-West Durham.
Proc. Geol. Assoc., 51, pp. 274-287.
42. ARMSTRONG, G. and KELL, J. (1951) The Tyne Tunnel.
Geological Mag., 88, pp. 257-361.
43. BEAUMONT, P. (1967) Glacial deposits of East Durham.
Ph.D. Thesis, University of Durham.
44. COUPLAND, G. and WOOLACOTT, D. (1926) The superficial deposits
near Sunderland and the Quaternary sequence in East
Durham.

45. DWERRYHOUSE, A.R. (1902) The Glaciation of Teesdale, Weardale and the Tyne Valley.
Quart. Jl. Geol. Soc., 58, pp. 572-608.
46. FRANCIS, E.A. (1970) Geology at Durham.
Trans. Nat. Hist. Soci., Durham, Northumberland, and Newcastle-upon-Tyne, vol.41, pp. 1-78.
47. HOWSE, R. (1864) On the Glaciation of the counties of Durham and Northumberland.
Trans. N. of England Min. Engrs., 13, pp. 169-185.
48. LEBOUR, G.A. (1894) Surface features in the Tyne valley.
Trans. Nat. Hist. Soc., Northumberland and Durham, 11, pp. 191-195.
49. MARSHALL, A. (1969) Glacial Deposits of the Team Wash.
M.Sc. Thesis, University of Durham.
50. MERRICK, E. (1909) Superficial Deposits around Newcastle-upon-Tyne.
Proc. Univ. Durham Phil. Soc., 3, p.141.
51. PEEL, R.F. (1941) The North Tyne Valley.
Geographical Journal, 98, pp. 5-19.
52. SMYTHE, J.A. (1912) Glacial Geology of Northumberland.
Trans. Nat. Hist. Soc., Northumberland and Durham, 4, pp. 86-116.
53. TRECHMANN, C.T. (1952) On the Pleistocene of Eastern Durham.
Proc. Yorks. Geol. Soc., 28, pp. 164-178.
54. TROTTER, F.M. and HOLLINGWORTH, S.E. (1932) Correlation of Northern Drifts.
Geological Mag., vol. 69, pp. 374-380.
55. VARIOUS (1931) Geology of Northumberland and Durham.
Geol. Assoc., 1931, p.67.

56. WOOLACOTT, D. (1905) The Superficial Deposits and Pre-glacial Valleys of the Northumberland and Durham Coalfield.
Quart. Jl. Geol. Soc., 61, p.68.
57. WOOLACOTT, D. (1921) The Interglacial Problem and the Glacial and Post-Glacial Sequence in Northumberland and Durham.
Geological Mag., 58, pp. 60-69.

APPENDIX 1.Rate of Face-Take.

$$\text{Area of Tunnel Face} - A = \frac{\pi D^2}{4}$$

$$\text{Rate of Face-Take} - S_F = \frac{V_F}{A} \cdot \text{X}$$

Where D is the unlined tunnel diameter (4.31m)

V_F is the volume of ground lost when the instrumentation array is intersected ($0.200 \text{ m}^3/\text{m}$).

X is the average rate of tunnel advance excluding weekends ($1.44\text{m}/\text{day}$).

$$A = \frac{\pi \cdot 4.31^2}{4} = 14.589 \text{ m}^2$$

$$S_F = \frac{0.200}{14.589} \cdot 1.44 = 0.0197 \text{ m/day}$$

$$= 0.82 \text{ mm/hour}$$

Volume of Settlement Trough

$$\text{Volume of Settlement Trough} = 2\pi \cdot i S_s \text{ max}$$

(calculated from Error Curve)

where $S_s \text{ max}$ is the maximum surface settlement

i is the point of inflexion of the Error Curve.

At zero days:

$$S_s \text{ max} = 6.4 \text{ mm} \quad i = 6.30$$

$$\text{Volume of Trough} = 0.202 \text{ m}^3/\text{m}$$

At 23 days:

$$S_s \text{ max} = 23.7 \text{ mm} \quad i = 6.15$$

$$\text{Volume of Trough} = 0.731 \text{ m}^3/\text{m}$$

At 51 days:

$$\begin{aligned} S_g \text{ max} &= 35.1 \text{ mm} & i &= 6.85 \\ \text{Volume of Trough} & & &= 1.205 \text{ m}^3/\text{m} \end{aligned}$$

At 149 days:

$$\begin{aligned} S_g \text{ max} &= 60.7 \text{ mm} & i &= 7.60 \\ \text{Volume of Trough} & & &= 2.313 \text{ m}^3/\text{m} \end{aligned}$$

At 224 days:

$$\begin{aligned} S_g \text{ max} &= 66.5 \text{ mm} & i &= 7.25 \\ \text{Volume of Trough} & & &= 2.417 \text{ m}^3/\text{m} \end{aligned}$$

APPENDIX 2 : FIELD AND EXPERIMENTAL DATA

	Page
Surface Settlement.....	165
Lateral Surface Movement Perpendicular to Centre Line.....	167
Normalised Lateral Surface Movement Perpendicular to Centre Line.....	168
Sub-surface Settlement (Boreholes 2,3 and 4).....	169
Ground Movement Vectors in Plane of Array.....	172
Ground Movement Vectors Parallel to Tunnel.....	177
X.R.F. Analysis Conditions.....	183
Moisture Content, Organic Content and Absorbed Moisture.....	184
X.R.D. Analyses.....	190
X.R.F. Analyses.....	192
Analysis of Consolidation Data.....	194
Lateral Sub-surface Movement towards Tunnel Face (1.1).....	195
Lateral Sub-surface Movement Perpendicular to Centre Line (2.2, 3.2, 4.2).....	203
Lateral Sub-surface Movement Parallel to Tunnel (2.1, 3.1, 4.1).....	259

SURFACE SETTLEMENT DATA (MM)

DATE	TUNNEL FACE POSITION			DAYS	SURFACE SETTLEMENT STATIONS										
	RINGS	FEET	METRES		J	I	H	G	F	E	D	C	B	A	
8:1:75	-57	-114	-34.79	-19	0.0	0.0	0.0	0.0	0.0	0.0	0.0	0.0	0.0	0.0	0.0
13:1:75	-50	-100	-30.48	-14	0.7	0.5	1.3	1.3	1.2	0.7	0.1	0.0	0.0	0.0	0.0
14:1:75	-47	-94	-28.65	-13	0.0	0.3	1.1	0.9	0.9	0.4	0.3	0.0	0.0	0.0	0.0
15:1:75	-43	-86	-26.21	-12	1.0	1.1	1.9	1.7	1.4	1.3	0.8	0.0	0.0	0.0	0.0
20:1:75	-32	-64	-19.51	-9	1.0	1.9	2.6	2.3	2.3	1.8	1.3	0.0	0.0	0.0	0.0
23:1:75	-21	-42	-12.80	-6	1.9	1.9	2.9	2.5	2.7	2.0	1.1	0.0	0.0	0.0	0.0
24:1:75	-18	-36	-10.97	-5	2.3	2.4	3.1	3.2	2.7	2.1	1.4	0.0	0.0	0.0	0.0
10:2:75	-14	-28	-8.53	-4	0.4	0.9	2.1	2.0	1.7	1.0	1.2	0.0	0.0	0.0	0.0
11:2:75	-11	-22	-6.71	-3	1.3	2.6	3.7	3.4	3.1	2.3	1.9	0.0	0.0	0.0	0.0
12:2:75	-7	-14	-4.27	-2	0.4	1.4	2.9	2.6	2.3	1.3	1.2	0.0	0.0	0.0	0.0
13:2:75	-3	-6	-1.83	-1	0.6	2.5	4.5	4.0	3.7	2.5	1.9	0.0	0.0	0.0	0.0
14:2:75	0	0	0.00	0	1.1	3.7	6.4	5.5	5.2	3.2	2.3	0.0	0.0	0.0	0.0
15:2:75	2	4	1.22	1	1.3	4.1	7.2	6.6	6.0	3.3	2.0	0.0	0.0	0.0	0.0
17:2:75	3	6	1.83	2	0.9	4.2	7.8	6.9	6.3	3.8	2.2	0.0	0.0	0.0	0.0
18:2:75	6	12	3.66	3	0.3	4.7	9.2	8.3	7.3	3.8	2.4	0.0	0.0	0.0	0.0
19:2:75	10	20	6.10	4	1.5	7.0	12.3	11.0	9.9	5.5	3.0	0.0	0.0	0.0	0.0
20:2:75	14	28	8.53	5	1.5	7.7	14.0	12.5	11.3	6.5	3.6	0.5	0.0	0.0	0.0
21:2:75	17	34	10.36	6	1.7	9.0	15.8	14.6	12.6	7.6	4.1	0.3	0.0	0.0	0.0
24:2:75	20	40	12.19	7	2.3	10.0	17.3	15.6	14.1	8.1	5.1	0.2	0.0	0.0	0.0
25:2:75	23	46	14.02	8	2.4	10.4	18.1	16.4	14.8	8.2	5.2	0.2	0.0	0.0	0.0
27:2:75	31	62	18.90	10	2.9	11.7	19.7	17.9	16.1	9.0	5.4	0.4	0.0	0.0	0.0
4:3:75	42	84	25.60	13	2.5	12.2	21.1	19.0	17.2	10.0	6.0	0.5	0.0	0.0	0.0
7:3:75	51	102	31.09	16	3.0	13.0	22.1	20.2	18.3	10.7	6.5	0.7	0.0	0.0	0.0
14:3:75	68	136	41.45	23	3.7	14.2	23.7	21.9	19.7	11.7	7.3	0.8	0.0	0.0	0.0
21:3:75	86	172	52.43	30	6.1	18.0	28.0	25.8	23.6	14.6	9.3	1.9	0.5	0.0	0.0
24:3:75	88	176	53.64	33	6.9	19.0	29.8	27.6	25.3	15.8	10.4	2.5	0.9	0.5	0.5
27:3:75	99	198	60.35	36	8.7	21.7	32.8	30.3	27.8	18.0	11.8	2.8	1.1	0.1	0.1
4:4:75	110	220	67.06	44	8.9	22.7	34.1	31.7	29.1	18.3	12.3	2.7	1.0	0.4	0.4
11:4:75	129	258	78.64	51	9.4	23.5	35.1	32.6	30.2	19.0	12.6	2.9	0.8	0.0	0.0
18:4:75	144	288	87.78	58	9.8	24.2	35.8	34.0	30.8	19.6	13.0	2.8	0.7	0.0	0.0
2:5:75	169	338	103.02	72	11.8	27.6	39.1	35.8	33.4	21.2	15.2	3.0	1.1	0.2	0.2
21:5:75	207	414	126.19	91	15.5	32.2	45.1	41.8	38.5	24.7	17.6	3.9	1.7	0.1	0.1

SURFACE SETTLEMENT DATA (MM)

DATE	TUNNEL FACE POSITION			DAYS	SURFACE SETTLEMENT STATIONS									
	RINGS	FEET	METRES		J	I	H	G	F	E	D	C	B	A
30:5:75	225	450	137.16	100	18.6	35.9	48.7	45.1	41.6	27.3	19.5	5.0	1.6	0.3
6:6:75	233	466	142.04	107	20.9	37.7	50.7	46.7	43.5	28.0	20.2	5.4	1.6	0.0
18:6:75	237	474	144.47	119	23.3	41.5	54.5	50.5	46.8	30.7	23.7	6.1	1.6	0.0
1:7:75	237	474	144.47	132	25.8	44.8	58.0	53.6	49.9	33.3	26.2	7.6	2.3	0.5
11:7:75	237	474	144.47	142	26.5	46.4	59.5	55.2	51.3	34.6	27.2	8.1	2.5	0.5
18:7:75	237	474	144.47	149	27.7	47.7	60.7	56.7	52.8	35.6	28.4	8.7	2.8	0.5
13:8:75	237	474	144.47	176	26.3	46.2	58.7	54.1	50.3	18.9	23.4	5.6	1.1	0.1
21:8:75	237	474	144.47	184	27.1	47.5	60.4	55.3	51.6	20.2	24.2	5.8	1.2	0.1
9:9:75	237	474	144.47	202	30.4	50.8	63.8	58.7	54.8	22.9	27.9	7.2	1.7	0.7
30:9:75	237	474	144.47	224	31.6	53.2	66.5	61.6	57.6	25.1	29.1	8.8	2.7	1.3

TUNNEL COMPLETED AT SHAFT C6 ON 10:6:75

LATERAL SURFACE MOVEMENT PERPENDICULAR TO CENTRE LINE (MM)

DATE	TUNNEL FACE POSITION			DAYS	LATERAL SURFACE MOVEMENT STATIONS									
	RINGS	FEET	METRES		J	I	H	G	F	E	D	C	B	A
8:1:75	-57	-114	-34.79	-11	0.0	0.0	0.0	0.0	0.0	0.0	0.0	0.0	0.0	0.0
15:1:75	-43	-86	-26.21	-12	-0.3	-0.3	0.0	-0.3	-0.3	0.0	0.6	0.3	0.3	0.0
24:1:75	-18	-36	-10.97	-5	0.0	-0.3	0.0	0.0	0.0	-0.3	0.0	0.0	0.0	-0.3
10:2:75	-14	-28	-8.53	-4	0.3	0.3	0.0	0.0	0.0	0.6	0.0	0.0	0.0	-0.3
12:2:75	-7	-14	-4.27	-2	0.6	0.3	0.0	0.0	1.2	0.9	0.3	-0.3	0.3	0.0
13:2:75	-3	-6	-1.83	-1	0.9	0.3	0.0	0.6	1.2	0.9	0.6	-0.3	-0.3	-0.9
14:2:75	0	0	0.00	0	0.9	1.2	0.0	0.6	1.2	1.2	0.6	-0.6	-0.3	-0.9
17:2:75	3	6	1.83	2	1.5	1.5	0.0	1.2	2.1	2.4	1.5	1.2	0.9	1.5
19:2:75	10	20	6.10	4	1.8	2.7	0.0	2.1	3.0	3.4	2.4	1.5	1.2	1.8
21:2:75	17	34	10.36	6	1.8	3.0	0.0	2.7	3.0	4.9	2.1	0.6	0.9	0.6
24:2:75	20	40	12.19	7	2.4	3.7	0.0	2.7	3.7	4.9	2.7	0.9	0.9	0.9
27:2:75	31	62	18.90	10	2.1	3.7	0.0	3.0	3.7	5.2	3.4	0.9	1.2	0.6
7:3:75	51	102	31.09	16	2.7	4.6	0.0	3.7	4.9	5.8	4.0	1.8	2.1	1.8
21:3:75	86	172	52.43	30	4.0	5.8	0.0	4.3	5.2	7.0	5.2	2.1	1.8	1.8
27:3:75	99	198	60.35	36	4.0	5.8	0.0	4.9	5.8	7.6	6.1	2.7	2.4	1.2
4:4:75	110	220	67.06	44	4.9	6.7	0.0	4.9	6.4	8.2	7.3	3.4	2.7	4.9
11:4:75	129	258	78.64	51	6.1	7.3	0.0	4.9	6.4	8.5	7.3	3.7	3.4	3.0
2:5:75	169	338	103.02	72	6.7	7.9	0.0	5.2	7.0	9.1	7.9	3.7	3.7	4.0
21:5:75	207	414	126.19	91	8.2	8.5	0.0	6.4	8.5	11.0	10.1	6.1	5.5	5.8
6:6:75	233	466	142.04	107	11.0	10.1	0.0	7.0	9.1	11.9	10.7	6.1	5.8	5.8
18:6:75	237	474	144.47	119	11.3	10.4	0.0	7.0	9.4	12.2	11.6	7.0	7.0	6.4
1:7:75	237	474	144.47	132	11.6	10.7	0.0	7.3	9.4	12.8	12.5	8.2	8.2	7.3
18:7:75	237	474	144.47	149	11.6	11.3	0.0	7.3	10.1	13.7	12.5	8.5	7.6	6.7
13:8:75	237	474	144.47	176	11.3	10.1	0.0	7.0	9.8	11.3	10.7	7.0	5.5	5.2
9:9:75	237	474	144.47	202	11.3	10.4	0.0	6.7	9.4	11.6	10.7	6.4	5.2	2.7
30:9:75	237	474	144.47	224	10.7	10.4	0.0	7.0	9.8	11.9	11.0	5.5	4.9	1.8

POSITIVE INDICATES MOVEMENT TOWARDS THE CENTRE LINE
 NEGATIVE INDICATES MOVEMENT AWAY FROM THE CENTRE LINE

NORMALISED LATERAL SURFACE MOVEMENT PERPENDICULAR TO CENTRE LINE (MM)

DATE	TUNNEL RINGS	FACE POSITION			LATERAL SURFACE MOVEMENT STATIONS										
		FEET	METRES	DAYS	J	I	H	G	F	E	D	C	B	A	
8:1:75	-57	-114	-34.79	-89	0.0	0.0	0.0	0.0	0.0	0.0	0.0	0.0	0.0	0.0	0.0
15:1:75	-43	-86	-26.21	-12	-0.3	-0.3	0.0	-0.3	-0.9	0.0	0.6	0.3	0.3	0.0	0.0
24:1:75	-18	-36	-10.97	-5	0.1	-0.2	0.0	0.0	0.0	-0.2	0.1	0.2	0.2	0.0	0.0
10:2:75	-14	-23	-8.53	-4	0.4	0.4	0.0	0.0	0.0	0.7	0.1	0.2	0.2	0.0	0.0
12:2:75	-7	-14	-4.27	-2	0.6	0.3	0.0	0.0	1.2	0.9	0.3	-0.3	0.3	0.0	0.0
13:2:75	-3	-6	-1.83	-1	1.3	0.5	0.0	0.7	1.4	1.2	1.0	0.2	0.4	0.0	0.0
14:2:75	0	0	0.00	0	1.3	1.4	0.0	0.7	1.4	1.5	1.0	-0.1	0.4	0.0	0.0
17:2:75	3	6	1.83	2	0.9	1.2	0.0	1.0	1.9	2.0	0.9	0.3	-0.3	0.0	0.0
19:2:75	10	20	6.10	4	1.1	2.4	0.0	1.9	2.8	2.8	1.7	0.4	-0.2	0.0	0.0
21:2:75	17	34	10.36	6	1.6	2.9	0.0	2.7	3.0	4.7	1.9	0.2	0.4	0.0	0.0
24:2:75	20	40	12.19	7	2.1	3.5	0.0	2.6	3.5	4.6	2.4	0.4	0.2	0.0	0.0
27:2:75	31	62	18.90	10	1.9	3.5	0.0	3.0	3.6	5.0	3.1	0.5	0.7	0.0	0.0
7:3:75	51	102	31.09	16	2.0	4.2	0.0	3.4	4.6	5.2	3.2	0.7	0.7	0.0	0.0
21:3:75	86	172	52.43	30	3.2	5.4	0.0	4.1	4.9	6.5	4.5	1.0	0.4	0.0	0.0
27:3:75	99	198	60.35	36	3.5	5.5	0.0	4.7	5.6	7.3	5.6	2.0	1.5	0.0	0.0
4:4:75	110	220	67.06	44	2.9	5.7	0.0	4.3	5.6	6.8	5.4	0.4	-1.2	0.0	0.0
11:4:75	129	258	78.64	51	4.9	6.7	0.0	4.5	5.9	7.6	6.1	1.8	0.9	0.0	0.0
2:5:75	169	338	103.02	72	5.1	7.1	0.0	4.7	6.4	8.0	6.3	1.3	0.5	0.0	0.0
21:5:75	207	414	126.19	91	5.9	7.4	0.0	5.7	7.6	9.2	7.7	2.6	0.9	0.0	0.0
6:6:75	233	466	142.04	107	8.7	8.9	0.0	6.3	8.2	10.2	8.4	2.6	1.2	0.0	0.0
18:6:75	237	474	144.47	119	8.7	9.1	0.0	6.3	8.4	10.3	9.0	3.2	1.9	0.0	0.0
1:7:75	237	474	144.47	132	8.7	9.2	0.0	6.5	8.3	10.6	9.6	3.8	2.4	0.0	0.0
18:7:75	237	474	144.47	149	8.9	9.9	0.0	6.5	9.0	11.7	9.8	4.5	2.3	0.0	0.0
13:8:75	237	474	144.47	176	9.2	9.0	0.0	6.4	8.9	9.7	8.6	3.9	1.3	0.0	0.0
9:9:75	237	474	144.47	202	10.2	9.8	0.0	6.4	9.0	10.8	9.6	4.8	3.0	0.0	0.0
30:9:75	237	474	144.47	224	9.9	10.0	0.0	6.8	9.5	11.3	10.2	4.4	3.4	0.0	0.0

POSITIVE INDICATES MOVEMENT TOWARDS THE CENTRE LINE
 NEGATIVE INDICATES MOVEMENT AWAY FROM THE CENTRE LINE

SUB-SURFACE SETTLEMENT DATA-BORFHOLE 2 (MM)

DATE	TUNNEL FACE POSITION			DAYS	SUB-SURFACE SETTLEMENT RINGS						
	RINGS	FEET	METRES		SURFACE	RING 1	RING 2	RING 3	RING 4	RING 5	RING 6
8:1:75	-57	-114	-34.79	-19	0.0	0.0	0.0	0.0	0.0	0.0	0.0
13:1:75	-50	-100	-30.48	-14	1.3	1.3	1.3	1.3	1.3	1.3	1.3
10:2:75	-14	-28	-8.53	-4	1.8	2.1	1.8	1.4	1.4	1.7	2.0
12:2:75	-7	-14	-4.27	-2	2.6	1.4	2.9	2.0	3.2	2.1	1.6
13:2:75	-3	-6	-1.83	-1	4.0	4.3	4.1	3.7	3.9	3.3	2.0
15:2:75	2	4	1.22	1	6.6	5.8	8.1	6.3	5.1	8.3	3.3
17:2:75	3	6	1.83	2	6.9	10.4	9.4	6.8	7.0	10.3	4.8
18:2:75	6	12	3.66	3	8.3	7.2	11.9	8.4	6.8	15.3	5.1
19:2:75	10	20	6.10	4	11.0	11.6	18.9	11.8	10.2	24.3	9.4
20:2:75	14	28	8.53	5	12.5	12.6	21.5	12.8	12.2	26.7	10.7
21:2:75	17	34	10.36	6	14.6	15.0	24.0	14.9	14.0	29.3	12.0
24:2:75	20	40	12.19	7	15.6	16.4	27.6	16.7	16.1	32.3	14.5
25:2:75	23	46	14.02	8	16.4	17.0	29.3	18.1	15.4	33.2	13.8
27:2:75	31	62	18.90	10	17.9	18.1	31.0	18.6	17.1	39.8	14.7
4:3:75	42	84	25.60	13	19.0	19.2	34.5	21.1	19.7	36.5	16.4
7:3:75	51	102	31.09	16	20.2	20.9	35.6	21.5	20.7	40.1	17.6
14:3:75	68	136	41.45	23	21.9	23.7	38.7	23.5	23.3	40.9	19.8
24:3:75	88	176	53.64	33	27.6	31.9	49.9	28.9	28.7	46.1	24.1
4:4:75	110	220	67.06	44	31.7	36.9	57.9	33.1	33.2	50.3	0.0
11:4:75	129	258	78.64	51	32.6	37.7	60.4	34.7	35.4	51.7	0.0
18:4:75	144	288	87.78	58	34.0	40.5	62.6	40.8	37.0	54.0	0.0
2:5:75	169	338	103.02	72	35.8	42.0	65.2	38.1	39.4	59.9	0.0
21:5:75	207	414	126.19	91	41.8	48.0	73.1	43.6	45.5	64.0	0.0
6:6:75	233	466	142.04	107	46.7	53.7	76.9	49.9	49.1	66.1	0.0
18:6:75	237	474	144.47	119	50.5	57.9	80.5	54.4	52.6	63.9	0.0
1:7:75	237	474	144.47	132	53.6	61.1	83.3	56.9	55.4	68.4	0.0
18:7:75	237	474	144.47	149	56.7	62.9	85.8	59.5	57.0	69.1	0.0
13:8:75	237	474	144.47	176	54.1	60.0	60.6	36.1	41.8	51.9	0.0
21:8:75	237	474	144.47	184	55.3	60.7	62.2	36.7	37.7	51.6	0.0
9:9:75	237	474	144.47	202	58.7	63.5	64.7	39.1	38.7	52.6	0.0
30:9:75	237	474	144.47	224	61.6	65.8	67.2	41.1	40.0	54.1	0.0

SUB-SURFACE SETTLEMENTS SHOWED NO DEVIATION FROM THE SURFACE SETTLEMENTS UNTIL 10:2:75

SUB-SURFACE SETTLEMENT DATA-BOREHOLE 3 (MM)

DATE	TUNNEL FACE POSITION			DAYS	SUB-SURFACE SETTLEMENT RINGS					
	RINGS	FEET	METRES		SURFACE	RING 1	RING 2	RING 3	RING 4	RING 5
8:1:75	-57	-114	-34.79	-19	0.0	0.0	0.0	0.0	0.0	0.0
13:1:75	-50	-100	-30.48	-14	1.2	1.2	1.2	1.2	1.2	1.2
10:2:75	-14	-28	-8.53	-4	1.6	0.8	1.0	1.1	1.2	0.5
12:2:75	-7	-14	-4.27	-2	2.3	1.6	1.8	2.3	2.7	1.7
15:2:75	2	4	1.22	1	6.0	4.7	4.0	6.1	4.1	3.0
17:2:75	3	6	1.83	2	6.3	7.3	5.5	6.3	5.9	3.8
18:2:75	6	12	3.66	3	7.3	6.9	5.0	8.0	5.9	3.5
19:2:75	10	20	6.10	4	9.9	10.9	9.6	11.1	10.2	5.8
20:2:75	14	28	8.53	5	11.3	12.4	10.7	13.3	14.1	5.5
21:2:75	17	34	10.36	6	12.6	13.5	9.3	14.6	10.7	5.5
24:2:75	20	40	12.19	7	14.1	15.8	15.0	17.1	15.0	6.2
25:2:75	23	46	14.02	8	14.8	16.3	15.0	17.1	13.4	5.9
27:2:75	31	62	18.90	10	16.1	14.4	16.5	23.1	14.2	6.7
4:3:75	42	84	25.60	13	17.2	18.0	18.7	20.3	16.4	7.9
7:3:75	51	102	31.09	16	18.3	18.1	20.4	21.3	17.4	9.2
14:3:75	68	136	41.45	23	19.7	18.9	22.8	22.9	19.3	9.8
24:3:75	88	176	53.64	33	25.3	24.6	30.2	28.6	23.8	17.0
4:4:75	110	220	67.06	44	29.1	29.6	40.7	33.1	29.8	19.5
11:4:75	129	258	78.64	51	30.2	29.7	43.4	35.1	28.3	0.0
18:4:75	144	288	87.78	58	30.6	33.8	47.1	37.7	32.2	0.0
2:5:75	169	338	103.02	72	33.4	34.1	47.9	39.5	33.2	0.0
21:5:75	207	414	126.19	91	38.5	40.3	53.0	45.0	0.0	0.0
6:6:75	233	466	142.04	107	43.5	45.6	57.5	50.1	0.0	0.0
18:6:75	237	474	144.47	119	46.8	49.9	62.9	54.2	0.0	0.0
1:7:75	237	474	144.47	132	49.9	52.2	63.7	56.0	0.0	0.0
18:7:75	237	474	144.47	149	52.8	54.2	67.7	58.9	0.0	0.0
13:8:75	237	474	144.47	176	50.3	56.1	47.9	61.6	54.7	0.0
9:9:75	237	474	144.47	202	54.8	60.2	53.4	66.9	0.0	0.0
30:9:75	237	474	144.47	224	57.6	62.6	57.2	70.8	0.0	0.0

SUB-SURFACE SETTLEMENTS SHOWED NO DEVIATION FROM THE SURFACE SETTLEMENTS UNTIL 10:2:75

SUB-SURFACE SETTLEMENT DATA-BOREHOLE 4 (MM)

DATE	TUNNEL FACE POSITION			DAYS	SUB-SURFACE SETTLEMENT RINGS				
	RINGS	FEET	METRES		SURFACE	RING 1	RING 2	RING 3	RING 4
8:1:75	-57	-114	-34.79	-19	0.0	0.0	0.0	0.0	0.0
13:1:75	-50	-100	-30.48	-14	0.7	0.7	0.7	0.7	0.7
10:2:75	-14	-28	-8.53	-4	1.1	0.8	1.2	1.1	1.1
12:2:75	-7	-14	-4.27	-2	1.3	1.3	0.6	1.7	1.1
15:2:75	2	4	1.22	1	3.3	2.3	4.7	2.8	0.1
17:2:75	3	6	1.83	2	3.8	4.4	4.4	3.7	0.7
18:2:75	6	12	3.66	3	3.8	2.9	3.1	1.8	0.1
19:2:75	10	20	6.10	4	5.5	6.5	5.4	4.6	2.8
20:2:75	14	28	8.53	5	6.5	7.5	6.3	4.8	3.0
21:2:75	17	34	10.36	6	7.6	8.1	6.2	5.4	2.1
24:2:75	20	40	12.19	7	8.1	9.0	7.2	6.0	2.6
25:2:75	23	46	14.02	8	8.2	8.4	6.7	5.6	1.2
27:2:75	31	62	18.90	10	9.0	8.3	6.8	5.8	2.1
4:3:75	42	84	25.60	13	10.0	9.9	8.1	7.1	3.0
7:3:75	51	102	31.02	16	10.7	10.9	8.5	7.1	2.9
14:3:75	68	136	41.45	23	11.7	12.4	9.7	8.0	3.4
24:3:75	88	176	53.64	33	15.8	16.2	10.3	8.1	3.5
4:4:75	110	220	67.06	44	18.3	18.2	11.8	8.3	3.2
11:4:75	129	258	78.64	51	19.0	19.4	12.7	8.6	3.1
18:4:75	144	288	87.78	58	19.6	19.4	13.3	9.5	3.0
2:5:75	169	338	103.02	72	21.2	30.1	15.1	11.0	4.4
21:5:75	207	414	126.19	91	24.7	26.2	18.7	14.3	7.3
6:6:75	233	466	142.04	107	28.0	30.0	21.9	17.3	9.4
18:6:75	237	474	144.47	119	30.7	32.5	24.3	19.4	10.8
1:7:75	237	474	144.47	132	33.3	34.9	26.5	20.7	11.4
18:7:75	237	474	144.47	149	35.6	35.9	28.8	21.3	11.8
13:8:75	237	474	144.47	176	18.9	19.8	12.8	9.7	1.5
21:8:75	237	474	144.47	184	20.2	20.5	14.4	10.8	2.0
9:9:75	237	474	144.47	202	22.9	23.9	16.8	13.0	3.5
30:9:75	237	474	144.47	224	25.1	26.7	19.2	14.9	4.7

SUB-SURFACE SETTLEMENTS SHOWED NO DEVIATION FROM THE SURFACE SETTLEMENTS UNTIL 10:2:75

GROUND MOVEMENT VECTORS IN PLANE OF ARRAY UP TO 51 DAYS ADVANCE (MM)

BOREHOLE	RING	HORIZONTAL	VERTICAL	VECTOR	ANGLE
1	SURFACE	0.00	35.10	35.10	0
2	SURFACE	0.30	32.60	32.60	0
2	1	3.89	37.70	37.90	5
2	2	3.54	60.40	60.50	3
2	3	9.73	34.70	36.04	15
2	4	11.32	35.40	37.17	17
2	5	12.41	51.70	53.17	13
3	SURFACE	6.40	30.20	30.87	11
3	1	6.39	29.70	30.38	12
3	2	12.50	43.40	45.16	16
3	3	15.81	35.10	38.50	24
3	4	12.09	28.30	30.77	23
4	SURFACE	8.23	19.00	20.71	23
4	1	4.32	19.40	19.88	12
4	2	5.42	12.70	13.81	23
4	3	5.68	8.60	10.31	33
4	4	4.15	3.10	5.18	53

POSITIVE INDICATES MOVEMENT TOWARDS TUNNEL
 NEGATIVE INDICATES MOVEMENT AWAY FROM TUNNEL
 ZERO ANGLE IS VERTICALLY DOWNWARDS

GROUND MOVEMENT VECTORS IN PLANE OF ARRAY FROM 51 TO 91 DAYS ADVANCE (MM)

BOREHOLE	RING SURFACE	HORIZONTAL	VERTICAL	VECTOR	ANGLE
1		0.00	10.00	10.00	0
2	SURFACE	1.83	9.25	9.43	11
2	1	0.16	10.30	10.30	0
2	2	-0.90	12.70	12.73	-4
2	3	-4.05	8.90	9.78	-24
2	4	-6.14	10.15	11.86	-31
2	5	-11.17	12.80	16.99	-41
3	SURFACE	1.83	8.30	8.50	12
3	1	5.66	10.60	12.02	28
3	2	-2.67	9.60	9.96	-15
3	3	-8.32	9.90	12.93	-40
4	SURFACE	0.91	5.70	5.77	9
4	1	-0.58	6.80	6.82	-4
4	2	-3.28	6.00	6.84	-28
4	3	-4.35	5.75	7.21	-37
4	4	-3.17	4.25	5.30	-36

POSITIVE INDICATES MOVEMENT TOWARDS TUNNEL
 NEGATIVE INDICATES MOVEMENT AWAY FROM TUNNEL
 ZERO ANGLE IS VERTICALLY DOWNWARDS

GROUND MOVEMENT VECTORS IN PLANE OF ARRAY FROM 91 TO 149 DAYS ADVANCE (MM)

BOREHOLE	RING	HORIZONTAL	VERTICAL	VECTOR	ANGLE
1	SURFACE	0.00	15.60	15.60	0
2	SURFACE	0.92	14.85	14.88	3
2	1	1.19	14.90	14.95	4
2	2	1.03	12.70	12.74	4
2	3	2.13	15.90	16.04	7
2	4	2.18	11.50	11.70	10
2	5	1.72	5.10	5.38	18
3	SURFACE	1.52	14.35	14.43	6
3	1	0.91	13.90	13.93	3
3	2	1.45	14.70	14.77	5
3	3	1.36	13.90	13.97	5
4	SURFACE	1.83	10.85	11.00	9
4	1	1.06	9.70	9.76	6
4	2	1.72	10.15	10.29	9
4	3	1.88	7.00	7.25	15
4	4	1.90	4.45	4.84	23

POSITIVE INDICATES MOVEMENT TOWARDS TUNNEL
 NEGATIVE INDICATES MOVEMENT AWAY FROM TUNNEL
 ZERO ANGLE IS VERTICALLY DOWNWARDS

GROUND MOVEMENT VECTORS IN PLANE OF ARRAY FROM 149 TO 176 DAYS ADVANCE (MM)

BOREHOLE	RING	HORIZONTAL	VERTICAL	VECTOR	ANGLE
1	SURFACE	0.00	-0.20	0.20	180
2	SURFACE	0.60	-2.60	2.67	192
2	1	-0.86	-2.90	3.02	-164
2	2	-0.12	-25.20	25.20	-180
2	3	-5.61	-23.35	24.01	-167
2	4	-7.87	-10.35	13.00	-143
2	5	-9.43	-17.20	19.62	-152
3	SURFACE	-0.30	-2.55	2.57	-174
3	1	-0.65	1.90	2.01	-18
3	2	-3.16	-19.80	20.05	-171
3	3	-8.48	2.70	8.90	-72
4	SURFACE	-1.22	-16.65	16.69	-176
4	1	-2.63	-16.10	16.31	-171
4	2	-6.35	-16.05	17.26	-159
4	3	-6.24	-11.65	13.22	-152
4	4	-3.55	-10.30	10.89	-161

POSITIVE INDICATES MOVEMENT TOWARDS TUNNEL
 NEGATIVE INDICATES MOVEMENT AWAY FROM TUNNEL
 ZERO ANGLE IS VERTICALLY DOWNWARDS

GROUND MOVEMENT VECTORS IN PLANE OF ARRAY FROM 176 TO 224 DAYS ADVANCE (MM)

BOREHOLE	RING SURFACE	HORIZONTAL	VERTICAL	VECTOR	ANGLE
1		0.00	7.80	7.80	0
2	SURFACE	0.62	7.50	7.53	4
2	1	0.23	5.80	5.80	2
2	2	-0.01	6.61	6.61	0
2	3	-0.10	5.00	5.00	-1
2	4	0.04	6.70	6.70	0
2	5	-0.84	2.20	2.35	-20
3	SURFACE	0.00	7.30	7.30	0
3	1	-0.14	6.50	6.50	-1
3	2	-0.18	9.30	9.30	-1
3	3	-0.22	9.20	9.20	-1
4	SURFACE	0.61	6.15	6.18	5
4	1	-0.16	6.90	6.90	-1
4	2	-0.03	6.40	6.40	0
4	3	-0.19	5.25	5.25	-2
4	4	-0.14	3.25	3.25	-2

POSITIVE INDICATES MOVEMENT TOWARDS TUNNEL
 NEGATIVE INDICATES MOVEMENT AWAY FROM TUNNEL
 ZERO ANGLE IS VERTICALLY DOWNWARDS

GROUND MOVEMENT VECTORS PARALLEL TO TUNNEL IN BOREHOLE 2 OFFSET 2.93M FROM CENTRE LINE (MM)

TIME	BOREHOLE	RING	HORIZONTAL	VERTICAL	VECTOR	ANGLE
UP TO 51	2	SURFACE	-3.00	32.60	32.74	-5
	2	1	-3.18	37.70	37.83	-4
	2	2	-1.40	60.40	60.42	-1
	2	3	-0.03	34.70	34.70	0
	2	4	-0.30	35.40	35.40	0
	2	5	-0.95	51.70	51.71	-1
51 TO 91	2	SURFACE	-8.95	9.25	12.87	-44
	2	1	-7.32	10.30	12.64	-35
	2	2	-6.71	12.70	14.36	-27
	2	3	-0.35	8.90	8.91	-2
	2	4	-0.42	10.15	10.16	-2
	2	5	-6.08	12.30	13.72	-26
91 TO 149	2	SURFACE	-4.90	14.85	15.64	-18
	2	1	-3.50	14.90	15.31	-13
	2	2	-2.09	12.70	12.87	-9
	2	3	-0.11	15.90	15.90	0
	2	4	0.18	11.50	11.50	0
	2	5	1.25	5.10	5.25	13

GROUND MOVEMENT VECTORS PARALLEL TO TUNNEL IN BOREHOLE 2 OFFSET 2.93M FROM CENTRE LINE (MM)

TIME	BOREHOLE	RING	HORIZONTAL	VERTICAL	VECTOR	ANGLE
149 TO 176	2	SURFACE	0.85	-2.60	2.74	162
	2	1	1.30	-2.90	3.18	156
	2	2	-0.12	-25.20	25.20	-180
	2	3	-15.27	-23.35	27.90	-147
	2	4	-14.82	-10.35	18.08	-125
	2	5	-7.86	-17.20	18.91	-156
176 TO 224	2	SURFACE	-2.00	7.50	7.76	-14
	2	1	-1.51	5.80	5.99	-14
	2	2	-1.04	6.60	6.68	-8
	2	3	0.43	5.00	5.02	4
	2	4	0.81	6.70	6.75	6
	2	5	1.17	2.20	2.49	28

POSITIVE INDICATES MOVEMENT AWAY FROM CHANNEL
 NEGATIVE INDICATES MOVEMENT TOWARDS CHANNEL
 ZERO ANGLE IS VERTICALLY DOWNWARDS

GROUND MOVEMENT VECTORS PARALLEL TO TUNNEL IN BOREHOLE 3 OFFSET 3.93M FROM CENTRE LINE (MM)

TIME	BOREHOLE	RING	HORIZONTAL	VERTICAL	VECTOR	ANGLE
UP TO 51	3	SURFACE	-5.05	30.20	30.62	-9
	3	1	-0.12	29.70	29.70	0
	3	2	-1.02	43.40	43.41	-1
	3	3	-3.42	35.10	35.27	-5
	3	4	-4.32	28.30	28.63	-8
51 TO 91	3	SURFACE	-4.92	8.30	9.65	-30
	3	1	0.08	10.60	10.60	0
	3	2	-5.56	9.60	11.09	-30
	3	3	-2.07	9.90	10.11	-11
91 TO 149	3	SURFACE	-3.72	14.35	14.82	-14
	3	1	-0.52	13.90	13.91	-2
	3	2	0.43	14.70	14.71	1
	3	3	1.55	13.90	13.99	6

GROUND MOVEMENT VECTORS PARALLEL TO TUNNEL IN BOREHOLE 3 OFFSET 3.93M FROM CENTRE LINE (MM)

TIME	BOREHOLE	RING	HORIZONTAL	VERTICAL	VECTOR	ANGLE
149 TO 176	3	SURFACE	0.50	-2.55	2.60	169
	3	1	0.09	1.90	1.90	2
	3	2	-4.44	-19.80	20.29	-168
	3	3	-2.41	2.70	3.62	-41
176 TO 224	3	SURFACE	-1.80	7.30	7.52	-13
	3	1	-0.25	6.50	6.50	-2
	3	2	-0.19	9.30	9.30	-1
	3	3	-0.36	9.20	9.21	-2

POSITIVE INDICATES MOVEMENT AWAY FROM CHANNEL
 NEGATIVE INDICATES MOVEMENT TOWARDS CHANNEL
 ZERO ANGLE IS VERTICALLY DOWNWARDS

GROUND MOVEMENT VECTORS PARALLEL TO TUNNEL IN BOREHOLE 4 OFFSET 7.65M FROM CENTRE LINE (MM)

TIME	BOREHOLE	RING	HORIZONTAL	VERTICAL	VECTOR	ANGLE
UP TO 51	4	SURFACE	-4.60	19.05	19.60	-13
	4	1	-1.26	19.40	19.44	-3
	4	2	-1.36	12.70	12.77	-6
	4	3	-1.31	8.60	8.70	-8
	4	4	-0.86	3.10	3.22	-15
51 TO 91	4	SURFACE	-1.52	5.70	5.90	-14
	4	1	-0.48	6.80	6.82	-4
	4	2	0.28	6.00	6.01	2
	4	3	0.29	5.75	5.76	2
	4	4	0.01	4.25	4.25	0
91 TO 149	4	SURFACE	-3.38	10.85	11.36	-17
	4	1	-2.35	9.70	9.98	-13
	4	2	-2.35	10.15	10.42	-13
	4	3	-1.02	7.00	7.07	-8
	4	4	-0.26	4.45	4.46	-3

GROUND MOVEMENT VECTORS PARALLEL TO TUNNEL IN BOREHOLE 4 OFFSET 7.65M FROM CENTRE LINE (MM)

TIME	BOREHOLE	RING	HORIZONTAL	VERTICAL	VECTOR	ANGLE
149 TO 176	4	SURFACE	0.30	-16.65	16.65	179
	4	1	0.93	-16.10	16.13	177
	4	2	4.58	-16.05	16.69	165
	4	3	-7.23	-11.65	13.71	-149
	4	4	2.48	-10.30	10.59	167
176 TO 224	4	SURFACE	-0.40	6.15	6.16	-3
	4	1	2.99	6.90	7.52	23
	4	2	-1.69	6.40	6.62	-14
	4	3	-2.12	5.25	5.66	-21
	4	4	-1.89	3.25	3.76	-30

POSITIVE INDICATES MOVEMENT AWAY FROM CHANNEL
 NEGATIVE INDICATES MOVEMENT TOWARDS CHANNEL
 ZERO ANGLE IS VERTICALLY DOWNWARDS

X.R.F. ANALYSIS CONDITIONS

ELEMENT	2θ	KV	MA	CRYSTAL	COUNTER	VACUUM PATH	TUBE	COLLIMATION
SI	109.00	60	16	PE	FLOW	YES	CHROMIUM	COARSE
AL	145.00	60	16	PE	FLOW	YES	CHROMIUM	COARSE
FE	25.50	40	8	PE	FLOW	YES	CHROMIUM	COARSE
MG-PEAK	45.03	40	8	THALLIUM-AP	FLOW	YES	CHROMIUM	COARSE
MG-BGRND	47.26	40	8	THALLIUM-AP	FLOW	YES	CHROMIUM	COARSE
CA	45.00	20	8	PE	FLOW	YES	CHROMIUM	COARSE
NA_PEAK	55.97	20	8	THALLIUM-AP	FLOW	YES	CHROMIUM	COARSE
NA-BGRND	58.63	20	8	THALLIUM-AP	FLOW	YES	CHROMIUM	COARSE
K	50.50	40	8	PE	FLOW	YES	CHROMIUM	COARSE
TI	36.52	40	8	PE	FLOW	YES	CHROMIUM	COARSE
S-PEAK	75.65	40	8	PE	FLOW	YES	CHROMIUM	COARSE
S-BGRND	73.53	40	8	PE	FLOW	YES	CHROMIUM	COARSE
P-PEAK	89.76	40	8	PE	FLOW	YES	CHROMIUM	FINE
P-BGRND	91.61	40	8	PE	FLOW	YES	CHROMIUM	FINE

MACHINE DRIFT MONITORED USING STANDARD ANALYSED EACH RUN

MOISTURE CONTENT, ORGANIC CONTENT AND ABSORBED MOISTURE (%)

SAMPLE NUMBER	MOISTURE CONTENT	ABSORBED MOISTURE	ORGANIC CONTENT	MOISTURE ABSORBED BY SILT MINUS ORGANICS
A1	46.117	0.949	3.657	1.030
A2	42.110	0.915	2.896	0.875
A3	45.750	0.967	3.780	0.995
A4	38.051	0.758	3.315	0.898
A5	41.469	0.852	2.649	0.937
A6	40.969	0.871	2.693	0.960
A7	42.437	0.898	2.898	1.011
A8	43.191	0.879	3.254	0.935
AVER-A	42.512	0.886	3.143	0.949
B1	45.773	0.941	3.874	1.230
B2	47.798	1.029	3.984	1.290
B3	41.705	0.853	2.707	0.932
B4	39.934	0.824	2.312	1.033
B5	41.503	0.808	2.848	1.001
AVER-B	43.343	0.891	3.145	1.097
C1	42.170	0.879	2.837	0.948
C2	46.997	0.991	3.921	1.108
C3	41.921	0.895	4.394	1.006
C4	41.526	0.843	2.605	0.956
C5	40.500	0.846	3.109	1.030
AVER-C	42.623	0.891	3.118	1.010
D1A	44.362	0.969	4.192	1.363
D1B	44.890	0.938	3.978	1.280
D1C	41.775	0.796	3.715	1.164
D1D	40.458	0.758	3.793	1.230
D1E	42.087	0.802	3.974	1.174
AVERAGE	42.714	0.963	3.930	1.242

MOISTURE CONTENT, ORGANIC CONTENT AND ABSORBED MOISTURE (%)

SAMPLE NUMBER	MOISTURE CONTENT	ABSORBED MOISTURE	ORGANIC CONTENT	MOISTURE ABSORBED BY SILT MINUS ORGANICS
D2A	39.125	0.816	2.904	0.881
D2B	39.686	0.837	2.834	0.897
D2C	41.335	0.862	2.596	0.915
D2D	43.251	0.877	2.689	0.948
D2E	42.053	0.859	2.925	0.883
AVERAGE	41.090	0.850	3.498	0.905
D3A	39.910	0.882	2.589	0.897
D3B	40.215	0.840	2.677	0.828
D3C	39.399	0.794	2.855	0.848
D3D	39.197	0.767	2.541	0.849
D3E	38.927	0.739	2.596	0.831
AVERAGE	39.529	0.804	2.652	0.851
D4A	38.718	0.953	2.969	1.071
D4B	48.793	0.900	3.012	1.153
D4C	42.968	0.858	2.784	0.987
D4D	41.080	0.855	2.538	1.185
D4E	43.075	0.893	2.749	1.263
AVERAGE	42.927	0.892	2.811	1.132
D5A	35.312	0.652	2.300	0.897
D5B	35.072	0.612	1.967	0.839
D5C	36.159	0.637	2.056	0.723
D5D	35.355	0.578	1.981	0.637
D5E	37.101	0.637	2.207	0.781
AVERAGE	35.800	0.623	2.102	0.776

MOISTURE CONTENT, ORGANIC CONTENT AND ABSORBED MOISTURE (%)

SAMPLE NUMBER	MOISTURE CONTENT	ABSORBED MOISTURE	ORGANIC CONTENT	MOISTURE ABSORBED BY SILT MINUS ORGANICS
D6A	41.104	0.804	2.911	0.942
D6B	41.562	0.904	2.891	0.939
D6C	41.835	0.909	2.882	1.001
D6D	40.480	0.909	2.892	1.145
AVERAGE	41.245	0.881	2.894	1.007
D7A	44.368	0.929	3.131	0.961
D7B	43.990	0.921	3.005	0.929
D7C	44.660	0.954	3.006	1.004
AVERAGE	44.339	0.935	3.047	0.965
D8A	42.384	0.912	2.850	0.828
D8B	41.545	0.899	2.741	0.799
D8C	42.146	0.877	2.661	0.778
D8D	41.575	0.862	2.803	0.808
D8E	44.045	0.861	2.897	0.890
AVERAGE	42.339	0.882	2.790	0.821
AVER-D	41.248	0.854	2.877	0.962
E1A	45.843	1.002	4.091	1.410
E1B	47.330	0.981	3.696	1.330
E1C	47.083	1.028	3.435	1.176
AVERAGE	47.376	1.004	3.741	1.305
E2A	37.787	0.818	3.645	1.078
E2B	38.370	0.740	3.355	1.059
E2C	39.261	0.794	3.038	1.027
AVERAGE	38.473	0.784	3.346	1.055

MOISTURE CONTENT, ORGANIC CONTENT AND ABSORBED MOISTURE (%)

SAMPLE NUMBER	MOISTURE CONTENT	ABSORBED MOISTURE	ORGANIC CONTENT	MOISTURE ABSORBED BY SILT MINUS ORGANICS
E3A	45.004	0.922	3.064	1.176
E3B	45.780	0.950	3.061	1.203
E3C	45.258	0.934	2.951	1.293
E3D	44.124	0.964	2.790	1.261
E3E	42.270	0.900	2.801	1.121
AVERAGE	44.487	0.934	2.933	1.211
E4A	47.603	0.904	3.246	1.065
E4B	48.733	0.898	2.828	1.101
E4C	48.616	0.894	3.162	1.053
E4D	43.925	0.845	2.967	0.972
E4E	41.673	0.834	2.626	0.942
E4F	44.328	0.813	2.735	0.935
E4G	47.291	0.865	2.899	0.947
AVERAGE	46.024	0.865	2.923	1.002
E5A	47.738	0.844	3.150	1.274
E5B	47.229	0.828	2.749	1.290
E5C	48.771	0.872	3.043	1.140
E5D	47.132	0.855	3.017	1.157
E5E	46.733	0.862	2.846	1.302
E5F	47.090	0.924	2.837	1.226
E5G	48.835	0.948	3.172	1.286
AVERAGE	47.647	0.876	2.973	1.232

MOISTURE CONTENT, ORGANIC CONTENT AND ABSORBED MOISTURE (%)

SAMPLE NUMBER	MOISTURE CONTENT	ABSORBED MOISTURE	ORGANIC CONTENT	MOISTURE ABSORBED BY SILT MINUS ORGANICS
E6A	44.504	0.947	2.516	0.999
E6B	45.576	0.957	2.204	0.951
E6C	46.299	0.977	2.688	0.930
E6D	45.409	0.970	2.563	1.005
E6E	45.404	0.987	2.240	0.925
AVERAGE	45.438	0.968	2.442	0.962
E7A	40.132	0.798	2.364	0.721
E7B	40.622	0.822	2.609	0.824
E7C	39.425	0.829	2.342	0.785
E7D	39.185	0.877	2.421	0.812
E7E	39.532	0.844	2.572	0.841
AVERAGE	39.779	0.834	2.462	0.797
AVER_E	44.174	0.895	2.974	1.116
F1A	42.968	1.005	3.932	1.320
F1B	43.800	1.025	3.831	1.271
F1C	42.153	0.970	3.503	1.251
F1D	42.838	0.976	3.540	1.245
F1E	45.572	1.017	4.094	1.284
F1F	43.873	1.014	3.647	1.296
F1G	42.899	1.008	3.717	1.269
F1H	43.319	1.028	3.801	1.390
F1I	45.220	1.038	4.094	1.321
F1J	45.299	1.049	3.645	1.291
AVERAGE	43.794	1.013	3.780	1.290

MOISTURE CONTENT, ORGANIC CONTENT AND ABSORBED MOISTURE (%)

SAMPLE NUMBER	MOISTURE CONTENT	ABSORBED MOISTURE	ORGANIC CONTENT	MOISTURE ABSORBED BY SILT MINUS ORGANICS
F2A	40.231	0.880	3.128	1.281
F2B	42.260	0.896	3.174	1.323
F2C	42.949	0.935	3.312	1.256
F2D	42.526	0.941	3.240	1.315
F2E	42.966	0.943	3.275	1.307
F2F	41.932	0.905	3.137	1.338
F2G	41.662	0.890	2.996	1.287
F2H	41.910	0.911	3.117	1.238
F2I	41.949	0.912	3.079	1.324
F2J	42.888	0.899	3.079	1.251
AVERAGE	42.127	0.911	3.154	1.293
F3A	40.504	0.764	3.292	1.348
F3B	44.568	0.901	3.367	1.262
F3C	48.135	0.957	3.357	1.292
F3D	47.077	0.972	3.189	1.299
F3E	46.025	0.920	3.499	1.391
F3F	45.057	0.890	3.072	1.224
F3G	45.127	0.900	2.836	1.198
F3H	45.614	0.868	3.205	1.202
F3I	44.043	0.882	3.223	1.226
F3J	46.056	0.933	3.234	1.234
AVERAGE	45.221	0.899	3.292	1.268
F4A	41.475	0.793	3.153	1.185
F4B	42.571	0.838	3.205	1.282
F4C	42.295	0.875	2.939	1.207
F4D	43.355	0.877	3.065	1.244
F4E	43.794	0.855	2.963	1.194
AVERAGE	42.698	0.855	3.065	1.207
AVER_F	43.460	0.919	3.323	1.264

PERCENTAGES CALCULATED RELATIVE TO DRY WEIGHT

X.R.D. ANALYSES_PERCENTAGES

SAMPLE	QUARTZ	KAOLINITE	ILLITE-MUSCOVITE		CALCITE	DOLOMITE	CHLORITE	SIDERITE	PYRITE
			MIXED	LAYER CLAYS			ORTHOCLASE	PLAGIOCLASE	
A1	49.0	16.6	22.8		3.5	5.6	*CHLOR,SID,*PYR,ORTH,PLAG=2.5		
A2	34.0	22.1	28.9		4.5	4.7	*CHLOR,SID,*PYR,ORTH,PLAG=5.8		
A3	47.0	15.5	24.4		3.5	7.4	*CHLOR,SID,*PYR,ORTH,PLAG=2.2		
A4	62.0	10.5	15.7		1.6	2.1	CHLOR,*ORTH,PLAG=3.1	PYR=5.0	
A5	45.0	19.2	22.9		5.5	6.0	CHLOR,*SID,ORTH,PLAG=1.4		
A6	42.0	14.9	27.4		5.8	6.1	CHLOR,SID,ORTH,*PLAG=3.8		
A7	42.0	16.2	27.0		4.6	5.7	CHLOR,SID,*PYR,*ORTH,PLAG=4.5		
A8	48.0	14.8	22.9		5.7	5.9	CHLOR,SID,*ORTH,PLAG=2.7		
B1	34.0	21.8	31.9		2.4	4.0	CHLOR,SID,*PYR,ORTH,PLAG=5.9		
B2	33.0	25.1	34.0		0.0	2.5	CHLOR,SID,*PYR,ORTH,PLAG=5.4		
B3	41.0	22.7	22.7		5.7	6.4	CHLOR,ORTH,PLAG=1.5		
B4	29.0	22.7	37.2		4.3	4.6	CHLOR,SID,PYR,ORTH,PLAG=2.2		
B5	40.0	19.1	24.5		7.9	5.0	CHLOR,SID,PYR,*ORTH,PLAG=3.5		
C1	47.0	15.5	26.6		3.3	3.0	*CHLOR,SID,*PYR,ORTH,PLAG=4.6		
C2	35.0	22.5	36.0		1.7	2.4	*CHLOR,SID,PYR,ORTH,PLAG=2.4		
C3	40.0	18.6	34.0		0.4	2.8	CHLOR,SID,PYR,*ORTH,PLAG=4.2		
C4	44.0	19.9	24.8		3.4	4.2	CHLOR,*PYR,*PLAG=3.7		
C5	54.0	12.7	22.0		3.6	3.1	CHLOR,*PYR,ORTH,PLAG=2.6		
D1C	31.0	25.8	35.6		1.7	1.4	CHLOR,SID,*PYR,ORTH,PLAG=4.5		
D2C	34.0	27.7	27.7		2.9	5.4	CHLOR,SID,ORTH,PLAG=2.3		
D3C	38.0	20.5	31.9		2.4	2.7	CHLOR,*PYR,*ORTH,PLAG=4.5		
D4C	79.0	5.5	8.8		2.2	1.7	*CHLOR,SID,*PYR,*ORTH,PLAG=2.8		
D5C	49.0	13.1	23.4		5.1	4.7	*CHLOR,SID,*PYR,ORTH,PLAG=4.7		
D6C	28.0	27.5	33.5		4.8	2.5	*CHLOR,SID,PYR,ORTH,*PLAG=3.7		
D7C	42.0	16.6	25.9		5.5	5.8	*CHLOR,SID,*PYR,ORTH,*PLAG=4.2		
D8C	42.0	16.2	29.3		3.2	4.2	CHLOR,SID,*PYR,ORTH,PLAG=5.1		

X.R.D. ANALYSES_PERCENTAGES

SAMPLE	QUARTZ	KAOLINITE	ILLITE-MUSCOVITE		CALCITE	DOLOMITE	CHLORITE	SIDERITE	PYRITE
			MIXED	LAYER CLAYS			ORTHOCLASE	PLAGIOCLASE	
E1C	49.0	21.7		20.9	4.0	3.7	CHLOR,SID,ORTH,PLAG=0.7		
E2C	60.0	12.8		17.5	3.5	5.0	CHLOR,SID,ORTH,PLAG=1.2		
E3C	43.0	14.4		30.6	4.8	4.1	*CHLOR,SID,*PYR,*ORTH,PLAG=3.1		
E4C	38.0	21.0		28.0	6.2	4.7	*CHLOR,SID,ORTH,PLAG=2.1		
E5C	52.0	16.8		19.9	5.3	4.4	CHLOR,SID,ORTH,*PLAG=1.6		
E6C	39.0	16.5		26.1	7.1	6.5	*CHLOR,*PYR,ORTH,*PLAG=4.8		
E7C	54.0	17.7		14.9	5.8	4.8	*CHLOR,SID,*PYR,*ORTH,PLAG=2.8		
F1D	41.0	19.0		29.0	4.4	3.6	CHLOR,SID,PYR,ORTH,PLAG=3.0		
F2D	55.0	14.9		16.7	5.7	6.0	CHLOR,SID,*ORTH,PLAG=1.9		
F3D	47.0	19.0		19.7	5.9	5.5	*CHLOR,SID,*PYR,ORTH,*PLAG=2.9		
F4D	50.0	15.6		22.9	2.9	4.9	CHLOR,SID,PYR,*ORTH,PLAG=3.7		
G1A	25.0	38.3		30.3	0.0	0.0	CHLOR,SID,*PYR,ORTH,PLAG=6.4		
G1B	54.0	20.6		24.4	0.0	0.0	CHLOR,ORTH=0.5		
G1C	43.0	19.0		37.0	0.0	0.0	ORTH,PLAG=1.0		
G1D	32.0	30.3		36.8	0.0	0.0	CHLOR,ORTH=0.9		
G1E	40.0	22.6		36.5	0.0	0.0	ORTH=0.9		
G1F	36.0	18.5		44.3	0.0	0.0	CHLOR=1.2		
G1G	51.0	21.0		26.6	0.0	0.0	CHLOR,ORTH,PLAG=1.4		
G1H	55.0	15.1		12.3	5.5	0.3	*PYR,ORTH,PLAG=1.2 SID=10.6		
G2A	41.0	23.0		28.1	0.0	1.5	CHLOR,SID,*PYR,*ORTH,PLAG=6.4		
G2B	41.0	22.1		35.6	0.0	0.0	ORTH=1.3		
G2C	55.0	22.0		22.0	0.0	0.0	ORTH=1.0		
G2D	30.0	31.6		35.7	0.0	0.0	CHLOR,ORTH,PLAG=2.7		
G2E	34.0	25.6		33.7	0.0	0.0	CHLOR,*ORTH=6.7		
G2F	47.0	23.0		29.1	0.0	0.0	ORTH,PLAG=0.9		
G2G	25.0	38.7		29.8	0.6	0.8	*SID,PYR,ORTH,PLAG=5.1		
G2H	19.0	41.8		35.4	0.5	0.9	SID,PYR,ORTH=1.3		

* INDICATES RELATIVELY SIGNIFICANT AMOUNT OF MINERAL PRESENT

X.R.F. ANALYSES (%)

SAMPLE	SiO2	AL2O3	FE2O3	MGO	CaO	NA2O	K2O	TiO2	S	P2O5	TOTAL
A1	57.21	15.02	5.43	2.53	3.56	0.73	3.25	0.83	0.97	0.14	89.66
A2	57.37	15.07	5.25	2.73	4.24	0.74	3.25	0.83	0.31	0.14	90.06
A3	55.79	14.71	5.90	2.74	4.30	0.74	2.40	0.84	0.42	0.14	88.00
A4	59.56	13.77	4.34	2.34	2.65	0.68	2.11	0.72	1.84	0.13	88.13
A5	56.70	14.13	5.44	2.84	4.95	0.82	2.36	0.82	0.24	0.14	88.45
A6	57.80	14.22	5.20	2.73	4.69	0.81	2.36	0.83	0.27	0.13	89.04
A7	56.81	14.14	5.88	2.77	5.05	0.79	2.38	0.81	0.24	0.14	89.01
A8	58.01	14.31	5.05	2.57	4.31	0.79	2.33	0.79	0.69	0.13	88.99
B1	56.27	14.26	6.48	2.38	3.53	0.73	3.28	0.82	-0.05	0.14	87.83
B2	55.30	15.96	6.98	2.54	1.44	0.72	3.93	0.88	3.39	0.13	91.28
B3	57.63	13.84	5.28	2.81	4.77	0.83	3.72	0.82	0.11	0.14	89.94
B4	57.75	14.69	4.99	2.90	4.58	0.86	3.85	0.84	0.35	0.12	90.93
B5	57.56	14.02	5.41	2.78	4.72	0.84	3.19	0.83	0.37	0.14	89.86
C1	58.19	14.04	5.38	2.73	4.47	0.87	3.84	0.82	0.27	0.13	90.73
C2	55.70	14.90	6.27	2.68	3.72	0.76	3.91	0.83	0.01	0.14	88.92
C3	56.67	14.94	5.35	2.65	2.95	0.75	3.07	0.83	0.56	0.14	87.91
C4	58.36	14.14	4.72	2.81	4.81	0.89	3.83	0.80	0.27	0.16	90.77
C5	58.18	14.47	5.28	2.53	3.63	0.78	3.79	0.79	-0.24	0.16	89.38
D1C	58.43	14.08	5.26	2.41	2.91	0.72	2.68	0.75	3.02	0.12	90.39
D2C	58.49	14.13	4.84	2.59	4.40	0.71	3.80	0.82	0.97	0.13	90.88
D3C	59.42	13.62	4.66	2.68	4.64	0.75	3.69	0.78	0.69	0.14	91.07
D4C	58.06	14.11	4.78	2.75	4.92	0.71	3.79	0.77	0.86	0.12	90.87
D5C	61.75	12.00	4.21	2.42	5.17	0.83	3.49	0.68	1.11	0.12	90.77
D6C	58.61	14.46	4.75	2.79	4.49	0.76	2.88	0.81	0.83	0.12	90.51
D7C	51.48	10.74	4.76	2.31	4.29	0.71	3.91	0.81	0.68	0.13	78.82
D8C	58.97	13.67	4.81	2.74	4.66	0.77	3.77	0.80	0.43	0.13	90.76
E1C	56.91	14.88	5.24	2.73	4.15	0.63	3.62	0.82	1.29	0.12	90.39
E2C	58.03	13.22	5.41	2.68	4.57	0.66	3.46	0.80	0.40	0.14	89.37
E3C	58.10	14.00	5.10	2.76	4.89	0.67	3.94	0.81	0.50	0.12	90.90
E4C	58.05	14.70	5.04	2.79	4.53	0.67	4.00	0.80	0.26	0.13	90.97
E5C	57.75	13.67	5.01	2.73	5.08	0.67	3.94	0.79	0.55	0.13	90.31
E6C	56.98	14.11	5.51	2.72	4.84	0.66	3.86	0.80	0.57	0.13	90.19
E7C	58.95	13.55	4.63	2.75	4.86	0.73	3.48	0.81	0.33	0.13	90.23

X.R.F. ANALYSES (%)

SAMPLE	SiO2	AL2O3	FE2O3	MGO	CAO	NA2O	K2O	TiO2	S	P2O5	TOTAL
F1C	57.98	14.14	4.82	2.72	3.42	0.97	3.95	0.81	4.76	0.13	93.70
F2C	56.26	13.60	5.58	2.69	4.90	0.87	3.91	0.80	4.56	0.15	93.31
F3C	56.44	14.84	5.44	2.76	4.58	0.72	4.14	0.84	1.38	0.13	91.26
F4C	58.06	13.78	4.88	2.80	5.02	0.79	3.94	0.82	1.25	0.14	91.48
G1A	52.08	23.18	5.84	2.38	0.49	0.36	4.74	1.08	-0.08	0.11	89.88
G1B	57.94	18.86	5.01	1.54	0.70	0.45	3.91	0.96	0.02	0.12	89.51
G1C	54.59	20.88	5.36	1.85	0.50	0.39	3.49	0.97	-0.33	0.13	87.83
G1D	54.52	21.15	5.63	1.76	0.50	0.40	3.45	1.01	-0.11	0.13	88.42
G1E	56.22	21.11	4.61	1.82	0.47	0.43	3.44	0.99	-0.36	0.13	88.85
G1F	57.27	19.41	4.38	1.63	0.64	0.45	3.36	0.93	-0.17	0.12	88.02
G1G	57.98	19.20	4.14	1.71	0.66	0.43	3.15	0.90	-0.28	0.12	88.01
G1H	48.15	16.61	13.23	1.65	2.38	0.33	3.09	0.86	-0.37	0.12	86.03
G2A	55.84	16.48	6.19	2.37	1.25	0.79	3.19	0.95	1.10	0.12	88.27
G2B	55.71	21.30	4.44	1.75	0.34	0.46	3.16	0.99	-0.33	0.10	87.92
G2C	57.57	19.28	4.56	1.50	0.45	0.54	2.85	0.99	0.50	0.10	88.45
G2D	54.21	20.45	5.69	1.77	0.47	0.41	2.41	0.99	0.47	0.11	87.00
G2E	54.79	20.47	5.60	1.82	0.42	0.42	2.40	0.97	0.58	0.10	87.58
G2F	54.19	21.36	5.09	1.85	0.35	0.46	2.52	1.00	-0.19	0.10	86.71
G2G	50.66	22.60	7.04	1.89	0.37	0.41	2.70	1.08	-0.32	0.12	86.54
G2H	50.42	21.92	7.67	1.83	0.37	0.45	2.68	1.07	-0.38	0.13	86.17
H1	53.67	19.45	6.15	2.40	4.15	0.60	3.19	0.86	0.31	0.10	89.88

CALCULATED ON A CO2, C AND H2O FREE BASIS

RECENT ALLUVIUM-UNDISTURBED

ANALYSIS OF CONSOLIDATION DATA

INITIAL MOISTURE CONTENT = 45.35 PERCENT
 FINAL MOISTURE CONTENT = 28.04 PERCENT
 NATURAL BULK DENSITY = 1.7549 GMS/CC
 NATURAL DRY DENSITY = 1.2073 GMS/CC
 FINAL BULK DENSITY = 1.9879 GMS/CC
 FINAL DRY DENSITY = 1.5526 GMS/CC
 SWELL PERCENTAGE = 0.00 PERCENT
 SWELL PRESSURE = 0.00 KN/M2

PRESSURE (KN/M2)	VOIDS RATIO	STRAIN PERCENT	CV (M2/YR)	MV (M2/MN)	PERMEABILITY (M/S)	CC/CS
0.00	1.1950					
26.97	1.1445	2.30	3.4950552	0.9683882	0.000000001049216	-0.0524668
51.49	1.1096	3.89	2.1521158	0.6692300	0.000000000446480	-0.1242757
102.97	1.0497	6.62	5.9643497	0.5596445	0.000000001034753	-0.1990579
154.46	1.0071	8.56	0.4892721	0.4077444	0.000000000061844	-0.2418195
205.95	0.9651	10.47	6.4968948	0.4099802	0.000000000825715	-0.3355542
308.92	0.9083	13.06	3.0920143	0.2850585	0.000000000273235	-0.3228413
411.89	0.8622	15.16	12.6847658	0.2374390	0.000000000933676	-0.3689339
823.79	0.7511	20.22	8.8228760	0.1492496	0.000000000408211	-0.3689500
1647.57	0.6462	25.00	12.8733931	0.0749772	0.000000000299215	-0.3485349
3295.15	0.5409	29.80	9.6532145	0.0401292	0.000000000120086	-0.3499921
1647.57	0.5479	29.48				0.0233328
823.79	0.5567	29.08				0.0291661
411.89	0.5681	28.56				0.0379158
205.95	0.5810	27.97				0.0430199
102.97	0.5975	27.22				0.0546863
51.49	0.6166	26.35				0.0634361
2.94	0.7068	22.24				0.0725746

Lateral Sub-surface Movement towards Tunnel Face

(1.1)

Positive indicates movement away from tunnel face

Negative indicates movement towards tunnel face

Displacement in mm.

1.1 -19.00

SURFACE DISPLACEMENT= 0.00

DEPTH	ORIGINAL DATA				DEPTH	AVERAGE	DIFFERENCE	DISPLACEMENT
	TOWARDS		AWAY					
0.0	0.	0.	0.	0.	0.0	0.000	0.000	0.000
1.0	656.	654.	872.	872.	1.0	-10.850	0.150	-0.150
2.0	668.	667.	858.	858.	2.0	-9.525	-0.025	-0.125
3.0	698.	696.	830.	830.	3.0	-6.650	-0.050	-0.075
4.0	704.	703.	824.	824.	4.0	-6.025	-0.025	-0.050
5.0	696.	695.	832.	832.	5.0	-6.825	-0.025	-0.025
6.0	694.	694.	836.	836.	6.0	-7.100	-0.100	0.075
7.0	712.	712.	816.	818.	7.0	-5.250	-0.150	0.225
8.0	728.	729.	804.	806.	8.0	-3.825	-0.125	0.350
9.0	738.	738.	792.	792.	9.0	-2.700	-0.100	0.450
10.0	755.	754.	776.	777.	10.0	-1.100	-0.100	0.550
11.0	808.	806.	725.	727.	11.0	4.050	-0.250	0.800
12.0	828.	828.	702.	703.	12.0	6.275	-0.025	0.825
13.0	836.	834.	696.	696.	13.0	6.950	-0.150	0.975
14.0	853.	855.	677.	676.	14.0	8.875	-0.125	1.100
15.0	856.	856.	674.	673.	15.0	9.125	-0.175	1.275
16.0	834.	835.	696.	696.	16.0	6.925	-0.175	1.450

1.1 -10.00

SURFACE DISPLACEMENT= 0.00

DEPTH	ORIGINAL DATA				DEPTH	AVERAGE	DIFFERENCE	DISPLACEMENT
	TOWARDS		AWAY					
0.0	0.	0.	0.	0.	0.0	0.000	0.000	0.000
1.0	666.	666.	883.	882.	1.0	-10.825	0.175	-0.175
2.0	678.	678.	868.	869.	2.0	-9.525	-0.025	-0.150
3.0	708.	707.	840.	842.	3.0	-6.675	-0.075	-0.075
4.0	715.	714.	834.	836.	4.0	-6.025	-0.025	-0.050
5.0	706.	707.	842.	842.	5.0	-6.775	0.025	-0.075
6.0	705.	705.	845.	846.	6.0	-7.025	-0.025	-0.050
7.0	723.	724.	826.	826.	7.0	-5.125	-0.025	-0.025
8.0	739.	741.	814.	816.	8.0	-3.750	-0.050	0.025
9.0	749.	750.	802.	804.	9.0	-2.675	-0.075	0.100
10.0	765.	766.	786.	788.	10.0	-1.075	-0.075	0.175
11.0	818.	820.	734.	736.	11.0	4.200	-0.100	0.275
12.0	839.	839.	712.	712.	12.0	6.350	0.050	0.225
13.0	846.	846.	706.	705.	13.0	7.025	-0.075	0.300
14.0	864.	866.	686.	686.	14.0	8.950	-0.050	0.350
15.0	867.	868.	684.	683.	15.0	9.200	-0.100	0.450
16.0	846.	846.	706.	706.	16.0	7.000	-0.100	0.550

1.1 -5.00

SURFACE DISPLACEMENT= 0.00

DEPTH	ORIGINAL DATA				DEPTH	AVERAGE	DIFFERENCE	DISPLACEMENT
	TOWARDS		AWAY					
0.0	0.	0.	0.	0.	0.0	0.000	0.000	0.000
1.0	654.	655.	870.	871.	1.0	-10.800	0.200	-0.200
2.0	668.	669.	856.	856.	2.0	-9.375	0.125	-0.325
3.0	696.	698.	828.	830.	3.0	-6.600	0.000	-0.325
4.0	704.	705.	822.	824.	4.0	-5.925	0.075	-0.400
5.0	695.	697.	830.	830.	5.0	-6.700	0.100	-0.500
6.0	693.	695.	834.	835.	6.0	-7.025	-0.025	-0.475
7.0	710.	713.	816.	817.	7.0	-5.250	-0.150	-0.325
8.0	728.	730.	804.	804.	8.0	-3.750	-0.050	-0.275
9.0	738.	740.	790.	792.	9.0	-2.600	0.000	-0.275
10.0	753.	757.	774.	774.	10.0	-0.950	0.050	-0.325
11.0	806.	808.	724.	724.	11.0	4.150	-0.150	-0.175
12.0	828.	828.	701.	702.	12.0	6.325	0.025	-0.200
13.0	834.	836.	694.	694.	13.0	7.050	-0.050	-0.150
14.0	854.	856.	674.	674.	14.0	9.050	0.050	-0.200
15.0	858.	834.	673.	674.	15.0	8.625	-0.675	0.475
16.0	834.	834.	696.	696.	16.0	6.900	-0.200	0.675

1.1 -4.00

SURFACE DISPLACEMENT= 0.00

DEPTH	ORIGINAL DATA				DEPTH	AVERAGE	DIFFERENCE	DISPLACEMENT
	TOWARDS		AWAY					
0.0	0.	0.	0.	0.	0.000	0.000	0.000	
1.0	650.	649.	860.	861.	-10.550	0.450	-0.450	
2.0	660.	660.	849.	849.	-9.450	0.050	-0.500	
3.0	690.	689.	820.	820.	-6.525	0.075	-0.575	
4.0	697.	695.	814.	814.	-5.900	0.100	-0.675	
5.0	687.	687.	823.	822.	-6.775	0.025	-0.700	
6.0	685.	684.	826.	826.	-7.075	-0.075	-0.625	
7.0	703.	703.	808.	806.	-5.200	-0.100	-0.525	
8.0	720.	720.	794.	795.	-3.725	-0.025	-0.500	
9.0	730.	731.	781.	782.	-2.550	0.050	-0.550	
10.0	747.	747.	765.	766.	-0.925	0.075	-0.625	
11.0	799.	800.	712.	713.	4.350	0.050	-0.675	
12.0	818.	818.	693.	694.	6.225	-0.075	-0.600	
13.0	826.	826.	685.	685.	7.050	-0.050	-0.550	
14.0	846.	847.	664.	666.	9.075	0.075	-0.625	
15.0	848.	847.	665.	664.	9.150	-0.150	-0.475	
16.0	826.	826.	686.	688.	6.950	-0.150	-0.325	

1.1 -3.00

SURFACE DISPLACEMENT= 0.00

DEPTH	ORIGINAL DATA				DEPTH	AVERAGE	DIFFERENCE	DISPLACEMENT
	TOWARDS		AWAY					
0.0	0.	0.	0.	0.	0.0	0.000	0.000	0.000
1.0	616.	618.	827.	824.	1.0	-10.425	0.575	-0.575
2.0	626.	628.	815.	812.	2.0	-9.325	0.175	-0.750
3.0	656.	657.	784.	784.	3.0	-6.375	0.225	-0.975
4.0	633.	634.	778.	778.	4.0	-7.225	-1.225	0.250
5.0	652.	653.	786.	786.	5.0	-6.675	0.125	0.125
6.0	650.	651.	792.	791.	6.0	-7.050	-0.050	0.175
7.0	669.	668.	772.	769.	7.0	-5.100	0.000	0.175
8.0	684.	684.	761.	760.	8.0	-3.825	-0.125	0.300
9.0	696.	696.	748.	747.	9.0	-2.575	0.025	0.275
10.0	712.	711.	731.	730.	10.0	-0.950	0.050	0.225
11.0	764.	763.	680.	680.	11.0	4.175	-0.125	0.350
12.0	785.	784.	659.	657.	12.0	6.325	0.025	0.325
13.0	793.	792.	650.	650.	13.0	7.125	0.025	0.300
14.0	812.	811.	631.	630.	14.0	9.050	0.050	0.250
15.0	814.	814.	630.	628.	15.0	9.250	-0.050	0.300
16.0	791.	791.	650.	650.	16.0	7.050	-0.050	0.350

1.1 -2.00

SURFACE DISPLACEMENT= 1.50

DEPTH	ORIGINAL DATA				DEPTH	AVERAGE	DIFFERENCE	DISPLACEMENT
	TOWARDS		AWAY					
0.0	0.	0.	0.	0.	0.0	0.000	0.000	1.500
1.0	620.	620.	830.	830.	1.0	-10.500	0.500	1.000
2.0	632.	633.	816.	816.	2.0	-9.175	0.325	0.675
3.0	663.	665.	788.	789.	3.0	-6.225	0.375	0.300
4.0	670.	671.	784.	783.	4.0	-5.650	0.350	-0.050
5.0	658.	660.	794.	794.	5.0	-6.750	0.050	-0.100
6.0	656.	658.	799.	799.	6.0	-7.100	-0.100	0.000
7.0	674.	675.	779.	778.	7.0	-5.200	-0.100	0.100
8.0	692.	693.	768.	769.	8.0	-3.800	-0.100	0.200
9.0	701.	703.	753.	754.	9.0	-2.575	0.025	0.175
10.0	716.	718.	738.	739.	10.0	-1.075	-0.075	0.250
11.0	768.	770.	688.	688.	11.0	4.050	-0.250	0.500
12.0	790.	791.	664.	664.	12.0	6.325	0.025	0.475
13.0	800.	799.	656.	655.	13.0	7.200	0.100	0.375
14.0	818.	819.	634.	635.	14.0	9.200	0.200	0.175
15.0	822.	822.	633.	632.	15.0	9.475	0.175	0.000
16.0	801.	801.	654.	654.	16.0	7.350	0.250	-0.250

1.1 -1.00

SURFACE DISPLACEMENT= 1.90

DEPTH	ORIGINAL DATA				DEPTH	AVERAGE	DIFFERENCE	DISPLACEMENT
	TOWARDS		AWAY					
0.0	0.	0.	0.	0.	0.0	0.000	0.000	1.900
1.0	634.	634.	840.	840.	1.0	-10.300	0.700	1.200
2.0	647.	650.	830.	828.	2.0	-9.025	0.475	0.725
3.0	675.	678.	802.	800.	3.0	-6.225	0.375	0.350
4.0	681.	683.	796.	795.	4.0	-5.675	0.325	0.025
5.0	670.	673.	806.	805.	5.0	-6.700	0.100	-0.075
6.0	666.	668.	812.	812.	6.0	-7.250	-0.250	0.175
7.0	686.	688.	792.	790.	7.0	-5.200	-0.100	0.275
8.0	702.	704.	780.	781.	8.0	-3.875	-0.175	0.450
9.0	713.	716.	765.	767.	9.0	-2.575	0.025	0.425
10.0	725.	727.	753.	756.	10.0	-1.425	-0.425	0.850
11.0	770.	772.	708.	711.	11.0	3.075	-1.225	2.075
12.0	797.	797.	684.	683.	12.0	5.675	-0.625	2.700
13.0	806.	806.	674.	673.	13.0	6.625	-0.475	3.175
14.0	824.	824.	655.	656.	14.0	8.425	-0.575	3.750
15.0	843.	844.	637.	636.	15.0	10.350	1.050	2.700
16.0	830.	830.	650.	650.	16.0	9.000	1.900	0.800

Lateral Sub-surface Movement Perpendicular to Centre Line

(2.2, 3.2, 4.2)

Positive indicates movement away from channel

Negative indicates movement towards channel

Displacement in mm.

2.2 -19.00

SURFACE DISPLACEMENT= 0.00

DEPTH	ORIGINAL DATA				DEPTH	AVERAGE	DIFFERENCE	DISPLACEMENT
	TOWARDS		AWAY					
0.0	0.	0.	0.	0.	0.0	0.000	0.000	0.000
1.0	906.	906.	622.	622.	1.0	14.200	-0.100	0.100
2.0	917.	917.	611.	611.	2.0	15.300	-0.200	0.300
3.0	914.	914.	614.	614.	3.0	15.000	-0.100	0.400
4.0	882.	881.	646.	646.	4.0	11.775	-0.025	0.425
5.0	864.	886.	664.	665.	5.0	10.525	0.525	-0.100
6.0	848.	850.	680.	682.	6.0	8.400	-0.100	0.000
7.0	860.	862.	669.	669.	7.0	9.600	-0.100	0.100
8.0	856.	858.	671.	674.	8.0	9.225	0.025	0.075
9.0	891.	892.	638.	638.	9.0	12.675	-0.225	0.300
10.0	937.	937.	592.	593.	10.0	17.225	-0.075	0.375
11.0	948.	948.	581.	582.	11.0	18.325	-0.075	0.450
12.0	964.	962.	566.	565.	12.0	19.850	-0.150	0.600
13.0	964.	965.	564.	564.	13.0	20.025	-0.175	0.775
14.0	970.	970.	559.	559.	14.0	20.550	-0.150	0.925
15.0	976.	976.	554.	554.	15.0	21.100	-0.100	1.025
16.0	978.	980.	551.	552.	16.0	21.375	-0.025	1.050

2.2 -10.00

SURFACE DISPLACEMENT= 0.30

DEPTH	ORIGINAL DATA				DEPTH	AVERAGE	DIFFERENCE	DISPLACEMENT
	TOWARDS		AWAY					
0.0	0.	0.	0.	0.	0.0	0.000	0.000	0.300
1.0	922.	922.	635.	638.	1.0	14.275	-0.025	0.325
2.0	934.	934.	624.	626.	2.0	15.450	-0.050	0.375
3.0	930.	932.	628.	629.	3.0	15.125	0.025	0.350
4.0	898.	898.	660.	662.	4.0	11.850	0.050	0.300
5.0	881.	881.	678.	680.	5.0	10.100	0.100	0.200
6.0	868.	867.	696.	697.	6.0	8.550	0.050	0.150
7.0	878.	880.	682.	684.	7.0	9.800	0.100	0.050
8.0	874.	874.	688.	688.	8.0	9.300	0.100	-0.050
9.0	908.	910.	652.	654.	9.0	12.800	-0.100	0.050
10.0	954.	954.	607.	608.	10.0	17.325	0.025	0.025
11.0	965.	966.	597.	598.	11.0	18.400	0.000	0.025
12.0	980.	982.	581.	582.	12.0	19.975	-0.025	0.050
13.0	982.	983.	580.	580.	13.0	20.125	-0.075	0.125
14.0	988.	988.	574.	576.	14.0	20.650	-0.050	0.175
15.0	992.	992.	570.	570.	15.0	21.100	-0.100	0.275
16.0	996.	996.	567.	568.	16.0	21.425	0.025	0.250

2.2 -5.00

SURFACE DISPLACEMENT=-14.32

DEPTH	ORIGINAL DATA				DEPTH	AVERAGE	DIFFERENCE	DISPLACEMENT
	TOWARDS		AWAY					
0.0	0.	0.	0.	0.	0.000	0.000	-14.320	
1.0	775.	773.	749.	751.	1.200	-13.100	-1.220	
2.0	893.	892.	638.	634.	12.825	-2.675	1.455	
3.0	919.	915.	604.	606.	15.600	0.500	0.955	
4.0	882.	879.	644.	648.	11.725	-0.075	1.030	
5.0	862.	862.	662.	665.	9.925	-0.075	1.105	
6.0	848.	848.	680.	682.	8.350	-0.150	1.255	
7.0	860.	860.	606.	668.	11.150	1.450	-0.195	
8.0	856.	856.	670.	672.	9.250	0.050	-0.245	
9.0	888.	892.	636.	632.	12.800	-0.100	-0.145	
10.0	938.	938.	590.	590.	17.400	0.100	-0.245	
11.0	949.	948.	580.	580.	18.425	0.025	-0.270	
12.0	962.	964.	564.	564.	19.950	-0.050	-0.220	
13.0	966.	964.	562.	562.	20.150	-0.050	-0.170	
14.0	970.	970.	556.	558.	20.650	-0.050	-0.120	
15.0	976.	976.	553.	553.	21.150	-0.050	-0.070	
16.0	979.	979.	550.	550.	21.450	0.050	-0.120	

2.2 -1.00

SURFACE DISPLACEMENT= -9.75

DEPTH	ORIGINAL DATA				DEPTH	AVERAGE	DIFFERENCE	DISPLACEMENT
	TOWARDS		AWAY					
0.0	0.	0.	0.	0.	0.0	0.000	0.000	-9.750
1.0	808.	808.	672.	672.	1.0	6.800	-7.500	-2.250
2.0	873.	874.	608.	608.	2.0	13.275	-2.225	-0.025
3.0	895.	899.	585.	586.	3.0	15.575	0.475	-0.500
4.0	856.	858.	623.	626.	4.0	11.625	-0.175	-0.325
5.0	840.	842.	643.	646.	5.0	9.825	-0.175	-0.150
6.0	824.	827.	659.	663.	6.0	8.225	-0.275	0.125
7.0	837.	840.	646.	648.	7.0	9.575	-0.125	0.250
8.0	833.	835.	650.	654.	8.0	9.100	-0.100	0.350
9.0	868.	871.	615.	616.	9.0	12.700	-0.200	0.550
10.0	914.	915.	570.	570.	10.0	17.225	-0.075	0.625
11.0	926.	927.	559.	559.	11.0	18.375	-0.025	0.650
12.0	940.	941.	545.	544.	12.0	19.800	-0.200	0.850
13.0	942.	943.	544.	542.	13.0	19.975	-0.225	1.075
14.0	947.	948.	538.	537.	14.0	20.500	-0.200	1.275
15.0	956.	955.	534.	531.	15.0	21.150	-0.050	1.325
16.0	959.	960.	520.	524.	16.0	21.875	0.475	0.850

2.2 +1.00

SURFACE DISPLACEMENT= -5.79

DEPTH	ORIGINAL DATA				DEPTH	AVERAGE	DIFFERENCE	DISPLACEMENT
	TOWARDS		AWAY					
0.0	0.	0.	0.	0.	0.000	0.000	-5.790	
1.0	802.	802.	620.	622.	9.050	-5.250	-0.540	
2.0	847.	848.	576.	576.	13.575	-1.925	1.385	
3.0	866.	868.	556.	557.	15.525	0.425	0.960	
4.0	832.	831.	592.	592.	11.975	0.175	0.785	
5.0	810.	809.	614.	615.	9.750	-0.250	1.035	
6.0	794.	793.	631.	632.	8.100	-0.400	1.435	
7.0	806.	807.	618.	618.	9.425	-0.275	1.710	
8.0	799.	798.	624.	627.	8.650	-0.550	2.260	
9.0	834.	833.	589.	591.	12.175	-0.725	2.985	
10.0	885.	886.	537.	539.	17.375	0.075	2.910	
11.0	903.	903.	521.	522.	19.075	0.675	2.235	
12.0	926.	924.	498.	498.	21.350	1.350	0.885	
13.0	934.	934.	489.	490.	22.225	2.025	-1.140	
14.0	906.	906.	519.	518.	19.375	-1.325	0.185	
15.0	901.	899.	527.	529.	18.600	-2.600	2.785	
16.0	934.	934.	489.	490.	22.225	0.825	1.960	

2.2 +6.00

SURFACE DISPLACEMENT= -3.35

DEPTH	ORIGINAL DATA				DEPTH	AVERAGE	DIFFERENCE	DISPLACEMENT
	TOWARDS		AWAY					
0.0	0.	0.	0.	0.	0.000	0.000	-3.350	
1.0	70.	69.	-124.	-122.	9.625	-4.675	1.325	
2.0	128.	129.	-178.	-174.	15.225	-0.275	1.600	
3.0	126.	129.	-179.	-172.	15.150	0.050	1.550	
4.0	87.	87.	-139.	-134.	11.175	-0.625	2.175	
5.0	67.	65.	-114.	-111.	8.925	-1.075	3.250	
6.0	48.	53.	-100.	-94.	7.375	-1.125	4.375	
7.0	64.	63.	-114.	-108.	8.725	-0.975	5.350	
8.0	49.	47.	-98.	-93.	7.175	-2.025	7.375	
9.0	95.	97.	-147.	-143.	12.050	-0.850	8.225	
10.0	139.	140.	-189.	-185.	16.325	-0.975	9.200	
11.0	165.	170.	-218.	-210.	19.075	0.675	8.525	
12.0	186.	189.	-235.	-231.	21.025	1.025	7.500	
13.0	196.	199.	-250.	-245.	22.250	2.050	5.450	
14.0	200.	203.	-248.	-250.	22.525	1.825	3.625	
15.0	207.	207.	-273.	-274.	24.025	2.825	0.800	
16.0	229.	230.	-273.	-273.	25.125	3.725	-2.925	

2.2 +13.00

SURFACE DISPLACEMENT= -1.83

DEPTH	ORIGINAL DATA				DEPTH	AVERAGE	DIFFERENCE	DISPLACEMENT
	TOWARDS		AWAY					
0.0	0.	0.	0.	0.	0.000	0.000	-1.830	
1.0	61.	61.	-144.	-142.	10.200	-4.100	2.270	
2.0	110.	114.	-194.	-191.	15.225	-0.275	2.545	
3.0	110.	112.	-195.	-191.	15.200	0.100	2.445	
4.0	69.	76.	-158.	-152.	11.375	-0.425	2.870	
5.0	42.	49.	-132.	-128.	8.775	-1.225	4.095	
6.0	29.	35.	-115.	-111.	7.250	-1.250	5.345	
7.0	42.	47.	-130.	-126.	8.625	-1.075	6.420	
8.0	25.	31.	-114.	-109.	6.975	-2.225	8.645	
9.0	70.	74.	-157.	-153.	11.350	-1.550	10.195	
10.0	115.	121.	-204.	-200.	16.000	-1.300	11.495	
11.0	142.	145.	-230.	-227.	18.600	0.200	11.295	
12.0	166.	170.	-252.	-250.	20.950	0.950	10.345	
13.0	177.	177.	-261.	-258.	21.825	1.625	8.720	
14.0	183.	186.	-269.	-268.	22.650	1.950	6.770	
15.0	185.	190.	-273.	-272.	23.000	1.800	4.970	
16.0	211.	216.	-301.	-300.	25.700	4.300	0.670	

2.2 +23.00

SURFACE DISPLACEMENT= -1.52

DEPTH	ORIGINAL DATA				DEPTH	AVERAGE	DIFFERENCE	DISPLACEMENT
	TOWARDS		AWAY					
0.0	0.	0.	0.	0.	0.000	0.000	-1.520	
1.0	66.	66.	-149.	-147.	10.700	-3.600	2.080	
2.0	111.	112.	-196.	-191.	15.250	-0.250	2.330	
3.0	110.	110.	-195.	-190.	15.125	0.025	2.305	
4.0	71.	71.	-159.	-154.	11.375	-0.425	2.730	
5.0	44.	46.	-132.	-127.	8.725	-1.275	4.005	
6.0	29.	32.	-115.	-110.	7.150	-1.350	5.355	
7.0	44.	44.	-132.	-127.	8.675	-1.025	6.380	
8.0	27.	30.	-114.	-109.	7.000	-2.200	8.580	
9.0	66.	72.	-158.	-152.	11.200	-1.700	10.280	
10.0	115.	117.	-204.	-201.	15.925	-1.375	11.655	
11.0	144.	147.	-232.	-229.	18.800	0.400	11.255	
12.0	167.	168.	-252.	-250.	20.925	0.925	10.330	
13.0	173.	172.	-260.	-259.	21.600	1.400	8.930	
14.0	182.	184.	-269.	-268.	22.575	1.875	7.055	
15.0	188.	188.	-274.	-272.	23.050	1.850	5.205	
16.0	207.	208.	-301.	-293.	25.225	3.825	1.380	

2.2 +30.00

SURFACE DISPLACEMENT= -0.91

DEPTH	ORIGINAL DATA				DEPTH	AVERAGE	DIFFERENCE	DISPLACEMENT
	TOWARDS		AWAY					
0.0	0.	0.	0.	0.	0.000	0.000	-0.910	
1.0	85.	86.	-127.	-126.	10.600	-3.700	2.790	
2.0	134.	134.	-176.	-174.	15.450	-0.050	2.840	
3.0	133.	133.	-174.	-171.	15.275	0.175	2.665	
4.0	91.	92.	-135.	-131.	11.225	-0.575	3.240	
5.0	68.	76.	-113.	-109.	9.150	-0.850	4.090	
6.0	49.	51.	-92.	-87.	6.975	-1.525	5.615	
7.0	66.	67.	-109.	-105.	8.675	-1.025	6.640	
8.0	50.	51.	-94.	-90.	7.125	-2.075	8.715	
9.0	91.	93.	-133.	-133.	11.250	-1.650	10.365	
10.0	138.	140.	-180.	-177.	15.875	-1.425	11.790	
11.0	168.	173.	-212.	-209.	19.050	0.650	11.140	
12.0	191.	195.	-233.	-230.	21.225	1.225	9.915	
13.0	198.	202.	-240.	-238.	21.950	1.750	8.165	
14.0	207.	209.	-249.	-246.	22.775	2.075	6.090	
15.0	213.	213.	-250.	-249.	23.125	1.925	4.165	
16.0	237.	235.	-274.	-274.	25.500	4.100	0.065	

2.2 +36.00

SURFACE DISPLACEMENT= -1.52

DEPTH	ORIGINAL DATA				DEPTH	AVERAGE	DIFFERENCE	DISPLACEMENT
	TOWARDS		AWAY					
0.0	0.	0.	0.	0.	0.000	0.000	-1.520	
1.0	63.	65.	-149.	-148.	10.625	-3.675	2.155	
2.0	110.	110.	-197.	-195.	15.300	-0.200	2.355	
3.0	107.	111.	-198.	-195.	15.275	0.175	2.180	
4.0	65.	68.	-156.	-153.	11.050	-0.750	2.930	
5.0	44.	46.	-134.	-135.	8.975	-1.025	3.955	
6.0	22.	26.	-112.	-111.	6.775	-1.725	5.680	
7.0	39.	42.	-129.	-127.	8.425	-1.275	6.955	
8.0	28.	30.	-117.	-114.	7.225	-1.975	8.930	
9.0	66.	71.	-158.	-155.	11.250	-1.650	10.580	
10.0	117.	115.	-204.	-203.	15.975	-1.325	11.905	
11.0	145.	148.	-236.	-234.	19.075	0.675	11.230	
12.0	166.	170.	-256.	-255.	21.175	1.175	10.055	
13.0	172.	176.	-264.	-262.	21.850	1.650	8.405	
14.0	182.	177.	-269.	-270.	22.450	1.750	6.655	
15.0	187.	185.	-273.	-274.	22.975	1.775	4.880	
16.0	209.	212.	-297.	-293.	25.275	3.875	1.005	

2.2 +43.00

SURFACE DISPLACEMENT= -0.30

DEPTH	ORIGINAL DATA				DEPTH	AVERAGE	DIFFERENCE	DISPLACEMENT
	TOWARDS		AWAY					
0.0	0.	0.	0.	0.	0.000	0.000	-0.300	
1.0	87.	86.	-128.	-124.	10.625	-3.675	3.375	
2.0	134.	132.	-175.	-171.	15.300	-0.200	3.575	
3.0	134.	133.	-175.	-172.	15.350	0.250	3.325	
4.0	88.	92.	-143.	-128.	11.275	-0.525	3.850	
5.0	68.	69.	-110.	-105.	8.800	-1.200	5.050	
6.0	48.	48.	-89.	-83.	6.700	-1.800	6.850	
7.0	64.	65.	-107.	-102.	8.450	-1.250	8.100	
8.0	47.	47.	-95.	-88.	6.925	-2.275	10.375	
9.0	90.	94.	-133.	-132.	11.225	-1.675	12.050	
10.0	140.	136.	-184.	-180.	16.000	-1.300	13.350	
11.0	170.	175.	-217.	-214.	19.400	1.000	12.350	
12.0	193.	194.	-235.	-232.	21.350	1.350	11.000	
13.0	197.	197.	-241.	-239.	21.850	1.650	9.350	
14.0	204.	206.	-249.	-247.	22.650	1.950	7.400	
15.0	211.	210.	-250.	-249.	23.000	1.800	5.600	
16.0	231.	238.	-276.	-273.	25.450	4.050	1.550	

2.2 +51.00

SURFACE DISPLACEMENT= 0.30

DEPTH	ORIGINAL DATA				DEPTH	AVERAGE	DIFFERENCE	DISPLACEMENT
	TOWARDS		AWAY					
0.0	0.	0.	0.	0.	0.000	0.000	0.300	
1.0	78.	78.	-138.	-136.	10.750	-3.550	3.850	
2.0	123.	129.	-183.	-182.	15.425	-0.075	3.925	
3.0	125.	128.	-186.	-183.	15.550	0.450	3.475	
4.0	78.	85.	-142.	-139.	11.100	-0.700	4.175	
5.0	56.	60.	-118.	-116.	8.750	-1.250	5.425	
6.0	36.	40.	-98.	-94.	6.700	-1.800	7.225	
7.0	53.	57.	-116.	-113.	8.475	-1.225	8.450	
8.0	40.	44.	-103.	-102.	7.225	-1.975	10.425	
9.0	82.	86.	-144.	-144.	11.400	-1.500	11.925	
10.0	130.	134.	-192.	-189.	16.125	-1.175	13.100	
11.0	159.	162.	-223.	-220.	19.100	0.700	12.400	
12.0	181.	182.	-243.	-241.	21.175	1.175	11.225	
13.0	187.	189.	-250.	-249.	21.875	1.675	9.550	
14.0	195.	194.	-256.	-256.	22.525	1.825	7.725	
15.0	198.	200.	-259.	-258.	22.875	1.675	6.050	
16.0	223.	225.	-282.	-286.	25.400	4.000	2.050	

2.2 +72.00

SURFACE DISPLACEMENT= 1.22

DEPTH	ORIGINAL DATA				DEPTH	AVERAGE	DIFFERENCE	DISPLACEMENT
	TOWARDS		AWAY					
0.0	0.	0.	0.	0.	0.000	0.000	1.220	
1.0	75.	77.	-150.	-150.	11.300	-3.000	4.220	
2.0	118.	118.	-196.	-195.	15.675	0.175	4.045	
3.0	119.	120.	-196.	-196.	15.775	0.675	3.370	
4.0	79.	78.	-157.	-154.	11.700	-0.100	3.470	
5.0	53.	55.	-133.	-130.	9.275	-0.725	4.195	
6.0	37.	38.	-117.	-114.	7.650	-0.850	5.045	
7.0	59.	61.	-139.	-136.	9.875	0.175	4.870	
8.0	49.	50.	-130.	-126.	8.875	-0.325	5.195	
9.0	87.	90.	-166.	-166.	12.725	-0.175	5.370	
10.0	132.	135.	-211.	-209.	17.175	-0.125	5.495	
11.0	164.	168.	-246.	-245.	20.575	2.175	3.320	
12.0	202.	204.	-278.	-277.	24.025	4.025	-0.705	
13.0	175.	175.	-253.	-251.	21.350	1.150	-1.855	
14.0	133.	135.	-210.	-211.	17.225	-3.475	1.620	
15.0	154.	154.	-230.	-232.	19.250	-1.950	3.570	

2.2 +91.00

SURFACE DISPLACEMENT= 2.13

DEPTH	ORIGINAL DATA				DEPTH	AVERAGE	DIFFERENCE	DISPLACEMENT
	TOWARDS		AWAY					
0.0	0.	0.	0.	0.	0.000	0.000	2.130	
1.0	69.	73.	-171.	-166.	11.975	-2.325	4.455	
2.0	111.	115.	-214.	-210.	16.250	0.750	3.705	
3.0	111.	115.	-214.	-211.	16.275	1.175	2.530	
4.0	54.	57.	-159.	-154.	10.600	-1.200	3.730	
5.0	38.	43.	-142.	-139.	9.050	-0.950	4.680	
6.0	24.	28.	-126.	-121.	7.475	-1.025	5.705	
7.0	41.	47.	-145.	-141.	9.350	-0.350	6.055	
8.0	45.	50.	-150.	-146.	9.775	0.575	5.480	
9.0	83.	86.	-185.	-182.	13.400	0.500	4.980	
10.0	127.	131.	-230.	-226.	17.850	0.550	4.430	
11.0	164.	168.	-267.	-266.	21.625	3.225	1.205	
12.0	189.	192.	-291.	-289.	24.025	4.025	-2.820	
13.0	165.	165.	-266.	-264.	21.500	1.300	-4.120	
14.0	127.	128.	-228.	-226.	17.725	-2.975	-1.145	
15.0	144.	146.	-246.	-244.	19.500	-1.700	0.555	

2.2 +107.00

SURFACE DISPLACEMENT= 1.52

ORIGINAL DATA								
DEPTH	TOWARDS		AWAY		DEPTH	AVERAGE	DIFFERENCE	DISPLACEMENT
0.0	0.	0.	0.	0.	0.0	0.000	0.000	1.520
1.0	77.	75.	-161.	-161.	1.0	11.850	-2.450	3.970
2.0	120.	114.	-205.	-206.	2.0	16.125	0.625	3.345
3.0	110.	113.	-205.	-205.	3.0	15.825	0.725	2.620
4.0	61.	55.	-147.	-148.	4.0	10.275	-1.525	4.145
5.0	44.	40.	-130.	-132.	5.0	8.650	-1.350	5.495
6.0	30.	27.	-115.	-114.	6.0	7.150	-1.350	6.845
7.0	47.	47.	-135.	-136.	7.0	9.125	-0.575	7.420
8.0	54.	51.	-138.	-139.	8.0	9.550	0.350	7.070
9.0	91.	93.	-176.	-175.	9.0	13.375	0.475	6.595
10.0	136.	133.	-220.	-220.	10.0	17.725	0.425	6.170
11.0	174.	171.	-259.	-259.	11.0	21.575	3.175	2.995
12.0	200.	198.	-289.	-284.	12.0	24.275	4.275	-1.280
13.0	172.	171.	-256.	-256.	13.0	21.375	1.175	-2.455
14.0	132.	131.	-220.	-220.	14.0	17.575	-3.125	0.670
15.0	148.	148.	-232.	-232.	15.0	19.000	-2.200	2.870

2.2 +119.00

SURFACE DISPLACEMENT= 3.05

DEPTH	ORIGINAL DATA				DEPTH	AVERAGE	DIFFERENCE	DISPLACEMENT
	TOWARDS		AWAY					
0.0	0.	0.	0.	0.	0.000	0.000	3.050	
1.0	96.	97.	-146.	-145.	12.100	-2.200	5.250	
2.0	140.	139.	-187.	-187.	16.325	0.825	4.425	
3.0	139.	137.	-185.	-188.	16.225	1.125	3.300	
4.0	79.	78.	-129.	-131.	10.425	-1.375	4.675	
5.0	63.	63.	-111.	-112.	8.725	-1.275	5.950	
6.0	49.	50.	-96.	-94.	7.225	-1.275	7.225	
7.0	66.	68.	-115.	-116.	9.125	-0.575	7.800	
8.0	72.	73.	-121.	-120.	9.650	0.450	7.350	
9.0	112.	112.	-159.	-159.	13.550	0.650	6.700	
10.0	155.	158.	-203.	-204.	18.000	0.700	6.000	
11.0	193.	196.	-240.	-241.	21.750	3.350	2.650	
12.0	221.	222.	-266.	-267.	24.400	4.400	-1.750	
13.0	192.	193.	-238.	-239.	21.550	1.350	-3.100	
14.0	151.	151.	-197.	-196.	17.375	-3.325	0.225	
15.0	169.	169.	-209.	-203.	18.750	-2.450	2.675	

2.2 +132.00

SURFACE DISPLACEMENT= 2.74

DEPTH	ORIGINAL DATA				DEPTH	AVERAGE	DIFFERENCE	DISPLACEMENT
	TOWARDS		AWAY					
0.0	0.	0.	0.	0.	0.000	0.000	2.740	
1.0	97.	97.	-142.	-140.	11.900	-2.400	5.140	
2.0	141.	141.	-187.	-187.	16.400	0.900	4.240	
3.0	140.	141.	-186.	-185.	16.300	1.200	3.040	
4.0	81.	80.	-127.	-127.	10.375	-1.425	4.465	
5.0	63.	64.	-110.	-110.	8.675	-1.325	5.790	
6.0	50.	51.	-94.	-93.	7.200	-1.300	7.090	
7.0	67.	69.	-115.	-113.	9.100	-0.600	7.690	
8.0	74.	80.	-121.	-118.	9.825	0.625	7.065	
9.0	111.	114.	-157.	-158.	13.500	0.600	6.465	
10.0	157.	160.	-202.	-201.	18.000	0.700	5.765	
11.0	197.	199.	-244.	-242.	22.050	3.650	2.115	
12.0	223.	224.	-266.	-266.	24.475	4.475	-2.360	
13.0	192.	194.	-238.	-236.	21.500	1.300	-3.660	
14.0	148.	150.	-194.	-195.	17.175	-3.525	-0.135	
15.0	166.	167.	-210.	-206.	18.725	-2.475	2.340	

2.2 +149.00

SURFACE DISPLACEMENT= 3.05

DEPTH	ORIGINAL DATA				DEPTH	AVERAGE	DIFFERENCE	DISPLACEMENT
	TOWARDS		AWAY					
0.0	0.	0.	0.	0.	0.000	0.000	3.050	
1.0	72.	68.	-166.	-162.	11.700	-2.600	5.650	
2.0	116.	114.	-210.	-210.	16.250	0.750	4.900	
3.0	118.	116.	-213.	-211.	16.450	1.350	3.550	
4.0	58.	56.	-153.	-152.	10.475	-1.325	4.875	
5.0	37.	39.	-133.	-133.	8.550	-1.450	6.325	
6.0	27.	28.	-120.	-120.	7.375	-1.125	7.450	
7.0	43.	43.	-139.	-138.	9.075	-0.625	8.075	
8.0	49.	44.	-146.	-145.	9.600	0.400	7.675	
9.0	87.	84.	-183.	-183.	13.425	0.525	7.150	
10.0	133.	132.	-227.	-228.	18.000	0.700	6.450	
11.0	173.	170.	-267.	-267.	21.925	3.525	2.925	
12.0	200.	197.	-291.	-291.	24.475	4.475	-1.550	
13.0	167.	165.	-261.	-261.	21.350	1.150	-2.700	
14.0	123.	121.	-215.	-216.	16.875	-3.825	1.125	
15.0	139.	139.	-225.	-233.	18.400	-2.800	3.925	

2.2 +176.00

SURFACE DISPLACEMENT= 3.65

DEPTH	ORIGINAL DATA				DEPTH	AVERAGE	DIFFERENCE	DISPLACEMENT
	TOWARDS		AWAY					
0.0	0.	0.	0.	0.	0.000	0.000	3.650	
1.0	84.	84.	-180.	-180.	13.200	-1.100	4.750	
2.0	116.	114.	-207.	-209.	16.150	0.650	4.100	
3.0	113.	110.	-207.	-209.	15.975	0.875	3.225	
4.0	30.	31.	-131.	-130.	8.050	-3.750	6.975	
5.0	24.	21.	-118.	-121.	7.100	-2.900	9.875	
6.0	59.	59.	-154.	-155.	10.675	2.175	7.700	
7.0	78.	73.	-173.	-176.	12.500	2.800	4.900	
8.0	85.	88.	-179.	-181.	13.325	4.125	0.775	
9.0	103.	99.	-198.	-201.	15.025	2.125	-1.350	
10.0	140.	137.	-237.	-235.	18.725	1.425	-2.775	
11.0	174.	173.	-268.	-270.	22.125	3.725	-6.500	
12.0	202.	202.	-299.	-299.	25.050	5.050	-11.550	
13.0	153.	152.	-249.	-249.	20.075	-0.125	-11.425	

2.2 +224.00

SURFACE DISPLACEMENT= 4.27

DEPTH	ORIGINAL DATA				DEPTH	AVERAGE	DIFFERENCE	DISPLACEMENT
	TOWARDS		AWAY					
0.0	0.	0.	0.	0.	0.000	0.000	4.270	
1.0	81.	82.	-190.	-189.	13.550	-0.750	5.020	
2.0	109.	108.	-216.	-217.	16.250	0.750	4.270	
3.0	107.	108.	-215.	-216.	16.150	1.050	3.220	
4.0	28.	28.	-135.	-137.	8.200	-3.600	6.820	
5.0	18.	18.	-124.	-127.	7.175	-2.825	9.645	
6.0	54.	54.	-157.	-159.	10.600	2.100	7.545	
7.0	71.	71.	-177.	-179.	12.450	2.750	4.795	
8.0	78.	77.	-185.	-185.	13.125	3.925	0.870	
9.0	99.	95.	-205.	-206.	15.125	2.225	-1.355	
10.0	137.	135.	-244.	-245.	19.025	1.725	-3.080	
11.0	175.	172.	-279.	-281.	22.675	4.275	-7.355	
12.0	205.	203.	-312.	-313.	25.825	5.825	-13.180	
13.0	150.	151.	-256.	-258.	20.375	0.175	-13.355	

3.2 -19.00

SURFACE DISPLACEMENT= 3.00

DEPTH	ORIGINAL DATA		DEPTH	AVERAGE	DIFFERENCE	DISPLACEMENT
	TOWARDS	AWAY				
0.0	0.	0.	0.0	0.000	0.000	3.000
1.0	916.	622.	1.0	14.750	0.350	2.650
2.0	787.	652.	2.0	4.300	2.200	0.450
3.0	754.	786.	3.0	-1.550	-0.150	0.600
4.0	704.	834.	4.0	-6.525	0.275	0.325
5.0	620.	921.	5.0	-15.000	0.300	0.025
6.0	644.	896.	6.0	-12.625	0.075	-0.050
7.0	675.	863.	7.0	-9.400	0.000	-0.050
8.0	696.	843.	8.0	-7.375	0.025	-0.075
9.0	698.	842.	9.0	-7.200	0.000	-0.075
10.0	724.	814.	10.0	-4.550	-0.050	-0.025
11.0	812.	729.	11.0	4.150	0.050	-0.075
12.0	813.	728.	12.0	4.200	0.000	-0.075
13.0	839.	706.	13.0	6.600	-0.100	0.025
14.0	893.	650.	14.0	12.150	-0.050	0.075
15.0	887.	556.	15.0	11.625	0.025	0.050

3.2 -10.00

SURFACE DISPLACEMENT= 0.00

DEPTH	ORIGINAL DATA		DEPTH	AVERAGE	DIFFERENCE	DISPLACEMENT
	TOWARDS	AWAY				
0.0	0.	0.	0.0	0.000	0.000	0.000
1.0	926.	636.	1.0	14.400	0.000	0.000
2.0	795.	769.	2.0	1.225	-0.875	0.875
3.0	760.	802.	3.0	-2.150	-0.750	1.625
4.0	710.	853.	4.0	-7.125	-0.325	1.950
5.0	628.	940.	5.0	-15.525	-0.225	2.175
6.0	652.	911.	6.0	-12.975	-0.275	2.450
7.0	684.	880.	7.0	-9.800	-0.400	2.850
8.0	704.	850.	8.0	-7.750	-0.350	3.200
9.0	706.	857.	9.0	-7.575	-0.375	3.575
10.0	733.	828.	10.0	-4.800	-0.300	3.875
11.0	820.	745.	11.0	3.725	-0.375	4.250
12.0	820.	744.	12.0	3.825	-0.375	4.625
13.0	848.	721.	13.0	6.350	-0.350	4.975
14.0	900.	665.	14.0	11.850	-0.350	5.325
15.0	896.	672.	15.0	11.250	-0.350	5.675

3.2 - 5.00

SURFACE DISPLACEMENT= 0.30

DEPTH	ORIGINAL DATA				DEPTH	AVERAGE	DIFFERENCE	DISPLACEMENT
	TOWARDS		AWAY					
0.0	0.	0.	0.	0.	0.0	0.000	0.000	0.300
1.0	914.	916.	619.	619.	1.0	14.800	0.400	-0.100
2.0	783.	784.	748.	744.	2.0	1.875	-0.225	0.125
3.0	750.	748.	782.	782.	3.0	-1.650	-0.250	0.375
4.0	698.	697.	832.	836.	4.0	-6.825	-0.025	0.400
5.0	616.	616.	920.	918.	5.0	-15.150	0.150	0.250
6.0	638.	638.	893.	892.	6.0	-12.725	-0.025	0.275
7.0	672.	672.	862.	860.	7.0	-9.450	-0.050	0.325
8.0	692.	693.	842.	840.	8.0	-7.425	-0.025	0.350
9.0	694.	694.	836.	839.	9.0	-7.175	0.025	0.325
10.0	718.	720.	812.	810.	10.0	-4.600	-0.100	0.425
11.0	808.	808.	727.	725.	11.0	4.100	0.000	0.425
12.0	808.	808.	724.	724.	12.0	4.200	0.000	0.425
13.0	850.	852.	702.	700.	13.0	7.500	0.800	-0.375
14.0	887.	887.	644.	644.	14.0	12.150	-0.050	-0.325
15.0	883.	886.	650.	650.	15.0	11.725	0.125	-0.450

3.2 -1.00

SURFACE DISPLACEMENT= 0.61

DEPTH	ORIGINAL DATA				DEPTH	AVERAGE	DIFFERENCE	DISPLACEMENT
	TOWARDS		AWAY					
0.0	0.	0.	0.	0.	0.000	0.000	0.610	
1.0	890.	890.	596.	594.	14.750	0.350	0.260	
2.0	759.	762.	728.	728.	1.625	-0.475	0.735	
3.0	727.	728.	760.	757.	-1.550	-0.150	0.885	
4.0	676.	676.	815.	819.	-7.050	-0.250	1.135	
5.0	592.	594.	900.	896.	-15.250	0.050	1.085	
6.0	614.	616.	872.	871.	-12.825	-0.125	1.210	
7.0	647.	648.	842.	842.	-9.725	-0.325	1.535	
8.0	670.	671.	822.	822.	-7.575	-0.175	1.710	
9.0	670.	672.	822.	820.	-7.500	-0.300	2.010	
10.0	698.	698.	786.	790.	-4.500	0.000	2.010	
11.0	735.	786.	702.	706.	4.075	-0.025	2.035	
12.0	787.	788.	700.	704.	4.275	0.075	1.960	
13.0	811.	812.	680.	682.	6.525	-0.175	2.135	
14.0	864.	864.	625.	626.	11.925	-0.275	2.410	

3.2 +1.00

SURFACE DISPLACEMENT= 1.55

DEPTH	ORIGINAL DATA		DEPTH	AVERAGE	DIFFERENCE	DISPLACEMENT
	TOWARDS	AWAY				
0.0	0.	0.	0.0	0.000	0.000	1.550
1.0	866.	560.	1.0	15.250	0.850	0.700
2.0	740.	687.	2.0	2.725	0.625	0.075
3.0	698.	728.	3.0	-1.425	-0.025	0.100
4.0	646.	780.	4.0	-6.700	0.100	0.000
5.0	562.	866.	5.0	-15.225	0.075	-0.075
6.0	580.	846.	6.0	-13.300	-0.600	0.525
7.0	614.	814.	7.0	-9.950	-0.550	1.075
8.0	639.	789.	8.0	-7.525	-0.125	1.200
9.0	640.	788.	9.0	-7.400	-0.200	1.400
10.0	669.	757.	10.0	-4.375	0.125	1.275
11.0	763.	666.	11.0	4.775	0.675	0.600
12.0	766.	662.	12.0	5.175	0.975	-0.375
13.0	793.	640.	13.0	7.650	0.950	-1.325
14.0	837.	592.	14.0	12.175	-0.025	-1.300
15.0	822.	606.	15.0	10.825	-0.775	-0.525

3.2 +6.00

SURFACE DISPLACEMENT= 1.83

ORIGINAL DATA					DEPTH	AVERAGE	DIFFERENCE	DISPLACEMENT
DEPTH	TOWARDS		AWAY					
0.0	0.	0.	0.	0.	0.0	0.000	0.000	1.830
1.0	150.	151.	-150.	-145.	1.0	14.900	0.500	1.330
2.0	19.	25.	-68.	-62.	2.0	4.350	2.250	-0.920
3.0	-54.	-47.	6.	11.	3.0	-2.950	-1.550	0.630
4.0	-134.	-131.	90.	93.	4.0	-11.200	-4.400	5.030
5.0	-180.	-176.	132.	135.	5.0	-15.575	-0.275	5.305
6.0	-159.	-156.	112.	116.	6.0	-13.575	-0.875	6.180
7.0	-127.	-123.	78.	81.	7.0	-10.225	-0.825	7.005
8.0	-109.	-105.	59.	63.	8.0	-9.400	-1.000	8.005
9.0	-107.	-102.	56.	60.	9.0	-8.125	-0.925	8.930
10.0	-59.	-53.	5.	9.	10.0	-3.150	1.350	7.580
11.0	22.	25.	-71.	-68.	11.0	4.650	0.550	7.030
12.0	35.	37.	-84.	-82.	12.0	5.950	1.750	5.280
13.0	73.	74.	-118.	-116.	13.0	9.525	2.825	2.455
14.0	101.	101.	-149.	-149.	14.0	12.500	0.300	2.155

3.2 +13.00

SURFACE DISPLACEMENT= 3.05

DEPTH	ORIGINAL DATA		DEPTH	AVERAGE	DIFFERENCE	DISPLACEMENT
	TOWARDS	AWAY				
0.0	0.	0.	0.0	0.000	0.000	3.050
1.0	141.	-166.	1.0	15.325	0.925	2.125
2.0	4.	-80.	2.0	4.175	2.075	0.050
3.0	-67.	-9.	3.0	-2.875	-1.475	1.525
4.0	-156.	80.	4.0	-11.800	-5.000	6.525
5.0	-199.	122.	5.0	-16.000	-9.700	7.225
6.0	-175.	97.	6.0	-13.575	-0.275	8.100
7.0	-143.	66.	7.0	-10.400	-1.000	9.100
8.0	-126.	48.	8.0	-8.700	-1.300	10.400
9.0	-125.	45.	9.0	-8.525	-1.325	11.725
10.0	-72.	-7.	10.0	-3.225	1.275	10.450
11.0	9.	-86.	11.0	4.750	0.650	9.800
12.0	24.	-101.	12.0	6.225	2.025	7.775
13.0	60.	-134.	13.0	9.725	3.025	4.750
14.0	87.	-164.	14.0	12.450	0.250	4.500

3.2 +23.00

SURFACE DISPLACEMENT= 3.50

DEPTH	ORIGINAL DATA		DEPTH	AVERAGE	DIFFERENCE	DISPLACEMENT
	TOWARDS	AWAY				
0.0	0.	0.	0.0	0.000	0.000	3.500
1.0	109.	-184.	1.0	14.725	0.325	3.175
2.0	3.	-77.	2.0	4.050	1.950	1.225
3.0	-67.	-9.	3.0	-2.850	-1.450	2.675
4.0	-156.	81.	4.0	-11.850	-5.050	7.725
5.0	-199.	121.	5.0	-15.950	-9.650	8.375
6.0	-176.	95.	6.0	-13.525	-9.825	9.200
7.0	-144.	56.	7.0	-10.425	-1.025	10.225
8.0	-127.	47.	8.0	-9.700	-1.300	11.525
9.0	-126.	46.	9.0	-8.550	-1.350	12.875
10.0	-73.	-7.	10.0	-3.225	1.275	11.600
11.0	9.	-86.	11.0	4.850	0.750	10.850
12.0	23.	-101.	12.0	6.225	2.025	8.825
13.0	60.	-137.	13.0	9.800	3.100	5.725
14.0	86.	-164.	14.0	12.475	0.275	5.450

3.2 +30.00

SURFACE DISPLACEMENT= 3.66

DEPTH	ORIGINAL DATA				DEPTH	AVERAGE	DIFFERENCE	DISPLACEMENT
	TOWARDS		AWAY					
0.0	0.	0.	0.	0.	0.000	0.000	3.660	
1.0	127.	132.	-171.	-171.	15.025	0.625	3.035	
2.0	12.	15.	-60.	-58.	3.625	1.525	1.510	
3.0	-49.	-47.	9.	7.	-2.800	-1.400	2.910	
4.0	-167.	-164.	118.	119.	-14.200	-7.400	10.310	
5.0	-181.	-178.	135.	137.	-15.775	-0.475	10.785	
6.0	-150.	-156.	110.	114.	-13.500	-0.800	11.585	
7.0	-127.	-125.	81.	83.	-10.400	-1.000	12.585	
8.0	-110.	-107.	63.	64.	-8.600	-1.200	13.785	
9.0	-110.	-106.	61.	64.	-8.525	-1.325	15.110	
10.0	-57.	-54.	4.	7.	-3.050	1.450	13.660	
11.0	25.	30.	-74.	-73.	5.050	0.950	12.710	
12.0	42.	40.	-87.	-87.	6.400	2.200	10.510	
13.0	80.	79.	-124.	-121.	10.100	3.400	7.110	
14.0	103.	105.	-150.	-147.	12.625	0.425	6.685	

3.2 +36.00

SURFACE DISPLACEMENT= 3.66

DEPTH	ORIGINAL DATA		DEPTH	AVERAGE	DIFFERENCE	DISPLACEMENT
	TOWARDS	AWAY				
0.0	0.	0.	0.0	0.000	0.000	3.660
1.0	112.	-100.	1.0	15.125	0.725	2.935
2.0	-3.	-74.	2.0	3.575	1.475	1.460
3.0	-65.	-11.	3.0	-2.700	-1.300	2.760
4.0	-154.	58.	4.0	-10.525	-3.725	6.485
5.0	-200.	122.	5.0	-16.050	-0.750	7.235
6.0	-178.	97.	6.0	-13.775	-1.075	8.310
7.0	-145.	65.	7.0	-10.525	-1.125	9.435
8.0	-131.	45.	8.0	-8.750	-1.350	10.785
9.0	-122.	45.	9.0	-8.400	-1.200	11.985
10.0	-69.	-10.	10.0	-2.950	1.550	10.435
11.0	11.	-93.	11.0	5.175	1.075	9.360
12.0	26.	-104.	12.0	6.525	2.325	7.035
13.0	63.	-137.	13.0	10.000	3.300	3.735
14.0	87.	-166.	14.0	12.625	0.425	3.310

3.2 +43.00

SURFACE DISPLACEMENT= 5.18

DEPTH	ORIGINAL DATA				DEPTH	AVERAGE	DIFFERENCE	DISPLACEMENT
	TOWARDS		AWAY					
0.0	0.	0.	0.	0.	0.000	0.000	5.180	
1.0	138.	138.	-171.	-169.	15.400	1.000	4.180	
2.0	19.	21.	-53.	-48.	3.525	1.425	2.755	
3.0	-41.	-40.	7.	14.	-2.550	-1.150	3.905	
4.0	-128.	-125.	98.	102.	-11.325	-4.525	8.430	
5.0	-181.	-174.	147.	151.	-16.325	-1.025	9.455	
6.0	-157.	-150.	122.	126.	-13.875	-1.175	10.630	
7.0	-120.	-116.	86.	91.	-10.325	-0.925	11.555	
8.0	-104.	-98.	68.	71.	-8.525	-1.125	12.680	
9.0	-101.	-97.	65.	69.	-8.275	-1.075	13.755	
10.0	-49.	-45.	10.	12.	-2.900	1.600	12.155	
11.0	35.	39.	-72.	-69.	5.375	1.275	10.880	
12.0	50.	53.	-84.	-82.	6.725	2.525	8.355	
13.0	85.	87.	-118.	-117.	10.175	3.475	4.880	
14.0	109.	110.	-141.	-143.	12.575	0.375	4.505	

3.2 +51.00

SURFACE DISPLACEMENT= 6.40

DEPTH	ORIGINAL DATA				DEPTH	AVERAGE	DIFFERENCE	DISPLACEMENT
	TOWARDS		AWAY					
0.0	0.	0.	0.	0.	0.000	0.000	6.400	
1.0	122.	125.	-190.	-130.	15.175	0.775	5.625	
2.0	7.	9.	-63.	-61.	3.500	1.400	4.225	
3.0	-53.	-51.	-2.	1.	-2.575	-1.175	5.400	
4.0	-145.	-147.	37.	91.	-11.750	-4.950	10.350	
5.0	-192.	-188.	134.	137.	-16.275	-0.975	11.325	
6.0	-168.	-165.	111.	114.	-13.950	-1.250	12.575	
7.0	-135.	-130.	79.	80.	-10.600	-1.200	13.775	
8.0	-116.	-109.	59.	60.	-8.600	-1.200	14.975	
9.0	-111.	-109.	53.	56.	-9.225	-1.025	16.000	
10.0	-61.	-55.	-1.	1.	-2.900	1.600	14.400	
11.0	23.	25.	-81.	-79.	5.200	1.100	13.300	
12.0	38.	39.	-95.	-93.	6.625	2.425	10.875	
13.0	70.	73.	-127.	-133.	10.075	3.375	7.500	
14.0	96.	97.	-153.	-151.	12.425	0.225	7.275	

3.2 +72.00

SURFACE DISPLACEMENT= 6.40

DEPTH	ORIGINAL DATA		DEPTH	AVERAGE	DIFFERENCE	DISPLACEMENT
	TOWARDS	AWAY				
0.0	0.	0.	0.0	0.000	0.000	6.400
1.0	120.	-102.	1.0	15.550	1.150	5.250
2.0	-3.	-72.	2.0	3.375	1.275	3.975
3.0	-61.	-13.	3.0	-2.400	-1.000	4.975
4.0	-148.	75.	4.0	-11.175	-4.375	9.350
5.0	-193.	121.	5.0	-15.750	-0.450	9.800
6.0	-171.	95.	6.0	-13.300	-0.600	10.400
7.0	-138.	60.	7.0	-9.975	-0.575	10.975
8.0	-117.	41.	8.0	-7.950	-0.550	11.525
9.0	-112.	37.	9.0	-7.475	-0.275	11.800
10.0	-63.	-15.	10.0	-2.375	2.125	9.675
11.0	21.	-95.	11.0	5.775	1.675	8.000

3.2 +91.00

SURFACE DISPLACEMENT= 8.23

DEPTH	ORIGINAL DATA		DEPTH	AVERAGE	DIFFERENCE	DISPLACEMENT
	TOWARDS	AWAY				
0.0	0.	0.	0.0	0.000	0.000	8.230
1.0	102.	-210.	1.0	15.650	1.250	6.980
2.0	-24.	-79.	2.0	2.700	0.600	6.380
3.0	-108.	6.	3.0	-5.725	-4.325	10.705
4.0	-188.	80.	4.0	-13.525	-6.725	17.430
5.0	-177.	71.	5.0	-12.375	2.025	14.505
6.0	-129.	25.	6.0	-7.725	4.975	9.530
7.0	-124.	19.	7.0	-7.200	2.200	7.330
8.0	-129.	25.	8.0	-7.700	-0.300	7.630
9.0	-122.	18.	9.0	-7.000	0.200	7.430
10.0	-99.	-6.	10.0	-4.700	-0.200	7.630
11.0	-28.	-72.	11.0	2.225	-1.875	9.505

3.2 +107.00

SURFACE DISPLACEMENT= 7.62

DEPTH	ORIGINAL DATA		DEPTH	AVERAGE	DIFFERENCE	DISPLACEMENT
	TOWARDS	AWAY				
0.0	0.	0.	0.0	0.000	0.000	7.620
1.0	120.	-201.	1.0	16.125	1.725	5.895
2.0	-15.	-67.	2.0	2.550	0.450	5.445
3.0	-98.	16.	3.0	-5.675	-4.275	6.720
4.0	-202.	124.	4.0	-16.375	-9.575	19.295
5.0	-168.	85.	5.0	-12.725	2.575	16.720
6.0	-117.	35.	6.0	-7.675	5.025	11.695
7.0	-113.	31.	7.0	-7.250	2.150	9.545
8.0	-118.	37.	8.0	-7.800	-0.400	9.945
9.0	-108.	28.	9.0	-6.875	0.325	9.620
10.0	-88.	3.	10.0	-4.600	-0.100	9.720
11.0	-8.	-64.	11.0	2.675	-1.425	11.145

3.2 +119.00

SURFACE DISPLACEMENT= 3.50

DEPTH	ORIGINAL DATA		DEPTH	AVERAGE	DIFFERENCE	DISPLACEMENT
	TOWARDS	AWAY				
0.0	0.	0.	0.0	0.000	0.000	8.500
1.0	138.	-185.	1.0	16.050	1.650	6.850
2.0	4.	-49.	2.0	2.550	0.450	6.400
3.0	-76.	31.	3.0	-5.525	-4.125	10.525
4.0	-185.	93.	4.0	-13.975	-7.175	17.700
5.0	-152.	105.	5.0	-12.875	2.425	15.275
6.0	-101.	54.	6.0	-7.800	4.900	10.375
7.0	-97.	50.	7.0	-7.375	2.025	8.350
8.0	-102.	54.	8.0	-7.850	-0.450	8.800
9.0	-91.	44.	9.0	-6.750	0.450	8.350
10.0	-70.	19.	10.0	-4.550	-0.050	8.400
11.0	-1.	-45.	11.0	2.225	-1.875	10.275

3.2 +132.00

SURFACE DISPLACEMENT= 9.45

DEPTH	TOWARDS	ORIGINAL DATA	AWAY	DEPTH	AVERAGE	DIFFERENCE	DISPLACEMENT
0.0	0.	0.	0.	0.0	0.000	0.000	9.450
1.0	141.	-183.	-124.	1.0	16.125	1.725	7.725
2.0	0.	-45.	-48.	2.0	2.175	0.075	7.650
3.0	-78.	34.	34.	3.0	-5.675	-4.275	11.925
4.0	-161.	95.	91.	4.0	-12.750	-5.950	17.875
5.0	-151.	105.	102.	5.0	-12.850	2.450	15.425
6.0	-100.	53.	54.	6.0	-7.775	4.925	10.500
7.0	-97.	51.	50.	7.0	-7.475	1.925	8.575
8.0	-102.	56.	56.	8.0	-7.925	-0.525	9.100
9.0	-92.	44.	47.	9.0	-6.850	0.350	8.750
10.0	-70.	20.	21.	10.0	-4.525	-0.025	8.775
11.0	0.	-46.	-47.	11.0	2.350	-1.750	10.525

3.2 +149.00

SURFACE DISPLACEMENT= 9.75

DEPTH	ORIGINAL DATA		DEPTH	AVERAGE	DIFFERENCE	DISPLACEMENT
	TOWARDS	AWAY				
0.0	0.	0.	0.0	0.000	0.000	9.750
1.0	120.	-191.	1.0	15.625	1.225	8.525
2.0	-19.	-72.	2.0	2.650	0.550	7.975
3.0	-89.	7.	3.0	-5.025	-3.625	11.600
4.0	-181.	91.	4.0	-13.600	-6.800	18.400
5.0	-174.	82.	5.0	-12.875	2.425	15.975
6.0	-123.	30.	6.0	-7.700	5.000	10.975
7.0	-119.	28.	7.0	-7.325	2.075	8.900
8.0	-124.	32.	8.0	-7.825	-0.425	9.325
9.0	-111.	20.	9.0	-6.600	0.600	8.725
10.0	-91.	-3.	10.0	-4.425	0.075	8.650
11.0	-23.	-70.	11.0	2.375	-1.725	10.375

3.2 +175.00

SURFACE DISPLACEMENT= 9.45

DEPTH	ORIGINAL DATA		DEPTH	AVERAGE	DIFFERENCE	DISPLACEMENT
	TOWARDS	AWAY				
0.0	C.	0.	0.0	0.000	0.000	9.450
1.0	128.	-212.	1.0	17.000	2.600	6.850
2.0	-21.	-67.	2.0	2.325	0.225	6.625
3.0	-97.	11.	3.0	-5.550	-4.150	10.775
4.0	-187.	101.	4.0	-14.475	-7.575	18.450
5.0	-163.	71.	5.0	-11.850	3.450	15.000
6.0	-95.	10.	6.0	-5.375	7.325	7.675
7.0	-89.	10.	7.0	-5.100	4.300	3.375
8.0	-103.	13.	8.0	-5.900	1.500	1.875
9.0	-98.	8.	9.0	-5.325	1.875	0.000
10.0	-77.	-15.	10.0	-3.100	1.400	-1.400
11.0	-20.	-69.	11.0	2.525	-1.575	0.175

3.2 +224.00

SURFACE DISPLACEMENT= 9.45

DEPTH	ORIGINAL DATA		DEPTH	AVERAGE	DIFFERENCE	DISPLACEMENT
	TOWARDS	AWAY				
0.0	0.	0.	0.0	0.000	0.000	9.450
1.0	129.	-214.	1.0	17.075	2.675	6.775
2.0	-21.	-67.	2.0	2.350	0.250	6.525
3.0	-96.	10.	3.0	-5.525	-4.125	10.650
4.0	-188.	101.	4.0	-14.425	-7.625	18.275
5.0	-163.	71.	5.0	-11.775	3.525	14.750
6.0	-96.	9.	6.0	-5.450	7.250	7.500
7.0	-90.	11.	7.0	-5.225	4.175	3.325
8.0	-101.	13.	8.0	-5.750	1.650	1.675
9.0	-98.	6.	9.0	-5.375	1.825	-0.150
10.0	-80.	-17.	10.0	-3.100	1.400	-1.550
11.0	-20.	-69.	11.0	2.575	-1.525	-0.025

4.2 +1.00

SURFACE DISPLACEMENT= 0.61

DEPTH	ORIGINAL DATA				DEPTH	AVERAGE	DIFFERENCE	DISPLACEMENT
	TOWARDS		AWAY					
0.0	0.	0.	0.	0.	0.000	0.000	0.610	
1.0	726.	730.	700.	703.	1.325	0.125	0.485	
2.0	736.	744.	690.	693.	2.425	0.525	-0.040	
3.0	744.	728.	682.	661.	3.225	0.625	-0.665	
4.0	706.	699.	716.	718.	-0.725	0.375	-1.040	
5.0	686.	678.	750.	742.	-3.200	0.100	-1.140	
6.0	658.	661.	773.	770.	-5.600	0.000	-1.140	
7.0	684.	714.	744.	721.	-1.675	0.025	-1.165	
8.0	695.	691.	731.	713.	-1.575	-0.175	-0.990	
9.0	723.	718.	694.	697.	1.250	0.450	-1.440	
10.0	753.	755.	677.	678.	3.825	0.225	-1.665	
11.0	770.	771.	660.	661.	5.500	0.200	-1.865	
12.0	780.	782.	649.	650.	6.575	0.175	-2.040	
13.0	820.	820.	610.	609.	10.525	0.325	-2.365	
14.0	828.	830.	598.	598.	11.550	0.050	-2.415	

4.2 +6.00

SURFACE DISPLACEMENT= 3.35

DEPTH	ORIGINAL DATA				DEPTH	AVERAGE	DIFFERENCE	DISPLACEMENT
	TOWARDS		AWAY					
0.0	0.	0.	0.	0.	0.000	0.000	3.350	
1.0	-6.	-5.	-40.	-40.	1.725	0.525	2.825	
2.0	5.	7.	-54.	-52.	2.950	1.050	1.775	
3.0	9.	12.	-57.	-55.	3.325	0.725	1.050	
4.0	-24.	-20.	-16.	-15.	4.0	-0.325	0.275	
5.0	-66.	-61.	20.	27.	5.0	-4.350	1.325	
6.0	-83.	-80.	41.	48.	6.0	-6.300	2.025	
7.0	-49.	-51.	7.	6.	7.0	-2.825	3.150	
8.0	-39.	-37.	-6.	-1.	8.0	-1.725	3.475	
9.0	-8.	-7.	-28.	-25.	9.0	0.950	3.325	
10.0	16.	16.	-61.	-59.	10.0	3.800	3.125	
11.0	34.	36.	-80.	-80.	11.0	5.750	2.675	
12.0	46.	45.	-91.	-90.	12.0	6.800	2.275	
13.0	88.	87.	-131.	-133.	13.0	10.975	1.500	
14.0	95.	93.	-138.	-141.	14.0	11.675	1.325	

4.2 +13.00

SURFACE DISPLACEMENT= 4.27

DEPTH	ORIGINAL DATA				DEPTH	AVERAGE	DIFFERENCE	DISPLACEMENT
	TOWARDS		AWAY					
0.0	0.	0.	0.	0.	0.000	0.000	4.270	
1.0	-17.	-14.	-52.	-48.	1.725	0.525	3.745	
2.0	-3.	0.	-67.	-65.	3.225	1.325	2.420	
3.0	0.	3.	-69.	-69.	3.525	0.925	1.495	
4.0	-34.	-32.	-31.	-34.	-0.025	1.075	0.420	
5.0	-82.	-77.	13.	11.	-4.575	-1.275	1.695	
6.0	-96.	-91.	26.	30.	-6.075	-0.475	2.170	
7.0	-58.	-54.	-5.	-3.	-2.600	-0.900	3.070	
8.0	-49.	-48.	-18.	-16.	-1.575	-0.175	3.245	
9.0	-20.	-19.	-46.	-46.	1.325	0.525	2.720	
10.0	4.	6.	-71.	-70.	3.775	0.175	2.545	
11.0	24.	25.	-93.	-92.	5.850	0.550	1.995	
12.0	32.	33.	-104.	-101.	6.750	0.350	1.645	
13.0	77.	76.	-146.	-146.	11.125	0.925	0.720	
14.0	81.	82.	-154.	-152.	11.725	0.225	0.495	

4.2 +23.00

SURFACE DISPLACEMENT= 4.88

DEPTH	ORIGINAL DATA				DEPTH	AVERAGE	DIFFERENCE	DISPLACEMENT
	TOWARDS		AWAY					
0.0	0.	0.	0.	0.	0.000	0.000	4.980	
1.0	-16.	-14.	-52.	-52.	1.850	0.650	4.230	
2.0	-3.	-5.	-69.	-68.	3.225	1.325	2.905	
3.0	1.	2.	-72.	-70.	3.625	1.025	1.880	
4.0	-33.	-32.	-33.	-31.	-0.025	1.075	0.805	
5.0	-81.	-80.	13.	15.	-4.725	-1.425	2.230	
6.0	-95.	-95.	26.	29.	-6.125	-0.525	2.755	
7.0	-55.	-55.	-12.	-8.	-2.250	-0.550	3.305	
8.0	-49.	-51.	-10.	-16.	-1.625	-0.225	3.530	
9.0	-19.	-18.	-45.	-45.	1.325	0.525	3.005	
10.0	4.	5.	-73.	-73.	3.875	0.275	2.730	
11.0	23.	24.	-92.	-93.	5.800	0.500	2.230	
12.0	33.	31.	-102.	-101.	6.675	0.275	1.955	
13.0	76.	74.	-148.	-145.	11.075	0.875	1.080	
14.0	82.	79.	-153.	-152.	11.650	0.150	0.930	

4.2 +36.00

SURFACE DISPLACEMENT= 6.69

DEPTH	ORIGINAL DATA				DEPTH	AVERAGE	DIFFERENCE	DISPLACEMENT
	TOWARDS		AWAY					
0.0	0.	0.	0.	0.	0.0	0.000	0.000	6.690
1.0	-15.	-16.	-55.	-53.	1.0	1.925	0.725	5.965
2.0	2.	3.	-72.	-70.	2.0	3.675	1.775	4.190
3.0	8.	9.	-77.	-70.	3.0	4.100	1.500	2.690
4.0	-27.	-29.	-31.	-31.	4.0	0.150	1.250	1.440
5.0	-79.	-77.	7.	8.	5.0	-4.275	-0.975	2.415
6.0	-98.	-98.	33.	33.	6.0	-6.550	-0.950	3.365
7.0	-56.	-57.	-11.	-9.	7.0	-2.325	-0.625	3.990
8.0	-52.	-52.	-17.	-16.	8.0	-1.775	-0.375	4.365
9.0	-14.	-8.	-46.	-47.	9.0	1.775	0.975	3.390
10.0	7.	11.	-74.	-71.	10.0	4.075	0.475	2.915
11.0	29.	29.	-92.	-93.	11.0	6.075	0.775	2.140
12.0	36.	38.	-103.	-101.	12.0	6.950	0.550	1.590
13.0	78.	82.	-149.	-144.	13.0	11.325	1.125	0.465
14.0	86.	87.	-156.	-155.	14.0	12.100	0.600	-0.135

4.2 +43.00

SURFACE DISPLACEMENT= 7.92

DEPTH	ORIGINAL DATA				DEPTH	AVERAGE	DIFFERENCE	DISPLACEMENT
	TOWARDS		AWAY					
0.0	0.	0.	0.	0.	0.000	0.000	7.920	
1.0	6.	10.	-37.	-36.	2.225	1.025	6.895	
2.0	22.	26.	-53.	-53.	3.850	1.950	4.945	
3.0	27.	32.	-59.	-56.	4.350	1.750	3.195	
4.0	-7.	-6.	-10.	-17.	0.575	1.675	1.520	
5.0	-62.	-57.	33.	35.	-4.675	-1.375	2.895	
6.0	-81.	-75.	49.	53.	-6.450	-0.850	3.745	
7.0	-40.	-36.	12.	8.	-2.400	-0.700	4.445	
8.0	-31.	-26.	3.	1.	-1.525	-0.125	4.570	
9.0	2.	3.	-26.	-30.	1.525	0.725	3.845	
10.0	26.	29.	-55.	-55.	4.125	0.525	3.320	
11.0	43.	46.	-76.	-75.	6.000	0.700	2.620	
12.0	52.	53.	-82.	-83.	6.750	0.350	2.270	
13.0	95.	94.	-130.	-128.	11.175	0.975	1.295	
14.0	102.	102.	-136.	-135.	11.875	0.375	0.920	

4.2 +51.00

SURFACE DISPLACEMENT= 8.23

DEPTH	ORIGINAL DATA				DEPTH	AVERAGE	DIFFERENCE	DISPLACEMENT
	TOWARDS		AWAY					
0.0	0.	0.	0.	0.	0.000	0.000	8.230	
1.0	-3.	-3.	-44.	-43.	2.025	0.825	7.405	
2.0	13.	14.	-62.	-60.	3.725	1.825	5.580	
3.0	18.	19.	-67.	-64.	4.200	1.600	3.980	
4.0	-18.	-18.	-27.	-16.	0.175	1.275	2.705	
5.0	-73.	-70.	25.	26.	-4.850	-1.550	4.255	
6.0	-89.	-89.	43.	46.	-6.675	-1.075	5.330	
7.0	-54.	-48.	-2.	-6.	-2.350	-0.650	5.980	
8.0	-38.	-37.	-7.	-5.	-1.575	-0.175	6.155	
9.0	-8.	-6.	-36.	-32.	1.350	0.550	5.605	
10.0	17.	17.	-65.	-63.	4.050	0.450	5.155	
11.0	35.	35.	-82.	-81.	5.825	0.525	4.630	
12.0	43.	42.	-92.	-91.	6.700	0.300	4.330	
13.0	86.	85.	-137.	-134.	11.050	0.850	3.480	
14.0	93.	91.	-143.	-142.	11.725	0.225	3.255	

4.2 +72.00

SURFACE DISPLACEMENT= 8.23

DEPTH	ORIGINAL DATA				DEPTH	AVERAGE	DIFFERENCE	DISPLACEMENT
	TOWARDS		AWAY					
0.0	0.	0.	0.	0.	0.000	0.000	8.230	
1.0	-15.	-14.	-55.	-55.	2.025	0.825	7.405	
2.0	5.	5.	-75.	-74.	3.975	2.075	5.330	
3.0	11.	10.	-81.	-79.	4.525	1.925	3.405	
4.0	-23.	-17.	-40.	-39.	0.975	2.075	1.330	
5.0	-81.	-78.	10.	11.	-4.500	-1.200	2.530	
6.0	-97.	-96.	27.	31.	-6.275	-0.675	3.205	
7.0	-56.	-55.	-5.	-3.	-2.575	-0.875	4.080	
8.0	-46.	-44.	-20.	-17.	-1.325	0.075	4.005	
9.0	-15.	-13.	-50.	-49.	1.775	0.975	3.030	
10.0	6.	7.	-76.	-75.	4.100	0.500	2.530	
11.0	24.	25.	-94.	-94.	5.925	0.625	1.905	
12.0	29.	27.	-101.	-99.	6.400	0.000	1.905	
13.0	74.	73.	-144.	-143.	10.850	0.650	1.255	
14.0	80.	77.	-152.	-151.	11.500	0.000	1.255	

4.2 +91.00

SURFACE DISPLACEMENT= 9.14

DEPTH	ORIGINAL DATA				DEPTH	AVERAGE	DIFFERENCE	DISPLACEMENT
	TOWARDS		AWAY					
0.0	0.	0.	0.	0.	0.000	0.000	9.140	
1.0	-29.	-28.	-72.	-72.	2.175	0.975	8.165	
2.0	-6.	-8.	-95.	-95.	4.425	2.525	5.640	
3.0	0.	0.	-101.	-99.	5.000	2.400	3.240	
4.0	-37.	-35.	-60.	-59.	1.175	2.275	0.965	
5.0	-92.	-90.	-10.	-9.	-4.075	-0.775	1.740	
6.0	-109.	-108.	12.	12.	-6.025	-0.425	2.165	
7.0	-68.	-64.	-34.	-36.	-1.550	0.150	2.015	
8.0	-61.	-62.	-35.	-36.	-1.300	0.100	1.915	
9.0	-34.	-33.	-64.	-62.	1.475	0.675	1.240	
10.0	-13.	-14.	-85.	-85.	3.575	-0.025	1.265	
11.0	6.	6.	-105.	-103.	5.500	0.200	1.065	
12.0	12.	13.	-115.	-113.	6.325	-0.075	1.140	
13.0	60.	58.	-161.	-160.	10.975	0.775	0.365	
14.0	65.	64.	-167.	-166.	11.550	0.050	0.315	

4.2 +107.00

SURFACE DISPLACEMENT= 8.84

DEPTH	ORIGINAL DATA				DEPTH	AVERAGE	DIFFERENCE	DISPLACEMENT
	TOWARDS		AWAY					
0.0	0.	0.	0.	0.	0.000	0.000	8.840	
1.0	-18.	-19.	-64.	-64.	1.0	2.275	7.765	
2.0	3.	4.	-85.	-88.	2.0	4.500	5.165	
3.0	9.	8.	-91.	-92.	3.0	5.000	2.765	
4.0	-22.	-26.	-45.	-52.	4.0	1.225	0.440	
5.0	-84.	-89.	5.	4.	5.0	-4.550	1.690	
6.0	-101.	-106.	3.	4.	6.0	-5.350	1.440	
7.0	-59.	-62.	-16.	-18.	7.0	-2.175	1.915	
8.0	-51.	-55.	-23.	-23.	8.0	-1.500	2.015	
9.0	-24.	-28.	-50.	-50.	9.0	1.200	1.615	
10.0	-6.	-8.	-73.	-73.	10.0	3.300	1.915	
11.0	13.	12.	-93.	-92.	11.0	5.250	1.965	
12.0	20.	16.	-103.	-103.	12.0	6.050	2.315	
13.0	67.	65.	-150.	-150.	13.0	10.800	1.715	
14.0	73.	71.	-155.	-156.	14.0	11.375	1.840	

4.2 +119.00

SURFACE DISPLACEMENT= 9.75

DEPTH	ORIGINAL DATA				DEPTH	AVERAGE	DIFFERENCE	DISPLACEMENT
	TOWARDS		AWAY					
0.0	0.	0.	0.	0.	0.000	0.000	9.750	
1.0	3.	2.	-46.	-49.	2.500	1.300	8.450	
2.0	26.	23.	-68.	-71.	4.700	2.800	5.650	
3.0	30.	27.	-73.	-74.	5.100	2.500	3.150	
4.0	-6.	-8.	-33.	-34.	1.325	2.425	0.725	
5.0	-64.	-69.	22.	23.	-4.425	-1.125	1.850	
6.0	-83.	-85.	40.	41.	-6.225	-0.625	2.475	
7.0	-41.	-44.	0.	-1.	-2.100	-0.400	2.875	
8.0	-34.	-37.	-5.	-6.	-1.500	-0.100	2.975	
9.0	-2.	-5.	-34.	-34.	1.525	0.725	2.250	
10.0	15.	13.	-55.	-55.	3.450	-0.150	2.400	
11.0	34.	32.	-75.	-75.	5.400	0.100	2.300	
12.0	42.	39.	-83.	-84.	6.200	-0.200	2.500	
13.0	87.	87.	-133.	-132.	10.975	0.775	1.725	
14.0	96.	97.	-138.	-138.	11.725	0.225	1.500	

4.2 +132.00

SURFACE DISPLACEMENT= 10.36

DEPTH	ORIGINAL DATA				DEPTH	AVERAGE	DIFFERENCE	DISPLACEMENT
	TOWARDS		AWAY					
0.0	0.	0.	0.	0.	0.000	0.000	10.360	
1.0	3.	-2.	-44.	-43.	2.200	1.000	9.360	
2.0	29.	25.	-69.	-69.	4.800	2.900	6.460	
3.0	34.	31.	-72.	-73.	5.250	2.650	3.810	
4.0	-5.	-6.	-30.	-33.	1.300	2.400	1.410	
5.0	-62.	-65.	26.	23.	-4.400	-1.100	2.510	
6.0	-79.	-82.	43.	43.	-6.175	-0.575	3.085	
7.0	-38.	-39.	1.	4.	-2.050	-0.350	3.435	
8.0	-29.	-33.	-2.	-2.	-1.450	-0.050	3.485	
9.0	-1.	-2.	-33.	-33.	1.575	0.775	2.710	
10.0	17.	15.	-53.	-54.	3.475	-0.125	2.835	
11.0	36.	33.	-73.	-73.	5.375	0.075	2.760	
12.0	44.	42.	-82.	-83.	6.275	-0.125	2.885	
13.0	90.	90.	-132.	-131.	11.075	0.875	2.010	
14.0	97.	97.	-136.	-135.	11.625	0.125	1.885	

4.2 +149.00

SURFACE DISPLACEMENT= 10.97

DEPTH	ORIGINAL DATA				DEPTH	AVERAGE	DIFFERENCE	DISPLACEMENT
	TOWARDS		AWAY					
0.0	0.	0.	0.	0.	0.000	0.000	10.970	
1.0	-24.	-22.	-69.	-69.	2.275	1.075	9.895	
2.0	3.	5.	-90.	-93.	4.775	2.875	7.020	
3.0	9.	12.	-98.	-97.	5.400	2.800	4.220	
4.0	-27.	-26.	-59.	-50.	1.375	2.475	1.745	
5.0	-92.	-92.	3.	1.	-4.700	-1.400	3.145	
6.0	-108.	-106.	20.	18.	-6.300	-0.700	3.845	
7.0	-61.	-60.	-25.	-23.	-1.825	-0.125	3.970	
8.0	-55.	-55.	-27.	-29.	-1.350	0.050	3.920	
9.0	-24.	-25.	-56.	-58.	1.625	0.825	3.095	
10.0	-7.	-6.	-77.	-79.	3.575	-0.025	3.120	
11.0	11.	12.	-97.	-98.	5.450	0.150	2.970	
12.0	19.	21.	-106.	-106.	6.300	-0.100	3.070	
13.0	66.	69.	-155.	-154.	11.100	0.900	2.170	
14.0	72.	75.	-162.	-159.	11.700	0.200	1.970	

4.2 +176.00

SURFACE DISPLACEMENT= 9.75

DEPTH	ORIGINAL DATA				DEPTH	AVERAGE	DIFFERENCE	DISPLACEMENT
	TOWARDS		AWAY					
0.0	0.	0.	0.	0.	0.000	0.000	9.750	
1.0	-16.	-15.	-72.	-73.	2.850	1.650	8.100	
2.0	9.	7.	-93.	-95.	5.100	3.200	4.900	
3.0	19.	19.	-101.	-103.	6.050	3.450	1.450	
4.0	-4.	-5.	-70.	-74.	3.375	4.475	-3.025	
5.0	-64.	-72.	-17.	-19.	-2.500	0.800	-3.825	
6.0	-111.	-114.	24.	22.	-6.775	-1.175	-2.650	
7.0	-76.	-78.	-17.	-23.	-2.850	-1.150	-1.500	
8.0	-58.	-57.	-38.	-40.	-0.925	0.475	-1.975	
9.0	-24.	-27.	-63.	-69.	2.025	1.225	-3.200	
10.0	-22.	-27.	-72.	-67.	2.250	-1.350	-1.850	
11.0	2.	-3.	-97.	-95.	4.775	-0.525	-1.325	
12.0	12.	6.	-106.	-101.	5.625	-0.775	-0.550	
13.0	57.	61.	-156.	-156.	10.750	0.550	-1.100	

4.2 +224.00

SURFACE DISPLACEMENT= 10.36

DEPTH	ORIGINAL DATA				DEPTH	AVERAGE	DIFFERENCE	DISPLACEMENT
	TOWARDS		AWAY					
0.0	0.	0.	0.	0.	0.000	0.000	10.360	
1.0	-16.	-14.	-80.	-82.	1.0	3.300	8.260	
2.0	7.	6.	-99.	-101.	2.0	5.325	4.835	
3.0	16.	14.	-108.	-109.	3.0	6.175	1.260	
4.0	-15.	-13.	-79.	-82.	4.0	3.325	-3.165	
5.0	-71.	-73.	-19.	-22.	5.0	-2.600	-3.865	
6.0	-114.	-115.	22.	21.	6.0	-6.800	-2.665	
7.0	-72.	-73.	-15.	-21.	7.0	-2.725	-1.640	
8.0	-53.	-54.	-38.	-40.	8.0	-0.725	-2.315	
9.0	-25.	-26.	-61.	-64.	9.0	1.850	-3.365	
10.0	-20.	-25.	-68.	-69.	10.0	2.300	-2.065	
11.0	2.	-2.	-94.	-94.	11.0	4.700	-1.465	
12.0	11.	8.	-103.	-102.	12.0	5.600	-0.665	
13.0	60.	63.	-156.	-156.	13.0	10.875	-1.340	

Lateral Sub-surface Movement Parallel to Tunnel

(2.1, 3.1, 4.1)

Positive indicates movement away from channel

Negative indicates movement towards channel

Displacement in mm.

2.1 -19.00

SURFACE DISPLACEMENT= 0.00

DEPTH	ORIGINAL DATA				DEPTH	AVERAGE	DIFFERENCE	DISPLACEMENT
	TOWARDS		AWAY					
0.0	0.	0.	0.	0.	0.0	0.000	0.000	0.000
1.0	700.	699.	830.	830.	1.0	-6.525	0.075	-0.075
2.0	698.	699.	832.	832.	2.0	-6.675	-0.175	0.100
3.0	714.	712.	818.	819.	3.0	-5.275	-0.175	0.275
4.0	722.	722.	810.	810.	4.0	-4.400	-0.100	0.375
5.0	736.	736.	796.	796.	5.0	-3.000	-0.100	0.475
6.0	750.	750.	784.	784.	6.0	-1.700	0.000	0.475
7.0	736.	736.	797.	797.	7.0	-3.050	-0.150	0.625
8.0	728.	729.	804.	804.	8.0	-3.775	-0.075	0.700
9.0	762.	762.	770.	772.	9.0	-0.450	-0.150	0.850
10.0	780.	780.	753.	753.	10.0	1.350	0.050	0.800
11.0	768.	769.	764.	765.	11.0	0.200	-0.100	0.900
12.0	760.	762.	772.	772.	12.0	-0.550	-0.150	1.050
13.0	758.	759.	774.	774.	13.0	-0.775	-0.075	1.125
14.0	760.	762.	772.	772.	14.0	-0.550	-0.150	1.275
15.0	762.	763.	770.	770.	15.0	-0.375	-0.075	1.350
16.0	750.	754.	782.	784.	16.0	-1.550	0.050	1.300

2.1 -10.00

SURFACE DISPLACEMENT= 0.00

DEPTH	ORIGINAL DATA				DEPTH	AVERAGE	DIFFERENCE	DISPLACEMENT
	TOWARDS		AWAY					
0.0	0.	0.	0.	0.	0.0	0.000	0.000	0.000
1.0	712.	713.	838.	840.	1.0	-6.325	0.275	-0.275
2.0	710.	712.	842.	842.	2.0	-6.550	-0.050	-0.225
3.0	724.	725.	826.	826.	3.0	-5.075	0.025	-0.250
4.0	732.	734.	819.	820.	4.0	-4.325	-0.025	-0.225
5.0	746.	748.	804.	806.	5.0	-2.900	0.000	-0.225
6.0	760.	762.	792.	794.	6.0	-1.600	0.100	-0.325
7.0	746.	748.	806.	806.	7.0	-2.950	-0.050	-0.275
8.0	738.	738.	813.	814.	8.0	-3.775	-0.075	-0.200
9.0	772.	772.	779.	782.	9.0	-0.425	-0.125	-0.075
10.0	792.	792.	762.	763.	10.0	1.475	0.175	-0.250
11.0	780.	782.	774.	778.	11.0	0.250	-0.050	-0.200
12.0	773.	773.	782.	785.	12.0	-0.525	-0.125	-0.075
13.0	770.	770.	784.	787.	13.0	-0.775	-0.075	0.000
14.0	773.	774.	782.	784.	14.0	-0.475	-0.075	0.075
15.0	773.	774.	782.	784.	15.0	-0.475	-0.175	0.250
16.0	763.	763.	794.	794.	16.0	-1.550	0.050	0.200

2.1 -5.00

SURFACE DISPLACEMENT= -3.10

DEPTH	ORIGINAL DATA				DEPTH	AVERAGE	DIFFERENCE	DISPLACEMENT
	TOWARDS		AWAY					
0.0	0.	0.	0.	0.	0.0	0.000	0.000	-3.100
1.0	662.	662.	866.	864.	1.0	-10.150	-3.550	0.450
2.0	704.	704.	825.	825.	2.0	-6.050	0.450	0.000
3.0	712.	712.	812.	815.	3.0	-5.075	0.025	-0.025
4.0	721.	719.	807.	807.	4.0	-4.350	-0.050	0.025
5.0	734.	734.	792.	793.	5.0	-2.925	-0.025	0.050
6.0	748.	748.	780.	782.	6.0	-1.650	0.050	0.000
7.0	734.	734.	792.	792.	7.0	-2.900	0.000	0.000
8.0	726.	726.	803.	803.	8.0	-3.850	-0.150	0.150
9.0	760.	759.	768.	769.	9.0	-0.450	-0.150	0.300
10.0	778.	776.	748.	752.	10.0	1.350	0.050	0.250
11.0	767.	767.	762.	765.	11.0	0.175	-0.125	0.375
12.0	760.	760.	770.	770.	12.0	-0.500	-0.100	0.475
13.0	758.	757.	772.	772.	13.0	-0.725	-0.025	0.500
14.0	760.	760.	768.	768.	14.0	-0.400	0.000	0.500
15.0	760.	761.	767.	769.	15.0	-0.375	-0.075	0.575
16.0	749.	749.	774.	779.	16.0	-1.375	0.225	0.350

2.1 -1.00

SURFACE DISPLACEMENT= 8.80

DEPTH	ORIGINAL DATA		DEPTH	AVERAGE	DIFFERENCE	DISPLACEMENT
	TOWARDS	AWAY				
0.0	0.	0.	0.0	0.000	0.000	8.800
1.0	736.	747.	1.0	-0.575	6.025	2.775
2.0	698.	784.	2.0	-4.350	2.150	0.625
3.0	692.	790.	3.0	-4.900	0.200	0.425
4.0	702.	781.	4.0	-3.875	0.425	0.000
5.0	712.	772.	5.0	-2.925	-0.025	0.025
6.0	724.	761.	6.0	-1.800	-0.100	0.125
7.0	711.	773.	7.0	-3.025	-0.125	0.250
8.0	705.	780.	8.0	-3.700	0.000	0.250
9.0	742.	744.	9.0	-0.125	0.175	0.075
10.0	757.	729.	10.0	1.400	0.100	-0.025
11.0	745.	741.	11.0	0.225	-0.075	0.050
12.0	736.	750.	12.0	-0.675	-0.275	0.325
13.0	736.	750.	13.0	-0.700	0.000	0.325
14.0	740.	750.	14.0	-0.425	-0.025	0.350
15.0	742.	746.	15.0	-0.150	0.150	0.200
16.0	728.	757.	16.0	-1.425	0.175	0.025

2.1 +1.00

SURFACE DISPLACEMENT= 4.40

DEPTH	ORIGINAL DATA				DEPTH	AVERAGE	DIFFERENCE	DISPLACEMENT
	TOWARDS		AWAY					
0.0	0.	0.	0.	0.	0.000	0.000	4.400	
1.0	676.	676.	747.	747.	-3.550	3.050	1.350	
2.0	665.	665.	760.	762.	-4.800	1.700	-0.350	
3.0	666.	666.	756.	757.	-4.525	0.575	-0.925	
4.0	674.	672.	750.	750.	-3.850	0.450	-1.375	
5.0	681.	681.	743.	743.	-3.100	-0.200	-1.175	
6.0	691.	690.	733.	735.	-2.175	-0.475	-0.700	
7.0	676.	677.	747.	749.	-3.575	-0.675	-0.025	
8.0	672.	673.	750.	752.	-3.925	-0.225	0.200	
9.0	712.	715.	711.	711.	0.125	0.425	-0.225	
10.0	731.	732.	692.	694.	1.925	0.625	-0.850	
11.0	722.	723.	703.	704.	0.950	0.650	-1.500	
12.0	718.	719.	708.	708.	0.525	0.925	-2.425	
13.0	715.	716.	710.	710.	0.275	0.975	-3.400	
14.0	701.	700.	725.	725.	-1.225	-0.825	-2.575	
15.0	698.	701.	730.	726.	-1.425	-1.125	-1.450	
16.0	698.	697.	729.	726.	-1.500	0.100	-1.550	

2.1 +6.00

SURFACE DISPLACEMENT= 3.40

DEPTH	ORIGINAL DATA				DEPTH	AVERAGE	DIFFERENCE	DISPLACEMENT
	TOWARDS		AWAY					
0.0	0.	0.	0.	0.	0.000	0.000	3.400	
1.0	-68.	-67.	15.	16.	-4.150	2.450	0.950	
2.0	-82.	-83.	31.	30.	-5.650	0.850	0.100	
3.0	-76.	-76.	21.	24.	-4.925	0.175	-0.075	
4.0	-67.	-66.	16.	20.	-4.225	0.075	-0.150	
5.0	-53.	-49.	-1.	0.	-2.525	0.375	-0.525	
6.0	-47.	-44.	-5.	-3.	-2.075	-0.375	-0.150	
7.0	-56.	-54.	4.	4.	-2.950	-0.050	-0.100	
8.0	-65.	-63.	17.	15.	-4.000	-0.300	0.200	
9.0	-23.	-18.	-32.	-27.	0.450	0.750	-0.550	
10.0	-9.	-9.	-41.	-38.	1.525	0.225	-0.775	
11.0	-25.	-23.	-29.	-26.	0.175	-0.125	-0.650	
12.0	-43.	-40.	-12.	-11.	-1.500	-1.100	0.450	
13.0	-46.	-45.	-7.	-4.	-2.000	-1.300	1.750	
14.0	-42.	-39.	-16.	-12.	-1.325	-0.925	2.675	
15.0	-33.	-29.	-25.	-21.	-0.400	-0.100	2.775	
16.0	-42.	-42.	-6.	-6.	-1.800	-0.200	2.975	

2.1 +13.00

SURFACE DISPLACEMENT= 1.00

DEPTH	ORIGINAL DATA				DEPTH	AVERAGE	DIFFERENCE	DISPLACEMENT
	TOWARDS		AWAY					
0.0	0.	0.	0.	0.	0.0	0.000	0.000	1.000
1.0	-89.	-90.	7.	10.	1.0	-4.900	1.700	-0.700
2.0	-105.	-105.	22.	26.	2.0	-6.450	0.050	-0.750
3.0	-97.	-95.	12.	17.	3.0	-5.525	-0.425	-0.325
4.0	-87.	-83.	4.	7.	4.0	-4.525	-0.225	-0.100
5.0	-66.	-64.	-16.	-11.	5.0	-2.575	0.325	-0.425
6.0	-62.	-58.	-21.	-16.	6.0	-2.075	-0.375	-0.050
7.0	-69.	-68.	-13.	-9.	7.0	-2.875	0.025	-0.075
8.0	-80.	-78.	-4.	0.	8.0	-3.850	-0.150	0.075
9.0	-37.	-34.	-44.	-41.	9.0	0.350	0.650	-0.575
10.0	-28.	-24.	-56.	-52.	10.0	1.400	0.100	-0.675
11.0	-40.	-37.	-44.	-40.	11.0	0.175	-0.125	-0.550
12.0	-56.	-56.	-24.	-21.	12.0	-1.675	-1.275	0.725
13.0	-61.	-59.	-21.	-18.	13.0	-2.025	-1.325	2.050
14.0	-54.	-53.	-28.	-25.	14.0	-1.350	-0.950	3.000
15.0	-45.	-45.	-37.	-35.	15.0	-0.450	-0.150	3.150
16.0	-55.	-55.	-24.	-24.	16.0	-1.550	0.050	3.100

2.1 +23.00

SURFACE DISPLACEMENT= 0.00

DEPTH	ORIGINAL DATA				DEPTH	AVERAGE	DIFFERENCE	DISPLACEMENT
	TOWARDS		AWAY					
0.0	0.	0.	0.	0.	0.000	0.000	0.000	
1.0	-94.	-94.	9.	11.	-5.200	1.400	-1.400	
2.0	-108.	-109.	23.	26.	-6.650	-0.150	-1.250	
3.0	-99.	-100.	13.	17.	-5.725	-0.625	-0.625	
4.0	-90.	-88.	3.	5.	-4.650	-0.350	-0.275	
5.0	-69.	-67.	-15.	-13.	-2.700	0.200	-0.475	
6.0	-65.	-64.	-21.	-17.	-2.275	-0.575	0.100	
7.0	-71.	-70.	-11.	-9.	-3.025	-0.125	0.225	
8.0	-81.	-79.	-4.	-1.	-3.875	-0.175	0.400	
9.0	-40.	-35.	-46.	-43.	0.350	0.650	-0.250	
10.0	-28.	-24.	-58.	-55.	1.525	0.225	-0.475	
11.0	-41.	-39.	-40.	-42.	0.050	-0.250	-0.225	
12.0	-57.	-57.	-26.	-23.	-1.625	-1.225	1.000	
13.0	-61.	-59.	-24.	-22.	-1.850	-1.150	2.150	
14.0	-53.	-53.	-20.	-26.	-1.275	-0.875	3.025	
15.0	-44.	-45.	-40.	-36.	-0.325	-0.025	3.050	
16.0	-56.	-57.	-26.	-26.	-1.525	0.075	2.975	

2.1 +30.00

SURFACE DISPLACEMENT= 0.00

DEPTH	ORIGINAL DATA				DEPTH	AVERAGE	DIFFERENCE	DISPLACEMENT
	TOWARDS		AWAY					
0.0	0.	0.	0.	0.	0.0	0.000	0.000	0.000
1.0	-75.	-74.	31.	32.	1.0	-5.300	1.300	-1.300
2.0	-91.	-88.	44.	45.	2.0	-6.700	-0.200	-1.100
3.0	-81.	-79.	34.	37.	3.0	-5.775	-0.675	-0.425
4.0	-71.	-70.	24.	28.	4.0	-4.925	-0.525	0.100
5.0	-45.	-45.	0.	3.	5.0	-2.325	0.575	-0.475
6.0	-47.	-43.	-1.	1.	6.0	-2.250	-0.550	0.075
7.0	-51.	-50.	5.	9.	7.0	-2.875	0.025	0.050
8.0	-45.	-46.	15.	18.	8.0	-3.100	0.600	-0.550
9.0	-20.	-15.	-25.	-22.	9.0	0.300	0.600	-1.150
10.0	-5.	-3.	-39.	-36.	10.0	1.675	0.375	-1.525
11.0	-18.	-18.	-26.	-22.	11.0	0.300	0.000	-1.525
12.0	-36.	-34.	-8.	-4.	12.0	-1.450	-1.050	-0.475
13.0	-41.	-39.	-7.	-1.	13.0	-1.800	-1.100	0.625
14.0	-32.	-33.	-11.	-7.	14.0	-1.175	-0.775	1.400
15.0	-24.	-24.	-20.	-17.	15.0	-0.275	0.025	1.375
16.0	-37.	-33.	-7.	-7.	16.0	-1.400	0.200	1.175

2.1 +36.00

SURFACE DISPLACEMENT= -1.75

DEPTH	ORIGINAL DATA				DEPTH	AVERAGE	DIFFERENCE	DISPLACEMENT
	TOWARDS		AWAY					
0.0	0.	0.	0.	0.	0.0	0.000	0.000	-1.750
1.0	-96.	-97.	16.	16.	1.0	-5.625	0.975	-2.725
2.0	-113.	-110.	29.	32.	2.0	-7.100	-0.600	-2.125
3.0	-102.	-101.	18.	22.	3.0	-6.075	-0.975	-1.150
4.0	-94.	-93.	10.	14.	4.0	-5.275	-0.975	-0.175
5.0	-65.	-63.	-16.	-13.	5.0	-2.475	0.425	-0.600
6.0	-64.	-61.	-21.	-17.	6.0	-2.175	-0.475	-0.125
7.0	-70.	-68.	-12.	-10.	7.0	-2.900	0.000	-0.125
8.0	-80.	-77.	-4.	0.	8.0	-3.825	-0.125	0.000
9.0	-38.	-37.	-43.	-40.	9.0	0.200	0.500	-0.500
10.0	-24.	-22.	-59.	-57.	10.0	1.750	0.450	-0.950
11.0	-39.	-38.	-45.	-41.	11.0	0.225	-0.075	-0.875
12.0	-56.	-55.	-26.	-23.	12.0	-1.550	-1.150	0.275
13.0	-61.	-59.	-24.	-20.	13.0	-1.900	-1.200	1.475
14.0	-56.	-54.	-31.	-29.	14.0	-1.250	-0.850	2.325
15.0	-48.	-44.	-36.	-36.	15.0	-0.500	-0.200	2.525
16.0	-55.	-56.	-26.	-24.	16.0	-1.525	0.075	2.450

2.1 +43.00

SURFACE DISPLACEMENT= -2.25

DEPTH	ORIGINAL DATA				DEPTH	AVERAGE	DIFFERENCE	DISPLACEMENT
	TOWARDS		AWAY					
0.0	0.	0.	0.	0.	0.0	0.000	0.000	-2.250
1.0	-79.	-77.	37.	40.	1.0	-5.825	0.775	-3.025
2.0	-93.	-91.	51.	54.	2.0	-7.225	-0.725	-2.300
3.0	-84.	-81.	42.	46.	3.0	-6.325	-1.225	-1.075
4.0	-75.	-72.	31.	36.	4.0	-5.350	-1.050	-0.025
5.0	-43.	-40.	3.	8.	5.0	-2.350	0.550	-0.575
6.0	-41.	-39.	1.	3.	6.0	-2.100	-0.400	-0.175
7.0	-51.	-47.	9.	12.	7.0	-2.975	-0.075	-0.100
8.0	-60.	-56.	16.	20.	8.0	-3.800	-0.100	0.000
9.0	-19.	-15.	-22.	-19.	9.0	0.175	0.475	-0.475
10.0	-4.	-1.	-37.	-33.	10.0	1.625	0.325	-0.800
11.0	-19.	-16.	-23.	-20.	11.0	0.200	-0.100	-0.700
12.0	-34.	-32.	-6.	-1.	12.0	-1.475	-1.075	0.375
13.0	-40.	-38.	-4.	-1.	13.0	-1.825	-1.125	1.500
14.0	-23.	-32.	-7.	-7.	14.0	-1.275	-0.875	2.375
15.0	-24.	-24.	-15.	-14.	15.0	-0.475	-0.175	2.550
16.0	-36.	-34.	-3.	-4.	16.0	-1.575	0.025	2.525

2.1 +51.00

SURFACE DISPLACEMENT= -3.00

DEPTH	ORIGINAL DATA		DEPTH	AVERAGE	DIFFERENCE	DISPLACEMENT
	TOWARDS	AWAY				
0.0	0.	0.	0.0	0.000	0.000	-3.000
1.0	-89.	29.	1.0	-5.950	0.650	-3.650
2.0	-103.	43.	2.0	-7.375	-0.875	-2.775
3.0	-94.	34.	3.0	-6.375	-1.275	-1.500
4.0	-84.	26.	4.0	-5.475	-1.175	-0.325
5.0	-55.	-4.	5.0	-2.500	0.400	-0.725
6.0	-52.	-9.	6.0	-2.175	-0.475	-0.250
7.0	-61.	1.	7.0	-3.050	-0.150	-0.100
8.0	-67.	8.	8.0	-3.800	-0.100	0.000
9.0	-26.	-29.	9.0	0.200	0.500	-0.500
10.0	-12.	-45.	10.0	1.700	0.400	-0.900
11.0	-25.	-32.	11.0	0.350	0.050	-0.950
12.0	-43.	-15.	12.0	-1.400	-1.000	0.050
13.0	-46.	-12.	13.0	-1.800	-1.100	1.150
14.0	-41.	-18.	14.0	-1.200	-0.800	1.950
15.0	-34.	-24.	15.0	-0.475	-0.175	2.125
16.0	-41.	-12.	16.0	-1.425	0.175	1.950

2.1 +72.00

SURFACE DISPLACEMENT= -5.60

DEPTH	ORIGINAL DATA				DEPTH	AVERAGE	DIFFERENCE	DISPLACEMENT
	TOWARDS		AWAY					
0.0	0.	0.	0.	0.	0.0	0.000	0.000	-5.600
1.0	-102.	-103.	25.	23.	1.0	-6.325	0.275	-5.875
2.0	-113.	-115.	40.	37.	2.0	-7.625	-1.125	-4.750
3.0	-105.	-106.	26.	27.	3.0	-6.600	-1.500	-3.250
4.0	-97.	-96.	17.	20.	4.0	-5.750	-1.450	-1.800
5.0	-70.	-66.	-10.	-6.	5.0	-3.000	-0.100	-1.700
6.0	-66.	-63.	-13.	-11.	6.0	-2.625	-0.925	-0.775
7.0	-74.	-71.	-5.	-2.	7.0	-3.450	-0.550	-0.225
8.0	-79.	-77.	-1.	2.	8.0	-3.925	-0.225	0.000
9.0	-39.	-36.	-37.	-36.	9.0	-0.050	0.250	-0.250
10.0	-23.	-22.	-54.	-53.	10.0	1.550	0.250	-0.500
11.0	-32.	-30.	-46.	-46.	11.0	0.750	0.450	-0.950
12.0	-41.	-40.	-36.	-34.	12.0	-0.275	0.125	-1.075
13.0	-53.	-53.	-26.	-24.	13.0	-1.400	-0.700	-0.375
14.0	-42.	-43.	-34.	-34.	14.0	-0.425	-0.025	-0.350
15.0	-39.	-38.	-39.	-37.	15.0	-0.025	0.275	-0.625
16.0	-39.	-38.	-39.	-37.	16.0	-0.025	1.575	-2.200

2.1 +91.00

SURFACE DISPLACEMENT=-11.95

DEPTH	ORIGINAL DATA				DEPTH	AVERAGE	DIFFERENCE	DISPLACEMENT
	TOWARDS		AWAY					
0.0	0.	0.	0.	0.	0.000	0.000	-11.950	
1.0	-122.	-120.	12.	13.	-6.675	-0.075	-11.875	
2.0	-144.	-144.	37.	37.	-9.050	-2.550	-9.325	
3.0	-116.	-114.	7.	10.	-6.175	-1.075	-8.250	
4.0	-115.	-112.	4.	5.	-5.900	-1.600	-6.650	
5.0	-96.	-92.	-12.	-9.	-4.175	-1.275	-5.375	
6.0	-101.	-98.	-10.	-7.	-4.550	-2.850	-2.525	
7.0	-97.	-95.	-11.	-8.	-4.325	-1.425	-1.100	
8.0	-102.	-100.	-7.	-3.	-4.800	-1.100	0.000	
9.0	-46.	-40.	-63.	-59.	0.900	1.200	-1.200	
10.0	-5.	-1.	-105.	-101.	5.000	3.700	-4.900	
11.0	-29.	-27.	-79.	-75.	2.450	2.150	-7.050	
12.0	-58.	-58.	-49.	-45.	-0.550	-0.150	-6.900	
13.0	-71.	-68.	-41.	-37.	-1.525	-0.825	-6.075	
14.0	-58.	-56.	-51.	-48.	-0.375	0.025	-6.100	
15.0	-55.	-55.	-55.	-52.	-0.075	0.225	-6.325	
16.0	-55.	-55.	-55.	-55.	0.000	1.600	-7.925	

2.1 +107.00

SURFACE DISPLACEMENT=-14.30

DEPTH	ORIGINAL DATA		DEPTH	AVERAGE	DIFFERENCE	DISPLACEMENT
	TOWARDS	AWAY				
0.0	0.	0.	0.0	0.000	0.000	-14.300
1.0	-114.	29.	1.0	-7.150	-0.550	-13.750
2.0	-134.	51.	2.0	-9.325	-2.825	-10.925
3.0	-106.	21.	3.0	-6.475	-1.375	-9.550
4.0	-105.	18.	4.0	-6.225	-1.925	-7.625
5.0	-86.	10.	5.0	-4.825	-1.925	-5.700
6.0	-93.	7.	6.0	-4.925	-3.225	-2.475
7.0	-88.	2.	7.0	-4.500	-1.600	-0.875
8.0	-92.	6.	8.0	-4.925	-1.225	0.350
9.0	-33.	-51.	9.0	0.975	1.275	-0.925
10.0	6.	-90.	10.0	4.775	3.475	-4.400
11.0	-19.	-64.	11.0	2.250	1.950	-6.350
12.0	-48.	-33.	12.0	-0.775	-0.375	-5.975
13.0	-59.	-27.	13.0	-1.675	-0.975	-5.000
14.0	-47.	-38.	14.0	-0.475	-0.075	-4.925
15.0	-43.	-40.	15.0	-0.075	0.225	-5.150

2.1 +119.00

SUPFACE DISPLACEMENT=-15.42

DEPTH	ORIGINAL DATA				DEPTH	AVERAGE	DIFFERENCE	DISPLACEMENT
	TOWARDS		AWAY					
0.0	0.	0.	0.	0.	0.000	0.000	-15.420	
1.0	-99.	-100.	49.	48.	-7.400	-0.800	-14.620	
2.0	-120.	-122.	73.	72.	-9.675	-3.175	-11.445	
3.0	-93.	-93.	43.	44.	-6.825	-1.725	-9.720	
4.0	-88.	-88.	39.	39.	-6.350	-2.050	-7.670	
5.0	-69.	-69.	20.	20.	-4.450	-1.550	-6.120	
6.0	-73.	-73.	23.	24.	-4.825	-3.125	-2.995	
7.0	-68.	-70.	21.	21.	-4.500	-1.600	-1.395	
8.0	-75.	-74.	27.	28.	-5.100	-1.400	0.005	
9.0	-20.	-15.	-30.	-29.	0.600	0.900	-0.895	
10.0	-22.	-22.	-68.	-68.	2.300	1.000	-1.895	
11.0	-3.	-2.	-43.	-45.	2.075	1.775	-3.670	
12.0	-30.	-31.	-16.	-14.	-0.775	-0.375	-3.295	
13.0	-42.	-44.	-7.	-5.	-1.850	-1.150	-2.145	
14.0	-29.	-28.	-18.	-16.	-0.575	-0.175	-1.970	
15.0	-24.	-25.	-21.	-21.	-0.175	0.125	-2.095	

2.1 +132.00

SURFACE DISPLACEMENT=-16.32

DEPTH	ORIGINAL DATA				DEPTH	AVERAGE	DIFFERENCE	DISPLACEMENT
	TOWARDS		AWAY					
0.0	0.	0.	0.	0.	0.0	0.000	0.000	-16.320
1.0	-97.	-99.	53.	56.	1.0	-7.625	-1.025	-15.295
2.0	-118.	-120.	75.	78.	2.0	-9.775	-3.275	-12.020
3.0	-91.	-93.	47.	49.	3.0	-7.000	-1.900	-10.120
4.0	-88.	-87.	41.	45.	4.0	-6.525	-2.225	-7.895
5.0	-67.	-67.	22.	23.	5.0	-4.475	-1.575	-6.320
6.0	-72.	-72.	27.	28.	6.0	-4.975	-3.275	-3.045
7.0	-68.	-67.	22.	23.	7.0	-4.500	-1.600	-1.445
8.0	-73.	-72.	30.	31.	8.0	-5.150	-1.450	0.005
9.0	-11.	-12.	-39.	-38.	9.0	1.350	1.650	-1.645
10.0	23.	26.	-68.	-65.	10.0	4.550	3.250	-4.895
11.0	-2.	-3.	-41.	-40.	11.0	1.900	1.600	-6.495
12.0	-29.	-28.	-13.	-12.	12.0	-0.800	-0.400	-6.095
13.0	-38.	-39.	-6.	-4.	13.0	-1.675	-0.975	-5.120
14.0	-27.	-26.	-16.	-15.	14.0	-0.550	-0.150	-4.970
15.0	-22.	-23.	-20.	-20.	15.0	-0.125	0.175	-5.145

2.1 +149.00

SURFACE DISPLACEMENT=-16.85

DEPTH	ORIGINAL DATA				DEPTH	AVERAGE	DIFFERENCE	DISPLACEMENT
	TOWARDS		AWAY					
0.0	0.	0.	0.	0.	0.0	0.000	0.000	-16.850
1.0	-124.	-122.	31.	31.	1.0	-7.700	-1.100	-15.750
2.0	-143.	-145.	51.	51.	2.0	-9.750	-3.250	-12.500
3.0	-117.	-121.	25.	25.	3.0	-7.200	-2.100	-10.400
4.0	-111.	-113.	18.	21.	4.0	-6.575	-2.275	-8.125
5.0	-91.	-92.	1.	0.	5.0	-4.600	-1.700	-6.425
6.0	-101.	-96.	2.	3.	6.0	-5.050	-3.350	-3.075
7.0	-90.	-92.	0.	0.	7.0	-4.550	-1.650	-1.425
8.0	-97.	-98.	4.	6.	8.0	-5.125	-1.425	0.000
9.0	-39.	-39.	-50.	-52.	9.0	0.600	0.900	-0.900
10.0	0.	-1.	-90.	-89.	10.0	4.450	3.150	-4.050
11.0	-25.	-25.	-67.	-65.	11.0	2.050	1.750	-5.800
12.0	-53.	-53.	-38.	-37.	12.0	-0.775	-0.375	-5.425
13.0	-61.	-63.	-30.	-28.	13.0	-1.650	-0.950	-4.475
14.0	-50.	-51.	-39.	-38.	14.0	-0.600	-0.200	-4.275
15.0	-45.	-46.	-45.	-45.	15.0	-0.025	0.275	-4.550

2.1 +176.00

SURFACE DISPLACEMENT=-16.00

DEPTH	ORIGINAL DATA				DEPTH	AVERAGE	DIFFERENCE	DISPLACEMENT
	TOWARDS		AWAY					
0.0	0.	0.	0.	0.	0.000	0.000	-16.000	
1.0	-128.	-128.	38.	37.	-8.275	-1.675	-14.325	
2.0	-142.	-143.	49.	47.	-9.525	-3.025	-11.300	
3.0	-108.	-110.	18.	17.	-6.325	-1.225	-10.075	
4.0	-60.	-61.	-28.	-30.	-1.575	2.725	-12.800	
5.0	-32.	-35.	-54.	-57.	1.100	4.000	-16.800	
6.0	-82.	-84.	-4.	-8.	-3.850	-2.150	-14.650	
7.0	-63.	-66.	-23.	-25.	-2.025	0.875	-15.525	
8.0	-79.	-80.	-15.	-11.	-3.325	0.375	-15.900	
9.0	-53.	-56.	-30.	-31.	-1.200	-0.900	-15.000	
10.0	-27.	-29.	-58.	-57.	1.475	0.175	-15.175	
11.0	-59.	-55.	-34.	-30.	-1.250	-1.550	-13.625	
12.0	-75.	-77.	-10.	-10.	-3.300	-2.900	-10.725	
13.0	-80.	-80.	-9.	-9.	-3.550	-2.850	-7.875	

2.1 +224.00

SURFACE DISPLACEMENT=-18.00

DEPTH	ORIGINAL DATA				DEPTH	AVERAGE	DIFFERENCE	DISPLACEMENT
	TOWARDS		AWAY					
0.0	0.	0.	0.	0.	0.0	0.000	0.000	-18.000
1.0	-136.	-137.	36.	33.	1.0	-8.550	-1.950	-16.050
2.0	-140.	-149.	50.	49.	2.0	-9.925	-3.425	-12.625
3.0	-116.	-116.	15.	15.	3.0	-6.575	-1.475	-11.150
4.0	-68.	-70.	-30.	-31.	4.0	-1.925	2.375	-13.525
5.0	-41.	-43.	-55.	-58.	5.0	0.725	3.625	-17.150
6.0	-89.	-90.	-9.	-13.	6.0	-3.925	-2.225	-14.925
7.0	-71.	-74.	-26.	-26.	7.0	-2.325	0.575	-15.500
8.0	-87.	-89.	-10.	-8.	8.0	-3.950	-0.250	-15.250
9.0	-62.	-63.	-32.	-34.	9.0	-1.475	-1.175	-14.075
10.0	-36.	-35.	-61.	-62.	10.0	1.275	-0.025	-14.050
11.0	-61.	-61.	-35.	-35.	11.0	-1.300	-1.600	-12.450
12.0	-80.	-80.	-13.	-18.	12.0	-3.225	-2.825	-9.625
13.0	-85.	-85.	-15.	-12.	13.0	-3.575	-2.875	-6.750

3.1 -19.00

SURFACE DISPLACEMENT= 0.00

DEPTH	ORIGINAL DATA				DEPTH	AVERAGE	DIFFERENCE	DISPLACEMENT'
	TOWARDS		AWAY					
0.0	0.	0.	0.	0.	0.0	0.000	0.000	0.000
1.0	664.	664.	874.	872.	1.0	-10.450	-0.150	0.150
2.0	725.	725.	814.	814.	2.0	-4.450	-0.150	0.300
3.0	738.	738.	802.	801.	3.0	-3.175	-0.075	0.375
4.0	745.	745.	793.	793.	4.0	-2.400	0.000	0.375
5.0	752.	753.	788.	788.	5.0	-1.775	0.025	0.350
6.0	764.	764.	775.	774.	6.0	-0.525	-0.025	0.375
7.0	774.	772.	758.	767.	7.0	0.275	-0.125	0.500
8.0	767.	767.	774.	774.	8.0	-0.350	0.050	0.450
9.0	774.	774.	767.	768.	9.0	0.325	-0.175	0.625
10.0	784.	786.	760.	761.	10.0	1.225	-0.075	0.700
11.0	771.	771.	770.	770.	11.0	0.050	-0.050	0.750
12.0	737.	768.	754.	754.	12.0	1.675	-0.125	0.875
13.0	782.	782.	758.	758.	13.0	1.200	0.000	0.875
14.0	739.	740.	800.	800.	14.0	-3.025	-0.025	0.900
15.0	755.	757.	788.	788.	15.0	-1.600	-0.100	1.000

3.1 -10.00

SURFACE DISPLACEMENT= 0.00

DEPTH	ORIGINAL DATA				DEPTH	AVERAGE	DIFFERENCE	DISPLACEMENT
	TOWARDS		AWAY					
0.0	0.	0.	0.	0.	0.000	0.000	0.000	
1.0	696.	679.	880.	880.	-9.625	0.675	-0.675	
2.0	737.	739.	820.	820.	-4.100	0.200	-0.875	
3.0	751.	753.	808.	808.	-2.800	0.300	-1.175	
4.0	758.	760.	799.	799.	-2.000	0.400	-1.575	
5.0	765.	767.	794.	794.	-1.400	0.400	-1.975	
6.0	778.	778.	781.	781.	-0.150	0.350	-2.325	
7.0	786.	788.	774.	774.	0.650	0.250	-2.575	
8.0	779.	781.	781.	781.	-0.050	0.350	-2.925	
9.0	788.	789.	772.	772.	0.825	0.325	-3.250	
10.0	798.	800.	766.	765.	1.675	0.375	-3.625	
11.0	784.	786.	776.	775.	0.475	0.375	-4.000	
12.0	801.	802.	760.	759.	2.100	0.300	-4.300	
13.0	795.	797.	766.	764.	1.550	0.350	-4.650	
14.0	753.	754.	808.	808.	-2.725	0.275	-4.925	
15.0	769.	769.	796.	793.	-1.275	0.225	-5.150	

3.1 -5.00

SURFACE DISPLACEMENT= 0.50

DEPTH	ORIGINAL DATA				DEPTH	AVERAGE	DIFFERENCE	DISPLACEMENT
	TOWARDS		AWAY					
0.0	0.	0.	0.	0.	0.0	0.000	0.000	0.500
1.0	664.	666.	868.	868.	1.0	-10.150	0.150	0.350
2.0	723.	725.	810.	810.	2.0	-4.300	0.000	0.350
3.0	738.	738.	798.	798.	3.0	-3.000	0.100	0.250
4.0	744.	744.	789.	789.	4.0	-2.250	0.150	0.100
5.0	751.	750.	784.	784.	5.0	-1.725	0.075	0.025
6.0	762.	762.	772.	770.	6.0	-0.450	0.050	-0.025
7.0	772.	772.	764.	764.	7.0	0.400	0.000	-0.025
8.0	765.	765.	772.	772.	8.0	-0.350	0.050	-0.075
9.0	772.	774.	762.	762.	9.0	0.550	0.050	-0.125
10.0	783.	783.	755.	757.	10.0	1.350	0.050	-0.175
11.0	768.	770.	765.	765.	11.0	0.200	0.100	-0.275
12.0	786.	786.	750.	750.	12.0	1.800	0.000	-0.275
13.0	780.	776.	755.	755.	13.0	1.150	-0.050	-0.225
14.0	738.	741.	797.	797.	14.0	-2.875	0.125	-0.350
15.0	753.	753.	784.	784.	15.0	-1.550	-0.050	-0.300

3.1 -1.00

SURFACE DISPLACEMENT= 1.30

DEPTH	ORIGINAL DATA				DEPTH	AVERAGE	DIFFERENCE	DISPLACEMENT
	TOWARDS		AWAY					
0.0	0.	0.	0.	0.	0.000	0.000	1.300	
1.0	649.	645.	846.	846.	-9.950	0.350	0.950	
2.0	702.	702.	790.	792.	-4.450	-0.150	1.100	
3.0	718.	720.	774.	776.	-2.900	0.300	0.800	
4.0	728.	730.	764.	764.	-1.750	0.650	0.150	
5.0	733.	732.	763.	764.	-1.550	0.250	-0.100	
6.0	742.	742.	753.	753.	-0.550	-0.050	-0.050	
7.0	750.	750.	745.	745.	0.250	-0.150	0.100	
8.0	746.	746.	750.	753.	-0.275	0.125	-0.025	
9.0	752.	753.	743.	744.	0.450	-0.050	0.025	
10.0	762.	763.	736.	738.	1.275	-0.025	0.050	
11.0	750.	750.	746.	748.	0.150	0.050	0.000	
12.0	766.	766.	729.	730.	1.825	0.025	-0.025	
13.0	760.	760.	736.	736.	1.200	0.000	-0.025	
14.0	718.	719.	776.	780.	-2.975	0.025	-0.050	
15.0	734.	734.	768.	768.	-1.700	-0.200	0.150	

3.1 +1.00

SURFACE DISPLACEMENT= 1.25

DEPTH	ORIGINAL DATA				DEPTH	AVERAGE	DIFFERENCE	DISPLACEMENT
	TOWARDS		AWAY					
0.0	0.	0.	0.	0.	0.0	0.000	0.000	1.250
1.0	614.	612.	812.	816.	1.0	-10.050	0.250	1.000
2.0	666.	665.	760.	763.	2.0	-4.800	-0.500	1.500
3.0	690.	688.	738.	740.	3.0	-2.500	0.600	0.900
4.0	701.	698.	726.	729.	4.0	-1.400	1.000	-0.100
5.0	699.	697.	729.	730.	5.0	-1.575	0.225	-0.325
6.0	707.	705.	722.	723.	6.0	-0.825	-0.325	0.000
7.0	716.	715.	711.	711.	7.0	0.225	-0.175	0.175
8.0	716.	712.	715.	716.	8.0	-0.075	0.325	-0.150
9.0	724.	720.	708.	708.	9.0	0.700	0.200	-0.350
10.0	735.	732.	701.	701.	10.0	1.625	0.325	-0.675
11.0	723.	719.	710.	712.	11.0	0.500	0.400	-1.075
12.0	738.	736.	692.	694.	12.0	2.200	0.400	-1.475
13.0	727.	728.	701.	702.	13.0	1.300	0.100	-1.575
14.0	684.	682.	744.	748.	14.0	-3.150	-0.150	-1.425
15.0	700.	701.	728.	728.	15.0	-1.375	0.125	-1.550

3.1 +6.00

SURFACE DISPLACEMENT= -1.45

DEPTH	ORIGINAL DATA				DEPTH	AVERAGE	DIFFERENCE	DISPLACEMENT
	TOWARDS		AWAY					
0.0	0.	0.	0.	0.	0.0	0.000	0.000	-1.450
1.0	-103.	-102.	103.	106.	1.0	-10.350	-0.050	-1.400
2.0	-81.	-80.	32.	35.	2.0	-5.700	-1.400	0.000
3.0	-44.	-42.	-5.	-2.	3.0	-1.975	1.125	-1.125
4.0	-30.	-26.	-21.	-17.	4.0	-0.450	1.950	-3.075
5.0	-35.	-31.	-14.	-11.	5.0	-1.025	0.775	-3.850
6.0	-24.	-21.	-23.	-21.	6.0	-0.025	0.475	-4.325
7.0	-16.	-12.	-33.	-30.	7.0	0.875	0.475	-4.800
8.0	-20.	-17.	-30.	-28.	8.0	0.525	0.925	-5.725
9.0	-13.	-11.	-36.	-34.	9.0	1.150	0.650	-6.375
10.0	-7.	-5.	-39.	-36.	10.0	1.575	0.275	-6.650
11.0	-21.	-19.	-29.	-25.	11.0	0.350	0.250	-6.900
12.0	-9.	-7.	-40.	-38.	12.0	1.550	-0.250	-6.650
13.0	-35.	-35.	-15.	-14.	13.0	-1.025	-2.225	-4.425
14.0	-60.	-59.	12.	13.	14.0	-3.600	-0.600	-3.825

3.1 +13.00

SURFACE DISPLACEMENT= -2.37

DEPTH	ORIGINAL DATA				DEPTH	AVERAGE	DIFFERENCE	DISPLACEMENT
	TOWARDS		AWAY					
0.0	0.	0.	0.	0.	0.000	0.000	-2.370	
1.0	-119.	-119.	97.	103.	-10.950	-0.650	-1.720	
2.0	-99.	-84.	28.	30.	-6.025	-1.725	0.005	
3.0	-61.	-58.	-11.	-8.	-2.500	0.600	-0.595	
4.0	-45.	-42.	-25.	-23.	-0.975	1.425	-2.020	
5.0	-47.	-44.	-22.	-18.	-1.275	0.525	-2.545	
6.0	-37.	-34.	-33.	-31.	-0.175	0.325	-2.870	
7.0	-25.	-22.	-46.	-41.	1.000	0.600	-3.470	
8.0	-30.	-27.	-42.	-39.	0.600	1.000	-4.470	
9.0	-23.	-20.	-48.	-44.	1.225	0.725	-5.195	
10.0	-17.	-16.	-50.	-47.	1.600	0.300	-5.495	
11.0	-33.	-31.	-38.	-37.	0.275	0.175	-5.670	
12.0	-19.	-18.	-50.	-49.	1.550	-0.250	-5.420	
13.0	-47.	-46.	-24.	-23.	-1.150	-2.350	-3.070	
14.0	-72.	-71.	2.	2.	-3.675	-0.675	-2.395	

3.1 +23.00

SURFACE DISPLACEMENT= -2.75

DEPTH	ORIGINAL DATA				DEPTH	AVERAGE	DIFFERENCE	DISPLACEMENT
	TOWARDS		AWAY					
0.0	0.	0.	0.	0.	0.0	0.000	0.000	-2.750
1.0	-148.	-147.	76.	66.	1.0	-10.975	-0.675	-2.075
2.0	-102.	-99.	27.	27.	2.0	-6.375	-2.075	0.000
3.0	-64.	-62.	-8.	-8.	3.0	-2.750	0.350	-0.350
4.0	-49.	-45.	-28.	-27.	4.0	-0.975	1.425	-1.775
5.0	-48.	-46.	-24.	-24.	5.0	-1.150	0.650	-2.425
6.0	-40.	-38.	-33.	-34.	6.0	-0.275	0.225	-2.650
7.0	-27.	-25.	-47.	-45.	7.0	1.000	0.600	-3.250
8.0	-31.	-28.	-43.	-43.	8.0	0.675	1.075	-4.325
9.0	-26.	-22.	-49.	-49.	9.0	1.250	0.750	-5.075
10.0	-20.	-16.	-52.	-52.	10.0	1.700	0.400	-5.475
11.0	-37.	-32.	-41.	-39.	11.0	0.275	0.175	-5.650
12.0	-19.	-19.	-53.	-52.	12.0	1.675	-0.125	-5.525
13.0	-46.	-49.	-27.	-26.	13.0	-1.050	-2.250	-3.275
14.0	-74.	-75.	-2.	0.	14.0	-3.675	-0.675	-2.600

3.1 +30.00

SURFACE DISPLACEMENT= -1.65

DEPTH	ORIGINAL DATA				DEPTH	AVERAGE	DIFFERENCE	DISPLACEMENT
	TOWARDS		AWAY					
0.0	0.	0.	0.	0.	0.000	0.000	-1.650	
1.0	-137.	-135.	89.	91.	-11.300	-1.000	-0.650	
2.0	-86.	-86.	9.	8.	-4.725	-0.425	-0.225	
3.0	-54.	-51.	-7.	-8.	-2.250	0.850	-1.075	
4.0	-52.	-52.	-13.	-9.	-2.050	0.350	-1.425	
5.0	-31.	-31.	-12.	-12.	-0.950	0.850	-2.275	
6.0	-28.	-32.	-19.	-19.	-0.550	-0.050	-2.225	
7.0	-13.	-10.	-33.	-32.	1.050	0.650	-2.875	
8.0	-17.	-14.	-31.	-30.	0.750	1.150	-4.025	
9.0	-11.	-8.	-37.	-37.	1.375	0.875	-4.900	
10.0	-4.	-2.	-41.	-39.	1.850	0.550	-5.450	
11.0	-20.	-18.	-28.	-26.	0.400	0.300	-5.750	
12.0	-7.	-6.	-38.	-38.	1.575	-0.225	-5.525	
13.0	-35.	-35.	-14.	-12.	-1.100	-2.300	-3.225	
14.0	-59.	-59.	11.	12.	-3.525	-0.525	-2.700	

3.1 +36.00

SURFACE DISPLACEMENT= -4.05

DEPTH	ORIGINAL DATA				DEPTH	AVERAGE	DIFFERENCE	DISPLACEMENT
	TOWARDS		AWAY					
0.0	0.	0.	0.	0.	0.000	0.000	-4.050	
1.0	-154.	-152.	80.	80.	-11.650	-1.350	-2.700	
2.0	-104.	-104.	25.	31.	-6.600	-2.300	-0.400	
3.0	-72.	-71.	-3.	0.	-3.500	-0.400	0.000	
4.0	-72.	-70.	-48.	-53.	-1.025	1.375	-1.375	
5.0	-47.	-43.	-27.	-25.	-0.950	0.850	-2.225	
6.0	-39.	-35.	-40.	-35.	0.025	0.525	-2.750	
7.0	-31.	-27.	-45.	-47.	0.850	0.450	-3.200	
8.0	-32.	-29.	-46.	-43.	0.700	1.100	-4.300	
9.0	-25.	-23.	-52.	-48.	1.300	0.800	-5.100	
10.0	-19.	-15.	-56.	-53.	1.875	0.575	-5.675	
11.0	-36.	-33.	-42.	-39.	0.300	0.200	-5.875	
12.0	-21.	-21.	-53.	-50.	1.525	-0.275	-5.600	
13.0	-51.	-47.	-28.	-25.	-1.125	-2.325	-3.275	
14.0	-74.	-73.	1.	0.	-3.700	-0.700	-2.575	

3.1 +43.00

SURFACE DISPLACEMENT= -5.10

DEPTH	ORIGINAL DATA				DEPTH	AVERAGE	DIFFERENCE	DISPLACEMENT
	TOWARDS		AWAY					
0.0	0.	0.	0.	0.	0.000	0.000	-5.100	
1.0	-114.	-114.	128.	132.	-12.200	-1.900	-3.200	
2.0	-86.	-85.	49.	53.	-6.825	-2.525	-0.675	
3.0	-55.	-53.	20.	23.	-3.775	-0.675	0.000	
4.0	-30.	-30.	-3.	0.	-1.425	0.975	-0.975	
5.0	-23.	-23.	-7.	-4.	-0.875	0.925	-1.900	
6.0	-16.	-15.	-17.	-15.	0.025	0.525	-2.425	
7.0	-9.	-5.	-27.	-24.	0.925	0.525	-2.950	
8.0	-13.	-9.	-24.	-22.	0.600	1.000	-3.950	
9.0	-8.	-4.	-29.	-27.	1.100	0.600	-4.550	
10.0	-1.	2.	-35.	-31.	1.675	0.375	-4.925	
11.0	-18.	-14.	-20.	-18.	0.150	0.050	-4.975	
12.0	-3.	0.	-33.	-29.	1.475	-0.325	-4.650	
13.0	-33.	-32.	-7.	-5.	-1.325	-2.525	-2.125	
14.0	-56.	-56.	18.	18.	-3.700	-0.700	-1.425	

3.1 +51.00

SURFACE DISPLACEMENT= -5.05

DEPTH	ORIGINAL DATA				DEPTH	AVERAGE	DIFFERENCE	DISPLACEMENT
	TOWARDS		AWAY					
0.0	0.	0.	0.	0.	0.000	0.000	-5.050	
1.0	-146.	-148.	92.	93.	-11.975	-1.675	-3.375	
2.0	-95.	-96.	39.	40.	-6.750	-2.450	-0.925	
3.0	-66.	-65.	11.	13.	-3.875	-0.775	-0.150	
4.0	-63.	-61.	-12.	-10.	-2.550	-0.150	0.000	
5.0	-39.	-33.	-18.	-16.	-0.950	0.850	-0.850	
6.0	-28.	-30.	-27.	-26.	-0.125	0.375	-1.225	
7.0	-21.	-16.	-36.	-34.	0.825	0.425	-1.650	
8.0	-22.	-18.	-35.	-33.	0.700	1.100	-2.750	
9.0	-15.	-12.	-40.	-40.	1.325	0.825	-3.575	
10.0	-7.	-5.	-45.	-41.	1.850	0.550	-4.125	
11.0	-24.	-21.	-32.	-29.	0.400	0.300	-4.425	
12.0	-13.	-10.	-44.	-43.	1.600	-0.200	-4.225	
13.0	-39.	-38.	-17.	-15.	-1.125	-2.325	-1.900	
14.0	-62.	-60.	7.	8.	-3.425	-0.425	-1.475	

3.1 +72.00

SURFACE DISPLACEMENT= -5.75

DEPTH	ORIGINAL DATA				DEPTH	AVERAGE	DIFFERENCE	DISPLACEMENT
	TOWARDS		AWAY					
0.0	0.	0.	0.	0.	0.0	0.000	0.000	-5.750
1.0	-160.	-157.	85.	87.	1.0	-12.225	-1.925	-3.825
2.0	-106.	-107.	34.	33.	2.0	-7.000	-2.700	-1.125
3.0	-78.	-79.	6.	6.	3.0	-4.225	-1.125	0.000
4.0	-57.	-62.	-18.	-16.	4.0	-2.125	0.275	-0.275
5.0	-51.	-49.	-22.	-27.	5.0	-1.275	0.525	-0.800
6.0	-44.	-42.	-30.	-29.	6.0	-0.675	-0.175	-0.625
7.0	-35.	-32.	-39.	-39.	7.0	0.275	-0.125	-0.500
8.0	-36.	-34.	-38.	-38.	8.0	0.150	0.550	-1.050
9.0	-30.	-27.	-44.	-44.	9.0	0.775	0.275	-1.325
10.0	-19.	-15.	-53.	-52.	10.0	1.775	0.475	-1.800
11.0	-29.	-27.	-45.	-45.	11.0	0.850	0.750	-2.550

3.1 +91.00

SURFACE DISPLACEMENT= -9.97

DEPTH	ORIGINAL DATA				DEPTH	AVERAGE	DIFFERENCE	DISPLACEMENT
	TOWARDS		AWAY					
0.0	0.	0.	0.	0.	0.000	0.000	-9.970	
1.0	-183.	-182.	74.	75.	-12.850	-2.550	-7.420	
2.0	-130.	-130.	25.	25.	-7.750	-3.450	-3.970	
3.0	-123.	-121.	20.	19.	-7.075	-3.975	0.005	
4.0	-100.	-98.	-54.	-55.	-2.225	0.175	-0.170	
5.0	-33.	-31.	-70.	-70.	1.900	3.700	-3.870	
6.0	-27.	-25.	-78.	-77.	2.575	3.075	-6.945	
7.0	-43.	-41.	-61.	-60.	0.925	0.525	-7.470	
8.0	-57.	-55.	-48.	-47.	-0.425	-0.025	-7.445	
9.0	-60.	-58.	-44.	-42.	-0.800	-1.300	-6.145	
10.0	-55.	-54.	-46.	-46.	-0.425	-1.725	-4.420	
11.0	-36.	-36.	-67.	-66.	1.525	1.425	-5.845	

3.1 +107.00

SURFACE DISPLACEMENT=-11.40

DEPTH	ORIGINAL DATA				DEPTH	AVERAGE	DIFFERENCE	DISPLACEMENT
	TOWARDS		AWAY					
0.0	0.	0.	0.	0.	0.0	0.000	0.000	-11.400
1.0	-173.	-176.	92.	91.	1.0	-13.300	-3.000	-8.400
2.0	-121.	-123.	40.	38.	2.0	-8.050	-3.750	-4.650
3.0	-115.	-115.	36.	33.	3.0	-7.475	-4.375	-0.275
4.0	-68.	-69.	-15.	-15.	4.0	-2.675	-0.275	0.000
5.0	-20.	-21.	-58.	-60.	5.0	1.925	3.725	-3.725
6.0	-16.	-17.	-64.	-66.	6.0	2.425	2.925	-6.650
7.0	-32.	-32.	-48.	-50.	7.0	0.850	0.450	-7.100
8.0	-46.	-47.	-32.	-34.	8.0	-0.675	-0.275	-6.825
9.0	-50.	-51.	-29.	-31.	9.0	-1.025	-1.525	-5.300
10.0	-42.	-44.	-33.	-36.	10.0	-0.425	-1.725	-3.575
11.0	-26.	-27.	-53.	-53.	11.0	1.325	1.225	-4.800

3.1 +11^o.00

SURFACE DISPLACEMENT=-12.25

DEPTH	ORIGINAL DATA				DEPTH	AVERAGE	DIFFERENCE	DISPLACEMENT
	TOWARDS		AWAY					
0.0	0.	0.	0.	0.	0.0	0.000	0.000	-12.250
1.0	-165.	-164.	113.	114.	1.0	-13.900	-3.600	-8.650
2.0	-104.	-104.	59.	57.	2.0	-8.100	-3.800	-4.850
3.0	-100.	-100.	55.	55.	3.0	-7.750	-4.650	-0.200
4.0	-72.	-72.	-19.	-21.	4.0	-2.600	-0.200	0.000
5.0	-3.	-2.	-42.	-45.	5.0	2.050	3.850	-3.850
6.0	2.	1.	-45.	-45.	6.0	2.325	2.825	-6.675
7.0	-14.	-14.	-29.	-29.	7.0	0.750	0.350	-7.025
8.0	-30.	-29.	-13.	-13.	8.0	-0.825	-0.425	-6.600
9.0	-34.	-32.	-10.	-9.	9.0	-1.175	-1.675	-4.925
10.0	-26.	-25.	-12.	-13.	10.0	-0.650	-1.950	-2.975
11.0	-9.	-9.	-34.	-34.	11.0	1.250	1.150	-4.125

3.1 +132.00

SURFACE DISPLACEMENT=-12.57

DEPTH	ORIGINAL DATA				DEPTH	AVERAGE	DIFFERENCE	DISPLACEMENT
	TOWARDS		AWAY					
0.0	0.	0.	0.	0.	0.000	0.000	-12.570	
1.0	-158.	-161.	115.	114.	-13.700	-3.400	-9.170	
2.0	-106.	-106.	61.	61.	-8.350	-4.050	-5.120	
3.0	-99.	-101.	59.	62.	-8.000	-4.900	-0.220	
4.0	-46.	-49.	4.	6.	-2.625	-0.225	0.005	
5.0	-2.	-2.	-39.	-40.	1.875	3.675	-3.670	
6.0	1.	2.	-44.	-45.	2.300	2.800	-6.470	
7.0	-15.	-13.	-28.	-29.	0.725	0.325	-6.795	
8.0	-29.	-29.	-13.	-13.	-0.800	-0.400	-6.395	
9.0	-31.	-33.	-11.	-11.	-1.050	-1.550	-4.845	
10.0	-24.	-22.	-16.	-15.	-0.375	-1.675	-3.170	
11.0	-8.	-8.	-33.	-32.	1.225	1.125	-4.295	

3.1 +149.00

SURFACE DISPLACEMENT=-13.70

DEPTH	ORIGINAL DATA				DEPTH	AVERAGE	DIFFERENCE	DISPLACEMENT
	TOWARDS		AWAY					
0.0	0.	0.	0.	0.	0.000	0.000	-13.700	
1.0	-164.	-166.	120.	123.	-14.325	-4.025	-9.675	
2.0	-129.	-129.	37.	35.	-8.250	-3.950	-5.725	
3.0	-127.	-129.	35.	34.	-8.125	-5.025	-0.700	
4.0	-78.	-78.	-14.	-18.	-3.100	-0.700	0.000	
5.0	-26.	-26.	-64.	-66.	1.950	3.750	-3.750	
6.0	-22.	-23.	-67.	-68.	2.250	2.750	-6.500	
7.0	-38.	-39.	-52.	-54.	0.725	0.325	-6.825	
8.0	-54.	-55.	-35.	-37.	-0.925	-0.525	-6.300	
9.0	-59.	-58.	-32.	-33.	-1.300	-1.800	-4.500	
10.0	-49.	-49.	-39.	-39.	-0.500	-1.800	-2.700	
11.0	-33.	-33.	-58.	-58.	1.250	1.150	-3.850	

3.1 +176.00

SURFACE DISPLACEMENT=-13.20

DEPTH	ORIGINAL DATA				DEPTH	AVERAGE	DIFFERENCE	DISPLACEMENT
	TOWARDS		AWAY					
0.0	0.	0.	0.	0.	0.000	0.000	-13.200	
1.0	-188.	-187.	137.	137.	-16.225	-5.925	-7.275	
2.0	-128.	-129.	38.	38.	-8.325	-4.025	-3.250	
3.0	-106.	-111.	19.	18.	-6.350	-3.250	0.000	
4.0	-62.	-65.	-62.	-62.	-0.075	2.325	-2.325	
5.0	-31.	-31.	-115.	-119.	4.300	6.100	-8.425	
6.0	-22.	-25.	-62.	-65.	2.000	2.500	-10.925	
7.0	-43.	-46.	-40.	-43.	-0.150	-0.550	-10.375	
8.0	-56.	-58.	-28.	-30.	-1.400	-1.000	-9.375	
9.0	-63.	-64.	-20.	-22.	-2.125	-2.625	-6.750	
10.0	-65.	-65.	-7.	-8.	-2.875	-4.175	-2.575	
11.0	-62.	-62.	-25.	-25.	-1.850	-1.950	-0.625	

3.1 +224.00

SURFACE DISPLACEMENT=-13.20

DEPTH	ORIGINAL DATA				DEPTH	AVERAGE	DIFFERENCE	DISPLACEMENT
	TOWARDS		AWAY					
0.0	0.	0.	0.	0.	0.000	0.000	-13.200	
1.0	-188.	-184.	135.	138.	-16.125	-5.825	-7.375	
2.0	-129.	-127.	38.	36.	-8.250	-3.950	-3.425	
3.0	-105.	-109.	19.	18.	-6.275	-3.175	-0.250	
4.0	-63.	-64.	-64.	-60.	-0.075	2.325	-2.575	
5.0	-33.	-29.	-114.	-115.	4.175	5.975	-8.550	
6.0	-22.	-23.	-64.	-64.	2.075	2.575	-11.125	
7.0	-44.	-45.	-42.	-42.	-0.125	-0.525	-10.600	
8.0	-52.	-57.	-28.	-27.	-1.350	-0.950	-9.650	
9.0	-63.	-63.	-21.	-24.	-2.025	-2.525	-7.125	
10.0	-67.	-67.	-8.	-8.	-2.950	-4.250	-2.875	
11.0	-63.	-62.	-24.	-26.	-1.875	-1.975	-0.900	

4.1 +6.00

SURFACE DISPLACEMENT= 0.00

DEPTH	ORIGINAL DATA				DEPTH	AVERAGE	DIFFERENCE	DISPLACEMENT
	TOWARDS		AWAY					
0.0	0.	0.	0.	0.	0.000	0.000	0.000	
1.0	27.	31.	-77.	-77.	5.300	0.000	0.000	
2.0	-38.	-34.	-10.	-9.	-1.325	-0.125	0.125	
3.0	-92.	-70.	43.	48.	-6.325	0.375	-0.250	
4.0	-167.	-167.	121.	118.	-14.325	-0.225	-0.025	
5.0	-159.	-155.	115.	117.	-13.650	0.050	-0.075	
6.0	-122.	-118.	74.	78.	-9.800	0.200	-0.275	
7.0	-56.	-55.	6.	7.	-3.100	0.100	-0.375	
8.0	-46.	-45.	0.	1.	-2.300	-0.100	-0.275	
9.0	-49.	-47.	-2.	1.	-2.375	0.125	-0.400	
10.0	-98.	-96.	47.	50.	-7.275	-0.075	-0.325	
11.0	-114.	-112.	62.	65.	-8.825	-0.025	-0.300	
12.0	-132.	-132.	84.	86.	-10.850	-0.050	-0.250	
13.0	-172.	-171.	123.	125.	-14.775	0.025	-0.275	
14.0	-174.	-175.	123.	126.	-14.950	-0.050	-0.225	

4.1 +13.00

SURFACE DISPLACEMENT= -2.20

DEPTH	ORIGINAL DATA				DEPTH	AVERAGE	DIFFERENCE	DISPLACEMENT
	TOWARDS		AWAY					
0.0	0.	0.	0.	0.	0.000	0.000	-2.200	
1.0	12.	12.	-81.	-80.	4.625	-0.675	-1.525	
2.0	-53.	-52.	-18.	-17.	-1.750	-0.550	-0.975	
3.0	-106.	-105.	37.	38.	-7.150	-0.450	-0.525	
4.0	-187.	-183.	111.	111.	-14.800	-0.700	0.175	
5.0	-170.	-168.	103.	102.	-13.575	0.125	0.050	
6.0	-129.	-128.	66.	66.	-9.725	0.275	-0.225	
7.0	-69.	-66.	-3.	-1.	-3.275	-0.075	-0.150	
8.0	-58.	-56.	-10.	-9.	-2.375	-0.175	0.025	
9.0	-61.	-59.	-10.	-10.	-2.500	0.000	0.025	
10.0	-107.	-107.	38.	38.	-7.250	-0.050	0.075	
11.0	-123.	-121.	52.	53.	-8.725	0.075	0.000	
12.0	-140.	-140.	72.	74.	-10.650	0.150	-0.150	
13.0	-182.	-184.	113.	115.	-14.850	-0.050	-0.100	
14.0	-185.	-186.	114.	115.	-15.000	-0.100	0.000	

4.1 +23.00

SURFACE DISPLACEMENT= -2.60

DEPTH	ORIGINAL DATA				DEPTH	AVERAGE	DIFFERENCE	DISPLACEMENT
	TOWARDS		AWAY					
0.0	0.	0.	0.	0.	0.000	0.000	-2.600	
1.0	9.	10.	-80.	-77.	4.400	-0.900	-1.700	
2.0	-54.	-54.	-15.	-13.	-2.000	-0.800	-0.900	
3.0	-108.	-106.	39.	44.	-7.425	-0.725	-0.175	
4.0	-179.	-178.	112.	115.	-14.600	-0.500	0.325	
5.0	-166.	-166.	103.	102.	-13.425	0.275	0.050	
6.0	-128.	-128.	65.	64.	-9.625	0.375	-0.325	
7.0	-66.	-64.	-2.	-1.	-3.175	0.025	-0.350	
8.0	-57.	-56.	-10.	-8.	-2.375	-0.175	-0.175	
9.0	-58.	-59.	-8.	-8.	-2.525	-0.025	-0.150	
10.0	-108.	-107.	37.	39.	-7.275	-0.075	-0.075	
11.0	-123.	-122.	52.	54.	-8.775	0.025	-0.100	
12.0	-139.	-141.	73.	74.	-10.675	0.125	-0.225	
13.0	-184.	-184.	113.	115.	-14.900	-0.100	-0.125	
14.0	-184.	-185.	115.	117.	-15.025	-0.125	0.000	

4.1 +36.00

SURFACE DISPLACEMENT= -4.40

DEPTH	ORIGINAL DATA				DEPTH	AVERAGE	DIFFERENCE	DISPLACEMENT
	TOWARDS		AWAY					
0.0	0.	0.	0.	0.	0.000	0.000	-4.400	
1.0	8.	9.	-77.	-76.	4.250	-1.050	-3.350	
2.0	-59.	-58.	-9.	-9.	-2.475	-1.275	-2.075	
3.0	-109.	-109.	43.	46.	-7.675	-0.975	-1.100	
4.0	-190.	-185.	115.	119.	-15.225	-1.125	0.025	
5.0	-169.	-167.	101.	104.	-13.525	0.175	-0.150	
6.0	-127.	-124.	60.	65.	-9.400	0.600	-0.750	
7.0	-64.	-64.	-14.	-4.	-2.750	0.450	-1.200	
8.0	-65.	-68.	-10.	-9.	-2.850	-0.650	-0.550	
9.0	-62.	-60.	-7.	-9.	-2.650	-0.150	-0.400	
10.0	-109.	-107.	42.	43.	-7.525	-0.325	-0.075	
11.0	-125.	-121.	49.	54.	-8.725	0.075	-0.150	
12.0	-139.	-140.	75.	77.	-10.775	0.025	-0.175	
13.0	-183.	-183.	116.	118.	-15.000	-0.200	0.025	
14.0	-188.	-189.	117.	118.	-15.300	-0.400	0.425	

4.1 +43.00

SURFACE DISPLACEMENT= -4.50

DEPTH	ORIGINAL DATA				DEPTH	AVERAGE	DIFFERENCE	DISPLACEMENT
	TOWARDS		AWAY					
0.0	0.	0.	0.	0.	0.000	0.000	-4.500	
1.0	27.	28.	-58.	-57.	4.250	-1.050	-3.450	
2.0	-39.	-38.	6.	8.	-2.275	-1.075	-2.375	
3.0	-93.	-90.	62.	64.	-7.725	-1.025	-1.350	
4.0	-168.	-174.	133.	133.	-15.200	-1.100	-0.250	
5.0	-150.	-148.	120.	121.	-13.475	0.225	-0.475	
6.0	-107.	-108.	81.	81.	-9.425	0.575	-1.050	
7.0	-46.	-46.	10.	11.	-2.825	0.375	-1.425	
8.0	-38.	-39.	8.	5.	-2.250	-0.050	-1.375	
9.0	-42.	-41.	10.	10.	-2.575	-0.075	-1.300	
10.0	-96.	-96.	58.	59.	-7.725	-0.525	-0.775	
11.0	-115.	-112.	71.	73.	-9.275	-0.475	-0.300	
12.0	-146.	-145.	93.	93.	-11.925	-1.125	0.825	
13.0	-168.	-169.	132.	134.	-15.075	-0.275	1.100	
14.0	-169.	-169.	133.	135.	-15.150	-0.250	1.350	

4.1 +51.00

SURFACE DISPLACEMENT= -4.60

DEPTH	ORIGINAL DATA				DEPTH	AVERAGE	DIFFERENCE	DISPLACEMENT
	TOWARDS		AWAY					
0.0	0.	0.	0.	0.	0.000	0.000	-4.600	
1.0	19.	18.	-64.	-63.	4.100	-1.200	-3.400	
2.0	-46.	-46.	2.	3.	-2.425	-1.225	-2.175	
3.0	-101.	-100.	56.	57.	-7.850	-1.150	-1.025	
4.0	-175.	-172.	123.	125.	-14.875	-0.775	-0.250	
5.0	-155.	-154.	111.	115.	-13.375	0.325	-0.575	
6.0	-115.	-111.	71.	72.	-9.225	0.775	-1.350	
7.0	-56.	-59.	3.	6.	-3.100	0.100	-1.450	
8.0	-46.	-43.	2.	1.	-2.300	-0.100	-1.350	
9.0	-49.	-48.	3.	2.	-2.550	-0.050	-1.300	
10.0	-98.	-97.	52.	53.	-7.500	-0.300	-1.000	
11.0	-111.	-111.	67.	68.	-8.925	-0.125	-0.875	
12.0	-128.	-130.	86.	87.	-10.775	0.025	-0.900	
13.0	-171.	-174.	127.	128.	-15.000	-0.200	-0.700	
14.0	-174.	-174.	127.	128.	-15.075	-0.175	-0.525	

4.1 +72.00

SURFACE DISPLACEMENT= -5.20

DEPTH	ORIGINAL DATA				DEPTH	AVERAGE	DIFFERENCE	DISPLACEMENT
	TOWARDS		AWAY					
0.0	0.	0.	0.	0.	0.000	0.000	-5.200	
1.0	4.	5.	-73.	-71.	3.825	-1.475	-3.725	
2.0	-58.	-58.	-10.	-10.	-2.400	-1.200	-2.525	
3.0	-114.	-113.	44.	45.	-7.900	-1.200	-1.325	
4.0	-181.	-186.	119.	117.	-15.075	-0.975	-0.350	
5.0	-169.	-166.	101.	101.	-13.425	0.275	-0.625	
6.0	-127.	-124.	62.	61.	-9.350	0.650	-1.275	
7.0	-61.	-61.	-5.	-3.	-2.850	0.350	-1.625	
8.0	-55.	-55.	-10.	-9.	-2.275	-0.075	-1.550	
9.0	-59.	-54.	-10.	-8.	-2.375	0.125	-1.675	
10.0	-107.	-108.	37.	39.	-7.275	-0.075	-1.600	
11.0	-122.	-122.	53.	54.	-8.775	0.025	-1.625	
12.0	-136.	-138.	70.	70.	-10.350	0.450	-2.075	
13.0	-179.	-181.	112.	113.	-14.625	0.175	-2.250	
14.0	-184.	-185.	113.	116.	-14.950	-0.050	-2.200	

4.1 +91.00

SURFACE DISPLACEMENT= -6.12

DEPTH	ORIGINAL DATA				DEPTH	AVERAGE	DIFFERENCE	DISPLACEMENT
	TOWARDS		AWAY					
0.0	0.	0.	0.	0.	0.000	0.000	-6.120	
1.0	-14.	-15.	-86.	-87.	3.600	-1.700	-6.420	
2.0	-77.	-79.	-22.	-21.	-2.825	-1.625	-2.795	
3.0	-132.	-131.	29.	29.	-8.025	-1.325	-1.470	
4.0	-207.	-205.	106.	105.	-15.575	-1.475	0.005	
5.0	-182.	-182.	86.	85.	-13.375	0.325	-0.320	
6.0	-142.	-139.	45.	44.	-9.250	0.750	-1.070	
7.0	-85.	-84.	-23.	-23.	-3.075	0.125	-1.195	
8.0	-72.	-74.	-25.	-24.	-2.425	-0.225	-0.970	
9.0	-76.	-75.	-25.	-28.	-2.450	0.050	-1.020	
10.0	-125.	-124.	24.	25.	-7.450	-0.250	-0.770	
11.0	-139.	-139.	39.	41.	-8.950	-0.150	-0.620	
12.0	-153.	-154.	56.	58.	-10.525	0.275	-0.895	
13.0	-199.	-199.	100.	102.	-15.000	-0.200	-0.695	
14.0	-200.	-203.	102.	103.	-15.200	-0.300	-0.395	

4.1 +107.00

SURFACE DISPLACEMENT= -7.40

DEPTH	ORIGINAL DATA				DEPTH	AVERAGE	DIFFERENCE	DISPLACEMENT
	TOWARDS		AWAY					
0.0	0.	0.	0.	0.	0.000	0.000	-7.400	
1.0	-6.	-7.	-72.	-74.	3.325	-1.975	-5.425	
2.0	-69.	-69.	-7.	-9.	-3.050	-1.850	-3.575	
3.0	-121.	-124.	45.	45.	-8.375	-1.675	-1.900	
4.0	-193.	-196.	117.	117.	-15.575	-1.475	-0.425	
5.0	-170.	-172.	97.	94.	-13.325	0.375	-0.800	
6.0	-126.	-129.	54.	53.	-9.050	0.950	-1.750	
7.0	-72.	-70.	-9.	-12.	-3.025	0.175	-1.925	
8.0	-57.	-65.	-10.	-10.	-2.550	-0.350	-1.575	
9.0	-66.	-69.	-6.	-6.	-3.075	-0.575	-1.000	
10.0	-112.	-114.	40.	39.	-7.625	-0.425	-0.575	
11.0	-128.	-129.	55.	49.	-9.025	-0.225	-0.350	
12.0	-143.	-145.	71.	72.	-10.775	0.025	-0.375	
13.0	-189.	-190.	115.	113.	-15.175	-0.375	0.000	
14.0	-191.	-193.	117.	117.	-15.450	-0.550	0.550	

4.1 +119.00

SURFACE DISPLACEMENT= -9.10

DEPTH	ORIGINAL DATA				DEPTH	AVERAGE	DIFFERENCE	DISPLACEMENT
	TOWARDS		AWAY					
0.0	0.	0.	0.	0.	0.000	0.000	-9.100	
1.0	11.	10.	-64.	-53.	3.450	-1.850	-7.250	
2.0	-53.	-54.	10.	10.	-3.175	-1.975	-5.275	
3.0	-105.	-107.	63.	63.	-8.450	-1.750	-3.525	
4.0	-176.	-177.	141.	134.	-15.700	-1.600	-1.925	
5.0	-151.	-153.	114.	114.	-13.300	0.400	-2.325	
6.0	-107.	-111.	72.	72.	-9.050	0.950	-3.275	
7.0	-50.	-102.	12.	12.	-4.400	-1.200	-2.075	
8.0	-44.	-43.	7.	6.	-2.500	-0.300	-1.775	
9.0	-48.	-51.	10.	9.	-2.950	-0.450	-1.325	
10.0	-96.	-95.	57.	58.	-7.650	-0.450	-0.875	
11.0	-111.	-112.	73.	71.	-9.175	-0.375	-0.500	
12.0	-127.	-127.	89.	89.	-10.800	0.000	-0.500	
13.0	-173.	-173.	132.	134.	-15.300	-0.500	0.000	
14.0	-175.	-176.	135.	135.	-15.525	-0.625	0.625	

4.1 +132.00

SURFACE DISPLACEMENT= -9.30

DEPTH	ORIGINAL DATA				DEPTH	AVERAGE	DIFFERENCE	DISPLACEMENT
	TOWARDS		AWAY					
0.0	0.	0.	0.	0.	0.000	0.000	-9.300	
1.0	11.	9.	-50.	-52.	3.050	-2.250	-7.050	
2.0	-52.	-54.	21.	13.	-3.500	-2.300	-4.750	
3.0	-105.	-107.	67.	65.	-8.600	-1.900	-2.850	
4.0	-181.	-184.	139.	140.	-16.100	-2.000	-0.850	
5.0	-150.	-151.	110.	113.	-13.100	0.600	-1.450	
6.0	-108.	-107.	72.	71.	-8.950	1.050	-2.500	
7.0	-54.	-49.	11.	12.	-3.150	0.050	-2.550	
8.0	-43.	-43.	10.	8.	-2.600	-0.400	-2.150	
9.0	-50.	-49.	9.	11.	-2.975	-0.475	-1.675	
10.0	-95.	-97.	58.	57.	-7.675	-0.475	-1.200	
11.0	-110.	-110.	73.	74.	-9.175	-0.375	-0.825	
12.0	-125.	-126.	90.	92.	-10.825	-0.025	-0.800	
13.0	-172.	-173.	135.	136.	-15.400	-0.600	-0.200	
14.0	-174.	-175.	136.	136.	-15.525	-0.625	0.425	

4.1 +149.00

SURFACE DISPLACEMENT= -9.50

DEPTH	ORIGINAL DATA				DEPTH	AVERAGE	DIFFERENCE	DISPLACEMENT
	TOWARDS		AWAY					
0.0	0.	0.	0.	0.	0.000	0.000	-9.500	
1.0	-11.	-13.	-76.	-79.	3.275	-2.025	-7.475	
2.0	-76.	-79.	-12.	-13.	-3.250	-2.050	-5.425	
3.0	-126.	-127.	42.	40.	-8.375	-1.675	-3.750	
4.0	-203.	-207.	110.	107.	-15.675	-1.575	-2.175	
5.0	-173.	-177.	92.	89.	-13.275	0.425	-2.600	
6.0	-131.	-133.	49.	49.	-9.050	0.950	-3.550	
7.0	-94.	-94.	-13.	-15.	-4.000	-0.800	-2.750	
8.0	-67.	-68.	-14.	-20.	-2.525	-0.325	-2.425	
9.0	-72.	-74.	-13.	-15.	-2.950	-0.450	-1.975	
10.0	-118.	-120.	34.	33.	-7.625	-0.425	-1.550	
11.0	-133.	-135.	49.	48.	-9.125	-0.325	-1.225	
12.0	-149.	-149.	67.	67.	-10.800	0.000	-1.225	
13.0	-196.	-196.	110.	112.	-15.350	-0.550	-0.675	
14.0	-197.	-198.	113.	115.	-15.575	-0.675	0.000	

4.1 +176.00

SURFACE DISPLACEMENT= -9.20

ORIGINAL DATA					DEPTH	AVERAGE	DIFFERENCE	DISPLACEMENT
DEPTH	TOWARDS		AWAY					
0.0	0.	0.	0.	0.	0.0	0.000	0.000	-9.200
1.0	-25.	-29.	-59.	-59.	1.0	1.600	-3.700	-5.500
2.0	-86.	-86.	-2.	-4.	2.0	-4.150	-2.950	-2.550
3.0	-136.	-140.	54.	55.	3.0	-9.625	-2.925	0.375
4.0	-224.	-223.	146.	140.	4.0	-18.325	-4.225	4.600
5.0	-193.	-195.	110.	107.	5.0	-15.125	-1.425	6.025
6.0	-86.	-87.	47.	46.	6.0	-6.650	3.350	2.675
7.0	33.	32.	-122.	-122.	7.0	7.725	10.925	-8.250
8.0	-44.	-47.	-41.	-39.	8.0	-0.275	1.925	-10.175
9.0	-80.	-81.	-10.	-9.	9.0	-3.550	-1.050	-9.125
10.0	-175.	-175.	88.	87.	10.0	-13.125	-5.925	-3.200
11.0	-172.	-172.	83.	82.	11.0	-12.725	-3.925	0.725
12.0	-157.	-155.	68.	70.	12.0	-11.250	-0.450	1.175
13.0	-200.	-202.	114.	114.	13.0	-15.750	-0.950	2.125

4.1 +224.00

SURFACE DISPLACEMENT= -9.60

ORIGINAL DATA								
DEPTH	TOWARDS		AWAY		DEPTH	AVERAGE	DIFFERENCE	DISPLACEMENT
0.0	0.	0.	0.	0.	0.0	0.000	0.000	-9.600
1.0	-32.	-33.	-62.	-65.	1.0	1.550	-3.750	-5.850
2.0	-91.	-91.	-3.	-3.	2.0	-4.400	-3.200	-2.650
3.0	-144.	-146.	50.	53.	3.0	-9.825	-3.125	0.475
4.0	-227.	-232.	140.	136.	4.0	-18.375	-4.275	4.750
5.0	-198.	-199.	106.	105.	5.0	-15.200	-1.500	6.250
6.0	-92.	-94.	2.	2.	6.0	-4.750	5.250	1.000
7.0	33.	31.	-125.	-125.	7.0	7.850	11.050	-10.050
8.0	-45.	-45.	-42.	-44.	8.0	-0.100	2.100	-12.150
9.0	-80.	-82.	-11.	-11.	9.0	-3.500	-1.000	-11.150
10.0	-179.	-179.	86.	84.	10.0	-13.200	-6.000	-5.150
11.0	-173.	-174.	93.	92.	11.0	-12.300	-4.000	-1.150
12.0	-157.	-158.	66.	68.	12.0	-11.225	-0.425	-0.725
13.0	-203.	-204.	114.	110.	13.0	-15.775	-0.975	0.250

DURHAM UNIVERSITY
SCIENCE
SECTION
12 JAN 1978